RESTRICTED REPORT 364R

CSIRO
AUSTRALIA

Division of
EXPLORATION GEOSCIENCE

Institute of Minerals, Energy and Construction

MAGNETIC PETROPHYSICS, PALAEOMAGNETISM AND TECTONIC ROTATIONS OF THE PORGERA INTRUSIVE COMPLEX, PAPUA NEW GUINEA

D.A. CLARK and P.W. SCHMIDT

P.O. Box 136
North Ryde
NSW 2113

January 1993

CSIRO
AUSTRALIA

Division of Exploration Geoscience
Institute of Minerals, Energy and Construction
51 Delhi Road, North Ryde, NSW. Postal Address: PO Box 136, North Ryde, NSW 2113
Telephone: (02) 887 8666. Telex: AA25817. Fax: (02) 887 8909

POLICY ON RESTRICTED REPORTS

Restricted Reports issued by this Division deal with projects where CSIRO has been granted privileged access to research material. Initially, circulation of Restricted Reports is strictly controlled, and we treat them as confidential documents at this stage. They should not be quoted publicly, but may be referred to as a "personal communication" from the author(s) if my approval is sought and given beforehand.

The results embodied in a Restricted Report may eventually form part of a more widely circulated CSIRO publication. Agreements with sponsors or companies generally specify that drafts will be first submitted for their approval, to ensure that proprietary information of a confidential nature is not inadvertently included.

After a certain period of time, the confidentiality of particular Restricted Reports will no longer be an important issue. It may then be appropriate for CSIRO to announce the titles of such reports, and to allow inspection and copying by other persons. This procedure would disseminate information about CSIRO research more widely to Industry. However, it will not be applicable to all Restricted Reports. Proprietary interests of various kinds may require an extended period of confidentiality. Premature release of Restricted Reports arising from continuing collaborative projects (especially AMIRA projects) may also be undesirable, and a separate policy exists in such cases.

You are invited to express an opinion about the security status of the enclosed Restricted Report. **Unless I hear to the contrary,** I will assume that in eighteen months time I have your permission to place this Restricted Report on open file, when it will be generally available to interested persons for reading, making notes, or photocopying, as desired.

B.E. Hobbs
Chief of Division

Floreat Park
Location: Underwood Avenue, Floreat Park
Postal Address: CSIRO Private Bag,
PO Wembley WA 6014
Telephone: (09) 387 0200
Fax: (09) 387 8642
Telex: AA92178

Townsville
Location: Davies Laboratory, University Road, Townsville
Postal Address: Private Mail Bag,
PO Aitkenvale QLD 4814
Telephone: (077) 71 9511
Fax: (077) 25 1009

Lindfield
Location: Bradfield Road, Lindfield
Postal Address: PO Box 218
Lindfield NSW 2070
Telephone: (02) 413 7733, 413 7211
Fax: (02) 413 7202
Telex: AA26296

RESTRICTED REPORT 364R Copy 10 of 11 copies

Report to Placer Exploration Ltd and the Porgera Joint Venture

	Copy No.
Placer/PJV	1-8
D.A. Clark	9
P.W. Schmidt	10
B.E. Hobbs	11

TABLE OF CONTENTS

LIST OF TABLES

LIST OF FIGURES

Fig.6. Zijderveld plots for the Waruwari altered hornblende diorite samples.

Fig.7. Zijderveld plots for the Waruwari andesite samples.

Fig.8. Zijderveld plots for the Haul Road dykes samples.

Fig.9. Zijderveld plots for the Tawisakale samples.

Fig.10. Zijderveld plots for the Mount Kare samples.

Fig.11. Zijderveld plots for the NE Porgera Complex samples.

Fig.12 Zijderveld plots for the Roamane hornblende diorite samples.

Fig.13. Zijderveld plots for the Rambari/Roamane augite hornblende diorite samples.

Fig.14. Zijderveld plots for the fresh and altered andesite samples from the underground mine.

Fig.15. Zijderveld plots for samples of altered host sediments and sulphide mineralisation.

Fig.16. Low and high temperature remanence components from the Tawisakale intrusion.

Fig.17. Low and high temperature remanence components from the NE Porgera Complex gabbros.

Fig.18. Low and high temperature remanence components from the Roamane hornblende diorite.

Fig.19. Low and high temperature remanence components from the Rambari/Roamane augite hornblende diorite.

Fig.20. Principal susceptibility axes of specimens from sites 01-11.

Fig.21. Principal susceptibility axes of specimens from Mt Kare.

Fig.22. Principal susceptibility axes of hornblende diorite specimens from the underground mine.

Fig.23. Principal susceptibility axes of augite hornblende diorite specimens from the underground mine.

EXECUTIVE SUMMARY

This report details magnetic properties of samples from the Porgera Intrusive Complex and from Mount Kare, Papua New Guinea. The aims of the study were:

(i) to assist magnetic interpretation by characterising the magnetic properties of the heterogeneous and variably altered intrusives and host rocks within the Porgera Intrusive Complex,

(ii) to define the bulk magnetisation of the known intrusive bodies, thereby enabling subtraction of the effects of shallow sources to reveal the signature of the interpreted large, deep magnetic body beneath the Porgera Complex,

(iii) to assist interpretation of the structure of the Porgera Complex by using palaeomagnetism to define the degree and timing of local tilting and rotation of intrusives by thin-skinned tectonic processes.

The interpreted large magnetic body at depth may represent a magma chamber that was the source of the high level stocks and the mineralising fluids at Porgera. The depth and geometry of this pluton is therefore relevant to the search for deeper mineralisation, possibly of porphyry copper type, at Porgera. Definitive modelling of the location and geometry of this body requires isolation of its magnetic signature from the complexities associated with the shallow intrusives. Given that the geometry of the near surface intrusives has been well defined by drilling, knowledge of representative magnetic properties should enable the magnetic anomalies due to shallow sources to be calculated reliably using standard polyhedral models.

Post-emplacement tilting of intrusives at Porgera was first suggested by palaeomagnetic results from four oriented block samples of hornblende diorite, collected from the mine adit. These samples all exhibited subvertical remanent magnetisation, substantially steeper than the geomagnetic field at any time from the Late Miocene to the present. This remanence direction indicates ~60° tilt of this intrusive to the north, subsequent to acquisition of the remanence.

This study has established representative magnetic properties for major rock types in the Porgera Intrusive Complex. The major results of the magnetic petrophysical study are summarised below:

* Relatively unaltered intrusive rocks of the Porgera Igneous Complex are moderately to strongly magnetic, whereas strongly altered intrusives, mineralised zones and country rocks are very weakly magnetic. Thus local magnetic anomalies at Porgera that are attributable to shallow sources arise from weakly altered intrusions. Alteration zones within intrusions may be detectable by high resolution magnetic surveys.

* Except for the small hornblende diorite intrusion at Yakatabari, Koenigsberger ratios are substantially less than unity, indicating that induced magnetisation is predominantly responsible for the anomalies associated with most of the Porgera Igneous Complex.

* There is evidence that hornblende diorite and hornblende diorite porphyry tend to be the most magnetic rock types in the complex, although all fresh intrusives sampled, from very mafic to intermediate compositions, have fairly high susceptibilities. The susceptibilities generally correspond to equivalent magnetite contents of 1-2 vol%.

* Altered ?intrusives from exposed mineralised zones at Mount Kare are very weakly magnetic. However drill core samples of fresh intrusives at depth are strongly magnetic and should be associated with a magnetic anomaly.

* Although a well-defined magnetic fabric is detectable for many localities, the susceptibility anisotropy is very weak and the effects of anisotropy on magnetic anomalies is negligible.

The main findings of the palaeomagnetic study are summarised below:

* Primary thermoremanent magnetisation is retained by most of the intrusives, unless they are highly altered. The primary magnetisation is carried by multidomain (titano)magnetite. In addition the remanence carried by the intrusives is weakly to heavily overprinted. The secondary component in relatively fresh intrusives in the mine area is probably associated with the weak, but pervasive, propylitic alteration and is carried by very fine-grained stoichiometric magnetite. This secondary magnetite is in the pseudosingle domain to single domain size range (several microns to submicron).

* Primary remanence directions have been rotated and are now steep up, in the case of normal polarity, or steep down, for reversed polarity. Thus a systematic tilt of the Porgera Igneous Complex since emplacement has been confirmed. The total degree of tilting has been 50°-60°, down to the south.

* In addition, there has been a systematic anticlockwise rotation of the Porgera Intrusive Complex, through about 45° on average, as indicated by rotation of originally northward declinations towards the NW (normal polarity) or southward declinations towards the SE (reversed polarity).

* Progressive tilting and anticlockwise rotation are tracked by secondary magnetisations acquired at various stages of the rotations. Thus the tectonic rotations are penecontemporaneous with the alteration, and therefore occurred relatively soon after emplacement, probably within 1 Ma. Although most of the tectonic movements were completed by the time of the latest remanence components, some rotations in the same sense continued after acquisition of secondary remanence.

* The tectonic rotations are evidently in response to thin-skinned tectonic processes and accompany the rapid uplift of the Complex. There is evidence that rapid tectonic rotations of epithermal and porphyry-type deposits in similar tectonic settings is commonplace. Palaeomagnetism is a powerful tool for detecting such rotations and could be particularly useful for elucidating the structural history of young deposits in tectonically active areas. The present study affords an example of the utility of the method for detecting hitherto unsuspected structural complications, which may have implications for locating further mineralised zones.

* The limited paleomagnetic data from altered rocks at Mount Kare indicate differential tectonic rotations at the two sites, suggesting that this deposit has been disrupted by tectonic movements.

Several recommendations concerning additional work are made:

(i) A number of intrusions are undersampled and there is scope for further work on drill core samples, in particular, as these become available during the current drilling programme. This would allow refinement of the magnetic models and would also provide information on tectonic rotations that may aid structural interpretation.

(ii) This study has illustrated the utility of the palaeomagnetic method for unravelling complex tectonic histories of young intrusive complexes. The possibility of applying palaeomagnetism to other porphyry-style or epithermal deposits should be investigated.

(iii) This study provides a foundation for a detailed study of the magnetic petrology of the Porgera intrusives. The aim would be to characterise the magmatic and hydrothermal processes that create, alter and destroy magnetic minerals in these rocks, as an aid to geological interpetation of magnetic surveys in the Porgera region and in analogous terrains. The present sample collection, supplemented if necessary to fill any gaps, could provide the material for detailed rock magnetic experiments, petrography, chemical analysis and electron microprobe analysis of opaque phases. These techniques would be used to determine the magnetic mineral abundance, composition, domain state and grainsize, and relate these to the rock composition, primary mineralogy and alteration. By integrating rock magnetic techniques and petrological studies, a much better understanding of the relationships between magnetic properties and geological factors, including igneous rock composition, magmatic conditions and hydrothermal processes, will be gained. Because mineralisation is also controlled by these factors, the association between mineralisation and magnetic anomaly patterns should become clearer as a result of magnetic petrological studies.

1. INTRODUCTION

This report details magnetic properties of samples from the Porgera Intrusive Complex and from Mount Kare, Papua New Guinea. The aims of the study were:

(i) to assist magnetic interpretation by characterising the magnetic properties of the heterogeneous and variably altered intrusives and host rocks within the Porgera Intrusive Complex,

(ii) to define the bulk magnetisation of the known intrusive bodies, thereby enabling subtraction of the effects of shallow sources to reveal the signature of the interpreted large, deep magnetic body beneath the Porgera Complex,

(iii) to assist interpretation of the structure of the Porgera Complex by using palaeomagnetism to define the degree and timing of local tilting and rotation of intrusives by thin-skinned tectonic processes.

The interpreted large magnetic body at depth may represent a magma chamber that was the source of the high level stocks and the mineralising fluids at Porgera. The depth and geometry of this pluton is therefore relevant to the search for deeper mineralisation, possibly of porphyry copper type, at Porgera. Definitive modelling of the location and geometry of this body requires isolation of its magnetic signature from the complexities associated with the shallow intrusives. Given that the geometry of the near surface intrusives has been well defined by drilling, knowledge of representative magnetic properties should enable the magnetic anomalies due to shallow sources to be calculated reliably using standard polyhedral models.

Post-emplacement tilting of intrusives at Porgera was first suggested by palaeomagnetic results from four oriented block samples of hornblende diorite, collected from the mine adit. These samples all exhibited subvertical remanent magnetisation, substantially steeper than the geomagnetic field at any time from the Late Miocene to the present. This remanence direction indicates ~60° tilt of this intrusive to the north, subsequent to acquisition of the remanence.

A total of 96 oriented samples were collected from the Porgera Complex in June, 1992, supplementing ten samples submitted earlier by K. Logan. In addition, nine oriented samples were collected from altered igneous rocks in surface workings at Mount Kare and three unoriented drill core samples from magnetic intrusive rocks at Mount Kare were taken from the remains of the core shed. Table 1 lists samples collected from the surface by CSIRO geophysicists, as well as previously submitted samples. Table 2 lists samples collected from the underground mine and Waruwari surface mine in June 1992.

The geology of the Porgera deposit has been summarised by Fleming *et al* (1986) and Handley and Henry (1990). Richards (1990) has presented a detailed petrological and geochemical study of the

Porgera intrusives and Richards *et al* (1991) and Richards (1992) have discussed the genesis of the mineralisation. The geochronology of the Porgera deposit has been studied by Richards and McDougall (1990). Richards *et al* (1990) have placed the magmatism at Porgera in a regional tectonic context and Sillitoe (1988) and Solomon (1990) have compared and contrasted Porgera-style magmatism and mineralisation to other intrusive-related gold deposits in Pacific island arcs.

The Porgera intrusives represent a comagmatic suite of mafic, alkaline (nepheline normative) rocks ranging in composition from alkali basalt through hawaiite (trachybasalt) to mugearite (basaltic trachyandesite) (Richards, 1990). Magnetite-rich spinel is a common primary phase that crystallised from the relatively oxidised magmas and can be quite abundant. Some secondary magnetite is also associated with ?deuteric alteration of primary olivine in the more mafic varieties. Secondary magnetite may also result from breakdown, under oxidising conditions, of primary hornblende and biotite during initial cooling. Thus relatively unaltered intrusives tend to be moderately to strongly magnetic. Propylitic alteration of varying intensity is pervasive throughout the Porgera Igneous Complex, but generally appears to have preserved magnetite, except in the most altered rocks. On the other hand, intense phyllic (sericite-carbonate) alteration, which is associated with gold-sulphide mineralisation at Waruwari, for example, destroys magnetite and produces weakly magnetic rocks.

The geochronological data of Richards and McDougall (1990) indicate an age of emplacement of 6.0 ± 0.3 Ma for the Porgera Intrusive Complex, with mineralisation occurring within 1 Ma of magmatism. Alteration ages range from 5.1 to 6.1 Ma. This young (Late Miocene) age for the Porgera Intrusive Complex implies that apparent polar wander since emplacement is very minor. Thus palaeomagnetic directions recorded at Porgera should lie close to the present geomagnetic field (for normal polarity remanence) or to its antipodal direction (in the case of reversed polarity remanence), unless there has been tectonic disturbance of the rocks since acquisition of the remanence.

The samples collected for this study are classified in Tables 1 and 2 according to the field names traditionally used at Porgera (Handley and Henry, 1990). Without whole rock chemical analyses and petrographic descriptions the samples cannot be matched exactly with Richards' (1990) classification of the Porgera intrusives, but approximate geochemically-based equivalents can be inferred from data given by Richards (1990) and Handley and Henry (1990), and are also given in the Tables. No unique correlation of the field names with the geochemical classification is possible, because the field names reflect alteration as well as primary composition. Overall the effect of alteration is to give the rocks a more felsic appearance in hand specimen than the chemical composition and primary mineralogy would indicate. Thus the field names suggest intermediate compositions, whereas geochemical and petrographic data indicate that the rocks are quite mafic.

Spinel phases are present to varying extents in all the intrusives at Porgera, although they are relatively rare in the mugearitic feldspar porphyries. According to the spinel compositions given by Richards (1990), the early-crystallising oxide phases are paramagnetic Mg-Al-Cr spinels. These occur in the more mafic rocks (alkali basalts, hawaiites and gabbroic cumulates) as microphenocrysts, a few hundred microns in diameter, enclosed in silicate phenocrysts. Spinel compositions evolved continuously towards ferromagnetic titanomagnetites during fractionation of the parental magma. Thus titanomagnetites with ~15-20 mole % ulvospinel occur as microphenocrysts in mugearites (evolved hornblende diorites and feldspar porphyries) and in the groundmass of the full spectrum of rock compositions. The continuous precipitation of spinel phases throughout magmatic differentiation indicates relatively high oxygen fugacity. Oxidising conditions in the magma are also conducive to production of secondary magnetite during deuteric alteration of olivine and subsolidus oxidation of hornblende and biotite. Secondary magnetite produced by these processes should be essentially pure, with negligible substitution of other cations for iron. The magnetic properties of the Porgera intrusives are predominantly attributable to primary titanomagnetites and secondary magnetite produced during initial cooling. The contribution of primitive chromian spinels is negligible.

2. ROCK MAGNETIC TECHNIQUES

Standard palaeomagnetic procedures (Collinson, 1983) were followed throughout this study. Block samples were collected underground and a portable petrol-powered drill was used to sample on the surface. Samples were oriented using both a sun compass (where possible) and a magnetic compass. The blocks and cores were subsampled in the laboratory to yield specimens of nominal 25mm diameter and 20mm height. Remanent magnetizations were measured using a CTF cryogenic magnetometer or an up-graded DIGICO balanced fluxgate magnetometer. The spinner unit and electronic drive unit of the latter have been interfaced to a personal computer.

The CSIRO susceptibility bridge/furnace (Ridley and Brown, 1980) was used to measure absolute susceptibilities. Anisotropy of magnetic susceptibility was determined using an up-graded DIGICO anisotropy delineator whose performance exceeds that of the original. Alternating field (AF) demagnetization was carried out by means of a Schonstedt GSD-1 demagnetizer. The CSIRO programmable carousel furnace, which allows multiple batches of samples to be processed unattended, was used for stepwise thermal demagnetisation.

Palaeomagnetic components isolated by thermal or AF demagnetisation were analysed by examination of orthogonal projections of vector end-ponts (Zijderveld plots) and the directions of linear segments, representing individual remanence components, were defined by principal component analysis (PCA), which is described by Kirschvink (1980).

3. BASIC MAGNETIC PROPERTIES

Table 3 gives bulk susceptibilities and natural remanent magnetisation (NRM) vectors for all the samples. Koenigsberger ratios (Q) calculated from these properties define the relative importance of remanent and induced magnetisation for each sample ($Q > 1$ indicates remanence is dominant, whereas $Q < 1$ indicates induced magnetisation is more intense than remanence). Results from individual localities will now be discussed separately.

Yakatabari

Sites 01 and 02 are both located in the relatively small, rootless Yakatabari intrusion that is exposed in the surface mine. The rock type is variably altered hornblende diorite (probably equivalent to mugearite in Robert's (1990) classification). Site 02 represents a fine-grained marginal phase of the intrusion. The susceptibility of the samples is correlated with the degree of alteration: the most altered sample (2B) is paramagnetic, whereas the majority of the samples from this site are fresher and have much higher susceptibilities (> 3000 μG/Oe). Within site 01 the susceptibility generally increases as the degree of alteration decreases from sample 1A-E.

The mean susceptibility of the site 01 samples is 2500 μG/Oe (.0314 SI) and for site 02 samples it is 3070 μG/Oe (0.0386 SI). NRM directions of specimens from sites 01 and 02 are somewhat scattered, but all lie within the NW up octant (Fig.1(a)). Palaeomagnetic cleaning of the specimens shows that the directional scatter reflects the presence of multiple remanence components, acquired at different times, rather than a simple primary thermoremanent magnetisation (see the next section). The variation in remanence directions recorded at Porgera records substantial tectonic rotation of intrusions during and since remanence acquistion, as well as one or more reversals of geomagnetic polarity.

Remanence intensities and Koenigsberger ratios are high for the Yakatabari samples, indicating that the main remanence carrier is very fine-grained magnetite, in the single domain (SD) to pseudosingle domain (PSD) size range, i.e. less than ~10 μm. Given the distinct grouping of remanence directions, the overall contribution of remanence to the magnetisation of the Yakatabari intrusion is substantial, dominating the contribution of induced magnetisation. The effective Q value is 4.5 for site 01 and even higher for the finer-grained marginal phase of site 02 ($Q = 9.1$). The mean remanence vector has similar inclination to the present field but is deflected towards the NW. The effect of this remanence direction on the associated anomaly is to deflect the anomaly axis towards a NW-SE orientation. After standard reduction to the pole, which assumes that the magnetisation is parallel to the present field, the local anomaly associated with this intrusion should exhibit a somewhat dipolar character, rather than a simple bullseye high, because the true magnetisation direction diverges from the assumed direction.

Although the moderately altered samples have less magnetite, and therefore have lower susceptibility, the remanent intensity does not decrease to the same extent and the Koenigsberger ratio is accordingly higher for these samples. This suggests that the magnetite in the moderately altered samples tends to be finer grained, and is therefore a more efficient remanence carrier. The most altered sample, 2B, has relatively weak remanence and a lower Q value because magnetite is almost completely absent and the susceptibility is dominated by paramagnetic silicates, which cannot carry remanence. Overall, remanence directions tend to be somewhat steeper for altered samples than for their fresher equivalents.

Site 01 is probably more representative of the bulk of the Yakatabari intrusion than the chilled margin at site 02. Thus the mean remanence and susceptibility for the site 01 samples probably provide the best estimate of the bulk properties of the intrusion.

Waruwari

Within the Waruwari pit highly altered hornblende diorite (mugearite) was collected at site 03, and variably altered andesite (?hawaiite) from the Roamane Fault zone was sampled at site 04. The most altered hornblende diorite samples are paramagnetic, with susceptibilities of~50 μG/Oe (0.63 * 10^{-3} SI), whereas moderately altered samples have moderate susceptibilities, up to ~800 μG/Oe (0.01 SI). NRM directions shown in Fig.1(b) are quite scattered, with both normal and reversed polarities evident. The distribution of remanence directions suggests that the subhorizontal remanence vectors represent subequal contributions from steep up and steep down components, which dominate the NRMs of other specimens. The scatter in NRM directions and the relatively low Q values of the less altered, higher susceptibility, samples ensure that the bulk remanence of the altered hornblende diorite at Waruwari is weak and the corresponding Koenigsberger ratio is low (~0.3). The resultant remanence direction is estimated to be steep up, although the mean NRM vector is ill-defined due to the great variability of remanence direction and intensity. The estimated average susceptibility of the altered hornblende diorite, assuming the sampling is representative, is ~180 μG/Oe (2.26 * 10^{-3} SI). In fact, the less altered, more magnetic samples are probably overrepresented in the collection because they were deliberately sought out to provide a contrast with the bulk of the exposed intrusive. Thus the true bulk susceptibility of this intrusive is probably somewhat lower than the above value. The relatively weak susceptibility accounts for the low magnetic response of the Waruwari intrusive.

The magnetic properties of the altered andesite samples from site 04 are very variable, reflecting variable alteration. Susceptibilities range from ~30 μG/Oe to 2150 μG/Oe (0.38-27.0 * 10^{-3}), with a mean value of 1100 μG/Oe (13.8 * 10^{-3} SI). NRM directions are very scattered (Fig.1(c)), with normal and reversed polarities represented. The effective Koenigsberger

ratio is low (Q = 0.2). An altered andesite sample previously collected from the Waruwari pit, W15, has similar properties to the altered site 04 samples. On the other hand, a relatively unaltered augite hornblende diorite sample (W13) previosly collected from Waruwari has high susceptibility (3980 μG/Oe = 50 * 10^{-3} SI), moderate NRM intensity (~390 μG) and a Q value of 0.24.

At both sites 03 and 04, palaeomagnetic cleaning shows that the scatter in remanence directions arises from variable overprinting of a hard reversed remanence component by a softer normal component (see next section).

Andesite and Hornblende Diorite Dykes (Sites 05 and 06)

Two parallel "dykes", a thin (4 m) fine-grained andesite intrusive (site 05) and a thicker, coarser-grained body of hornblende diorite (site 06), intrude black sediments beside the Haul Road between Tawisakale and Waruwari. Both bodies are conformable with the host sediments, suggesting that they are sills that have been tilted to the south, along with the sediments, subsequent to emplacement. The rock compositions are probably similar for the two intrusives, with the difference in appearance attributable to finer grain size in the rapidly chilled thin dyke/sill.

Apart from sample 5A, which is from the narrow chilled margin of the intrusive, the andesite has high susceptibility, increasing away from the dyke margins towards the centre. *In situ* susceptibility measurements fall in the range 21-44 * 10^{-3} SI (1670-3500 μG/Oe), except at the dyke margins, where the SI susceptibility drops to ~0.46 * 10^{-3} (37 μG/Oe). The mean susceptibility of samples 5B-F is 5240 μG/Oe (66 * 10^{-3} SI), somewhat higher than the *in situ* measurements, which are reduced by unevenness of the exposed surfaces.

The hornblende diorite dyke is also strongly magnetic, with an average susceptibility of ~6400 μG/Oe (80 * 10^{-3} SI). The susceptibilities of baked sediments and altered hornblende diorite at the dyke margins are much lower, in the paramagnetic range.

NRM directions are scattered within the NE and SE up octants for the andesite dyke and the NW up and SW up octants for the hornblende diorite dyke (Fig.1(d)-(e)). Koenigsberger ratios are low for the dykes (Q = 0.14 and 0.11 for sites 05 and 06 respectively). Palaeomagnetic cleaning of specimens from the dykes suggests that a dominant normal component and a subordinate reversed component, with highly overlapped stability spectra, contribute to the observed NRM.

Tawisakale

Hornblende diorite porphyry (mugearite) samples from the unmineralised Tawisakale intrusion have high susceptibilities (~5000 μG/Oe = 63 * 10^{-3} SI). *In situ* susceptibilities were quite consistent at ~40 * 10^{-3} SI. NRM directions are scattered within the NE quadrant, with inclinations ranging from shallow up to steep down (Fig.1(f)). The effective Q value (0.16) is low, indicating that remanence is subordinate to induced magnetisation for the Tawisakale samples. The distribution of NRM directions reflects variable contributions from a harder, relatively steep down reversed component underlying a generally subordinate, softer normal component with somewhat shallower shallower inclination.

Mount Kare

Highly altered ?intrusives from hard rock workings at Mount Kare were sampled at sites 08 and 09. These rocks are very weakly magnetic, probably due to the intense alteration in the mineralised zones. The susceptibilities are less than 30 μG/Oe (0.38 * 10^{-3} SI), averaging 17 μG/Oe (0.21 * 10^{-3} SI). Remanent magnetisation is also weak, but dominates induced magnetisation, probably reflecting the presence of secondary haematite in these samples. NRMs are broadly reversed with respect to the present field (Fig.1(g)-(h)).

Three drill core samples of relatively fresh intrusive rocks intersected at depth beneath Mount Kare were retrieved from the ruins of the core shed. Although these samples had been baked in the fire that destroyed the sheds, the magnetic mineralogy has probably been preserved. These samples are quite magnetic, with an average susceptibility of 3350 μG/Oe (42 * 10^{-3} SI). Remanent magnetisation is comparable to induced magnetisation for these samples, but the NRM carried by the cores is probably thermoremanence acquired in the fire.

NE Porgera Complex

At sites 10 and 11 alkali gabbro was sampled in road cuts west of the Kogai River, away from the mineralised area of the Porgera Complex. Although precise grid co-ordinates were not known, comparison with the 1:10,000 topographic and geological maps suggests that sites 10 and 11 are mapped as the Kogai Diorite and Sluice Diorite respectively. These samples appear more mafic than the intrusives sampled in and around the mine area and are less altered. The mean susceptibility of the moderately magnetic samples from site 10 is 1200 μG/Oe (15.1 * 10^{-3} SI), whereas samples from site 11 are more magnetic, with a mean susceptibility of 4790 μG/Oe (60.2 * 10^{-3} SI).

NRMs are relatively weak for these samples and the site mean Koenigsberger ratios are accordingly low (~0.1), indicating that magnetisation by induction predominates for this rock type. NRM directions lie predominantly in the NE up octant for site 10 and

are scattered about a NNE direction with moderate inclination for site 11 (Fig.1(i)-(j)). Palaeomagnetic cleaning shows that this intrusion carries remanence dominated by a relatively soft component of normal polarity, underlain by harder reversed component.

Roamane Hornblende Diorite

Hornblende diorite (hawaiite) samples collected from the underground mine have quite variable suceptibilities, with a range of ~600 μG/Oe to ~9400 μG/Oe (~2.5-11.8 * 10^{-3} SI), but overall are strongly magnetic. The average susceptibility is 5530 μG/Oe (69.5 * 10^{-3} SI). NRM directions are quite consistently directed steeply upwards (Fig.2(a)), reflecting a ubiquitous subvertical remanence component that dominates the NRM of this intrusive. NRM intensities for individual samples range from ~200 to ~2100 μG and Q values from 0.3 to 1.2. The mean NRM vector has an intensity of 1010 μG, with dec = 38°, inc = -83°. The corresponding Q value is 0.45, indicating that remanence makes a substantial contribution to the total magnetisation, but is nevertheless subordinate to induced magnetisation.

Rambari/Roamane Augite Hornblende Diorite

Augite hornblende diorite (alkali basalt/gabbro) from the underground mine has somewhat variable magnetic properties, but is moderately magnetic overall. Susceptibilities of samples of this rock type range from ~300 μG/Oe (3.8 * 10^{-3} SI) to ~4800 μG/Oe (60.3 * 10^{-3} SI), with a mean of 2140 μG/Oe (26.9 * 10^{-3} SI), which is substantially less than that of the hornblende diorite.

NRM directions are much more scattered for the augite hornblende diorite than for the hornblende diorite (Fig.2(b)), reflecting the presence of normal and reversed components within each sample. The relatively weak NRM intensities and low Q values of these samples result from superposition of subequal, nearly antiparallel remanence components. As a result, remanence makes a very minor contribution to the magnetisation of the augite hornblende diorite at Roamane.

Roamane Andesite

Only two samples of fresh andesite (?alkali basalt) were collected from the underground mine, whereas six samples of highly altered andesite were taken. The relatively unaltered samples have high susceptibility (~3500 μG/Oe = 44 * 10^{-3} SI), whereas their altered equivalents are paramagnetic, with susceptibilities of only 10-80 μG/Oe (0.13-1.0 * 10^{-3} SI).

The fresh andesites have moderate NRM intensities, but the magnetisation is dominated by induction ($Q \approx 0.3$). NRMs of the altered andesites are weak and Q values are low. Palaeomagnetic cleaning indicates that the NRMs consist of multiple components with overlapped stability spectra.

Sulphide Mineralisation

Sulphide-bearing mineralised samples W14, from Waruwari, and 28/19, from Roamane both have very low susceptibilities and very weak remanence, reflecting almost total destruction of ferromagnetic minerals by the intense alteration associated with the mineralising fluids.

Sediments

Three samples of sedimentary country rock, variably altered, were taken from the underground mine. All had very weak susceptibility and remanence, reflecting the absence of primary ferromagnetic minerals in these reduced, organic-rich, pyritic sediments.

Discussion

The magnetic property measurements discussed above indicate that relatively unaltered intrusive rocks of the Porgera Igneous Complex are moderately to strongly magnetic, whereas strongly altered intrusives, mineralised zones and country rocks are very weakly magnetic. Thus local magnetic anomalies at Porgera that are attributable to shallow sources arise from weakly altered intrusions. The susceptibility distributions for the sampled rock types are plotted in Fig.3.

Except for the small hornblende diorite intrusion at Yakatabari, Koenigsberger ratios are substantially less than unity, indicating that induced magnetisation is predominantly responsible for the anomalies associated with most of the Porgera Igneous Complex.

Figure 3 offers evidence that hornblende diorite and hornblende diorite porphyry tend to be the most magnetic rock types in the complex, although all fresh intrusives sampled, from very mafic to intermediate composition, have fairly high susceptibilities. The susceptibilities generally correspond to equivalent magnetite contents of 1-2 vol%. This presumably reflects the ubiquitous presence of magnetite-rich spinel in the groundmass, as well as secondary magnetite produced by high-temperature breakdown of mafic silicates under oxidising conditions. Titanomagnetite microphenocrysts that occur additionally in hornblende diorites and hornblende diorite porphyries may account for the generally higher susceptibility of these rock types. Phenocrystic spinels in the more mafic intrusives are paramagnetic, suggesting that the susceptibility of these rocks arises from groundmass titanomagnetites and secondary magnetite.

Spinel phenocrysts are rare in feldspar porphyries, which are not represented in the present collection, but published chemical analyses indicate high normative magnetite (~5 wt%) in these rocks (Richards, 1990). Normative magnetite calculations tend to overestimate true magnetite contents in these rocks, because ferric iron contents are underestimated for clinopyroxene and ignored for hornblende and biotite. However, high normative magnetite correlates with modal magnetite. Furthermore, the normative magnetite is similar for the feldspar porphyries and

the other rock types that are known to have high susceptibilities. Thus the high normative magnetite values suggest that the feldspar porphyries contain groundmass magnetite and should have moderate to high susceptibility.

4. PALAEOMAGNETISM OF THE INTRUSIVE COMPLEX

The low latitude of Porgera implies a shallow geomagnetic field. The recent geomagnetic field, averaged over a few thousand years, coincides with the axial geocentric dipole field corresponding to the latitude of Porgera (5.5°S), i.e. dec = 0°, inc = -11°. The present field direction at Porgera (dec = 5.5°, inc = -26°) reflects secular variation and is anomalously steep. The northward drift of the Australian Plate during the Tertiary is reflected in progressively steeper palaeofields with increasing age. However, the amount of movement since emplacement of the Porgera Complex in the Late Miocene is only ~10°. Based on the data of Idnurm (1985), the 5-6 Ma palaeomagnetic pole for the Australian Plate lies at 80°S, 120°E. The corresponding dipole field direction is dec = 3°, inc = -26° (for normal polarity), or dec = 183°, inc = +26° (for reversed polarity). Thus palaeomagnetic directions recorded at Porgera should lie close to the present geomagnetic field (for normal polarity remanence) or to its antipodal direction (in the case of reversed polarity remanence), unless there has been tectonic disturbance of the rocks since acquisition of the remanence.

A recent refinement of the Late Cretaceous and Cenozoic geomagnetic polarity time scale, based on a global analysis of marine magnetic anomalies was published by Cande and Kent (1992). The data indicate that the geomagnetic field had normal polarity from 6.3 Ma to 6.0 Ma, reversed polarity in the interval 6.0-5.9 Ma, normal polarity again from 5.9 Ma to 5.7 Ma, followed by reversed polarity until 5.0 Ma, with several subsequent reversals between 5.0 Ma and 4.0 Ma.

NRM directions from many of the Porgera intrusives are scattered, suggesting a complex magnetic/tectonic history, rather than a simple thermoremanent magnetisation that records initial cooling of the intrusives. AF and thermal demagnetisation reveals the presence of multicomponent magnetisations and, in many cases, allows the remanence components to be resolved. Only fully resolved remanence components represent magnetically recorded palaeofield directions.

The most appropriate method of displaying palaeomagnetic cleaning data is the Zijderveld plot, which is explained in Fig.4. Representative Zijderveld plots for AF and thermal demagnetisation of samples from Porgera and Mount Kare are shown in Figs.5-15, along with stereoplots, plots of intensity versus treatment and the corresponding stability spectra. The palaeomagnetic data from each locality will be discussed separately, before integrating the information to interpret the magnetic and tectonic history of the Porgera area.

Yakatabari

Fig.5 shows Zijderveld plots for the Yakatabari samples. The hornblende diorite samples from Yakatabari fall into two cateogories: the more altered samples from site 01 (01A-B), which have moderate to steep up NRM directions in the NW quadrant, and the remainder of the samples from sites 01 and 02, which have NW shallow up NRM directions. AF and thermal demagnetisation of specimens from samples 01A and 01B show that the NRMs are essentially monocomponent, demagnetising steadily towards the origin, with no change in direction. These magnetisations have moderate coercivities, predominantly in the range 50-150 Oe (5-15 mT, SI), and mostly unblock between 550°C and 570°C, i.e. just below the Curie point of magnetite. This indicates that the remanence carrier in these somewhat altered rocks is fine-grained, pseudosingle domain, nearly pure magnetite. The direction of the remanence component indicates that the intrusion has been rotated since acquisition of the characteristic remanence.

The other samples carry a more complex remanence, dominated by a NW, shallow up component. A number of specimens respond to AF and thermal cleaning by gradual migration of the remanence direction to the lower hemisphere (e.g. 01C1, 02C2, 02D2, 02E1, 02E2, 02F3, 02G1). In these specimens the remanence appears to be heading towards a steep down direction. The hard component is not fully resolved by thermal demagnetisation, however, largely because of the very square-shouldered thermal demagnetisation curve, whereby the residual remanence unblocks suddenly between 550°C and 570°C. In the case of AF demagnetisation, the residual remanence is overwhelmed by noise at high demagnetising fields, preventing isolation of the hard component. In some specimens, e.g. 01D1, 01E1, the hard reversed component is absent, and the NRM consists only of the NNW shallow up component that dominates the NRM of this intrusion.

Because the hard component is not resolved, its tectonic significance is unclear. The demagnetisation trends suggest, however, that this reversed component has steep inclination, and therefore reflects tectonic rotation since acquisition. The dominant, softer component has similar inclination to the Late Miocene normal polarity field, but is rotated anticlockwise. This suggests that this component was acquired subsequent to the tilting of the intrusion, but before an anticlockwise rotation about a subvertical axis.

Waruwari

The strongly altered hornblende diorite samples from site 03 in the Waruwari pit are very weakly magnetised. NRM directions are very scattered, suggesting complex multicomponent remanence, which is probably associated with a prolonged alteration. AF and thermal cleaning reveal noisy demagnetisation trends, with little directional consistency between apparent linear segments. Figure 6 shows Zijderveld plots for the site 03 samples. The only characteristic remanence component at this site is a NNE-NW directed component with moderate to steep negative inclination.

This component is present in samples 03A-D and 03G. There is some indication of an underlying hard component of reversed polarity in some specimens, e.g. 03B2, 03E2 and 03F2. The latter specimen carries almost antiparallel normal and reversed components: NNW up and SSE down, with moderate inclinations. Overall acquisition of remanence at site 03 has spanned at least one geomagnetic reversal, and is characterised by reamnence components with highly overlapped blocking temperature spectra, which indicates chemical, rather than purely thermal, overprinting. The scattered remanence directions are attributable to this complex magnetic history and preclude quantitative tectonic interpretation of the palaeomagnetic data from this site. However the presence of anomalously steep remanence components indicates tectonic tilting in the same sense as at the nearby Yakatabari sites, i.e. down to the south.

The variably altered andesite samples from site 04 in the Waruwari pit, however, have retained a more readily interpretable palaeomagnetic record. Figure 7 presents Zijderveld plots for this site. The less altered samples 04A-C exhibit two well-defined components: a NW up softer magnetisation and a harder SW down magnetisation. The response to AF and thermal demagnetisation is similar. The discrete blocking temperature spectra of these components suggests predominantly thermal, rather than chemical, overprinting.

The more altered andesite samples 04D-E exhibit somewhat more complex responses to cleaning. Specimen 04D1 carries almost antiparallel normal and reversed components. After initial removal of a minor normal magnetisation, the latter component is still being removed after 550°C treatment, as the residual remanence intensity *increases*. This implies that a high temperature normal component, probably coaxial with the well-defined reversed component, has been revealed, but not demagnetised by cleaning to 550°C.

Specimen 04E2 also has antiparallel normal and reversed components, which have steep inclinations, plus a high temperature SW down component that resembles the characteristic component of other samples from this site. In addition there is an unresolved high temperature component. The final direction of this component is indeterminate, but the demagnetisation trend suggests that it is of normal polarity.

The palaeomagnetic directions obtained from site 04, which is close to the Roamane Fault Zone, indicate tilting down to the south since acquisition of the steep normal and reversed components, with some rotation about a subvertical axis also occurring between acquisition of components of opposite polarity, given that the declinations of the normal and reversed components are not 180° apart. These rotations may be quite localised, reflecting movements on the adjacent Roamane Fault.

Haul Road Dykes

Andesite and hornblende diorite "dykes" conformable with the enclosing sediments are exposed in the Haul Road, between

Waruwari and Tawisakale, at sites 05 and 06 respectively. At this locality the beds, and the sheet-like intrusions, are dipping at 75° to 190° magnetic. Figure 8 shows Zijderveld plots for samples from sites 05 and 06. Initial thermal demagnetisation to 200°C removes substantial remanence components that have no consistent directions from sample to sample and are interpreted as palaeomagnetic noise carried by magnetic grains with low stability. Thereafter, well-defined linear demagnetisation trends towards the origin are observed, indicating a single component of magnetisation. These characteristic components have very steep inclinations. For the narrow andesite dyke (site 05), the characteristic components have NE-E declinations, whereas for the thicker hornblende diorite intrusive the declinations are SE to SW. There is no indication of underlying harder components in these rocks.

The palaeomagnetic directions from these steeply south-dipping "dykes" are rotated ~70°-80° with respect to the Late Miocene (or younger) geomagnetic field direction, indicating tectonic tilting of ~70°-80° to the south since acquisition of the remanence. This tilt is consistent with the present bedding attitude. Thus tilting of the beds in this area post-dates the palaeomagnetic signature and restoring the beds to the horizontal, by rotating about an approximately E-W axis, rotates the observed palaeomagnetic directions into the Late Miocene palaeofield direction.

Thus the palaeomagnetism of the Haul Road "dykes" confirms that they are sills, intruded into originally flat-lying sediments, and that this locality has subsequently been tilted ~75° to the south.

Tawisakale

Compared to the noisy palaeomagnetic signatures from many of the samples from Yakatabari, Waruwari and the Haul Road, the samples from Tawisakale respond well to palaeomagnetic cleaning. Zijderveld plots for the Tawisakale samples are presented in Fig.9. Two well-defined remanence components are present in all the Tawisakale samples: a low temperature normal component, directed ~N with moderate negative inclination, and a high temperature reversed component, which has a SE steep down direction. Figure 16 shows the directions of well-resolved low and high temperature components. The high temperature component departs substantially from the Late Miocene field direction, whereas the low temperature component is more consistent with palaeofield directions of the last 6 Ma. This indicates that the high temperature component predates tectonic rotation of the intrusion, whilst the low temperature component was acquired later, after most of the tectonic rotation had occurred.

Only the low temperature component is removed during initial thermal demagnetisation up to 300°C-400°C, after which it is completely demagnetised. The remaining high temperature component, which has intensities of several hundred μG, is consistently removed between 400°C and 670°C. The latter temperature represents the Curie point of haematite. Thus the

high temperature component is carried by haematite, as well as by magnetite. Since magnetite is a relatively abundant primary phase in this intrusion, magnetite should record primary thermoremanence, as well as any subsequent thermal overprinting. The portion of early, high temperature, remanence carried by magnetite is therefore interpreted as primary. This implies that haematite was present in this rock type from the time of initial cooling and is therefore either a primary mineral or a product of penecontemporaneous alteration. Tawisakale is the only intrusion encountered in this study for which haematite, as well as magnetite, records a reliable palaeomagnetic signature.

The discrete unblocking temperature spectra of the two remanence components, and the relative age of the components deduced from their directions, suggest that the low temperature component represents a thermal overprint of the primary magnetisation. The relative simplicity of the palaeomagnetic signature reflects the absence of chemical overprinting at this site, which is consistent with the weak alteration of the unmineralised Tawisakale intrusion. The reversed polarity of the inferred primary component at Tawisakale contrasts with the normal polarity of the probable primary component detected in several other intrusions, e.g. Yakatabari, Waruwari, and Roamane (to be discussed).

Mount Kare

Zijderveld plots for the Mount Kare samples are given in Fig.10. After removal of minor paleomagnetic noise components by thermal demagnetisation to 200°C, specimens from site 08 demagnetise steadily towards the origin, defining an essentially monocomponent remanence of reversed polarity, directed SE and shallow down. Substantial unblocking occurs above 550°C and the remanence is totally demagnetised by 570°C. This shows that magnetite is the remanence carrier in these rocks. Because magnetite is only present in trace amounts in these very weakly magnetic rocks, the palaeomagnetic signal is probably carried by rare magnetite grains that have escaped destruction, perhaps protected by enclosure within silicate hosts, during the intense alteration of these rocks. The inclination of the characteristic remanence component from site 08 is consistent with the Late Miocene palaeofield inclination, but the declination departs significantly from the essentially south-directed palaeofield. This indicates ~45° of anticlockwise rotation of site 08 about a subvertical axis since acquisition of the remanence.

The palaeomagnetic signature at site 09 is more complex and less consistent between samples. Sample 09B has an NRM direction that is anomalous with respect to the other samples from this site. Thermal demagnetisation reveals a steep down component, with an unresolved high temperature component. The other samples from site 09 have well grouped directions of reversed polarity, with declination s slightly west of south and moderate positive inclinations. Thermal demagnetisation of specimen 09C1 shows that the remanence becomes slightly steeper and the declination swings to the SW, before disappearing above 550°C. The weak remanence of this specimen is also carried by traces of magnetite. The cleaned

remanence direction implies some clockwise rotation and southward tilting of this site. Thus different tectonic movements have occurred at sites 08 and 09, implying some tectonic disruption of the Mount Kare intrusives.

NE Porgera Complex

The intrusives sampled at sites 10 and 11 appear more mafic than the rocks of the mine area and are relatively fresh. Thermal demagnetisation resolves two remanence components, a low temperature north-directed magnetisation with moderate negative inclination, and an ESE steep down high temperature component (Fig.11). The remanence is demagnetised by 570°C. Overlap of the unblocking temperature spectra of the two components ranges from minimal to moderate. The former case corresponds to demagnetisation trends consisting of two linear segments with a sharp elbow, whereas overlapped spectra are indicated by a curved trend joining the linear segments that define the low and high temperature components.

Figure 17 shows directions of well-resolved low and high temperature components from these intrusives. Both the remanence components diverge from unrotated palaeofield directions. However the departure of the low temperature component from the Late Miocene normal field is less than the discrepancy between the high temperature component and the reversed Late Miocene field. Thus the low temperature component appears to have been acquired later than the high temperature component, after initiation of the tectonic rotation, but before movement had ceased. The low temperature component is interpreted as a thermal overprint, accompanied by some chemical remagnetisation in some samples, of a primary thermoremanence, represented by the high temperature direction. The overprinting occurred during the tilting of the intrusions. Again the sense of rotation is down to the south, rotating originally shallow remanence directions into the presently observed steep orientations.

Roamane Hornblende Diorite

The hornblende diorite samples previously collected from the adit of the Porgera mine have well-grouped, nearly vertical, upward ponting NRMs. AF cleaning shows that this is a simple monocomponent, stable remanence for samples A and C, but the NRM of sample D consists of a vertical up soft component and a harder vertical down component (Fig.12). Sample B also has indications of an unresolved harder component underlying the steep up magnetisation. The vertical axis of magnetisation implies tilting to the south through ~80° since acquisition of the remanence.

The extensive collection of hornblende diorite samples from the Roamane intrusion made in June 1992 has enabled the palaeomagnetism of this intrusion to be well characterised. Nearly all samples carry the steep up characteristic component, which dominates the NRM of this rock type. For a number of samples, detailed thermal demagnetisation resolves a minor high temperature component in these samples (Fig.12). When resolved, this component has reversed polarity and is consistently

directed south, with moderate positive inclination. Overall the palaeomagnetic signatures of the Roamane hornblende diorite samples can be classified into four categories:

(i) essentially monocomponent remanence, corresponding to the ubiquitous vertical up component, that is removed steadily up to 550°C-570°C (e.g. 25/27, 25/28, 26/9, 26/30, 28/1, 28/3, 28/4, 28/18, 31/25),

(ii) NRMs consisting of well-defined "low" ($\lesssim$ 500°C) and high temperature components, or soft and hard components in the case of AF cleaning, (e.g. 25G (AF), 28/5, 31/23, 31/24),

(iii) NRMs consisting of the ubiquitous steep up component, plus a minor, poorly resolved, high temperature or high coercivity component of reversed polarity (e.g. 26/10, 28/6, 28/18, 31/25)

(iv) a few specimens for which the unblocking temperature spectra of the normal and reversed polarity components are completely overlapped, so that a quasilinear segment on the Zijderveld plots that represents a hybrid remanence is seen (e.g. 25G, 28C). However, AF demagnetisation of specimen 25G3 appears to totally remove the soft component, allowing the direction of the hard component to be determined for this sample.

When the Zijderveld plots are closely examined, nearly all the samples in category (i) show evidence of small, unresolved high temperature components, i.e. they could be classified as category (iii). It appears, therefore, that all the hornblende diorite samples carry minor high temperature components, although these cannot always be properly resolved. The remanence directions after successive high temperature steps generally trend along a great circle path towards the direction of the high temperature component, even though a stable end point is not necessarily reached before the residual palaeomagnetic signal is swamped by noise. Directions of well-resolved components, as determined by PCA, are plotted in Fig.18.

The ubiquitous vertical up component that dominates the NRM of the Roamane hornblende diorite implies substantial tilting of this intrusion, ~80° down to the south, since acquisition of this component. The minor reversed, high temperature component has lower inclination (~60°) and is consistent with acquisition at an intermediate stage of the tectonic tilting. On average, the high temperature component appears to have been acquired after approximately 30° of tilting had already occurred. Both the high and "low" temperature components are carried by magnetite *sensu lato*, but the high temperature component is associated with minor amounts of very fine-grained magnetite, in the single domain (i.e. submicron) size range, as evidenced by its very high stability to AF demagnetisation. As the high temperature component is younger than the dominant "low" temperature component, this suggests that small amounts of ultrafine secondary magnetite were produced during alteration and acquired a very stable chemical remanence with high unblocking temperatures.

Augite Hornblende Diorite (Roamane/Rambari)

Whereas the remanence of the hornblende diorite samples from underground is dominated by the vertical up component, with a very minor reversed component that is often difficult to resolve, the augite hornblende diorite carries well-defined normal and reversed components that are often of comparable magnitude (Fig.13). The directions of the "low" and high temperature components appear to be identical to those of the corresponding components carried by the hornblende diorite, but the high temperature component is much more prominent for the augite hornblende diorite.

The low temperature component alone is steadily removed during thermal demagnetisation up to 400°C-500°C, or by AF demagnetisation to 100-150 Oe (10-15 mT). Thereafter a reversed component, directed SSE with moderate to steep positive inclination, is defined by linear demagnetisation trends directly towards the origin. The reversed high temperature component is stable up to ~570°C and to > 1000 Oe (100 mT) AF. These properties indicate that the reversed component is carried by very fine-grained magnetite in the PSD and SD size ranges (i.e. from ~20μm to submicron).

The "low" temperature, softer component is carried by MD magnetite *sensu lato*. The unblocking temperatures of the two components may reflect compositional differences, whereby the less stable component is carried by titaniferous magnetite, which has a lower Curie point than pure magnetite, and the high temperature component is carried by stoichiometric magnetite.
Directions of well-resolved components from the augite hornblende diorite, as determined by PCA, are plotted in Fig.19. The "low" temperature component has very steep inclination (~80°), whereas the high temperature component has a distribution of directions that suggests some vertical streaking, or slight bimodality, of inclinations. The inclinations range from +40° to +70°, suggesting that the reversed components were acquired at slightly different stages of the tectonic tilting. The normal component is interpreted as primary thermoremanence, carried by titanomagnetite, that has been rotated into the vertical by southward tilting. The reversed component is a secondary magnetisation, carried by fine-grained magnetite, acquired at an intermediate stage of tilting. This interpretation implies that the PSD/SD magnetite is associated with alteration, probably produced by breakdown of mafic silicates. The fresh augite hornblende diorite sample from Waruwari, W13,

Andesite and Altered Andesite

Figure 14 shows Zijderveld plots for fresh and altered andesite samples from the Porgera mine. Thermal demagnetisation of a specimen from sample 25E consistently removes a NNE shallow up component up to 580°C. However the demagnetisation trend just bypasses the origin, revealing a residual minor component of reversed polarity, which cannot be fully resolved. The other relatively unaltered andesite sample has a very steep up magnetisation, analogous to that of the hornblende diorite.

The unblocking temperatures and the high coercivity indicate that the weak high temperature remanence of the altered andesite samples is carried by traces of SD magnetite. Some samples (e.g. 25C, 28/6) have somewhat higher NRM intensity associated with a steep low temperature component of normal polarity, as well as the characteristic reversed high temperature component. Most of the other samples show at least a hint of this normal component. Interpretation of the thermal demagnetisation data from the altered andesite samples is complicated by the production of new magnetic minerals at high temperatures, as indicated by a substantial increase in magnetisation. Magnetic noise picked up by this new magnetic material tends to swamp the residual palaeomagnetic signal in these samples. However, the data for the andesite and altered andesite samples are consistent with the presence of remanence components similar to those found in other intrusives, albeit with much weaker intensities and in differing proportions. The minor steep up component in some of the altered samples may represent a residual primary remanence carried by very small amounts of (titano)magnetite that have survived destruction during the alteration. The strong remanence of the weakly altered sample 26/16 is dominated by this primary component, wheras the other weakly altered sample has an apparently younger, because shallower, dominant component. The reversed high temperature component that is present in most of the samples appears to have a range of inclinations ranging from shallow down to steep down, suggesting a range of ages for this component with respect to tilting. The reversed component in some cases appears to have been acquired early in the tilting history, and in other cases after all or most of the tilting had been completed.

Other Rock Types

Figure 15 shows Zijderveld plots for samples of altered host sediments and sulphide mineralisation. The near-ubiquitous south down reversed component is present in these samples, although not always well-resolved. By analogy with the other rock types, is interpeted as an alteration component acquired during the tectonic tilting event. In some samples a normal low temperature component is also present. Overall, these samples are not very good palaeomagnetic recorders and detailed interpreatation of their palaeomagnetism is not justified.

Discussion

Several of the intrusions carry clear-cut palaeomagnetic signatures that are readily intepretable in terms of thermal and/or chemical overprinting of primary thermoremanence. Because the palaeofield axis is well constrained for this young intrusive complex, the tectonic rotations, and relative timing of the various remanence components, can be determined from the well-defined palaeomagnetic directions obtained from these intrusions. Some other bodies or rock types, particularly those affected strongly by alteration, have more complex paleomagnetic signatures, reflecting multiple remanence components with overlapped stability spectra. However, the insights gained from

the sites that are well behaved palaeomagnetically greatly aids interpretation of the more complicated demagnetisation data from the samples for which remanence components are not well resolved.

The well-resolved palaeomagnetic components isolated from each intrusion are summarised below, together with the interpretion of each component as primary thermoremanence, secondary thermal overprint, or secondary thermochemical overprint associated with alteration. Here, LT and HT refer to lower and higher temperature components respectively; P = primary thermo-remanence, ST = secondary thermal overprint, SC = secondary chemical overprint; (N) = normal polarity, (R) = reversed polarity.

INTRUSION	**LT COMPONENT** (dec,inc;α_{95})	**HT COMPONENT** (dec,inc;α_{95})	**Nature of Remanence**
Roamane Hb diorite	(001,-83;4)	(163,+54;20)	Primary (N) SC (R)
Aug Hb dio (Roamane/Rambari)	(356,-77;5)	(158,+56;6)	Primary (N) SC (R)
Tawisakale	(357,-41;7)	(125,+67;3)	Primary (R) ST (N)
NE Porgera Complex	(022,-46;8)	(109,+56;8)	Primary (R) ST/SC (N)
Haul Rd Dykes	~(23,-83)		Primary (N)
Waruwari (andesite)	~(299,-45)	~(211,+48)	SC (N) Primary? (R)
Waruwari (Hb diorite)	(345,-49;27)	?	SC? (N) SC? (R)
Yakatabari	(316,-15;18)	?	SC (N) Primary? (R)

The inferred tectonic motions since acquisition of each component are:

INTRUSION	PRIMARY COMPONENT		SECONDARY COMPONENT	
	Tilt	Rotation	Tilt	Rotation
Roamane Hb diorite	57°S±4°	-2°±29°	27°S±20°	-20°±34°
Aug Hb dio (Roamane/Rambari)	51°S±5°	-7°±23°	30°S±6°	-25°±10°
Tawisakale	41°S±3°	-58°±7°	15°S±7°	-6°±10°
NE Porgera Complex	30°S±8°	-74°±15°	20°S±8°	+19°±11°
Haul Rd Dykes	~60°S	?	-	-
Waruwari (andesite)	~20°S	?	~20°S	?
Waruwari (Hb diorite)	-	-	23°S±27°	?
Yakatabari	?	?	11°N±18°	-47°±19°

It should be noted that the path of a finite rotation cannot be inferred uniquely from initial and rotated orientations of directional markers, such as remanence vectors. However, where a sequence of progressively rotated vectors is found, the sequence of rotations can be satisfactorily deduced. The principle of parsimony can also be invoked, implying that the simplest motion consistent with the initial and final orientations, and any other data, should be preferred. The observed rotations of palaeomagnetic directions have been resolved into tilting about an approximately E-W axis, which mainly affects the inclination, and rotation about a vertical axis (defined positive clockwise), which affects the declination. This approach is justified by the ubiquity and progressive nature of southward tilting as the major detected rotation. Subsequent minor rotations about a steeply plunging axis are practically undetectable for primary remanence directions that have been rotated into subvertical orientations. On the other hand, change in declination is readily detectable for secondary magnetisations, acquired after most of the tilting, which have shallow to moderate inclinations.

In the underground mine, fresh hornblende diorite samples retain strong primary remanence, only lightly overprinted by alteration. Augite hornblende diorite samples, on the other hand, are more strongly overprinted and generally retain well-defined primary and secondary magnetisations. The samples from Tawisakale and the NE Porgera Complex also show distinct primary and secondary remanence components. Palaeomagnetic data from the other localities are less clear-cut, reflecting overlapped stability spectra associated with chemical overprinting, but are nevertheless interpretable, particularly when the behaviour of samples from the well-behaved rock types is available for comparison.

The consistent indications of tilting down to the south of the intrusions suggest that the whole of the exposed portion of the Porgera Complex has been tilted in response to thin-skinned tectonics in the Late Miocene, rotating shallow palaeomagnetic directions into steep orientations. Anticlockwise deflection of declinations, typically through about 45°(±20°), are also indicated for all intrusions, suggesting that the whole complex has undergone anticlockwise rotation. Variations from the average deflection of declination may reflect differential local rotations due to movements on nearby faults, or may represent variations in the timing of secondary remanence acquisition with respect to the general anticlockwise rotation. The latter interpretation would indicate that the anticlockwise rotation was taking place during the alteration episode. The fact that individual samples from Tawisakale and the NE Porgera Complex show anticlockwise rotation of the primary component, but not of the thermal overprint component, suggests that the anticlockwise rotation was completed relatively soon after emplacement, before magmatic and hydrothermal activity in the Complex had ceased. Rotation of the primary magnetisation about a steeply plunging axis cannot be resolved for the Roamane intrusives, because the direction is almost vertical.

Similarly, the lesser tilting indicated for secondary, alteration-related, magnetisations implies that the major tectonic rotations had been partially completed before the alteration. This tightly constrains the initiation of tilting to the period between emplacement and alteration, i.e. ~5-6 Ma. However, in some cases further tilting, in the same sense, continued after the rocks were altered, as the secondary magnetisations are also steeper than the palaeofield. Secondary magnetisations recorded by augite hornblende diorite samples from Roamane/Rambari, for example, indicate variable degrees of tilting, ranging from very little to substantial. This indicates that the alteration event(s) were penecontemporaneous with the final stages of tectonic tilting. Lum *et al* (1992) have recognised that rapid rotation of shallow level intrusive bodies associated with porphyry and epithermal mineralisation in the SW Pacific is commonplace. These authors stress the extreme mobility of fault blocks in this region, with rotations about horizontal and vertical axes, substantial vertical movements and lateral translations. Deposits are often tilted 20-30° and sometimes more, with rotations of 25° in 100,000 years not unusual. These rotations often accompany uplift, with typical

elevation rates of 2 km in a million years. Thus the inferred tectonic history at Porgera is not unusual for this tectonic environment.

Inferred primary magnetisations of different intrusions may have either polarity, indicating slight differences in age of emplacement. Nedachi *et al* (1984, 1985) have applied magneto-stratigraphy to unravelling the relative ages of 3-5 Ma intrusives at Panguna. The rarity of cross-cutting relationships at Porgera suggests that magnetostratigraphy may have application to resolving slight age differences between the Porgera intrusives. K-Ar dating probably cannot date the intrusives sufficiently precisely to determine the intrusive sequence, particularly given problems with excess argon in these rocks (Richards and McDougall, 1990). Based on the geochronological constraints, the geomagnetic polarity time scale (Cande and Kent, 1992) and the relative degree of interpreted tectonic rotation of palaeomagnetic directions, the following sequence of events at Porgera can be tentatively inferred:

1. Emplacement of Rambari augite hornblende diorite and Roamane hornblende diorite in either of the normal polarity intervals (a) 6.3-6.0 Ma or (b) 5.9-5.7 Ma. The Waruwari hornblende diorite intrusion may also have similar age because, although no primary remanence appears to have survived the alteration, the alteration signature of this intrusion appears to be quite early. The Haul Road dykes also appear to be early.

2. Commencement of southward tilting, through about 10° before emplacement of the the Tawisakale hornblende diorite porphry and through about 30° before intrusion of the NE Porgera Complex gabbro. These intrusions were emplaced during a reversed polarity interval(s), either 6.0-5.9 Ma or, more probably, 5.7-5.0 Ma. The Waruwari andesite and the Yakatabari intrusion may also have been intruded at this time. Alteration of the Waruwari hornblende diorite was probably initiated around 5.8 Ma (normal polarity), continuing into this reversed polarity period. The earlier brief reversed polarity chron is a possibility only if the earliest intrusives are older than 6.0 Ma, i.e. case 1(a) above.

3. Continuing southward tilting, and initiation of anticlockwise rotation, during the episode of pervasive propylitic alteration that is recorded by secondary chemical remanence in the augite hornblende diorites and hornblenede diorites from the underground mine and Waruwari. This occurred during the reversed polarity chron from 5.7-5.0 Ma.

4. After most of the tectonic rotations were complete, thermal or thermochemical overprinting of the Tawisakale and NE Porgera Complex intrusions occurred during a normal polarity chron, probably soon after 5.0 Ma. At Yakatabari, the alteration overprint appears to have occurred before most of the anticlockwise rotation. It is possible, however, that the anomalous declination of the overprint component at Yakatabari reflects later local movements on the Roamane Fault.

5. MAGNETIC FABRIC OF THE INTRUSIVE COMPLEX

The susceptibility anisotropy of the samples was found to be very weak and the effects of anisotropy on magnetic anomalies associated with the Porgera Complex is therefore negligible. Anisotropies range from less than 1% (i.e. A < 1.01) to a few percent, at most. However, the weak magnetic fabric defined by the susceptibility ellipsoids reflects slight preferred dimensional orientation of magnetite grains in the rocks and therefore provides an indication of petrofabric. Magnetic fabric of intrusives generally reflects magmatic flow and subsequent deformation, and may therefore provide useful structural information.

The susceptibility ellipsoids of the samples collected in June 1993 are given in Tables 5 and 6. Principal susceptibility axes for sites 01-11 are plotted in Fig.20, those from Mount Kare in Fig.21, those for hornblende diorite samples from underground in Fig.22, and for augite hornblende diorite underground samples in Fig.23. Major susceptibility axes represent magnetic lineations, whereas minor axes represent poles (normals) to the magnetic foliation. The magnetic foliation plane contains the major and intermediate axes.

Each of the Yakatabari sites (01 and 02) shows a distictly orthorhombic magnetic fabric, with well-grouped magnetic lineations lying within a well-defined foliation plane. At site 01 the lineations plunge SSE within a SW-dipping foliation, whereas at site 02 the foliation dips WSW and contains a SSE-plunging lineation. The fabrics at the two sites are very similar in character, but the fabric at site 02, in the marginal phase, is rotated clockwise with respect to the site 01 fabric, perhaps reflecting shearing due to movements on the nearby Roamane Fault.

At Waruwari, both the altered hornblende diorite and the variably altered andesite have predominantly linear fabrics, with rotational symmetry about a steeply plunging lineation. On the other hand, the Haul Road dykes show no clear magnetic fabric, with scattering and intermingling of all three principal susceptibility axes.

The Tawisakale intrusion has a magnetic fabric with orthorhombic symmetry. The foliation is ~NW-SE vertical with a subhorizontal NW-SE lineation. The NE Porgera Complex at site 10 has a poorly defined foliation with moderate dip to the SW and a hint of a south-plunging lineation, whereas at site 11 the foliation is absent and the magnetic fabric is essentially a pure steeply-plunging lineation.

At Mount Kare, site 08 has no distinct magnetic fabric, but site 09 has a subvertical E-W foliation containing a lineation with shallow plunge to the east (Fig.22). The differences may reflect the differing tectonic movements inferred for these two sites from the palaeomagnetism.

In the underground mine, both the hornblende diorite and augite hornblende diorite intrusions have essentially uniaxial prolate magnetic fabrics, with a subvertical lineation (Figs.22-23).

Overall there is no very clear pattern to the magnetic fabric data, except for a preponderance of lineation-dominant fabrics, several with steeply plunging magnetic lineations. Given the tectonic complications within the Complex, and the fact that several geological variables, including magma flow and deformation, can influence such weakly developed magnetic fabrics, it is not surprising that the interpretation of the data is not straightforward. The widespread occurrence of subvertical lineations, however, suggests that the magnetic fabrics may reflect a vertical stress field imposed on the intrusions after the main tectonic rotations had occurred. This stress field is presumably associated with the continuing rapid uplift of the Porgera Complex. Deviations from this general pattern may reflect local structural conditions and could conceivably have application to structural interpretation in the mine area. However, the present data indicate that only a more sophisticated approach, which integrates magnetic fabric measurements with other structural data, is likely to be useful in this context.

6. CONCLUSIONS

Magnetic Petrophysics

This study has established representative magnetic properties for major rock types in the Porgera Intrusive Complex. Given the known geometry of the shallow intrusions, this information should enable definitive modelling of the magnetic effects of shallow sources at Porgera. Subtraction of the calculated fields arising from known intrusions will reveal the magnetic signature of the deeper sources, including the inferred large body at depth, which probably represents the magma chamber from which the exposed intrusives are derived. Exploration for additional Porgera-style mineralisation at depth, and for possible porphry copper mineralisation beneath the exposed complex, needs to be guided by detailed magnetic modelling of the deeper zones of the Porgera Intrusive Complex. The major results of the magnetic petrophysical study are summarised below:

(i) Relatively unaltered intrusive rocks of the Porgera Igneous Complex are moderately to strongly magnetic, whereas strongly altered intrusives, mineralised zones and country rocks are very weakly magnetic. Thus local magnetic anomalies at Porgera that are attributable to shallow sources arise from weakly altered intrusions. Alteration zones within intrusions may be detectable by high resolution magnetic surveys.

(ii) Except for the small hornblende diorite intrusion at Yakatabari, Koenigsberger ratios are substantially less than unity, indicating that induced magnetisation is predominantly responsible for the anomalies associated with most of the Porgera Igneous Complex.

(iii) There is evidence that hornblende diorite and hornblende diorite porphyry tend to be the most magnetic rock types in the complex, although all fresh intrusives sampled, from very mafic to intermediate compositions, have fairly high susceptibilities. The susceptibilities generally correspond to equivalent magnetite contents of 1-2 vol%. This reflects the ubiquitous presence of magnetite-rich spinel in the groundmass, as well as secondary magnetite produced by high-temperature breakdown of mafic silicates under oxidising conditions. In addition, hornblende diorite and hornblende diorite porphyry contain relatively abundant titanomagnetite microphenocrysts that increase the susceptibility of these evolved rock types. Feldspar porphyries are not represented in this collection. Titanomagnetite microphenocrysts occur in feldspar porphyries, but are rare, suggesting that these rocks should have lower susceptibility than hornblende diorites. However, the high normative magnetite of feldspar porphyries, comparable to that of other intrusive types at Porgera, suggest that feldspar porphyries contain groundmass magnetite and have moderate to strong susceptibilities.

(iv) The average susceptibilities and Koenigsberger ratios of the well-sampled intrusives are given below:

	Susceptibility (μG/Oe)	Q
Roamane Hb Diorite	5530	0.45
Augite Hb Diorite (Rambari/Roamane)	2140	0.07
Yakatabari Hb Diorite	2790	6.8
Waruwari Altered Hornblende Diorite	180	0.34
Haul Rd Andesite Dyke	4370	0.14
Haul Rd Hb Diorite Dyke	6420	0.11
Tawisakale Hornblende Diorite Porphyry	4840	0.16
NE Porgera Complex Gabbro	3000	0.10

(v) Although the Koenigsberger ratio of the Roamane hornblende diorite intrusion is less than one, it is still significantly larger than the Q value of the augite hornblende diorite, the NE Porgera Complex gabbro and the Tawisakale intrusion. This reflects the dominance of the steep up primary component of remanence in the Roamane hornblende diorite, with only minor alteration-related overprinting. In the other intrusions, however, there is substantial overprinting of the primary remanence by a secondary component of opposite polarity. Partial cancellation of opposing remanence components results in a lower NRM intensity for these intrusions. Remanent magnetisation needs

to be incorporated into models of the Yakatabari intrusion and, to a lesser extent, the Roamane hornblende diorite.

(vi) Altered ?intrusives from exposed mineralised zones at Mount Kare are very weakly magnetic. However drill core samples of fresh intrusives at depth are strongly magnetic.

(vii) Although a well-defined magnetic fabric is detectable for many localities, the susceptibility anisotropy is very weak and the effects of anisotropy on magnetic anomalies is negligible.

Palaeomagnetism and Tectonics

The low latitude of Porgera implies a shallow geomagnetic field. The 5-6 Ma palaeomagnetic pole for the Australian Plate lies at 80°S, 120°E. The corresponding dipole field direction is dec = 3°, inc = -26° (for normal polarity), or dec = 183°, inc = +26° (for reversed polarity). Thus palaeomagnetic directions recorded at Porgera should lie close to the present geomagnetic field (for normal polarity remanence) or to its antipodal direction (in the case of reversed polarity remanence), unless there has been tectonic disturbance of the rocks since acquisition of the remanence. The geomagnetic field had normal polarity from 6.3 Ma to 6.0 Ma, reversed polarity in the interval 6.0-5.9 Ma, normal polarity again from 5.9 Ma to 5.7 Ma, followed by reversed polarity until 5.0 Ma, with several subsequent reversals between 5.0 Ma and 4.0 Ma. Because the palaeofield axis is well constrained for this young intrusive complex, the tectonic rotations, and relative timing of the various remanence components, can be determined from the well-defined palaeomagnetic directions obtained from these intrusions.

NRM directions from many of the Porgera intrusives are scattered, suggesting a complex magnetic/tectonic history, rather than a simple thermoremanent magnetisation that records initial cooling of the intrusives. AF and thermal demagnetisation reveals the presence of multicomponent magnetisations and, in many cases, allows the remanence components to be resolved. Only fully resolved remanence components represent magnetically recorded palaeofield directions.

The main findings of the palaeomagnetic study are summarised below:

(i) Primary thermoremanent magnetisation is retained by most of the intrusives, unless they are highly altered. The primary magnetisation is carried by multidomain (titano)magnetite. In addition the remanence carried by the intrusives is weakly to heavily overprinted. The secondary component in relatively fresh intrusives in the mine area is probably associated with the weak, but pervasive, propylitic alteration and is carried by very fine-grained stoichiometric magnetite. This secondary magnetite is in the pseudosingle domain to single domain size range (several microns to submicron). Overprinting in the Tawisakale and NE Porgera Complex intrusions may be predominantly thermal, rather than chemical.

(ii) Primary remanence directions have been rotated and are now steep up, in the case of normal polarity, or steep down, for reversed polarity. Thus a systematic tilt of the Porgera Igneous Complex since emplacement has been confirmed. The total degree of tilting has been 50°-60°, down to the south. Originally flat-lying sills are now dipping steeply to the south, and originally vertical stocks have shallow plunge to the north, unless disrupted by faults.

(iii) In addition, there has been a systematic anticlockwise rotation of the Porgera Intrusive Complex, through about 45° on average, as indicated by rotation of originally northward declinations towards the NW (normal polarity) or southward declinations towards the SE (reversed polarity). This rotation is more obvious for secondary magnetisations, which have shallower inclinations, than for primary directions, which are often so steep that rotations about a vertical axis are undetectable. Variations in the degree of rotation (±20°) since emplacement may indicate small local rotations in response to movements on nearby faults.

(iv) Progressive tilting and anticlockwise rotation are tracked by secondary magnetisations acquired at various stages of the rotations. Thus the tectonic rotations are penecontemporaneous with the alteration, and therefore occurred relatively soon after emplacement, probably within 1 Ma. Although most of the tectonic movements were completed by the time of the latest remanence components, some rotations in the same sense continued after acquisition of secondary remanence.

(v) The tectonic rotations are evidently in response to thin-skinned tectonic processes and accompany the rapid uplift of the Complex. There is evidence that rapid tectonic rotations of epithermal and porphyry-type deposits in similar tectonic settings is commonplace. Palaeomagnetism is a powerful tool for detecting such rotations and could be particularly useful for elucidating the structural history of young deposits in tectonically active areas. The present study affords an example of the utility of the method for detecting hitherto unsuspected structural complications.

(vi) The preferred interpretation of the magnetic and tectonic history of the Porgera Igneous Complex is summarised below:

1. Early emplacement of Rambari augite hornblende diorite and Roamane hornblende diorite, most probably during the normal polarity interval 5.9-5.7 Ma. The Waruwari hornblende diorite intrusion may also have similar age because, although no primary remanence appears to have survived the alteration, the alteration signature of this intrusion appears to be quite early.

2. Commencement of southward tilting, through about 10° before emplacement of the the Tawisakale hornblende diorite porphry and through about 30° before intrusion of the NE Porgera Complex gabbro. These intrusions were emplaced during a reversed polarity interval, probably 5.7-5.0 Ma. The Waruwari andesite and the

Yakatabari intrusion may also have been intruded at this time. Alteration of the Waruwari hornblende diorite was probably initiated around 5.8 Ma (normal polarity), continuing into this reversed polarity period.

3. Continuing southward tilting, and initiation of anticlockwise rotation, during the episode of pervasive propylitic alteration that is recorded by secondary chemical remanence in the augite hornblende diorites and hornblenede diorites from the underground mine and Waruwari. This occurred during the reversed polarity chron from 5.7-5.0 Ma.

4. After most of the tectonic rotations were complete, thermal or thermochemical overprinting of the Tawisakale and NE Porgera Complex intrusions occurred during a normal polarity chron, probably soon after 5.0 Ma. At Yakatabari, the alteration overprint appears to have occurred before most of the anticlockwise rotation. It is possible, however, that the anomalous declination of the overprint component at Yakatabari reflects later local movements on the Roamane Fault.

(vii) The limited palaeomagnetic data from altered rocks at Mount Kare indicate differential tectonic rotations at the two sites, suggesting that this deposit has been disrupted by tectonic movements.

7. RECOMMENDATIONS

Several recommendations concerning additional work are made:

(i) A number of intrusions are undersampled and there is scope for further work on drill core samples, in particular, as these become available during the current drilling programme. This would allow refinement of the magnetic models and would also provide information on tectonic rotations that may aid structural interpretation.

(ii) This study has illustrated the utility of the palaeomagnetic method for unravelling complex tectonic histories of young intrusive complexes. The possibility of applying palaeomagnetism to other porphyry-style or epithermal deposits should be investigated.

(iii) This study provides a foundation for a detailed study of the magnetic petrology of the Porgera intrusives. The aim would be to characterise the magmatic and hydrothermal processes that create, alter and destroy magnetic minerals in these rocks, as an aid to geological interpetation of magnetic surveys in the Porgera region and in analogous terrains. The present sample collection, supplemented if necessary to fill any gaps, could provide the material for detailed rock magnetic experiments, petrography, chemical analysis and electron microprobe analysis of opaque phases. These techniques would be used to determine the magnetic mineral abundance, composition, domain state and grainsize, and relate these to the rock composition, primary mineralogy and alteration. By integrating rock magnetic

techniques and petrological studies, a much better understanding of the relationships between magnetic properties and geological factors, including igneous rock composition, magmatic conditions and hydrothermal processes, will be gained. Because mineralisation is also controlled by these factors, the association between mineralisation and magnetic anomaly patterns should become clearer as a result of magnetic petrological studies.

8. REFERENCES

Cande, S.C. and Kent, D.V., 1992. A new geomagnetic polarity time scale for the Late Cretaceous and Cenozoic. J. Geophys. Res., 97, 13,917-13,951.

Fleming, A.W., Handley, G.A., Williams, K.L., Hills, A.L. and Corbett, G.J., 1986. The Porgera gold deposit, Papaua New Guinea. Econ. Geol., 81, 660-680.

Handley, G.A. and Henry, D.D., 1990. Porgera gold deposit, *in* F.E. Hughes (Ed.), Geology of the Mineral Deposits of Australia and Papua New Guinea, Aus. IMM, Melborne, 1717-1724.

Hollister, V.F., 1975. An appraisal of the nature and source of porphyry copper deposits. Minerals Sc. Engng, 7, 225-233.

Idnurm, M., 1985. Late Mesozoic and Cenozoic plaeomagnetism of Australia - I. A redetermined apparent polar wander path. Geophys. J. R. astron. Soc., 83, 399-418.

Kirschvink, J., 1980. The least-squares line and plane and the analysis of palaeomagnetic data. Geophys. J. R. astron. Soc., 62, 699-718.

Lum, J.A., Clark, A.L. and Coleman, P.J., 1992. Gold Potential of the Southwest Pacific. East-West Center, Honolulu.

Nedachi, M., Enjoji, M., Urashima, Y. and Manser, W., 1984. Preliminary study on the rock magnetism of the intrusives from the Panguna ore deposit, Bouganville, Papua New Guinea. Kagoshima University Research Center for the South Pacific, Report 6, Subject I. Prompt Report of 3rd Scientific Survey of South Pacific.

Nedachi, M., Enjoji, M., Urashima, Y. and Manser, W., 1985. On the paleomagnetism of the intrusives from the Panguna porphyry copper deposit, Bouganville, Papua New Guinea. Kagoshima University Research Center for the South Pacific, Occasional Papers, 5, 13-26.

Richards, J.P., 1990. Petrology and geochemistry of alkalic intrusives at the Porgera gold deposit, Papua New Guinea. J. Geochem. Explor., 35, 141-190.

Richards, J.P., 1992. Magmatic-epithermal transitions in alkalic systems: Porgera gold deposit, Papua New Guinea. Geology, 20, 547-550.

Richards, J.P., Chappell, B.W. and McCulloch, M.T., 1990. Intraplate-type magmatism in a continent-island arc collision zone: Porgera intrusive complex, Papaua New Guinea. Geology, 18, 958-961.

Richards, J.P. and McDougall, I., 1990. Geochronology of the Porgera gold deposit, Papua New Guinea: resolving the effects of excess argon on K-Ar and $^{40}Ar/^{39}Ar$ age estimates for magmatism and mineralization. Geochim. Cosmochim. Acta, 54, 1397-1415.

Richards, J.P., McCulloch, M.T., Chappell, B.W. and Kerrich, R., 1991. Sources of metals in the Porgera gold deposit, Papua New Guinea: evidence from alteration, isotope, and noble metal geochemistry. Geochim. Cosmochim. Acta, 55, 565-580.

Sillitoe, R.H., 1979. Some thoughts on gold-rich porphyry copper deposits. Mineral. Deposita, 14, 161-174.

Sillitoe, R.H., 1988. Gold deposits in western Pacific island arcs: the magmatic connection, *in* Keays, R.R. *et al* (Eds), The Geology of Gold Deposits: the Perspective in 1988. Econ. Geol. Monograph 6, 274-291.

Solomon, M., 1990. Subduction, arc reversal, and the origin of porphyry copper-gold deposits in island arcs. Geology, 18, 630-633.

Ware, G.H., 1979. In-situ induced-polarization and magnetic susceptibility measurements - Yerington mine. Geophysics, 44, 1417-1428.

TABLE 1. LIST OF SURFACE SAMPLES

Site	N	Locality	Lithology		Comments
			FIELD NAME	GEOCHEMICAL CLASSIFICATION	
01	5	Yakatabari	Hb Diorite	Mugearite	Slightly altered, degree of alteration decreasing from 01A to 01E.
02	7	Yakatabari	Hb Diorite	Mugearite	Similar to site 01, but finer grained.
03	7	Waruwari	Hb Diorite	Mugearite?	All samples altered, 03E is very altered, 03G is least altered.
04	5	Saddle (RFZ) in pit	Andesite	Hawaiite?	Altered fine grained intermediate phase.
05	6	Beside Waruwari Haul Road	Andesite	Hawaiite?	4 m thick conformable dyke/ sill intruding black seds. 05A is chilled margin.
06	8	" "	Hb diorite	Hawaiite?	Thick, apparently conformable intrusive (sill?), similar to site 05, but coarser grained. 06E,H chilled margin; 06F is altered margin; 06G is baked contact.
07	5	Tawisakale	Hb diorite porphyry	Mugearite	Unmineralised intrusion.

Site	N	Locality	Lithology		Comments
			FIELD NAME	GEOCHEMICAL CLASSIFICATION	
08	4	Mt Kare	?andesite		Highly altered, mineralised intrusives in pit.
09	5	Mt Kare	?diorite		Highly altered, mineralised intrusives in tunnel.
10	4	NE Porgera Complex (Kogai Diorite?)	aug. Hb diorite	Alkali gabbro	Fresh, mafic gabbro from outside mineralised zone.
11	6	NE Porgera Complex (Sluice Diorite?)	aug. Hb diorite	Alkali gabbro	Fresh, mafic gabbro from outside mineralised zone.

Sample	Rock type	Location
Peruk A	Andesite	Float from E flank of Peruk
Peruk B	Altered andesite	"
C1	Fresh intrusive, baked in fire	Drill core from holes into Mt Kare intrusion
C2	"	"
MK11	"	"

PREVIOUSLY SUBMITTED SAMPLES

Site	Locality (Porgera Grid)	Lithology		Comments
		FIELD NAME	GEOCHEMICAL	
PG1	Tawisakale (72050E,45000N)	Hb dior. porph.	Mugearite	Measured at Sydney University 2400 m ASL
PG2	Out of Rudi's tunnel (72140E,45160N)	Andesite	Hawaiite?	2650 m ASL
PG3	Little Waruwari (71040E,45670N)	Hb diorite	Mugearite?	Altered 2650 m ASL
PG4	Yakatabari (71500,45500N)	Hb diorite	Mugearite	2700 m ASL
PG5	Rambari (71440E,45820N)	Andesite	Hawaiite?	Altered 2750 m ASL
PG6	Rambari (71420E,45860N)	Hb diorite	Hawaiite?	Altered 2750 M ASL
PG7	Roamane (71800E,45920N)	Hb diorite	Hawaiite?	Altered and weathered 2650 m ASL
PG8	Peruk (72290E,46210N)	Andesite	Hawaiite?	2600 m ASL
PG9	Btwn Roamane/Rambari (72000E,46060N)	Andesite	Hawaiite?	2600 m ASL

TABLE 2. LIST OF UNDERGROUND AND SURFACE MINE SAMPLES

Sample	Rock type		Mine Grid Location	
	FIELD NAME	GEOCHEMICAL CLASSIFICATION		
28 LEVEL				
28A	Aug Hb diorite	Alkali gabbro?	Adit drive, ~200m in; 50m E of bend	
28B	Altered sediment		Adit drive, ~200m past bend	
28C	Hb diorite	Hawaiite?	Fresh air drive (escape route)	
28/1	Hb diorite	Hawaiite?	11375N	22270E
28/2	Hb diorite	Hawaiite?	11375N	22260E
28/3	Hb diorite	Hawaiite?	11375N	22180E
28/4	Hb diorite	Hawaiite?	11375N	22195E
28/5	Hb diorite	Hawaiite?	11375N	22240E
28/6	Alt. andesite	Alkali basalt?	11270N	22165E
28/7	Alt. andesite	Alkali basalt?	11265N	22180E
28/16	Andesite	Alkali basalt?	11355N	22400E
28/17	Alt. andesite	Alkali basalt?	11360N	22400E
28/18	Hb diorite	Hawaiite?	11375N	22400E
28/19	Sulphides			
Previously submitted samples			(Porgera Grid)	
PG A	Hb diorite	Hawaiite?	Adit 1275m in (71570E,45600N)	
PG B	Hb diorite	Hawaiite?	Adit 1033m in (71800E,45685N)	
PG C	Hb diorite	Hawaiite?	Adit 1432m in (71420E,45550N)	
PG D	Hb diorite	Hawaiite?	Adit 275m in	

Sample	Rock type		Mine Grid Location
	FIELD NAME	GEOCHEMICAL CLASSIFICATION	
26 LEVEL			
26/9	Hb diorite	Hawaiite?	Decline 26L to 25L
26/10	Hb diorite	Hawaiite?	Decline 26L to 25L
26/11	Aug Hb diorite	Alkali gabbro?	Decline 26L to 25L
26/12	Aug Hb diorite	Alkali gabbro?	Decline 26L to 25L
26/20	Aug Hb diorite	Alkali gabbro?	11445N 22445E (incline 28L to 31L)
26/21	Aug Hb diorite	Alkali gabbro?	11442N 22420E (incline 28L to 31L)
26/22	Aug Hb diorite	Alkali gabbro?	Incline 28L to 31L
26/29	Aug Hb diorite	Alkali gabbro?	
26/30	Hb diorite	Hawaiite?	
26/31	Aug Hb diorite	Alkali gabbro?	
31 LEVEL			
31/23	Hb diorite	Hawaiite?	11385N 22345E
31/24	Hb diorite	Hawaiite?	11390N 22370E
31/25	Hb diorite	Hawaiite?	11390N 22390E
25 LEVEL			
25A	Andesite (altered)	Alkali basalt?	24 cross-cut, 30m in; footwall fault zone
25B	Black sediment		24 cross-cut, 20m in; veined zone in footwall
25C	Andesite (altered)	Alkali basalt?	24 cross-cut, 15m in
25D	Andesite (altered)	Alkali basalt?	21 cross-cut, N side
25E	Andesite (chilled margin)	Alkali basalt?	21 cross-cut, S side

Sample	Rock type		Mine Grid Location
	FIELD NAME	GEOCHEMICAL CLASSIFICATION	
25F	Altered sediment		21 cross-cut, S side corner of 105 drive
25G	Hb diorite	Hawaiite?	33 cross-cut, foot-wall drive
25/26	Hb diorite	Hawaiite?	
25/27	Hb diorite	Hawaiite?	
25/28	Hb diorite	Hawaiite?	
WARUWARI			
W/13	Aug Hb diorite	Alkali gabbro?	Waruwari pit
W/14	Sulphides		Waruwari pit
W/15	Alt. andesite	Alkali basalt?	Waruwari pit

TABLE 3. BASIC MAGNETIC PROPERTIES OF THE PORGERA AND MOUNT KARE SURFACE SAMPLES

Site	N	Bulk susceptibility (μG/Oe)	NRM (J[μG];D°,I°)	Q
01A	3	890	9150;300,-67	25
01B	3	1890	3380;310,-52	4.4
01C	3	2730	2940;324,-28	2.6
01D	5	3920	4660;318,-10	2.9
01E	1	3110	5540;335,-11	4.0
Site 01	5	2500	4580;335,-39	4.5
02A	3	1680	7670;305,-24	11
02B	2	35	26;354,-21	1.8
02C	4	3990	20,390;321,-03	12
02D	3	3430	13,960;320,-03	9.9
02E	4	5160	19,620;322,-04	9.3
02F	2	3240	8820;317,-14	6.6
02G	1	3890	10,820;308,-12	6.8
Site 02	7	3070	11,470;318,-08	9.1
YAK (Hb diorite)	2	2790	7780;318,-16	6.8

Site	N	Bulk susceptibility (μG/Oe)	NRM (J[μG];D°,I°)	Q
03A	2	275	70;027,-64	0.62
03B	2	44	27;294,+14	1.5
03C	3	41	17;333,-48	1.0
03D	4	60	34;312,-72	1.4
03E	4	36	26;166,+01	1.8
03F	3	43	1;151,+56	0.07
03G	4	774	68;303,-62	0.21
Site 03	7	182	25;317,-68	0.34
WARUWARI: Altered Hb diorite				
04A	3	1740	141;268,+07	0.20
04B	3	1500	142;326,-16	0.23
04C	3	2150	199;300,-26	0.23
04D	2	27	0.2;236,+74	0.02
04E	3	102	5;273,+13	0.12
Site 04	5	1100	88;298,-14	0.20
WARUWARI: andesite				
PG3	1	4120	13,460;089,+06	8.0*
(Hb diorite: Little Waruwari)				

Site	N	Bulk susceptibility (μG/Oe)	NRM (J[μG];D°,I°)	Q
05A	3	41	26;045;-69	1.5
05B	2	3610	417;026,-37	0.28
05C	3	5930	196;140,-37	0.08
05D	3	5250	200;045,-46	0.09
05E	3	5600	208;031,-41	0.09
05F	4	5790	613;024,-40	0.26
Site 05 (andesite dyke)	6	4370	250;037,-45	0.14
06A	3	6790	171;298,-67	0.06
06B	3	6460	288;244,-57	0.11
06C	3	6910	243;310,-73	0.09
06D	2	5870	494;264,-58	0.21
06E	3	6200	312;243,-53	0.12
06F	3	41	3;201,-57	0.16
06G	3	37	0.8;165,-66	0.05
06H	3	6270	272;310,-25	0.11
06A-E,H (Hb diorite)	6	6420	278;273,-58	0.11

Site	N	Bulk susceptibility (μG/Oe)	NRM (J[μG];D°,I°)	Q
07A	3	4980	570;084,+56	0.28
07B	3	5220	427;041,+38	0.20
07C	3	4950	388;025,+11	0.19
07D	3	4960	361;019,-24	0.18
07E	4	5000	175;037,+51	0.09
PG1	1	3920	305;030,+14	0.19
Site 07	6	4840	310;038,+28	0.16
TAWISAKALE: Hb diorite porphyry				
PG2	1	37	23;282,+43	1.5
RUDI'S TUNNEL: altered andesite				
PG5 (alt. andesite)	1	75	49;160,-26	1.6
PG6 (alt. Hb diorite)	1	51	15;108,-01	0.72
RAMBARI				
PG7	1	4	372;023,-31	233*
ROAMANE: altered and weathered Hb diorite				
PG9	1	2070	1590;271,-37	1.9
BTWN ROAMANE & RAMBARI: andesite				

Site	N	Bulk susceptibility (μG/Oe)	NRM (J[μG];D°,I°)	Q
08A	1	19	8;128,+15	1.1
08B	2	9	7;132,+13	1.9
08C	1	27	15;133,+12	1.4
08D	1	20	10;129,+13	1.2
Site 08	4	18	10;131,+13	1.4
09A	1	20	53;201,+54	6.5
09B	2	13	6;323,+63	1.0
09C	2	10	64;203,+47	16
09D	2	16	59;197,+39	9.0
09E	1	15	41;203,+46	6.7
Site 09	5	15	44;201,+48	7.2
Sites 08 & 09	2	17	24;186,+45	3.5
MT KARE: altered ?intrusives				
10A	2	570	26;072,-38	0.11
10B	3	1590	99;035,-37	0.15
10C	4	667	21;063,-30	0.08
10D	4	1960	79;058,-35	0.10
Site 10	4	1200	55;050,-37	0.11

Site	N	Bulk susceptibility (μG/Oe)	NRM (J[μG];D°,I°)	Q
11A	3	4230	129;035,-37	0.07
11B	3	3530	182;000,-30	0.13
11C	4	4050	242;012,-58	0.15
11D	3	3760	130;017,-24	0.08
11E	4	4230	267;024,-40	0.15
11F	4	8940	299;060,-72	0.08
Site 11	6	4790	195;021,-49	0.10
Sites 10 & 11	2	3000	123;029,-47	0.10
NE Porgera Complex: gabbro				
Peruk A (andesite)	6	4750	1460;_,_	0.75
Peruk B (alt. andesite)	1	30	-	-
PG8 (PERUK: andesite)	1	3080	11,600;218,-10	9.2*
C1 (Mt Kare)	3	4300	1210;-,-	0.69
C2 (Mt Kare)	2	4690	4340;-,-	2.3
MK11 (Mt Kare)	4	1070	563;-,-	1.3

N = no. of specimens, samples or sites used to calculate mean properties

Bulk susceptibility = $(k_1+k_2+k_3)/3$, where $k_{1,2,3}$ are the principal axes of the mean susceptibility tensor.

Susceptibility: 1 μG/Oe = 4p * 10^{-6} SI = 0.0000126 SI

= 0.0126 * 10^{-3} SI

1 vol% magnetite corresponds to a susceptibility of ~3000 μG/Oe = 38 * 10^{-3} SI.

The NRM is calculated as the mean of N remanence vectors, weighted according to their intensity.

J = NRM intensity in μG (1 μG = 1 mA/m, SI)

D = NRM declination, positive clockwise from true north

I = NRM inclination, positive downwards

Q = Koenigsberger ratio = remanent intensity/induced intensity

= J/kF, where F = 0.41 Oe (= 41,000 nT, SI)

* Samples collected close to the natural surface with high Q values. The remanence carried by these samples may be due to nearby lightning strikes and could therefore be unrepresentative of the bulk prperties.

TABLE 4. BASIC MAGNETIC PROPERTIES OF MINE SAMPLES

Sample	N	Bulk susceptibility (μG/Oe)	NRM (J[μG];D°,I°)	Q
25G	5	4560	595;078,-12	0.32
28C	4	2240	838;026,-38	0.91
25/27	5	6820	1040;307,-70	0.37
25/28	2	3880	787;006,-79	0.49
26/9	6	6830	946;104,-84	0.34
26/10	1	2500	446;357,-79	0.44
26/30	1	627	194;094,-84	0.75
28/1	6	8730	828;037,-81	0.23
28/3	1	5700	1230;011,-79	0.53
28/4	2	8080	1450;305,-83	0.44
28/5	4	9440	1510;317,-87	0.39
28/18	5	6870	1580;003,-80	0.56
31/23	1	7430	1140;255,-89	0.37
31/24	5	1430	350;163,-73	0.60
31/25	3	7420	1170;332,-78	0.38
PGA	1	7250	2070;044,-84	0.70
PGB	1	2300	1160;161,-75	1.2
PGC	1	8730	1640;112,-88	0.46
PGD	1	4220	1150;080,-64	0.66
Hb diorite (Roamane)	19	5530	1010;038,-83	0.45

Sample	N	Bulk susceptibility (μG/Oe)	NRM (J[μG];D°,I°)	Q
28A	6	4840	462;358,-01	0.23
26/11	3	938	189;146,+12	0.49
26/12	5	1470	126;134,-47	0.21
26/20	3	1160	64;144,+22	0.13
26/21	4	3530	287;150,-12	0.20
26/22	5	3530	194;331,-74	0.13
26/29	3	266	292;155,+56	2.7
26/31	1	1350	386;166,-53	0.70
Aug Hb diorite (Roamane/Rambari)	8	2140	65;103,-36	0.07
25E	4	2710	648;031,-17	0.58
28/16	2	4200	470;036,-85	0.27
Andesite (Roamane)	2	3460	465;031,-45	0.33
25A	6	45	4.4;070,+44	0.22
25C	5	10	1.8;178;+39	0.44
25D	6	41	2.5;104,-06	0.15
28/6	6	78	7.3;191,-58	0.43
28/7	7	14	2.2;196,+36	0.38
28/17	3	56	1.5;118,+38	0.07
Altered andesite (Roamane)	6	41	1.5;142,-01	0.09

Sample	N	Bulk susceptibility (μG/Oe)	NRM (J[μG];D°,I°)	Q
W13	1	3980	386;166,-53	0.24
(Aug Hb diorite, Waruwari)				
W14	2	7	1.6;339,-37	0.57
(Sulphides, Waruwari)				
W15	4	52	1.1;166,-79	0.05
(altered andesite, Waruwari)				
25B	2	27	0.5;194,+57	0.05
25F	6	4	0.5;337,-11	0.28
28B	4	36	16;176,+53	1.1
28/19	2	11	0.9;337,-27	0.20
Sediments/ Mineralisation	4	19	3.9;179,+57	0.50

N = no. of specimens, samples or sites used to calculate mean properties

Bulk susceptibility = $(k_1+k_2+k_3)/3$, where $k_{1,2,3}$ are the principal axes of the mean susceptibility tensor.

Susceptibility: 1 μG/Oe = $4\pi * 10^{-6}$ SI = 0.0000126 SI

$= 0.0126 * 10^{-3}$ SI

The NRM is calculated as the mean of N remanence vectors, weighted according to their intensity.

J = NRM intensity in μG (1 μG = 1 mA/m, SI)

D = NRM declination, positive clockwise from true north

I = NRM inclination, positive downwards

Q = Koenigsberger ratio = remanent intensity/induced intensity

= J/kF, where F = 0.41 Oe (= 41,000 nT, SI)

TABLE 5. MAGNETIC FABRIC OF PORGERA AND MOUNT KARE SURFACE SAMPLES

Sample	Susceptibility Ellipsoid	A	L	F	P	T
01A	909;166,23 894;284,48 879;060,33	1.034	1.017	1.017	1.000	0.0004
01B	1906;150,37 1889;262,27 1792;018,41	1.063	1.009	1.054	0.957	0.711
01C	2769;147,32 2734;259,31 2652;022,42	1.044	1.013	1.030	0.982	0.412
01D	3966;144,45 3919;293,41 3866;037,16	1.026	1.012	1.014	0.998	0.075
01E	3176;148,41 3113;307,47 3073;049,11	1.034	1.020	1.013	1.007	-0.217
Site 01 Mean tensor	2544;149,37 2506;272,36 2458;030,33	1.035	1.015	1.020	0.996	0.119
Site 01, all specimens; unit tensors (N = 14)	1.037;152,39 1.003;271,35 0.981;027,36	1.040	1.023	1.017	1.006	-0.149

Sample	Susceptibility Ellipsoid	A	L	F	P	T
02A	1767;209,22 1679;319,40 1601;098,42	1.104	1.053	1.049	1.004	-0.036
02B	36.2;027,44 35.3;221,46 35.2;124,07	1.027	1.024	1.004	1.020	-0.740
02C	4093;197,47 3987;320,27 3930;068,31	1.042	1.027	1.014	1.012	-0.297
02D	3541;216,55 3434;315,07 3353;050,34	1.056	1.031	1.024	1.007	-0.126
02E	5241;216,52 5157;346,27 5050;089,25	1.038	1.016	1.021	0.995	0.131
02F	3365;197,24 3244;341,62 3224;100,15	1.044	1.037	1.006	1.031	-0.714
02G	3996;198,24 3894;316,46 3812;091,34	1.048	1.026	1.022	1.005	-0.094
Site 02 (N=7)	3141;204,38 3063;328,35 3007;08 ,32	1.044	1.025	1.019	1.007	-0.155

Sample	Susceptibility Ellipsoid	A	L	F	P	T
Site 02, all specimens; unit tensors (N = 19)	1.021;205,38 0.998;332;37 0.981;088,30	1.040	1.023	1.017	1.006	-0.149
03A	282;317,68 274;166,22 268;071,10	1.052	1.030	1.022	1.008	-0.152
03B	45.1;006,43 44.3;197,47 44.0;071,06	1.024	1.017	1.007	1.009	-0.152
03C	42.2;051,58 41.4;210,30 40.7;306,10	1.035	1.019	1.016	1.002	-0.062
03D	61.7;297,49 60.3;100,40 58.6;197,09	1.052	1.024	1.028	0.996	0.079
03E	36.5;339,86 36.1;159,04 35.9;249,00	1.016	1.011	1.005	1.006	-0.383
03F	44.1;350,89 43.2;183,01 43.0;093,00	1.026	1.022	1.004	1.018	-0.683

Sample	Susceptibility Ellipsoid	A	L	F	P	T
03G	779;063,70 773;231,20 769;323,04	1.014	1.008	1.005	1.003	-0.251
Site 03 (N=7)	184;345,79 181;175,11 181;085,02	1.018	1.016	1.016	1.014	-0.818
Site 03, all specimens; unit tensors (N = 22)	1.012;359,79 0.995;181,11 0.981;088,30	1.018	1.017	1.008	1.016	-0.906
04A	1765;262,75 1731;013,05 1711;104,14	1.032	1.020	1.017	1.008	-0.262
04B	1501;061,18 1496;225,72 1493;330,05	1.006	1.004	1.002	1.002	-0.358
04C	2198;244,56 2165;344,07 2077;079,34	1.058	1.015	1.042	0.974	0.460

Sample	Susceptibility Ellipsoid	A	L	F	P	T
04D	27.0;030,53 26.8;197,36 26.7;292,06	1.013	1.009	1.004	1.005	-0.411
04E	103;322,83 102;095,05 101;186,05	1.023	1.013	1.009	1.0044	-0.175
Site 04 (N=5)	1117;248,61 1103;352,08 1085;086,28	1.030	1.013	1.017	0.996	0.137
Site 04, all specimens; unit tensors (N = 12)	1.011;258,67 0.999;359,05 0.990;091,23	1.021	1.012	1.010	1.002	-0.086
05A	41.9;212,31 41.4;022,58 41.0;119,04	1.023	1.014	1.009	1.005	-0.234
05B	3905;175,33 3614;062,31 3310;300,42	1.180	1.081	1.092	0.990	0.064
05C	6008;206,34 5999;305,14 5777;054,53	1.040	1.002	1.038	0.924	0.924

Sample	Susceptibility Ellipsoid	A	L	F	P	T
05D	5451;054,20 5351;158,32 4943;297,51	1.103	1.019	1.083	0.941	0.622
05E	5741;111,38 5678;016,06 5389;278,51	1.065	1.011	1.054	0.959	0.654
05F	5987;015,23 5795;252,52 5586;119,28	1.072	1.033	1.038	0.996	0.062
Site 05 (N=6)	4472;192,11 4390;092,40 4247;294,48	1.033	1.019	1.034	0.985	0.283
Site 05, all specimens; unit tensors (N = 15)	1.023;192,11 1.005;093,40 0.972;295,48	1.052	1.018	1.034	0.985	0.307

Sample	Susceptibility Ellipsoid	A	L	F	P	T
06A	6828;245,84 6798;096,05 6743;006,03	1.013	1.006	1.007	0.999	0.094
06B	6492;097,52 6453;285,38 6438;192,04	1.009	1.006	1.002	1.004	-0.435
06C	6922;242,50 6904;339,06 6827;074,39	1.023	1.013	1.011	1.002	-0.067
06D	5924;161,60 5874;292,21 5808;031,21	1.020	1.009	1.011	0.997	0.137
06E	6268;347,06 6200;079,13 6145;233,76	1.020	1.011	1.009	1.002	-0.108
06F	41.4;021,44 40.7;123,12 40.6;224,44	1.021	1.016	1.005	1.011	-0.538
06G	38.1;007,30 37.1;131,45 36.8;257,31	1.034	1.027	1.008	1.019	-0.555
06H	6332;264,28 6289;008,24 6174;132,52	1.026	1.007	1.019	0.988	0.465

Sample	Susceptibility Ellipsoid	A	L	F	P	T
Site 06 (N=8)	4837;270,46 4820;164,15 4807;061,40	1.006	1.004	1.003	1.001	-0.146
Site 06, all specimens; unit tensors (N = 22)	1.004;353;34 0.999;239,30 0.997;119,41	1.007	1.005	1.002	1.002	-0.465
07A	5013;123,63 4998;314,27 4924;222,04	1.018	1.003	1.015	0.988	0.988
07B	5222;118,08 5192;243,77 5110;026,10	1.022	1.006	1.016	0.990	0.461
07C	5028;126,22 4922;351,60 4886;224,19	1.029	1.022	1.008	1.014	-0.484
07D	5003;294,22 4965;128,67 4924;026,05	1.016	1.008	1.008	0.999	0.044

Sample	Susceptibility Ellipsoid	A	L	F	P	T
07E	5058;131,21 5014;315,69 4919;221,01	1.028	1.009	1.019	0.990	0.368
Site 07 (N=5)	5059;125,18 5021;304,73 4807;061,40	1.021	1.008	1.013	0.994	0.269
Site 07, all specimens; unit tensors (N = 17)	1.009;125,16 1.002;303,74 0.989;035,01	1.021	1.007	1.013	0.994	0.288
Site 08, all specimens; mean tensor (N = 4)	18.4;254,37 18.3;148,20 18.2;036,47	1.008	1.002	1.006	0.996	0.593
Site 08, all specimens; unit tensors (N = 4)	1.004;233,41 1.001;132,12 0.996;029,46	1.008	1.003	1.005	0.998	0.224

Sample	Susceptibility Ellipsoid	A	L	F	P	T
Site 09, all specimens; mean tensor (N = 5)	13.7;086,32 13.4;182,10 13.3;287,56	1.003	1.002	1.012	1.008	-0.233
Site 09, all specimens; unit tensors (N =)	1.018;087,29 0.996;183,11 0.987;291,58	1.031	1.022	1.009	1.013	-0.407
10A	581;240,30 569;341,19 560;098,54	1.039	1.021	1.017	1.004	-0.105
10B	1614;171,35 1579;338,55 1575;077,06	1.025	1.022	1.003	1.019	-0.781
10C	673;183,40 667;065,29 661;311,37	1.019	1.009	1.010	0.999	0.068
10D	1975;269,29 1965;156,35 1947;028,41	1.014	1.005	1.009	0.996	0.301

Sample	Susceptibility Ellipsoid	A	L	F	P	T
Site 10 (N = 4)	1322;188,40 1314;289,12 1304;032,47	1.0144	1.007	1.007	0.999	-0.045
Site 10, all specimens; unit tensors (N = 12)	1.008;210,39 0.999;113,08 0.992;013,49	1.016	1.009	1.007	1.002	-0.131
11A	4279;084,79 4223;195,04 4198;285,10	1.019	1.013	1.006	1.007	-0.386
11B	3580;123,68 3515;339,18 3490;245,12	1.025	1.018	1.007	1.011	-0.441
11C	4094;226,76 4025;355,09 4021;087,11	1.018	1.017	1.001	1.016	-0.885
11D	3800;276,55 3739;100,35 3726;009,02	1.020	1.016	1.004	1.013	-0.633
11E	4281;237,53 4208;046,37 4192;140,05	1.021	1.017	1.004	1.013	-0.630

Sample	Susceptibility Ellipsoid	A	L	F	P	T
11F	9018;146,61 8931;297,26 8877;032,13	1.015	1.009	1.006	1.003	-0.189
Site 11 (N=6)	4829;195,78 4773;295,02 4762;026,11	1.014	1.012	1.002	1.009	-0.676
Site 11, all specimens; unit tensors (N = 19)	1.009;188,80 0.996;294,03 0.995;025,10	1.014	1.013	1.001	1.012	-0.845

N = no. of specimens, samples or sites used to calculate mean susceptibility tensor

Principal susceptibility axes are given in the form: $k_i;D_i,I_i$ ($i = 1,2,3$ for major, intermediate and minor axes respectively). The k_i are expressed in $\mu G/Oe$.

(D_1,I_1) represents the direction of the magnetic lineation.

(D_3,I_3) represents the magnetic foliation pole.

The magnetic fabric is characterised by the following parameters:

A = anisotropy magnitude = k_1/k_3,
L = lineation magnitude = k_1/k_2, $\quad (A,L,F \geq 1)$
F = foliation magnitude = k_2/k_3,
P = prolateness of susceptibility ellipsoid = L/F $\quad (P > 0)$,
T = ellipsoid shape parameter = $2(n2-n3)/(n1-n3) - 1 \quad (-1 \leq T \leq 1)$
where n1,n2,n3 are the natural logarithms of k_1,k_2,k_3.

TABLE 6. MAGNETIC FABRIC OF UNDERGROUND AND SURFACE MINE SAMPLES

Sample	Susceptibility Ellipsoid	A	L	F	P	T
25G	4602;235,63 4550;100,20 4514;003,18	1.019	1.011	1.008	1.003	-0.1764
28C	2288;077,34 2227;225,51 2199;336,16	1.040	1.027	1.013	1.025	-0.364
25/27	6899;291,81 6824;141,08 6750;051,05	1.022	1.011	1.011	1.000	0.006
25/28	3927;001,32 3890;151,54 3811;262,14	1.030	1.009	1.021	0.989	0.384
26/9	7272;048,61 7161;267,23 6045;169,16	1.203	1.016	1.185	0.857	0.833
26/10	2544;070,26 2511;193,48 2442;323,30	1.042	1.013	1.029	0.985	0.367
26/30	641;202,61 624;051,25 615;315,12	1.044	1.027	1.016	1.011	-0.264
28/1	8824;348,78 8732;252,01 8646;162,12	1.021	1.011	1.010	1.001	-0.030

Sample	Susceptibility Ellipsoid	A	L	F	P	T
28/3	5851;228,02 5698;320,34 5554;135,56	1.053	1.027	1.026	1.001	-0.021
28/4	8164;074,31 8158;203,46 7928;325,27	1.030	1.001	1.029	0.973	0.950
28/5	9551;034,64 9423;248,22 9337;152,13	1.023	1.014	1.009	1.004	-0.190
28/18	6960;043,46 6891;218,44 6756;311,03	1.030	1.010	1.020	0.990	0.333
31/23	7548;210,70 7428;351,16 7324;085,12	1.031	1.016	1.014	1.002	-0.067
31/24	1502;112,64 1432;297,26 1358;206,02	1.106	1.049	1.054	0.995	0.046
31/25	7516;281,87 7389;159,02 7364;069,03	1.021	1.017	1.003	1.014	-0.670
Hb diorite (Roamane) (N = 15)	5567;040,74 5521;251,14 5423;159,08	1.027	1.008	1.018	0.990	0.364

Sample	Susceptibility Ellipsoid	A	L	F	P	T
Hb diorite (Roamane); all specimens, unit tensors (N = 51)	1.014;077,73 1.000;264,13 0.986;173,02	1.029	1.014	1.015	0.985	0.405
28A	4872;345,07 4838;200,81 4809;076,05	1.013	1.007	1.006	1.001	-0.071
26/11	949;274,53 935;122,34 929;023,13	1.022	1.014	1.007	1.007	-0.333
26/12	1491;002,69 1459;227,15 1446;133,14	1.032	1.022	1.009	1.013	-0.417
26/20	1167;072,59 1160;175,08 1152;269,30	1.013	1.007	1.007	1.000	-0.003
26/21	3600;174,86 3512;350,04 3489;080,00	1.032	1.025	1.007	1.019	-0.585
26/22	3567;350,64 3522;120,17 3497;216,19	1.020	1.013	1.007	1.006	-0.282
26/29	269;036,75 265;171,11 263;264,11	1.025	1.016	1.010	1.006	-0.230

Sample	Susceptibility Ellipsoid	A	L	F	P	T
26/31	1385;017,47 1350;213,42 1329;116,08	1.042	1.026	1.016	1.010	-0.241
Aug Hb diorite, Roamane (N = 8)	2155;357,73 2132;171,17 2120;261,02	1.017	1.011	1.006	1.005	-0.324
Aug Hb diorite Roamane; all specimens, unit tensors (N = 30)	1.009;000,74 0.997;171,16 0.993;262,02	1.016	1.012	1.004	1.008	-0.515
25E	2732;217,32 2708;047,58 2683;309,05	1.018	1.009	1.017	1.000	0.017
28/16	4295;268,79 4249;053,09 4046;144,06	1.062	1.011	1.050	0.963	0.634
Andesite, Roamane (N = 2)	3507;244,68 3483;050,21 3367;142,05	1.042	1.007	1.035	0.973	0.663
Andesite, Roamane; all specimens, unit tensors (N = 6)	1.010;225,56 1.002;043,34 0.988;134,01	1.022	1.008	1.014	0.994	0.273

25A	45.7;224,41 44.7;016,45 44.0;121,14	1.039	1.022	1.016	1.007	-0.173
25C	10.2;217,45 10.1;090,31 10.0;341,29	1.021	1.012	1.009	1.002	-0.109
25D	41.9;244,33 41.4;096,53 41.0;345,16	1.021	1.011	1.010	1.000	-0.010
28/6	79.1;263,82 78.1;105,08 77.7;014,03	1.019	1.012	1.006	1.006	-0.325
28/7	13.8;115,76 13.7;345,09 13.6;254,10	1.012	1.009	1.004	1.005	-0.420
28/17	56.7;081,77 55.6;336,04 55.4;245,13	1.024	1.020	1.004	1.017	-0.698
Altered andesite, Roamane (N = 6)	41.1;227,74 40.6;060,15 40.4;329,03	1.016	1.011	1.005	1.006	-0.363
Altered andesite; Roamane; all specimens, unit tensors	1.008;217,66 0.999;069,21 0.992;335,13	1.016	1.010	1.006	1.003	-0.211

(N = 32)

W13 (Aug Hb diorite)	4009;277,35 3981;079,53 3919;181,09	1.023	1.015	1.017	0.914	0.375
W14 (Sulphide)	7.0;214,75 6.9;358,13 6.7;090,09	1.050	1.025	1.025	1.000	0.007
W15 (altered andesite)	53.0;238,81 52.3;037,09 52.2;128,03	1.015	1.013	1.002	1.011	-0.750
25B	27.3;091,11 26.5;000,05 26.4;244,78	1.036	1.030	1.006	1.025	-0.690
25F	4.3;125,46 4.2;014,19 4.0;269,38	1.073	1.027	1.044	0.984	0.227
28B	36.2;205,37 35.7;075,40 35.5;319,28	1.020	1.016	1.005	1.011	-0.525
28/19	11.1;358,18 11.0;143,68 10.6;264,12	1.047	1.011	1.036	0.976	0.535

Sample	Susceptibility Ellipsoid	A	L	F	P	T
Sediments/ Mineralisation; Roamane (N = 4)	19.5;121,39 19.5;216,06 19.3;313,51	1.011	1.001	1.010	0.992	0.760
Sediments/ mineralisation; Roamane; all specimens, unit tensors (N = 14)	1.016;131,45 1.004;020,20 0.980;274,38	1.036	1.012	1.024	0.989	0.311

Symbols as for Table 5.

Fig.1. NRM directions of specimens from sites 01-11.

a

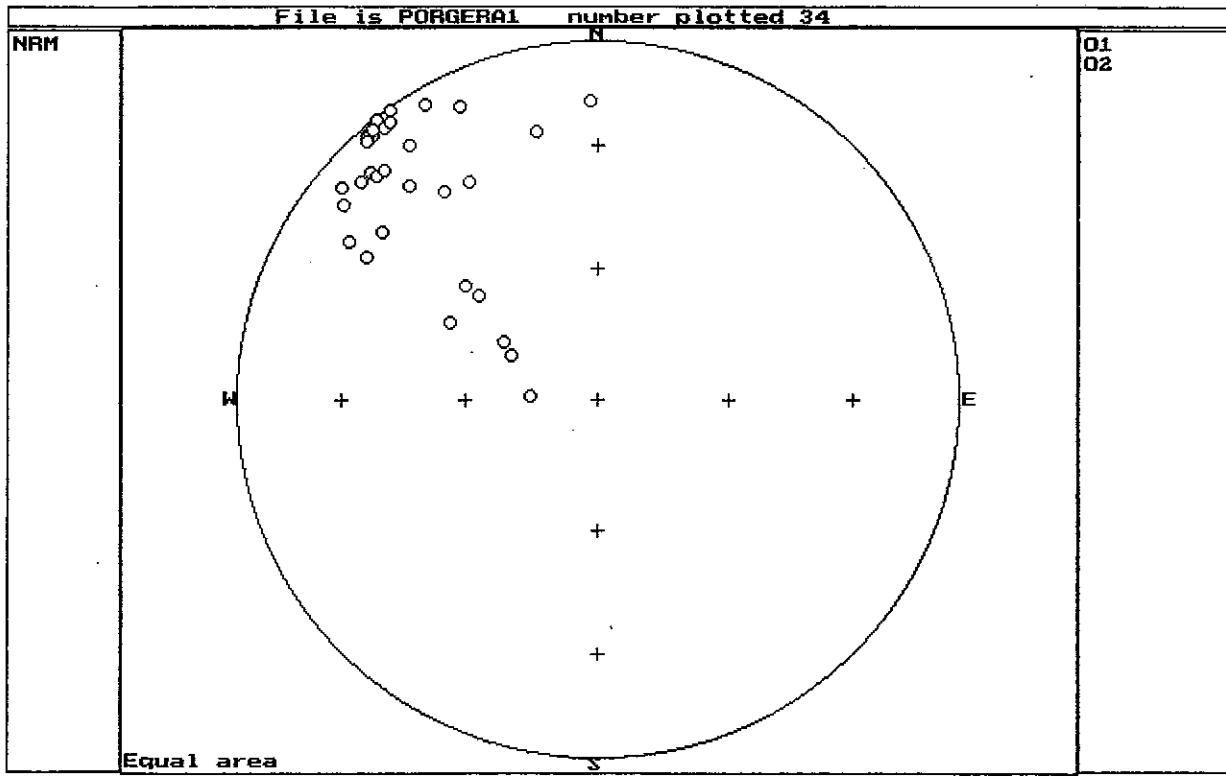
File is PORGERA1 number plotted 34
NRM
O1
O2
N
W
E
S
Equal area

b

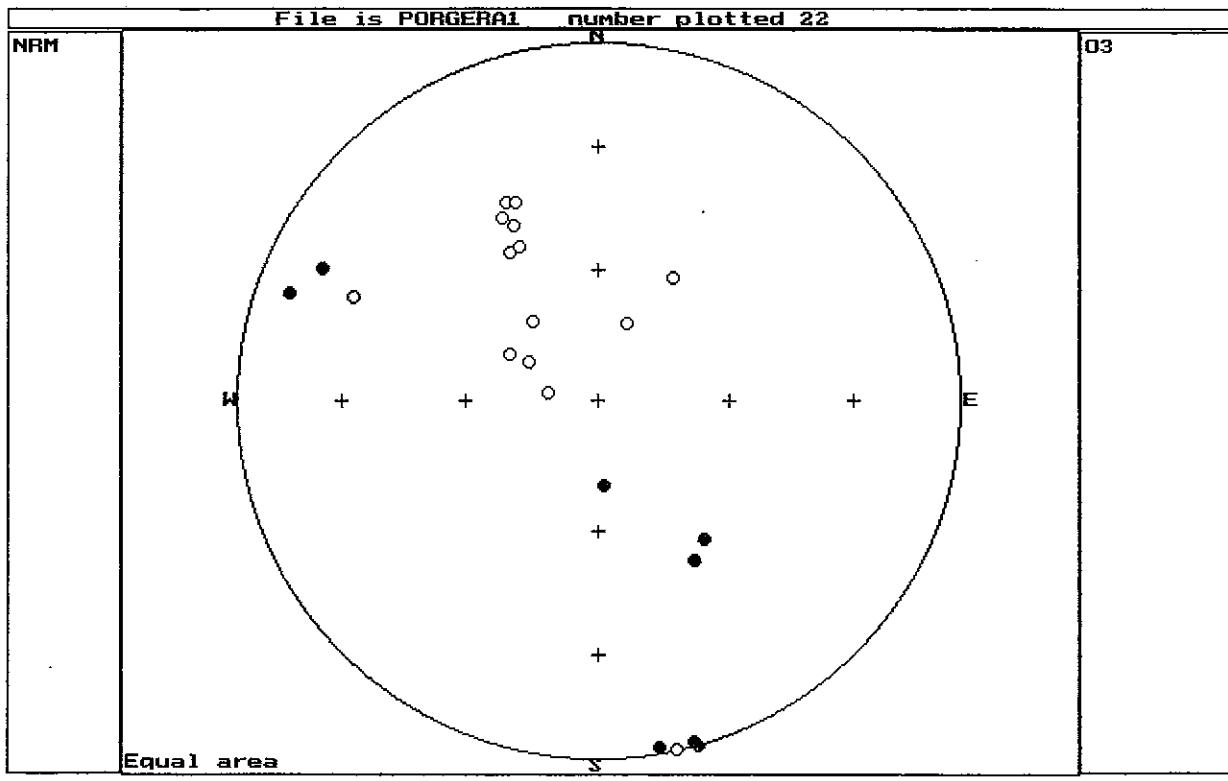
File is PORGERA1 number plotted 22
NRM
O3
N
W
E
S
Equal area

c

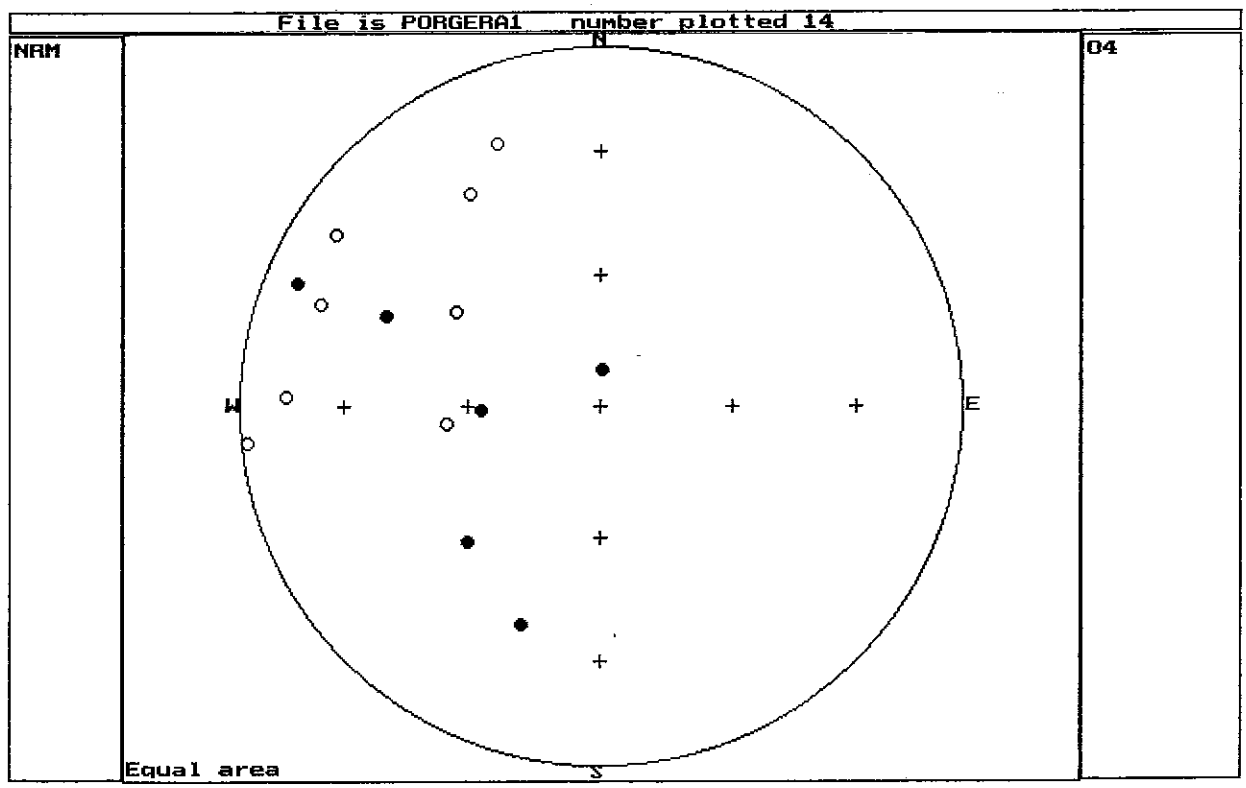
File is PORGERA1 number plotted 14
NRM
04
N
W
E
S
Equal area

d

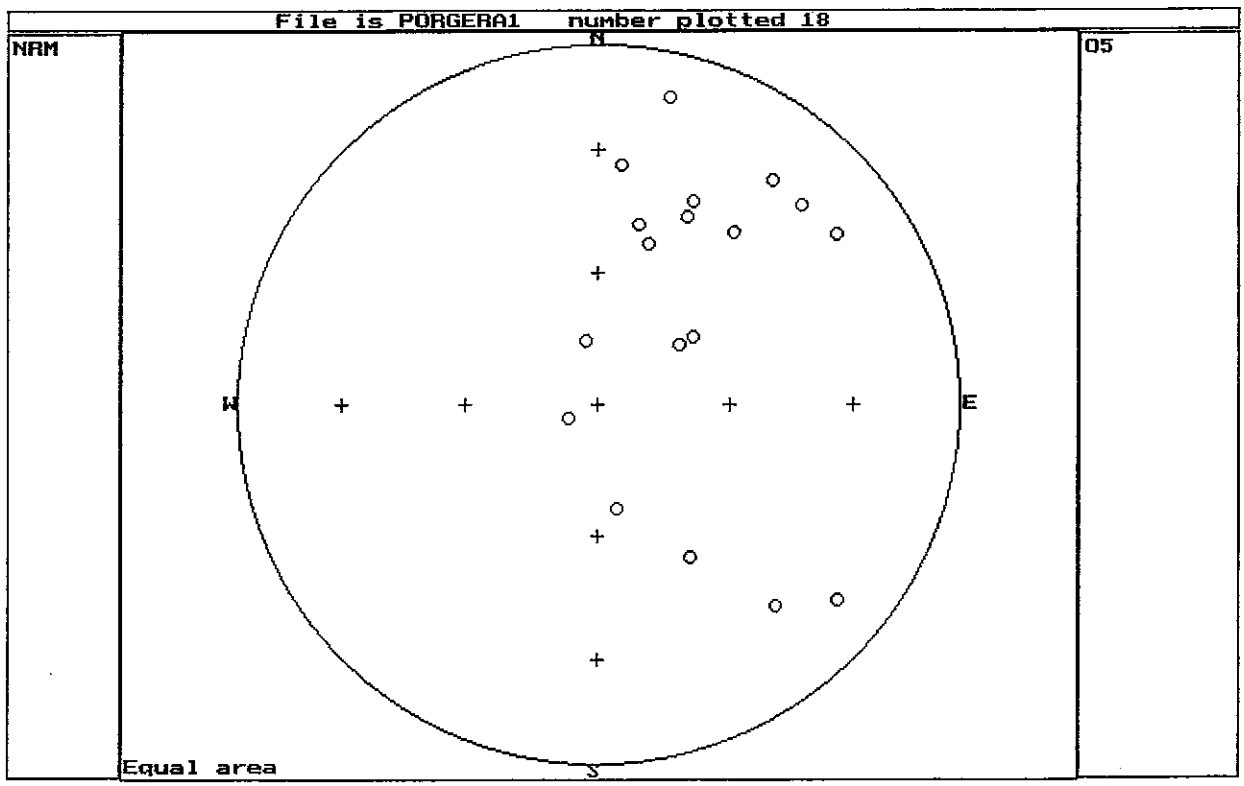
File is PORGERA1 number plotted 18
NRM
05
N
W
E
S
Equal area

e

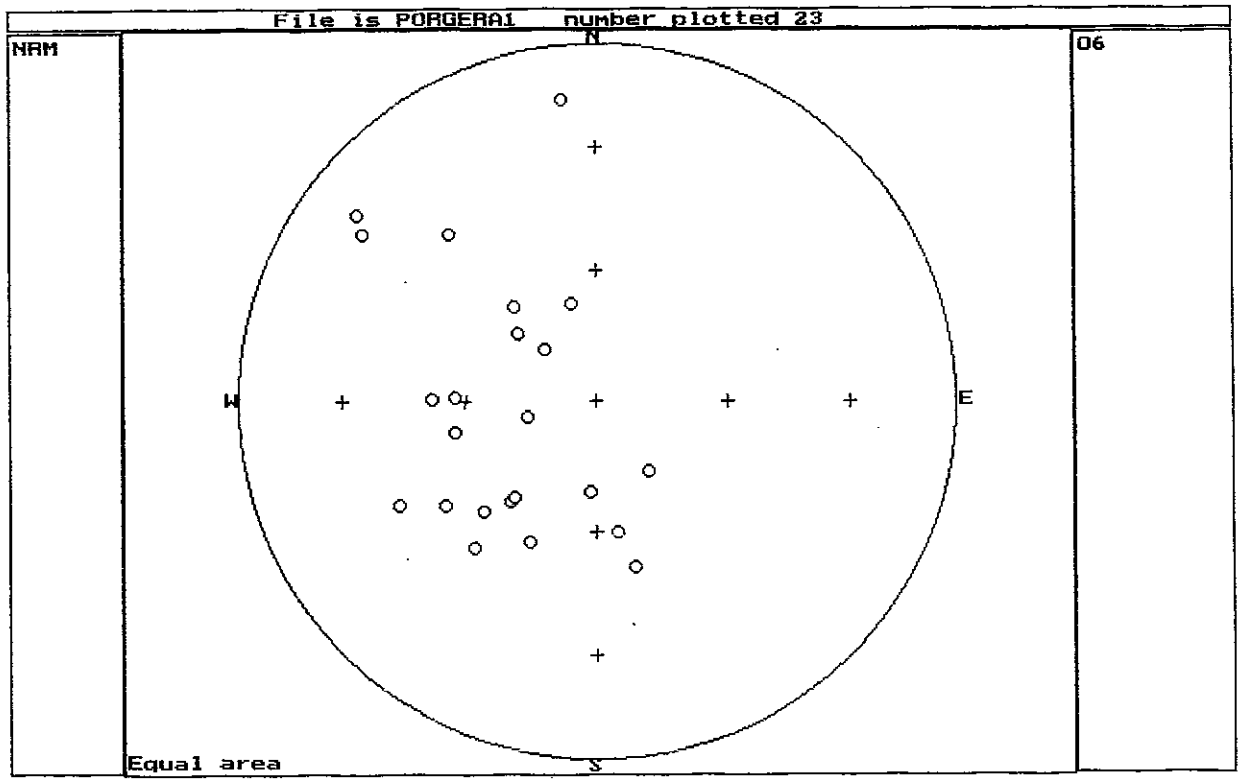
File is PORGERA1 number plotted 23
NRM
06
N
W
E
S
Equal area

f

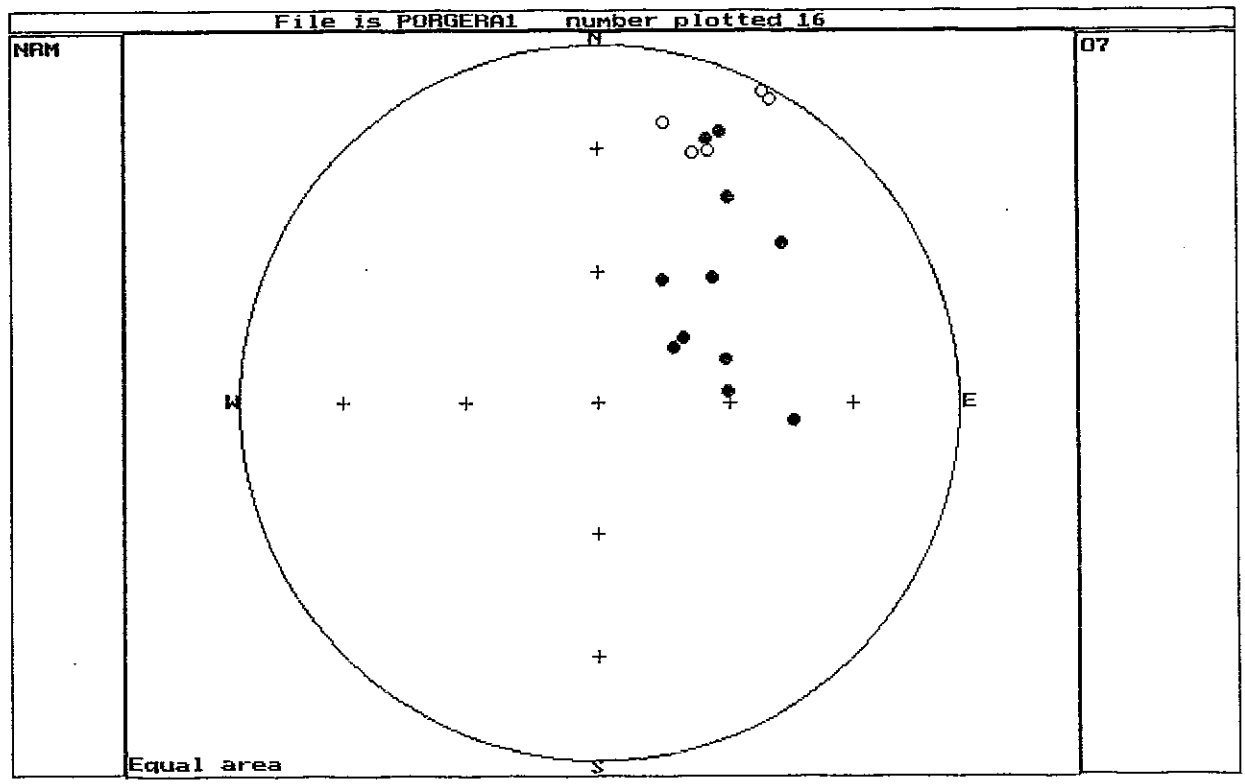
File is PORGERA1 number plotted 16
NRM
07
N
W
E
S
Equal area

g

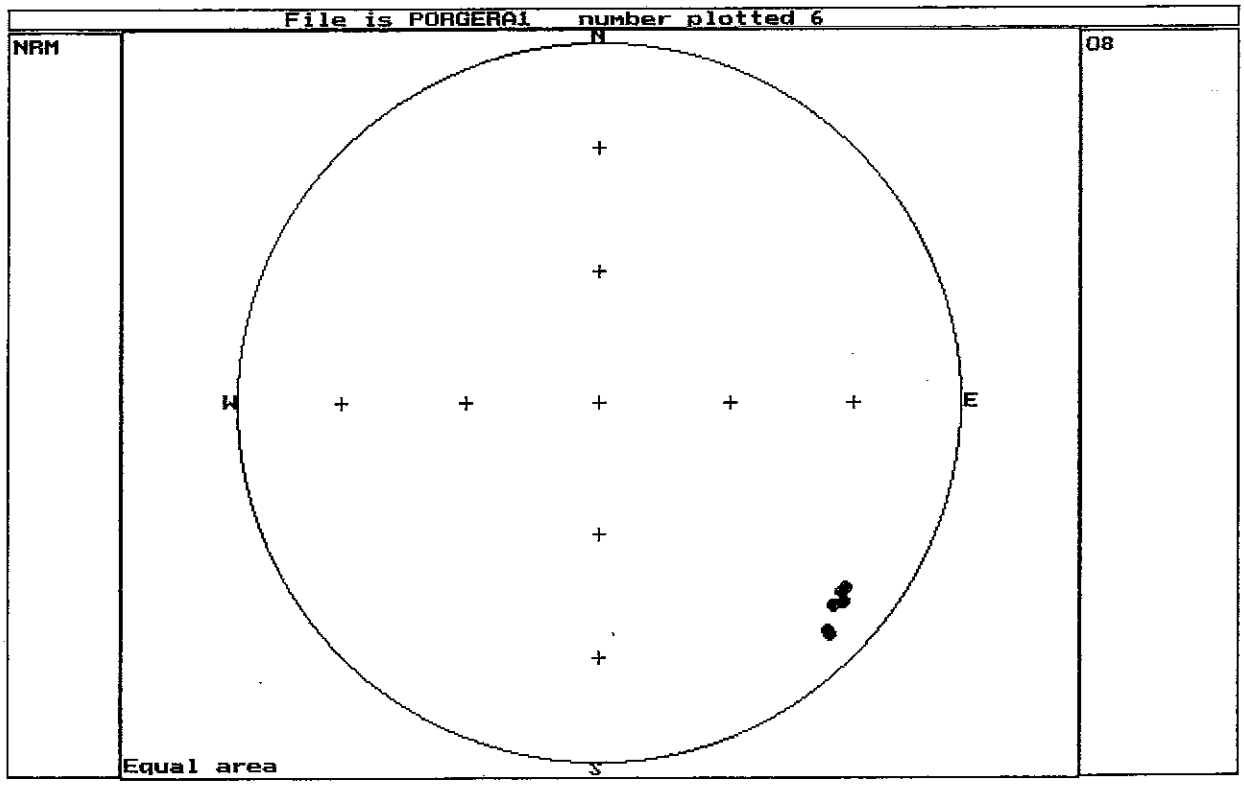
File is PORGERA1 number plotted 6
NRM
O8
N
W
E
S
Equal area

h

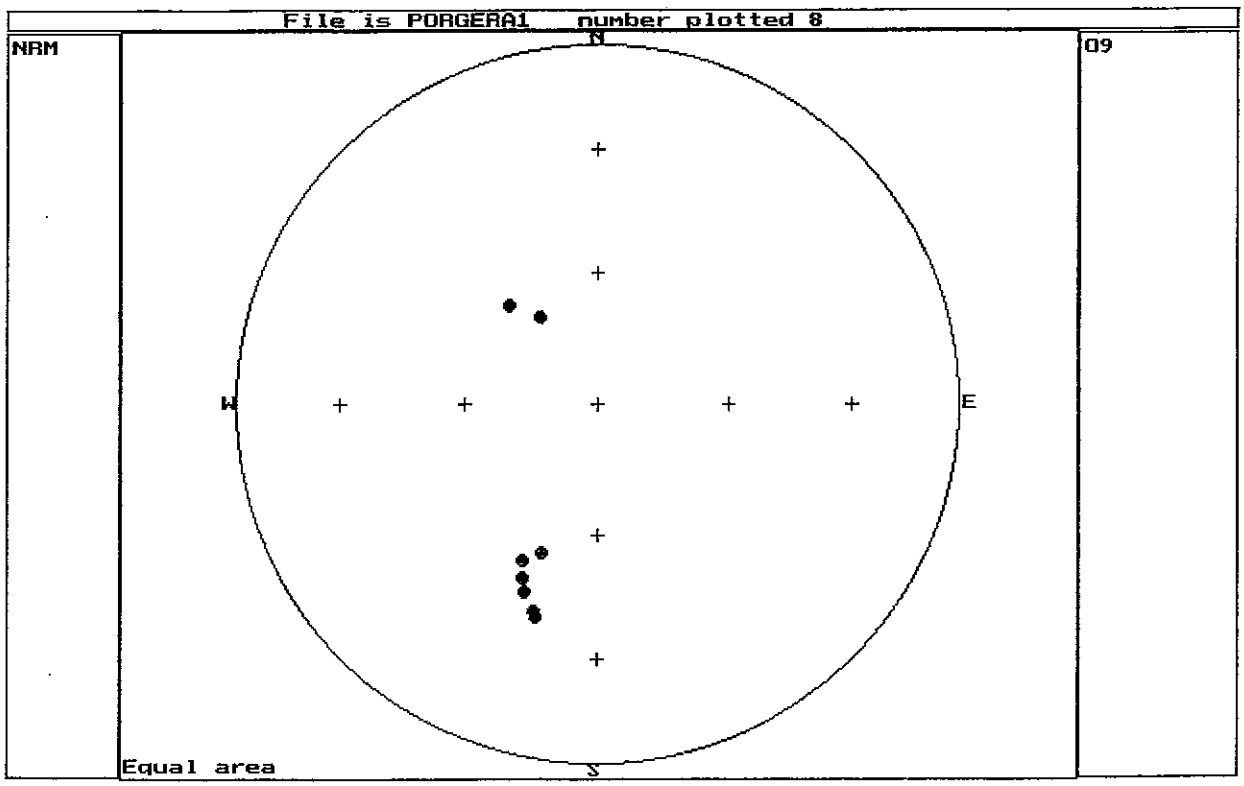
File is PORGERA1 number plotted 8
NRM
O9
N
W
E
S
Equal area

i

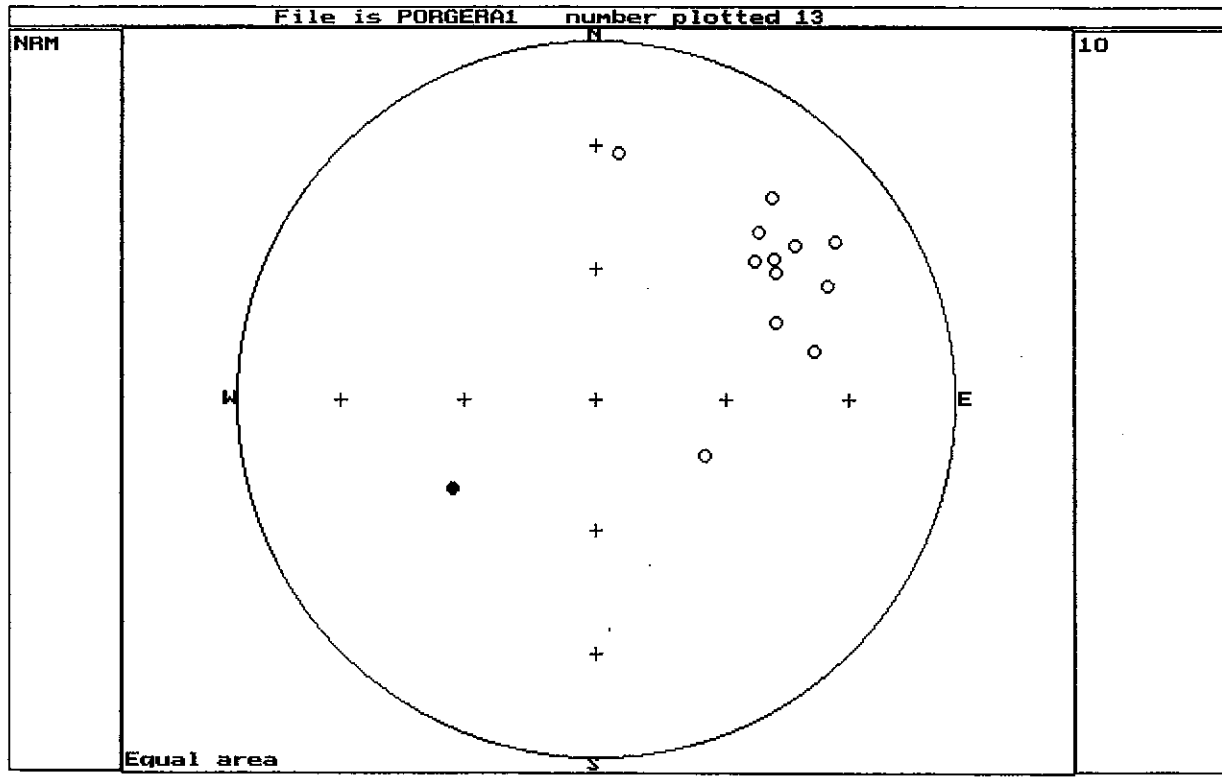
File is PORGERA1 number plotted 13
NRM
10
N
W
E
S
Equal area

j

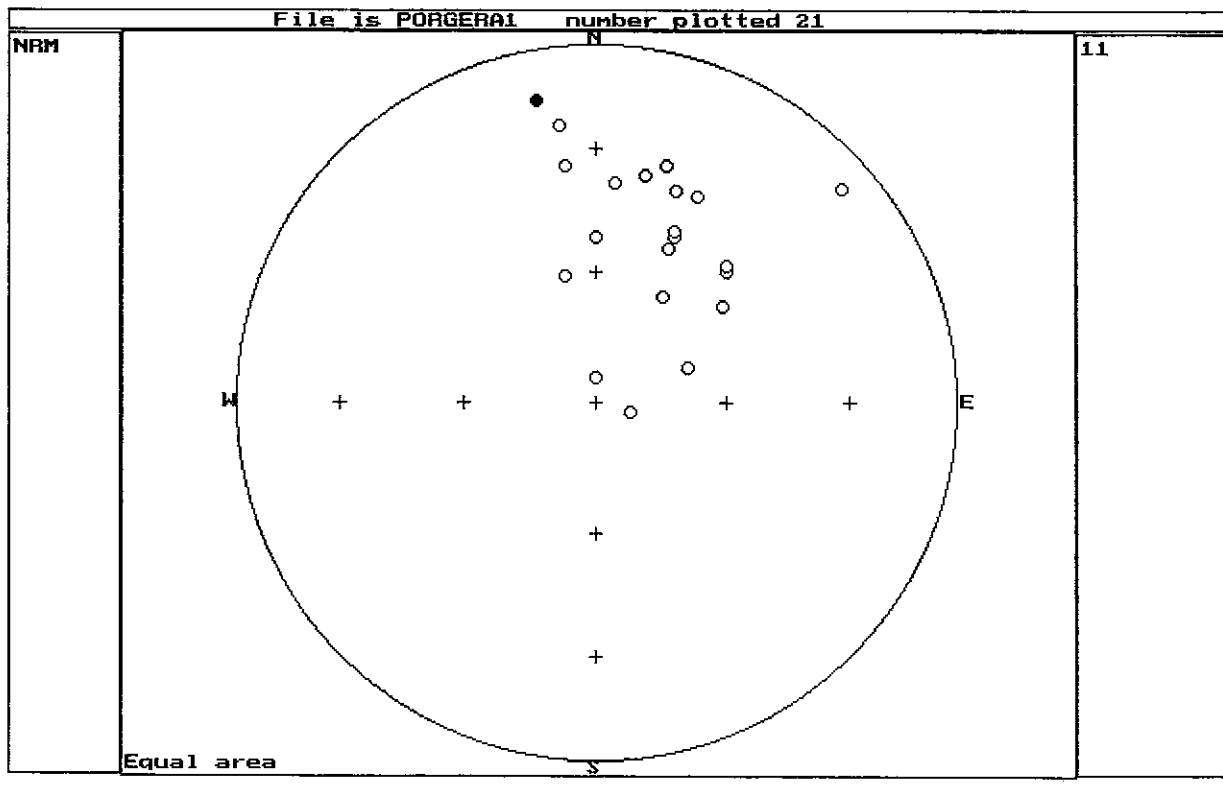
File is PORGERA1 number plotted 21
NRM
11
N
W
E
S
Equal area

Fig.2. NRM directions of specimens from underground mine samples. (a) hornblende diorite, (b) augite hornblende diorite, (c) andesite, (d) altered andesite, (e) altered sediments and sulphide mineralisation

a

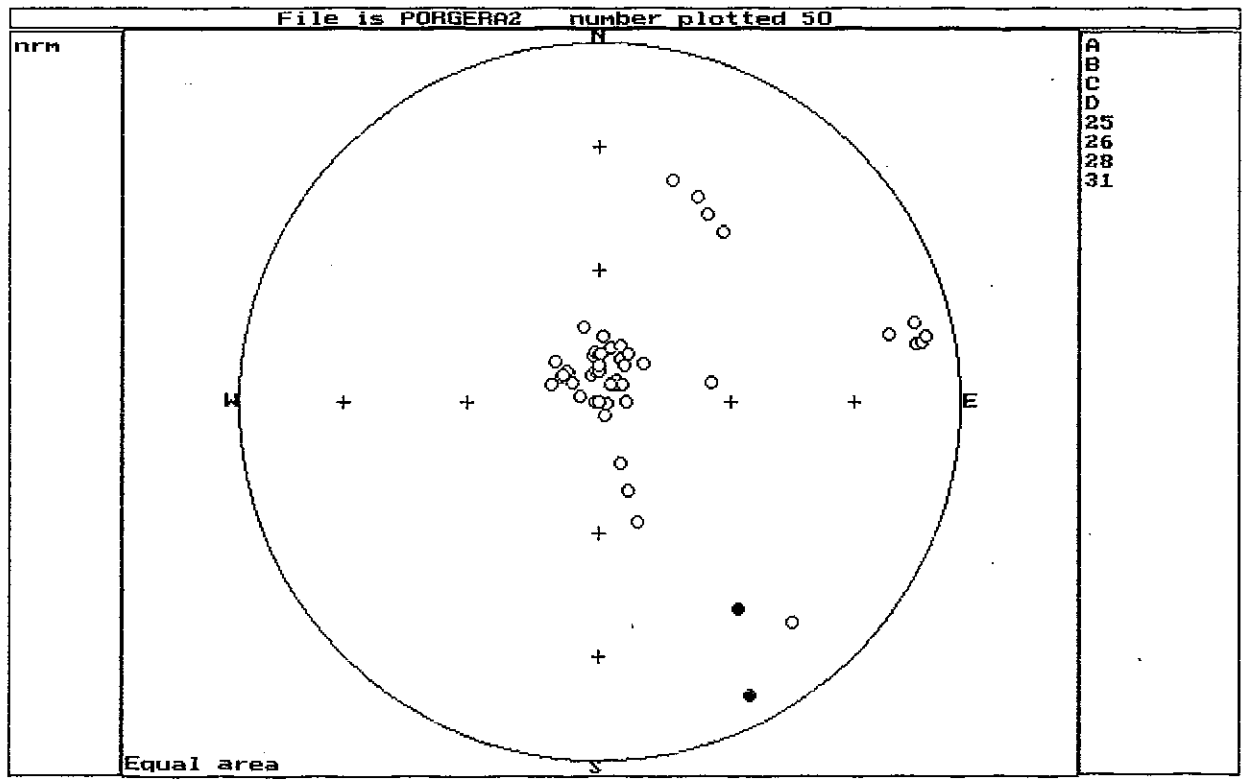
File is PORGERA2 number plotted 50
nrm
N
W
E
S
A
B
C
D
25
26
28
31
Equal area

b

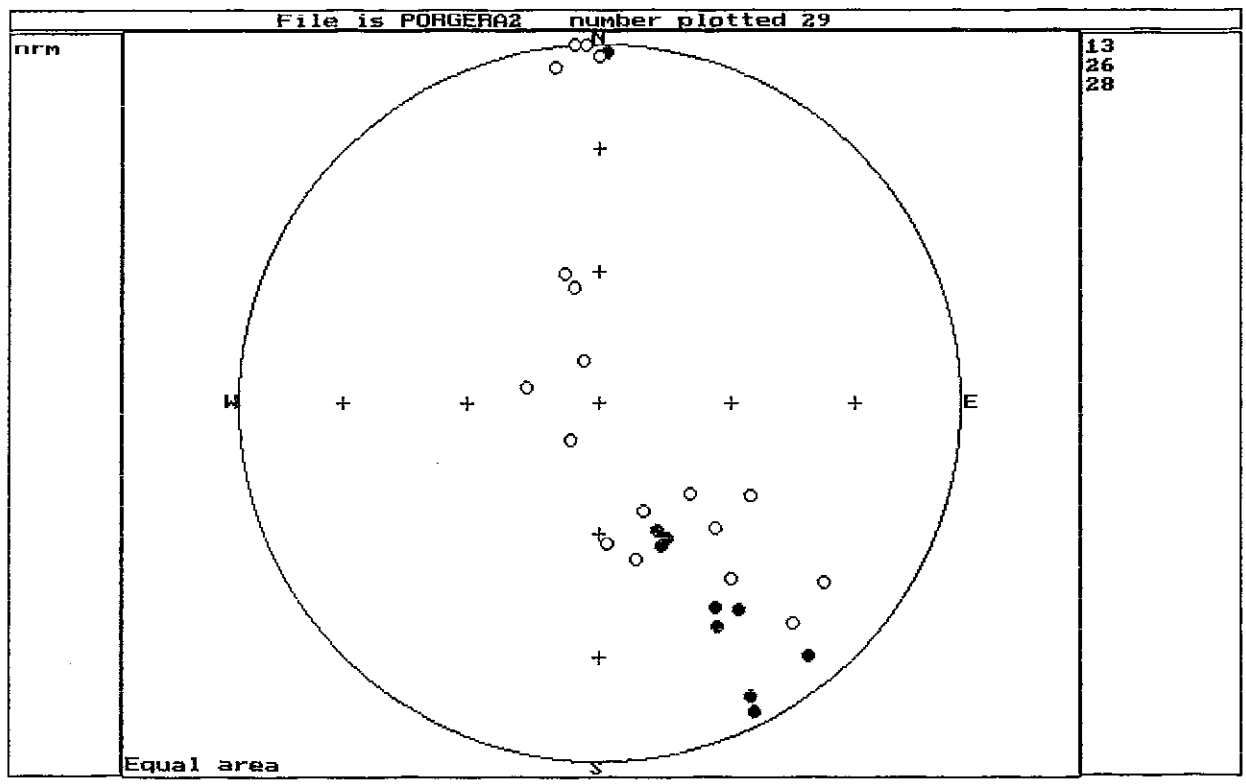
File is PORGERA2 number plotted 29
nrm
N
W
E
S
13
26
28
Equal area

c

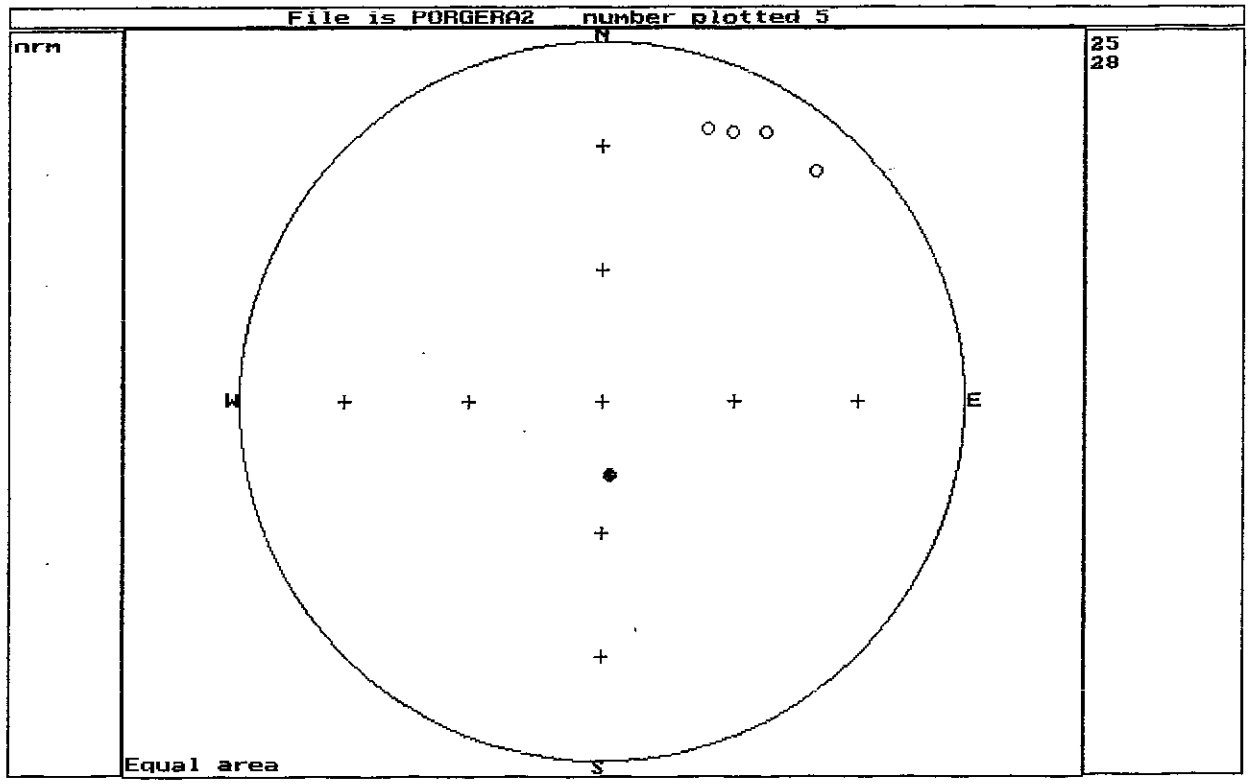
File is PORGERA2 number plotted 5
nrm
25
28
N
W
E
S
Equal area

d

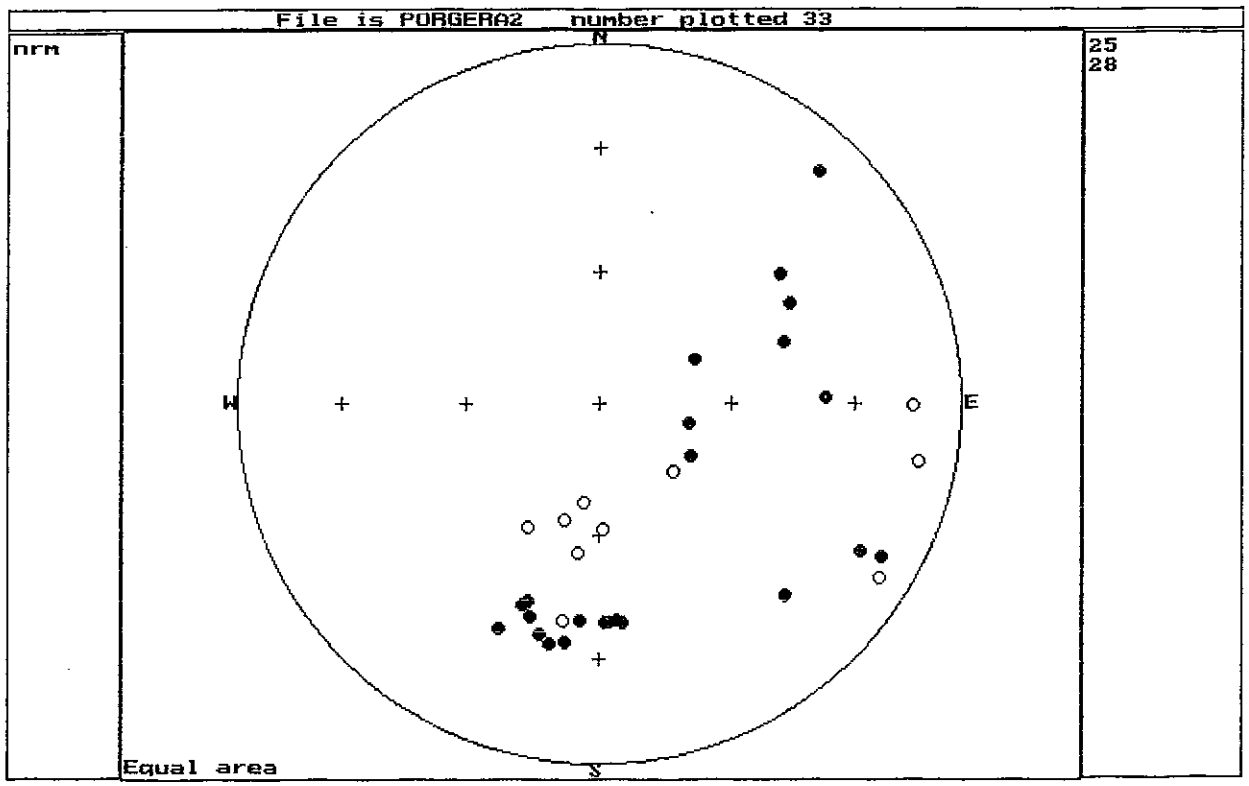
File is PORGERA2 number plotted 33
nrm
25
28
N
W
E
S
Equal area

e

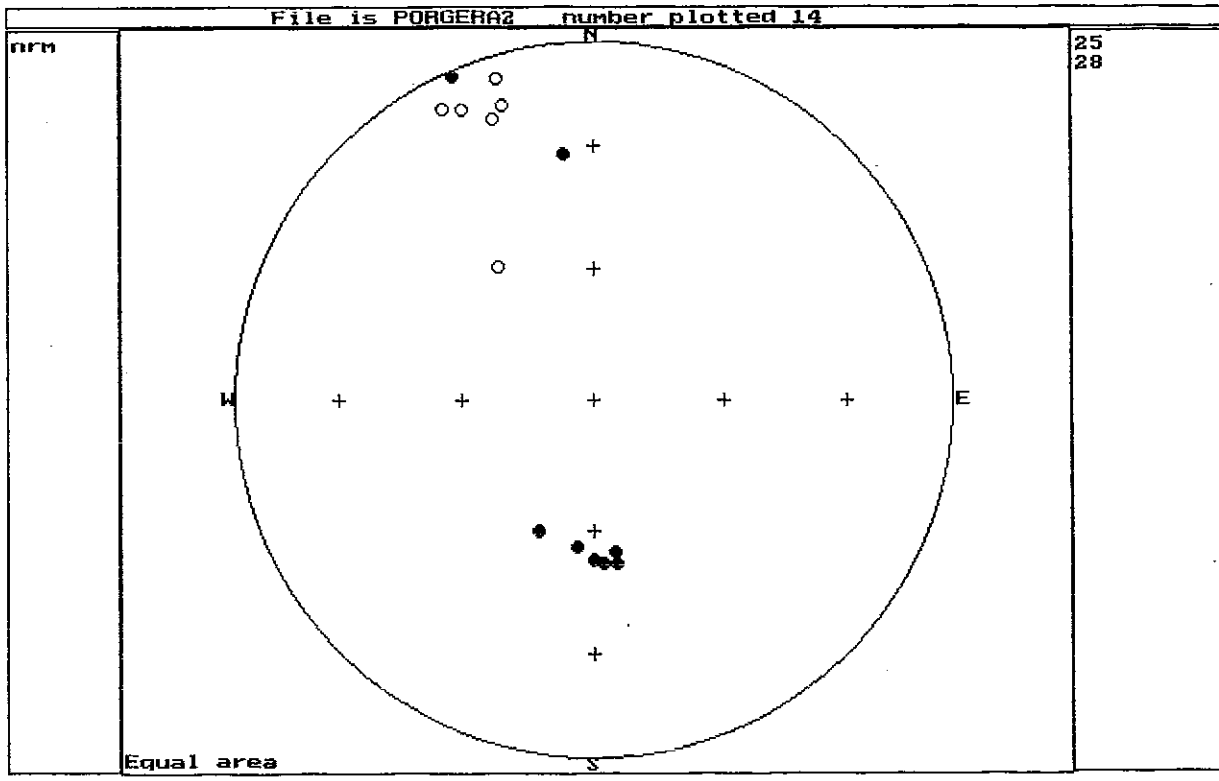

Fig.3. Susceptibility distributions for sampled rock types.

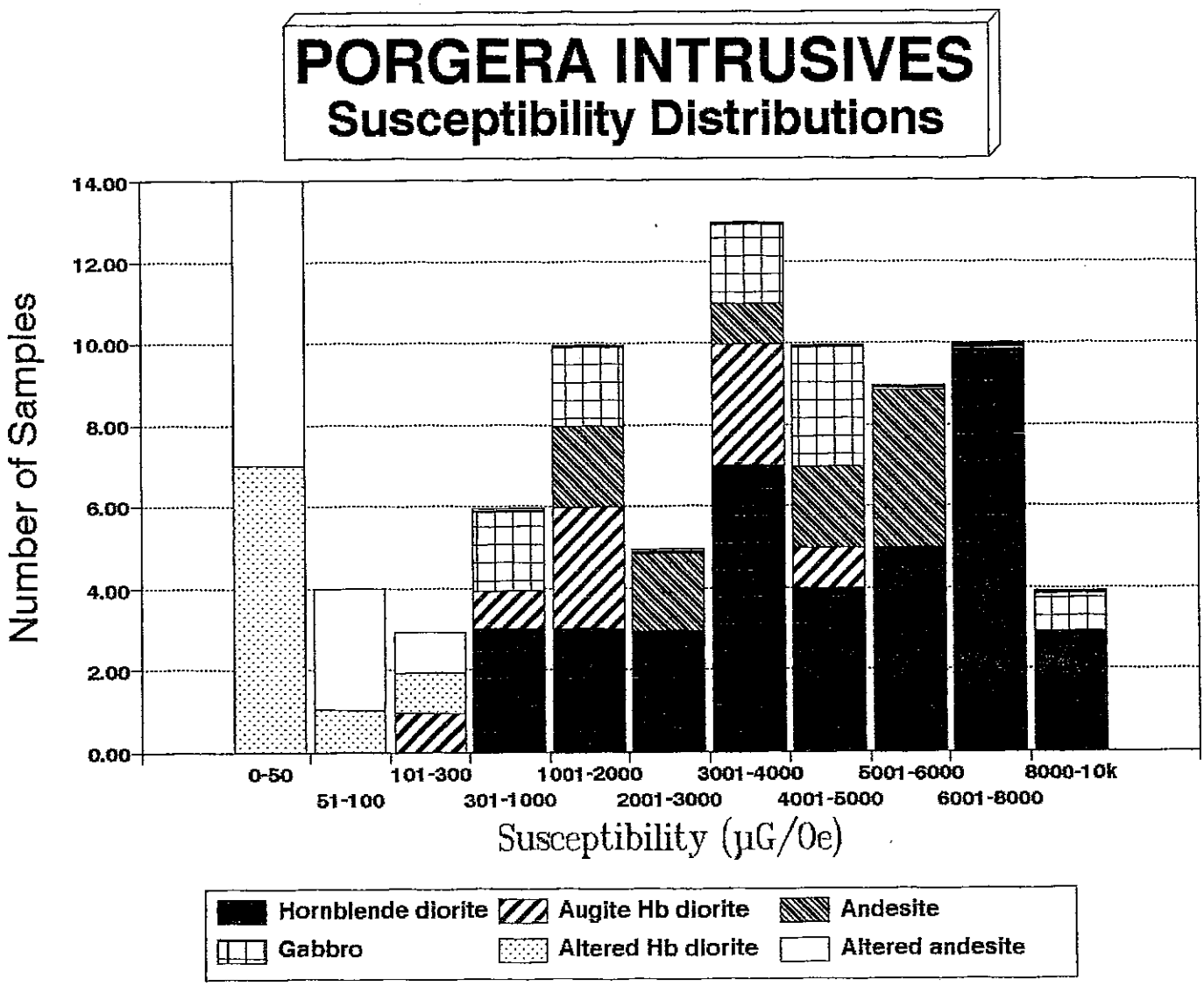
PORGERA INTRUSIVES
Susceptibility Distributions
Number of Samples
14.00
12.00
10.00
8.00
6.00
4.00
2.00
0.00
0-50
51-100
101-300
301-1000
1001-2000
2001-3000
3001-4000
4001-5000
5001-6000
6001-8000
8000-10k
Susceptibility (µG/Oe)
Hornblende diorite
Augite Hb diorite
Andesite
Gabbro
Altered Hb diorite
Altered andesite

Magnetisation is a three dimensional vector quantity and difficulties arise when representing such on a flat surface. Two separate figures are required to display a three dimensional vector. Stereographic plots and an intensity decay curve have been very useful, especially when the direction of the cleaned magnetisation is of paramount importance. However, when an appreciation of the full vectorial nature of a magnetisation is required, orthogonal projections (Zijderveld, 1967) provide an ideal method of combining both the magnitude and directional information. This greatly assists the recognition and identification of multi-component magnetisations.

(a) This illustration portrays the magnetisation decay during eight demagnetisation steps, from an oblique perspective (southeast-up octant). $\tilde{J}_1 - \tilde{J}_2$ represents the vector difference between the first and second demagnetisation step, i.e. the magnetisation removed during the second step.

(b) By simply plotting the vector end-points the diagram is greatly clarified and a soft $(\tilde{J}_s)$ and hard $(\tilde{J}_h)$ magnetisation are evident, yet a unique identification of the direction or intensity of either is not possible from this single figure.

(c) Linear combination of magnetisations yields a resultant NRM $(\tilde{J}_o)$.

(d) By projecting vector end-points onto the horizontal plane and a vertical plane allows the composition of the magnetisation to be visualised.

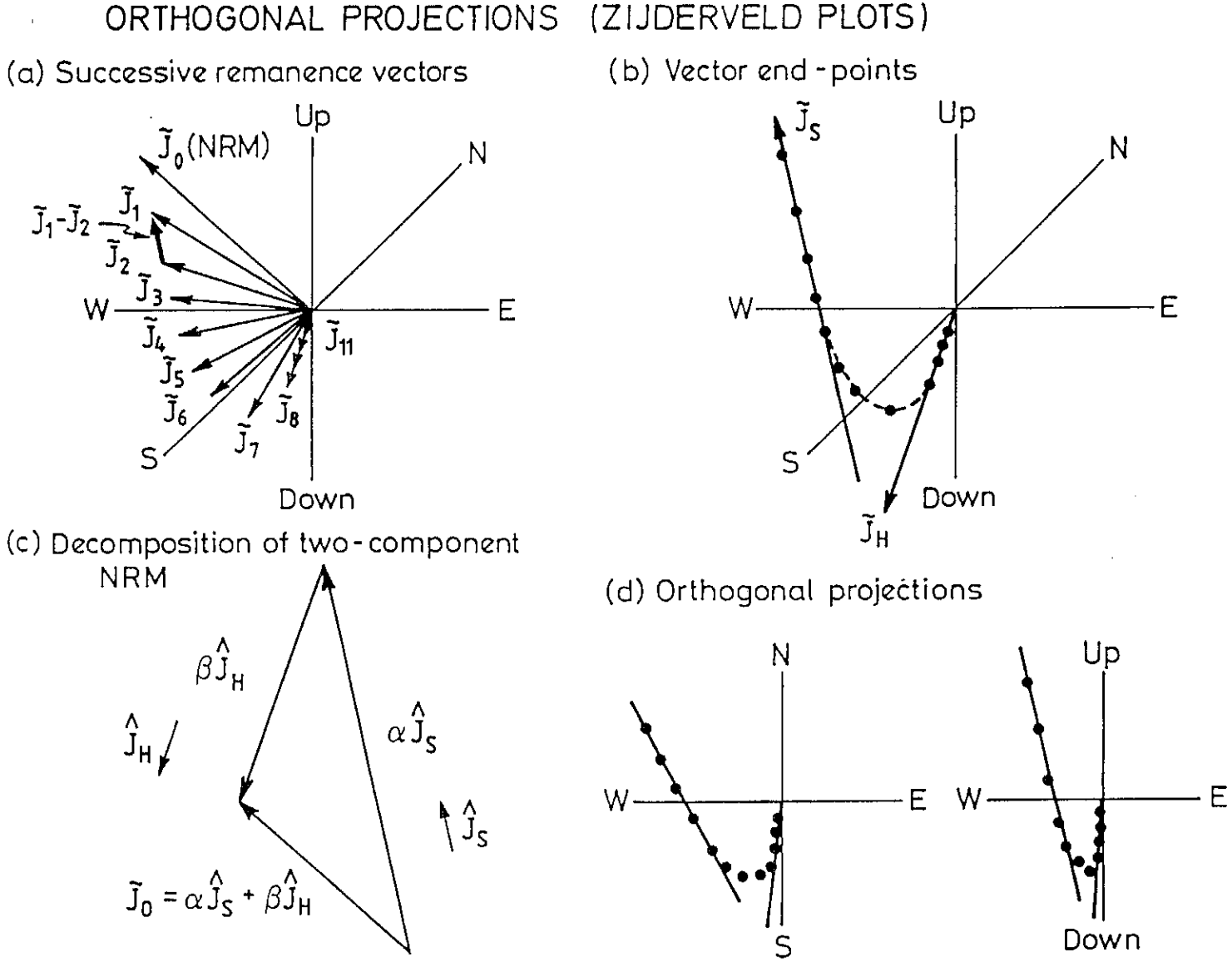
ORTHOGONAL PROJECTIONS (ZIJDERVELD PLOTS)
(a) Successive remanence vectors
Up
N
W
E
S
Down
$\tilde{J}_0$(NRM)
$\tilde{J}_1$
$\tilde{J}_1-\tilde{J}_2$
$\tilde{J}_2$
$\tilde{J}_3$
$\tilde{J}_4$
$\tilde{J}_5$
$\tilde{J}_6$
$\tilde{J}_7$
$\tilde{J}_8$
$\tilde{J}_{11}$
(b) Vector end-points
$\tilde{J}_S$
$\tilde{J}_H$
(c) Decomposition of two-component NRM
$\beta\hat{J}_H$
$\alpha\hat{J}_S$
$\hat{J}_H$
$\hat{J}_S$
$\tilde{J}_0 = \alpha\hat{J}_S + \beta\hat{J}_H$
(d) Orthogonal projections

Fig.4

Fig.5. Zijderveld plots for the Yakatabari samples.

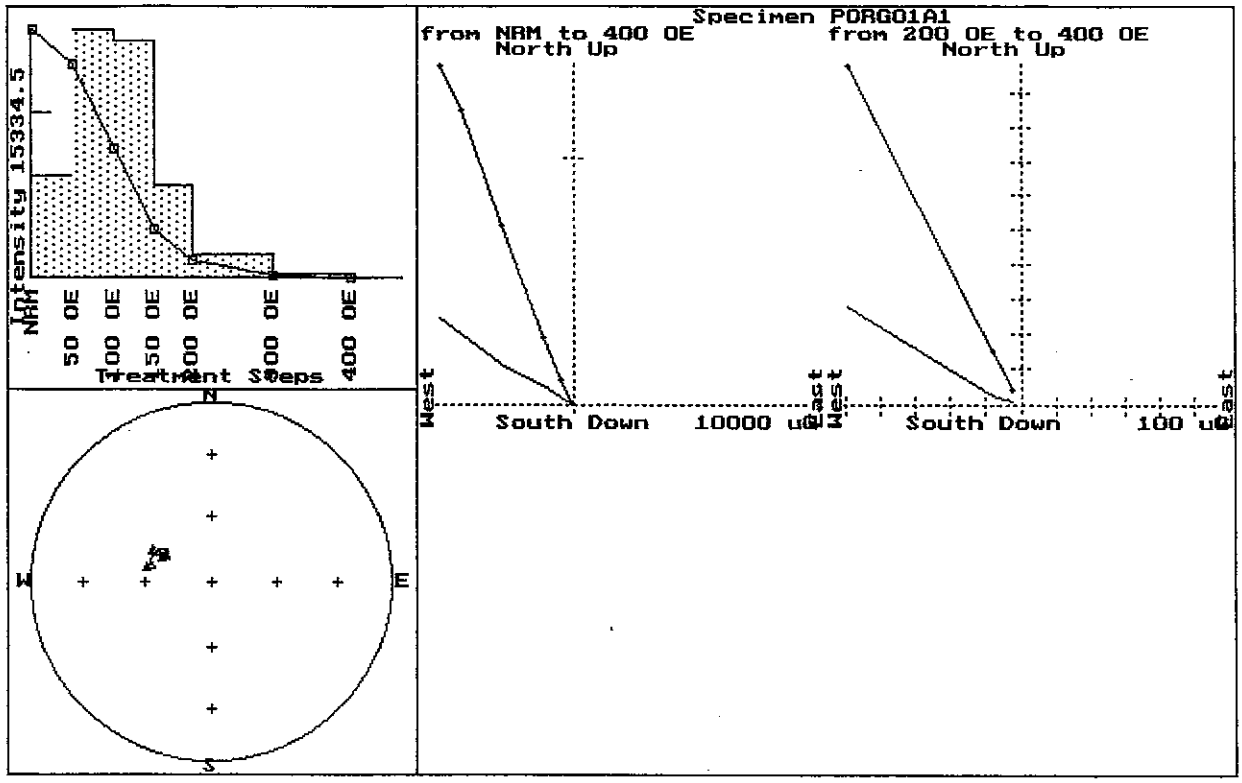
Intensity 15334.5
NRM
50 OE
100 OE
150 OE
200 OE
300 OE
400 OE
Treatment Steps
N
W
E
S
Specimen PORG01A1
from NRM to 400 OE
North Up
West
South Down
10000 uG
East
from 200 OE to 400 OE
North Up
West
South Down
100 uG
East

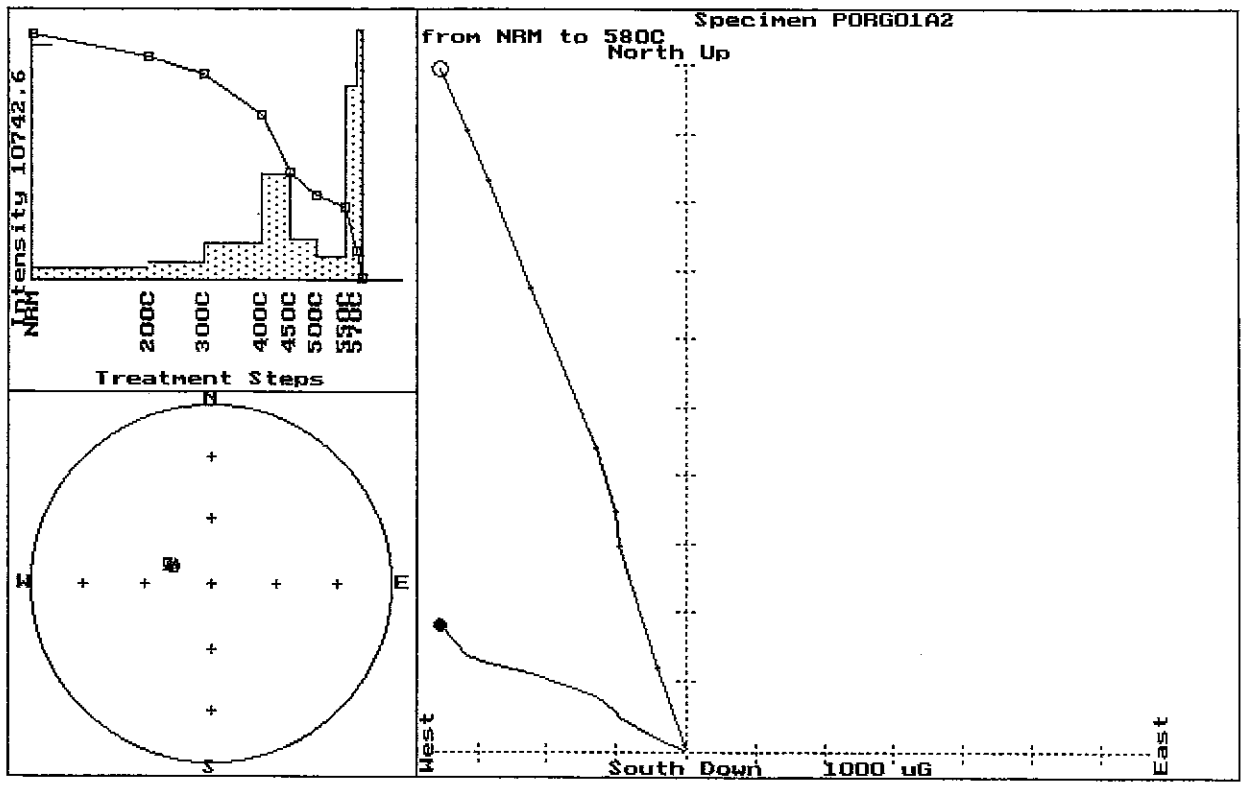
Intensity 10742.6
NRM
200C
300C
400C
450C
500C
550C
580C
Treatment Steps
N
W
E
S
Specimen PORG01A2
from NRM to 580C
North Up
West
South Down
1000 uG
East

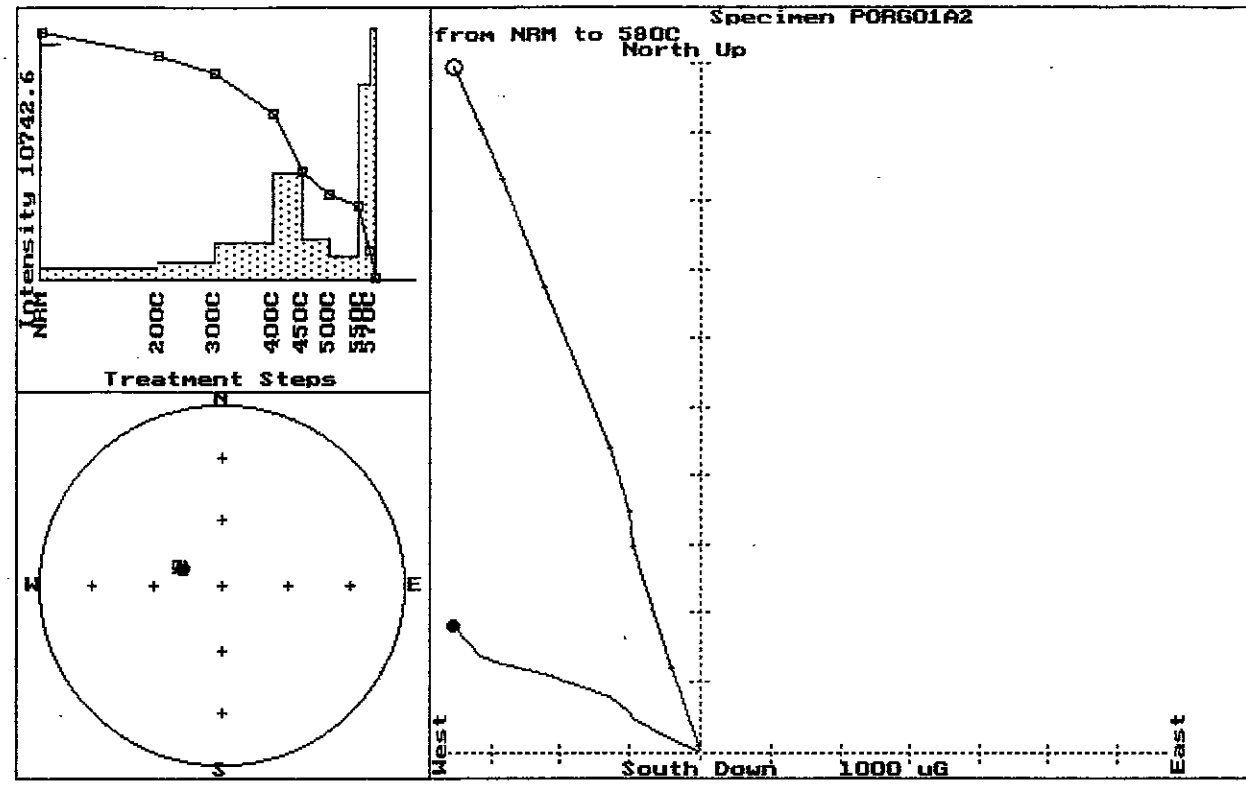
Intensity 10742.6
NRM
200C
300C
400C
450C
500C
550C
Treatment Steps
N
E
W
S
Specimen PORGO1A2
from NRM to 580C
North Up
West
South Down
1000 uG
East

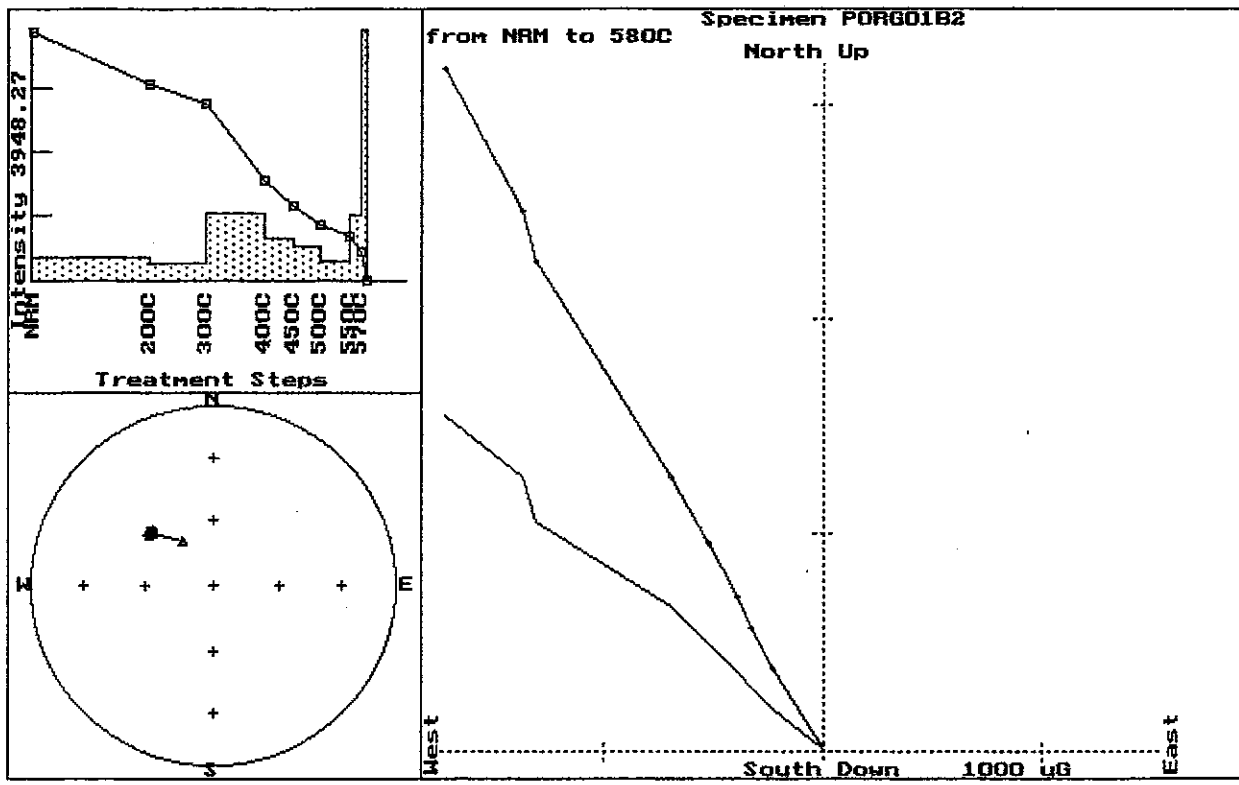
Intensity 3948.27
NRM
200C
300C
400C
450C
500C
550C
Treatment Steps
N
E
W
S
Specimen PORGO1B2
from NRM to 580C
North Up
West
South Down
1000 uG
East

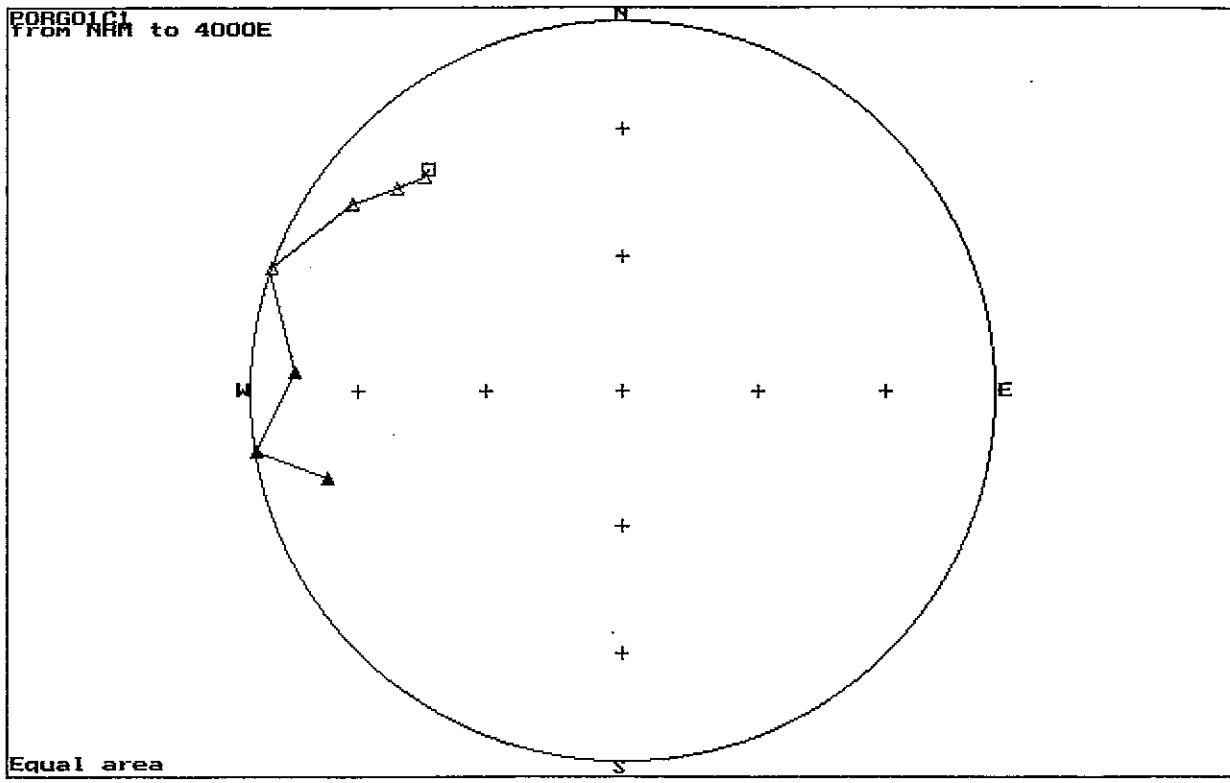
PORGO1C1
from NRM to 4000E
N
W
E
S
Equal area

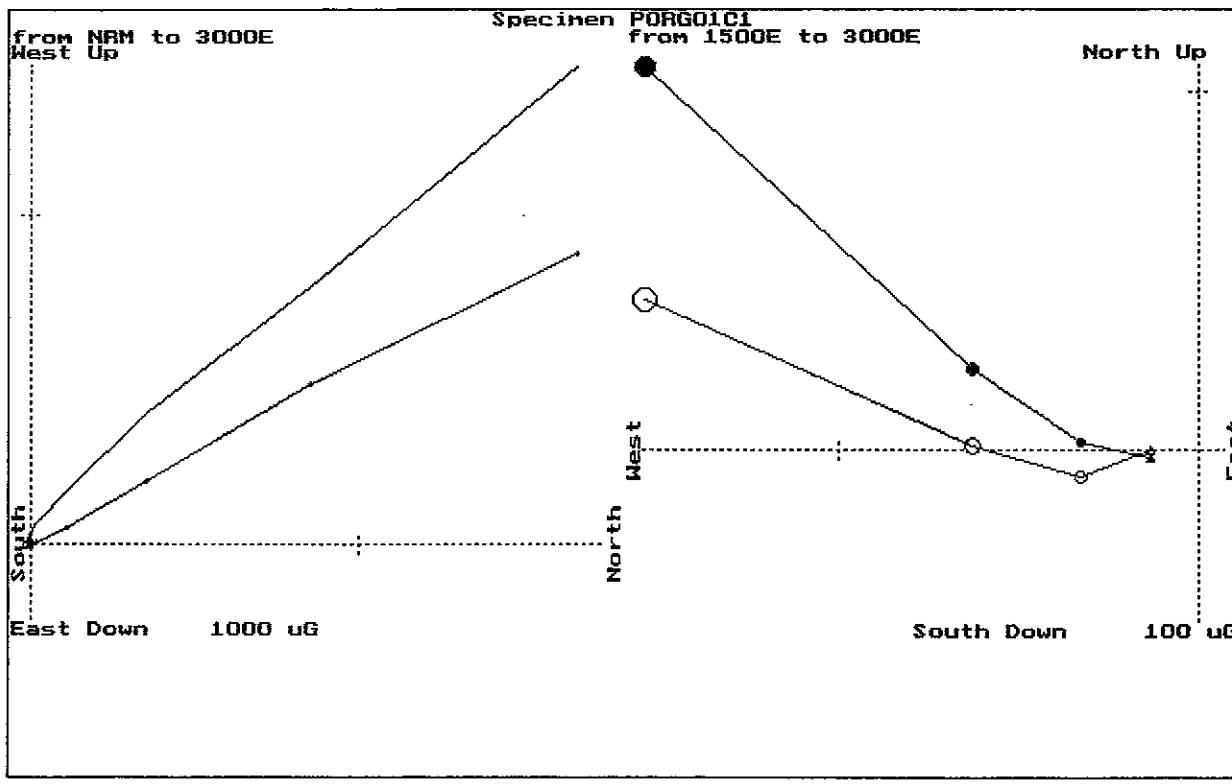
Specimen PORGO1C1
from NRM to 3000E
West Up
from 1500E to 3000E
North Up
South
North
West
East
East Down 1000 uG
South Down 100 uG

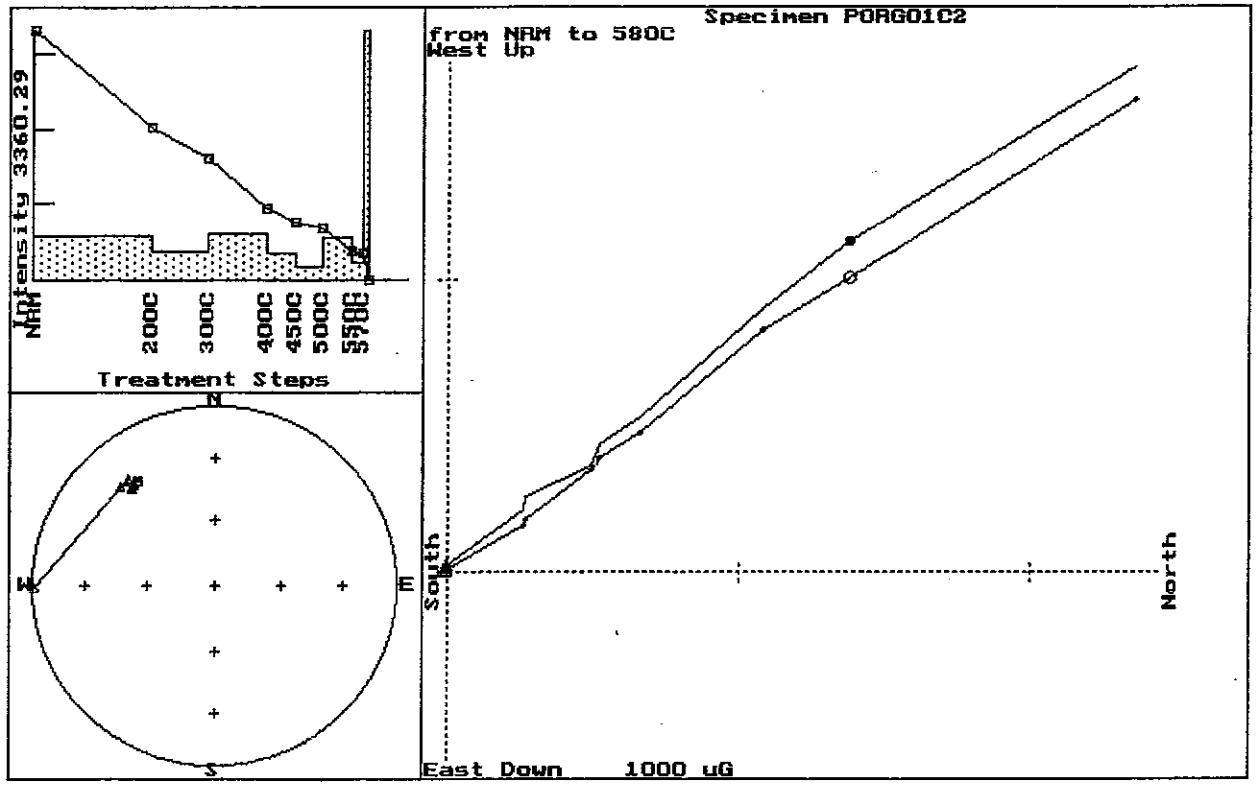
Specimen PORGO1C2
from NRM to 580C
West Up
Intensity 3360.29
NRM
200C
300C
400C
450C
500C
550C
580C
Treatment Steps
N
E
S
W
South
North
East Down
1000 uG

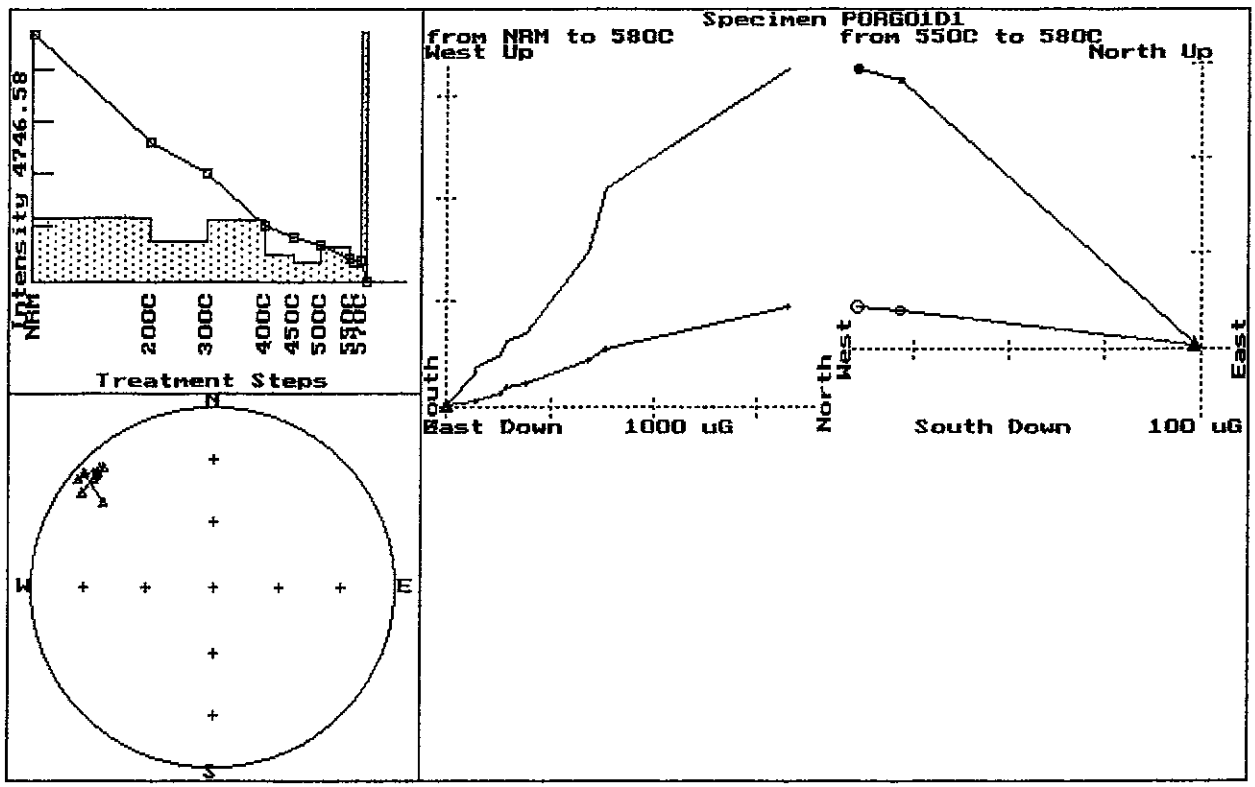
Specimen PORGO1D1
from NRM to 580C
West Up
from 550C to 580C
North Up
Intensity 4746.58
NRM
200C
300C
400C
450C
500C
550C
580C
Treatment Steps
N
E
S
W
South
East Down
1000 uG
North
West
East
South Down
100 uG

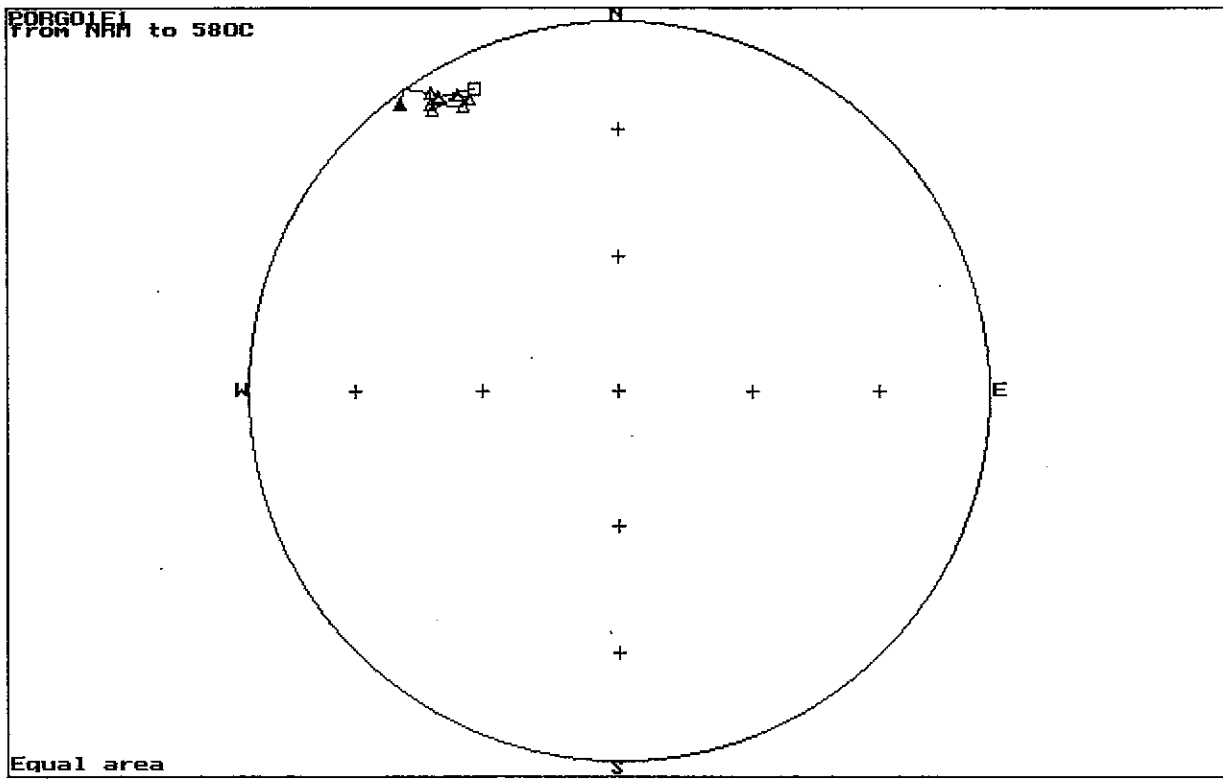
PORGO1E1
from NRM to 580C
N
W
E
S
Equal area

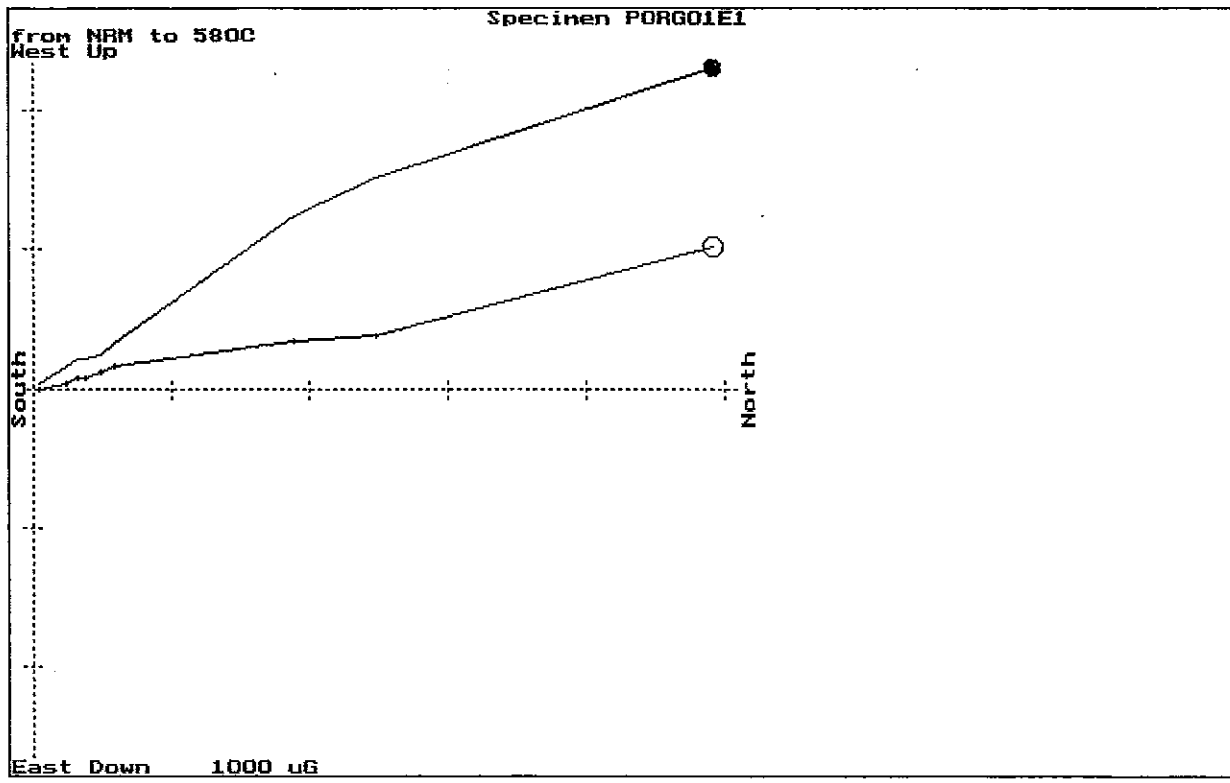
Specimen PORGO1E1
from NRM to 580C
West Up
South
North
East Down
1000 uG

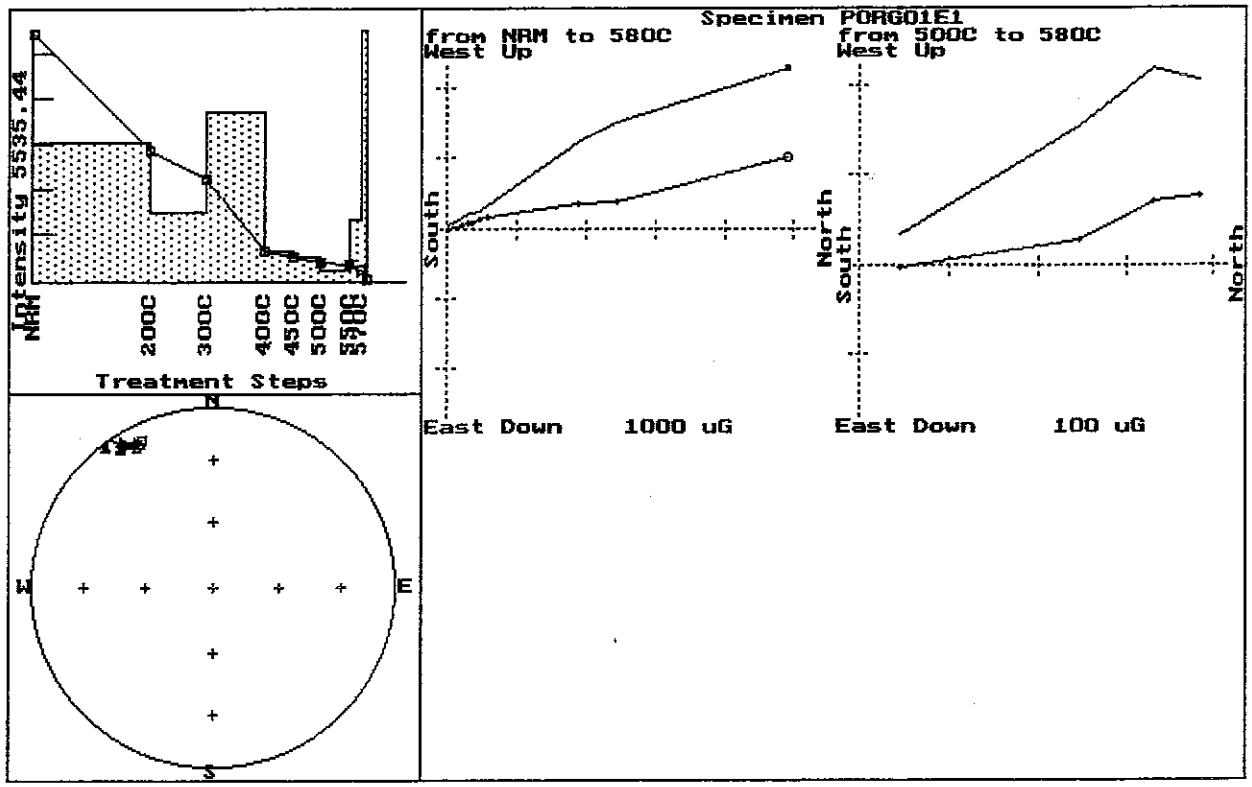
Intensity 5535.44
NRM
200C
300C
400C
450C
500C
580C
Treatment Steps
N
E
S
W
Specimen PORG01E1
from NRM to 580C
West Up
South
East Down
1000 uG
from 500C to 580C
West Up
North
South
North
East Down
100 uG

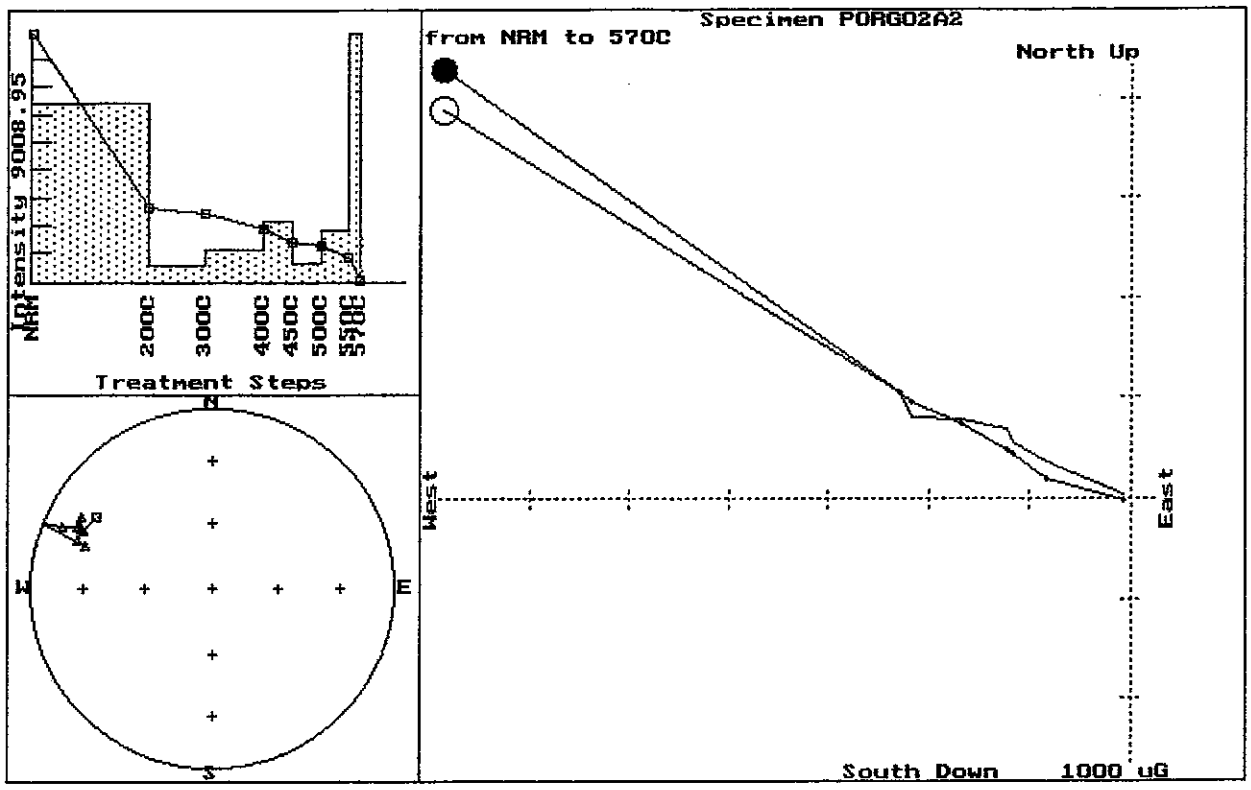
Intensity 9008.95
NRM
200C
300C
400C
450C
500C
570C
Treatment Steps
N
E
S
W
Specimen PORG02A2
from NRM to 570C
North Up
West
East
South Down
1000 uG

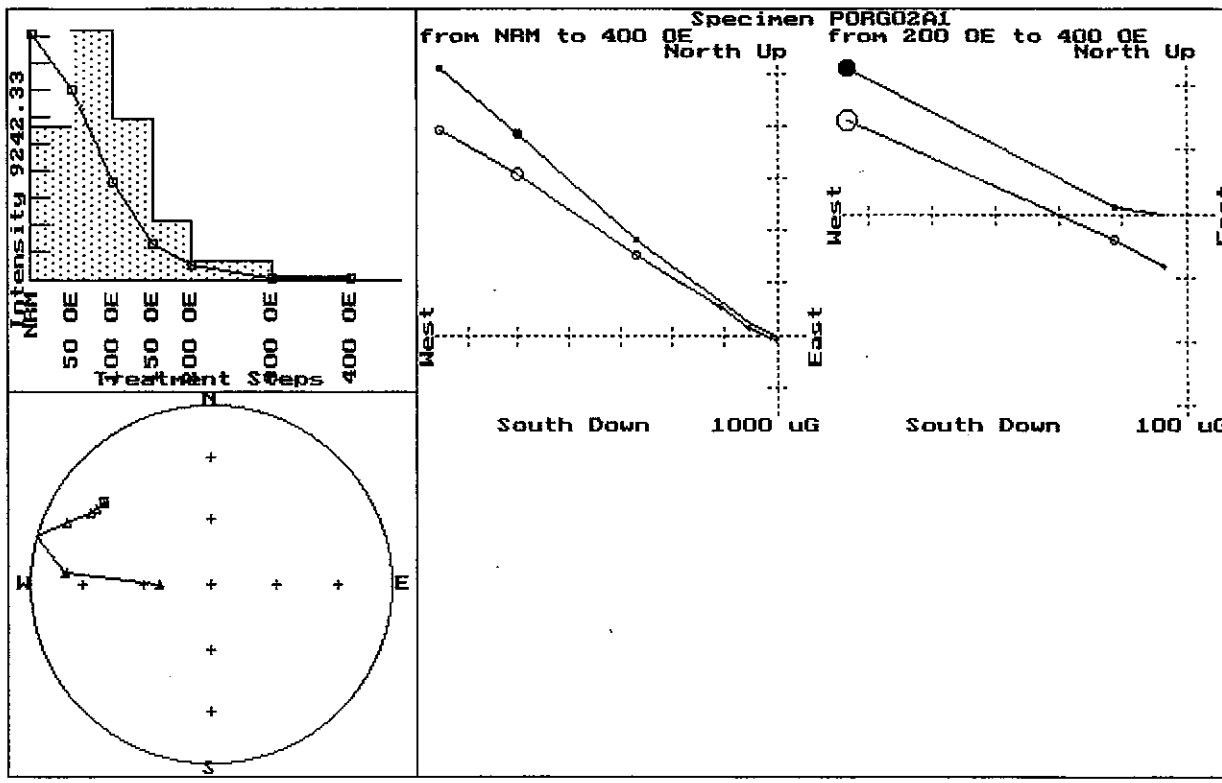
Intensity 9242.33
NRM
50 OE
100 OE
150 OE
200 OE
300 OE
400 OE
Treatment Steps
N
W
E
S
Specimen PORG02A1
from NRM to 400 OE
North Up
West
East
South Down
1000 uG
from 200 OE to 400 OE
North Up
West
East
South Down
100 uG

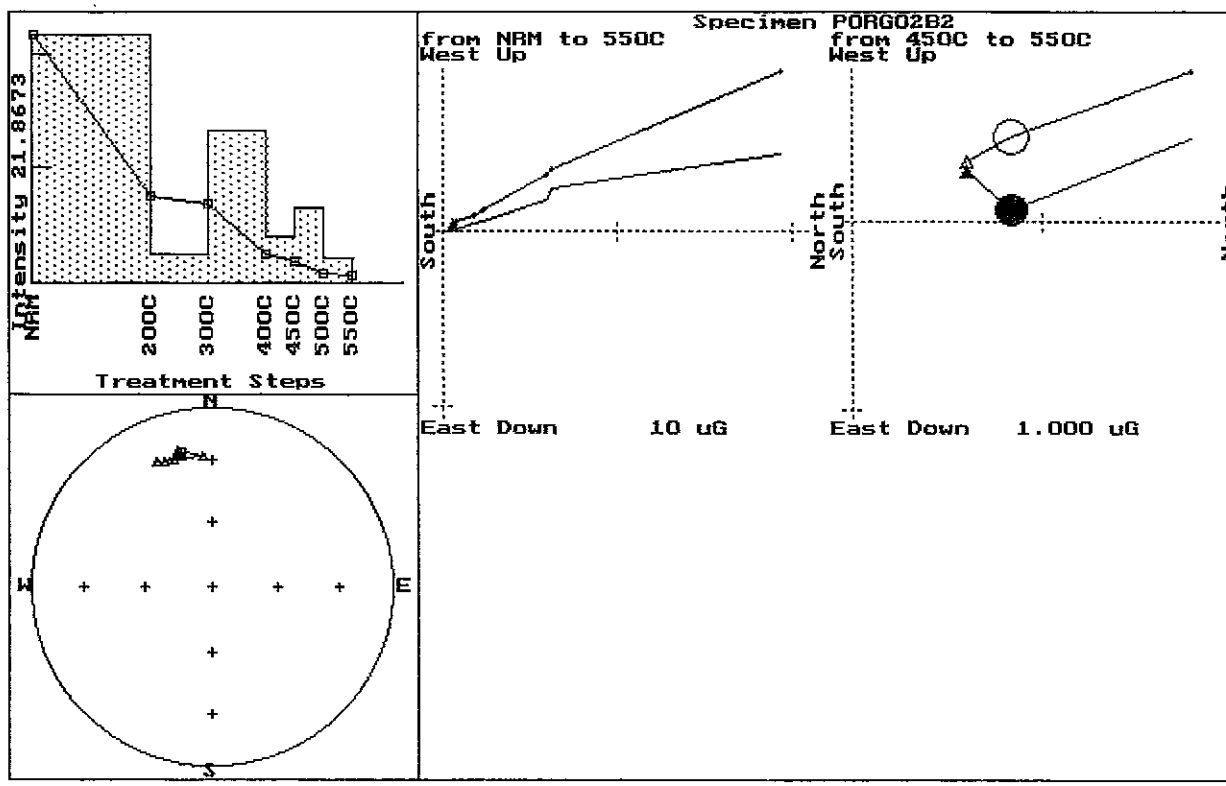
Intensity 21.8673
NRM
200C
300C
400C
450C
500C
550C
Treatment Steps
N
W
E
S
Specimen PORG02B2
from NRM to 550C
West Up
South
East Down
10 uG
from 450C to 550C
West Up
North
South
East Down
1.000 uG

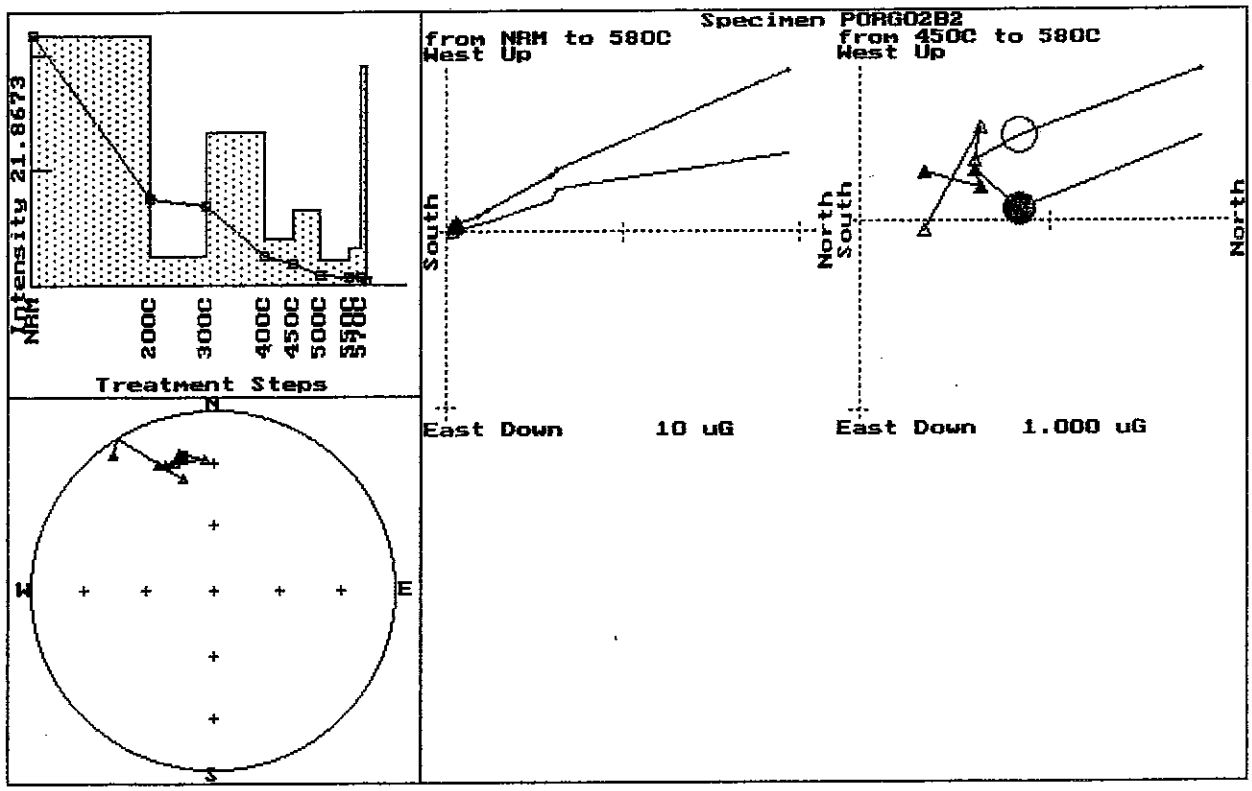
Intensity 21.8673
NRM
200C
300C
400C
450C
500C
580C
Treatment Steps
N
W
E
S
Specimen PORG02B2
from NRM to 580C
West Up
South
East Down
10 uG
from 450C to 580C
West Up
North
South
East Down
1.000 uG

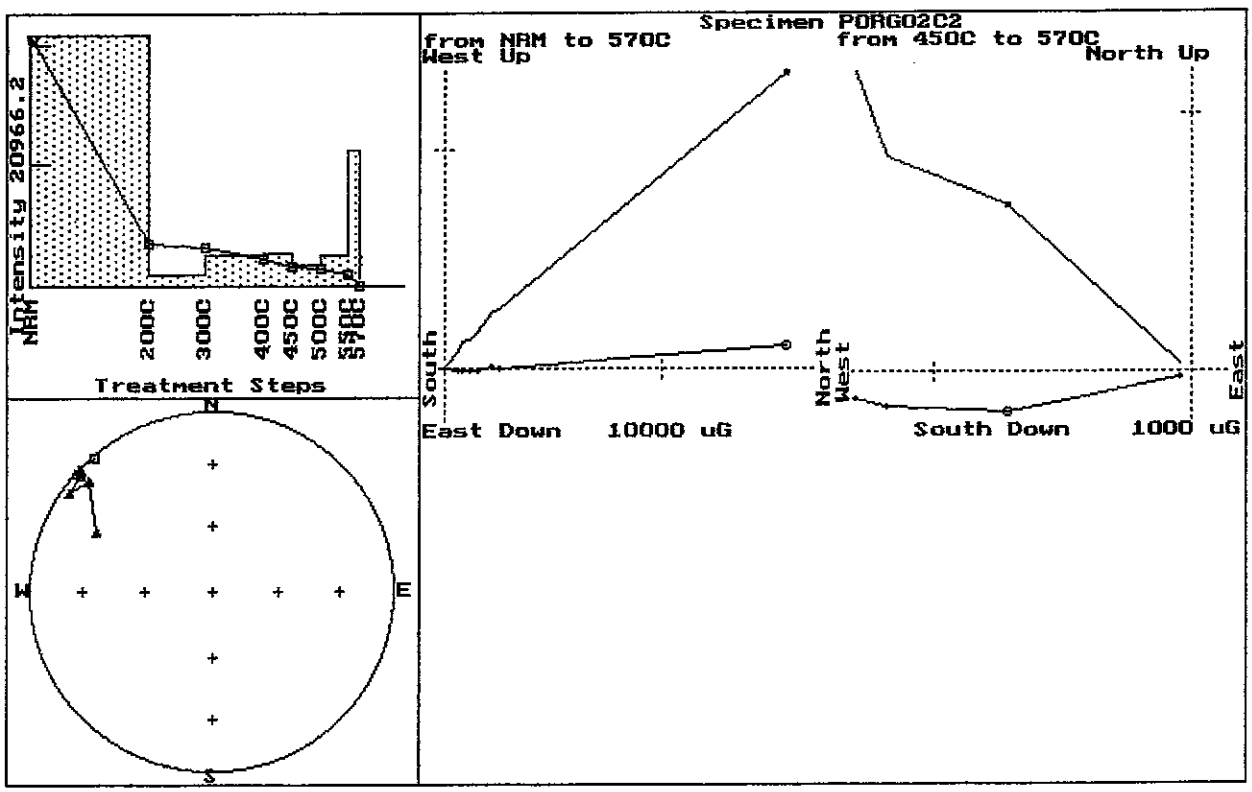
Intensity 20966.2
NRM
200C
300C
400C
450C
500C
570C
Treatment Steps
N
W
E
S
Specimen PORG02C2
from NRM to 570C
West Up
South
East Down
10000 uG
from 450C to 570C
North Up
North
West
East
South Down
1000 uG

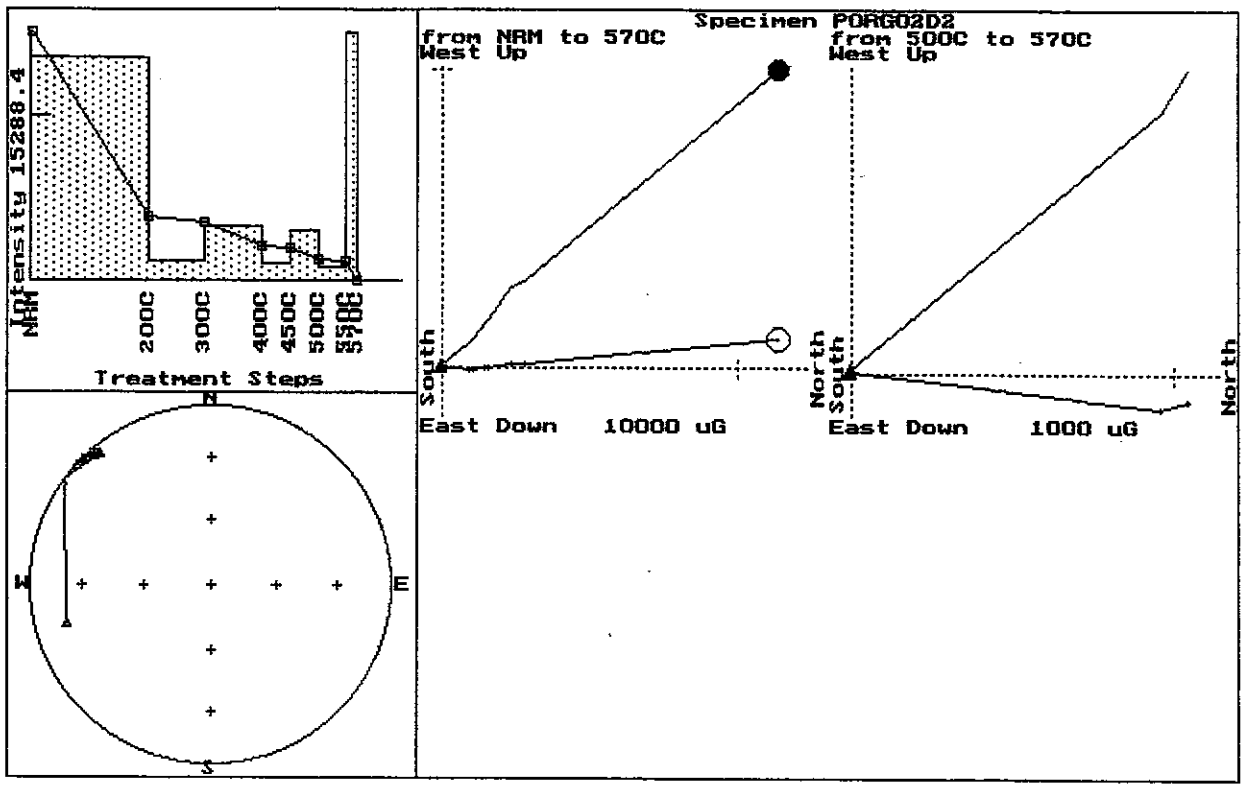
Intensity 15288.4
NRM
200C
300C
400C
450C
500C
570C
Treatment Steps
N
E
S
W
Specimen PORG02D2
from NRM to 570C
West Up
South
East Down
10000 uG
from 500C to 570C
West Up
North
South
East Down
1000 uG
North

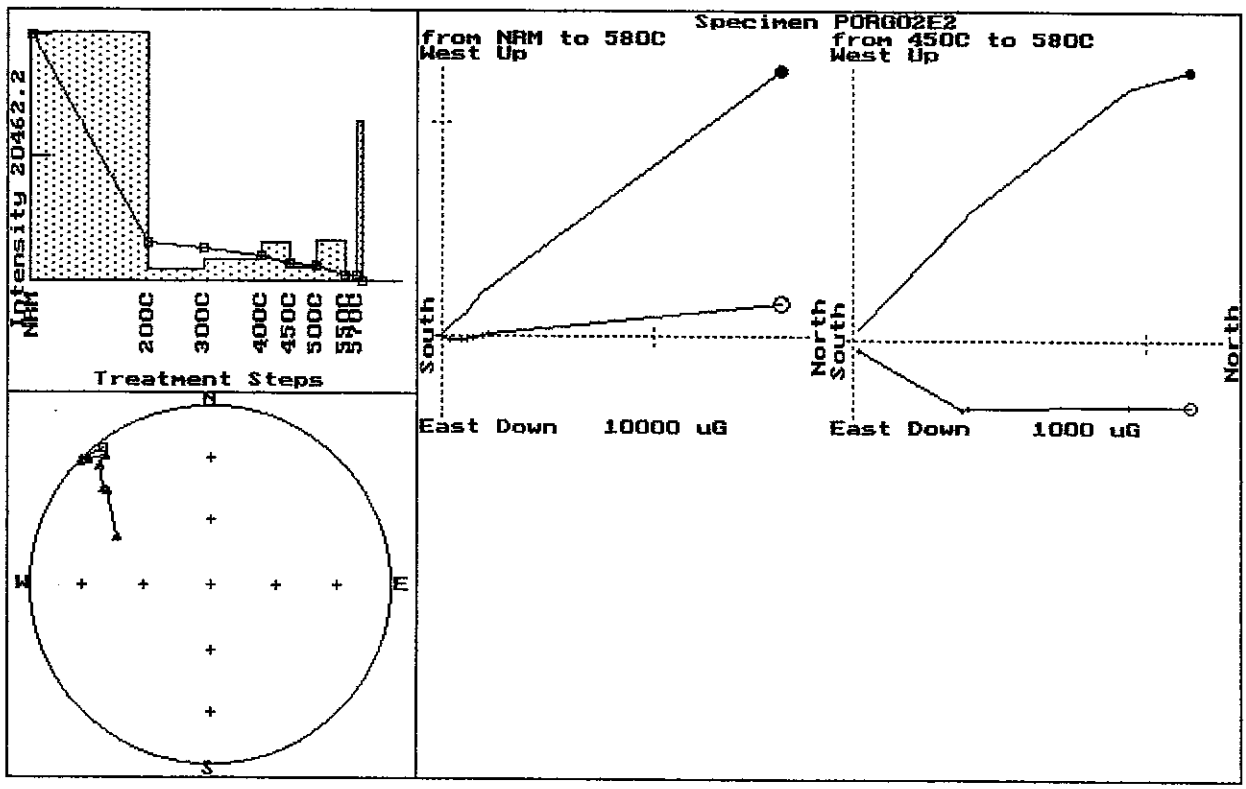
Intensity 20462.2
NRM
200C
300C
400C
450C
500C
580C
Treatment Steps
N
E
S
W
Specimen PORG02E2
from NRM to 580C
West Up
South
East Down
10000 uG
from 450C to 580C
West Up
North
South
East Down
1000 uG
North

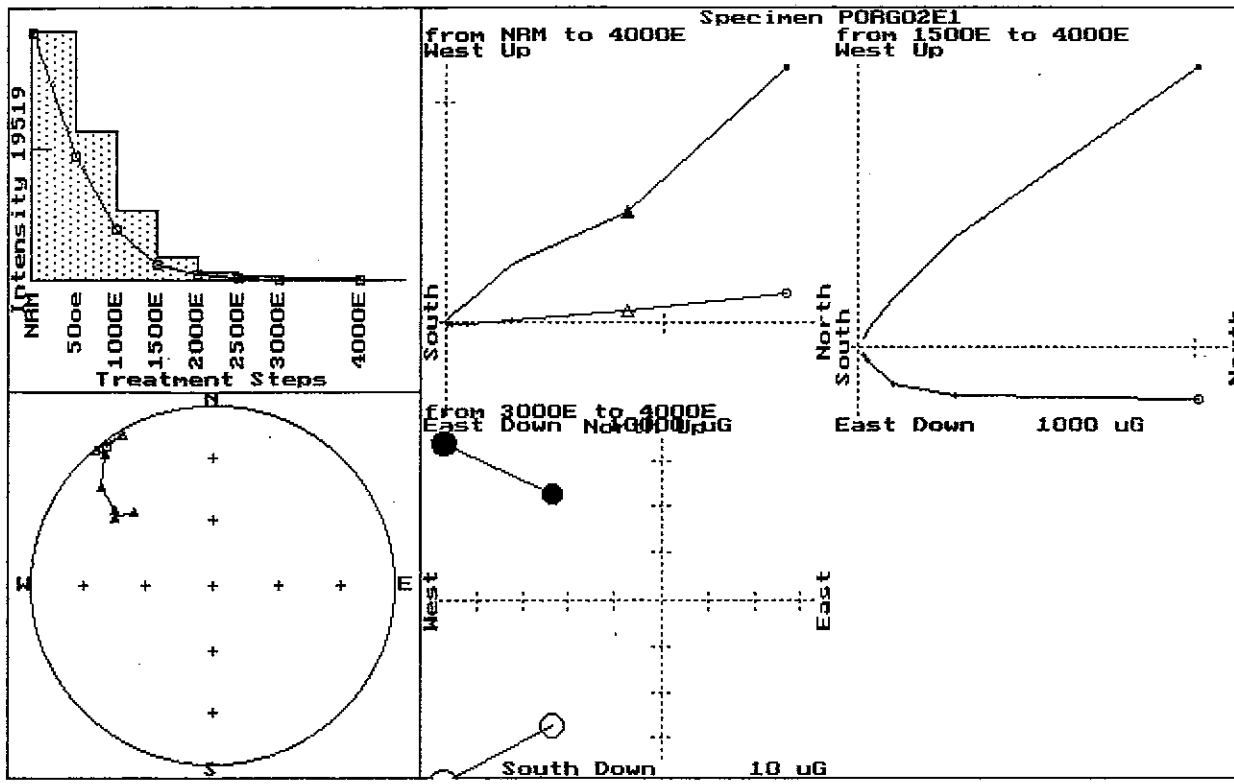
Specimen PORG02E1
Intensity 19519
NRM
50oe
1000E
1500E
2000E
2500E
3000E
4000E
Treatment Steps
from NRM to 4000E
West Up
South
from 1500E to 4000E
West Up
North
South
North
from 3000E to 4000E
East Down
East Down 1000 uG
West
East
South Down 10 uG

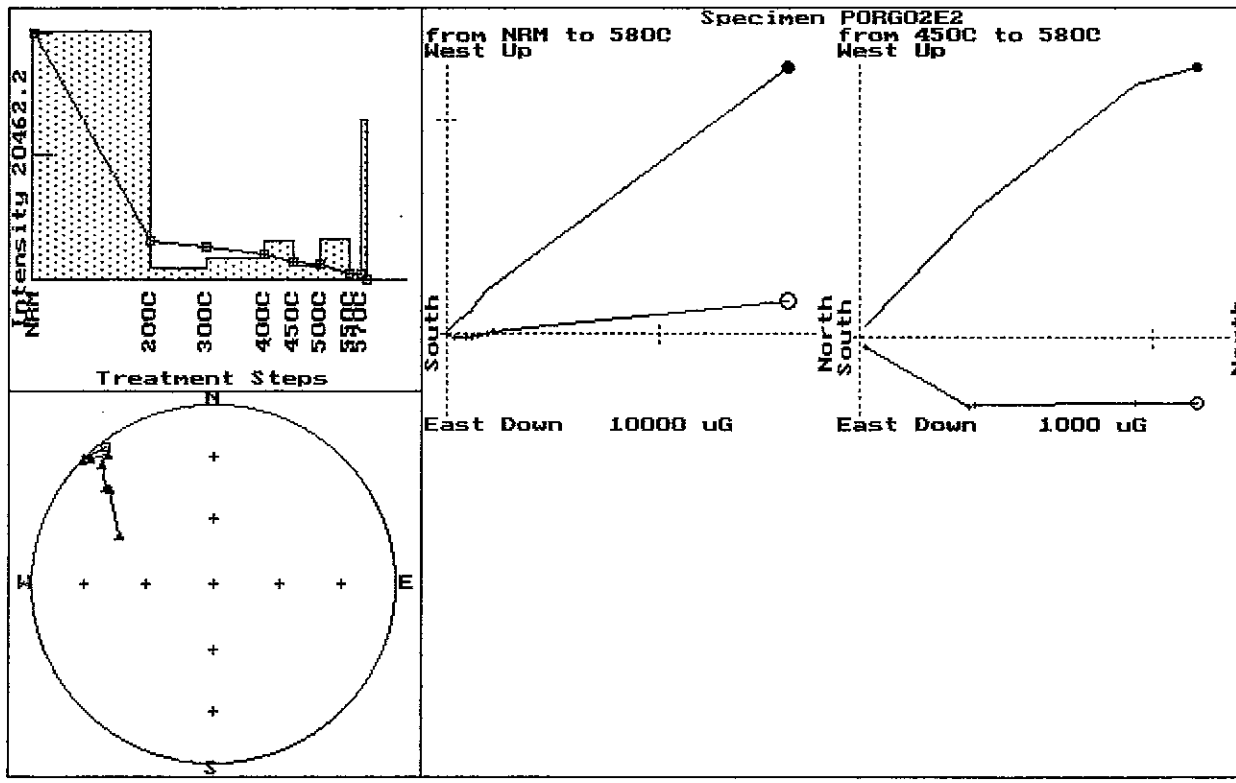
Specimen PORG02E2
Intensity 20462.2
NRM
200C
300C
400C
450C
500C
Treatment Steps
from NRM to 580C
West Up
South
East Down 10000 uG
from 450C to 580C
West Up
North
South
North
East Down 1000 uG

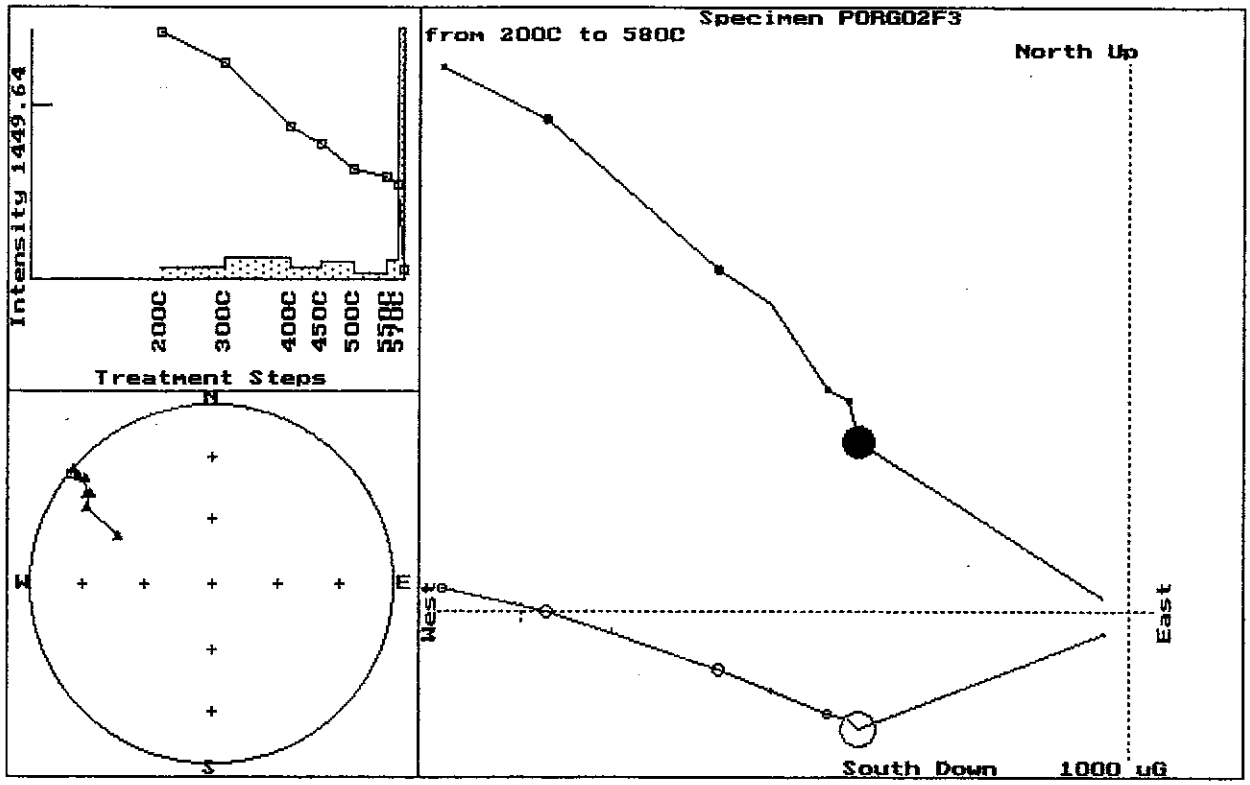
Specimen PORG02F3
from 200C to 580C
North Up
Intensity 1449.64
200C
300C
400C
450C
500C
580C
Treatment Steps
N
E
S
W
West
East
South Down
1000 uG

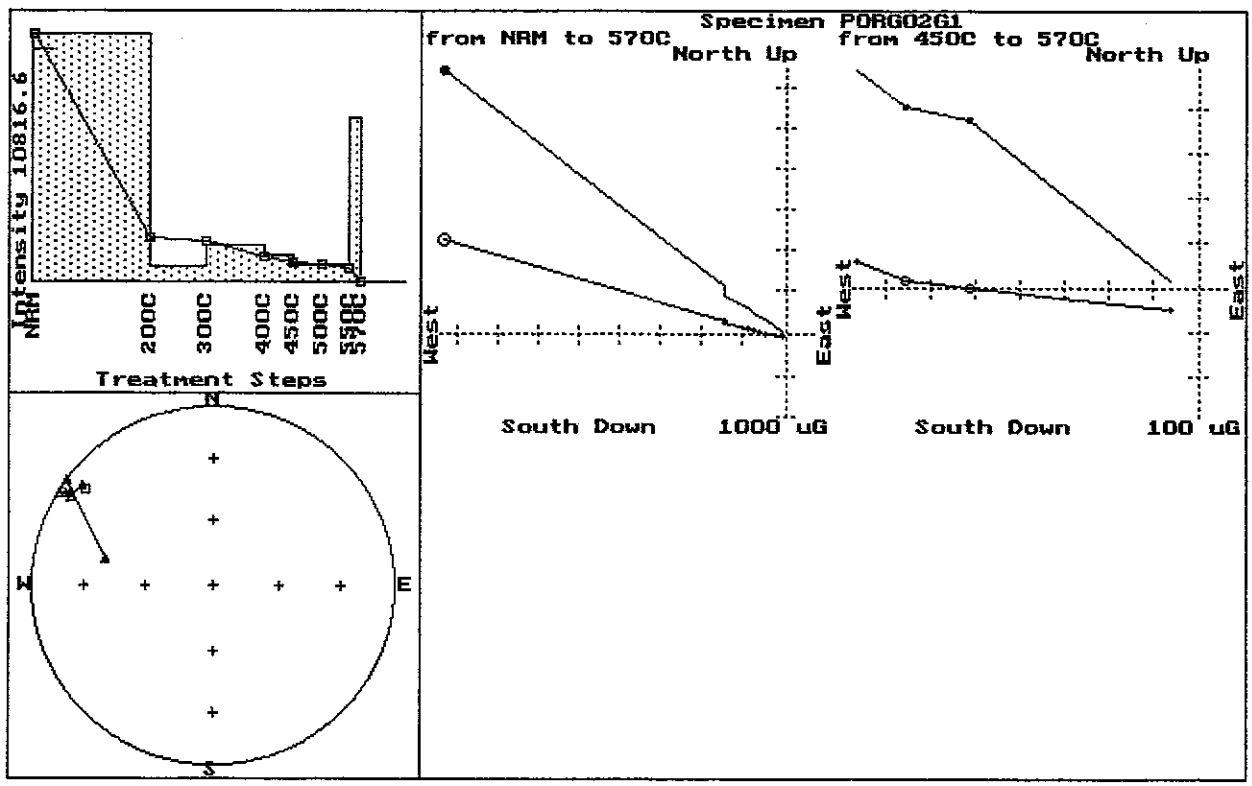
Specimen PORG02G1
from NRM to 570C
North Up
from 450C to 570C
North Up
Intensity 10816.6
NRM
200C
300C
400C
450C
500C
570C
Treatment Steps
N
E
S
W
West
East
South Down
1000 uG
West
East
South Down
100 uG

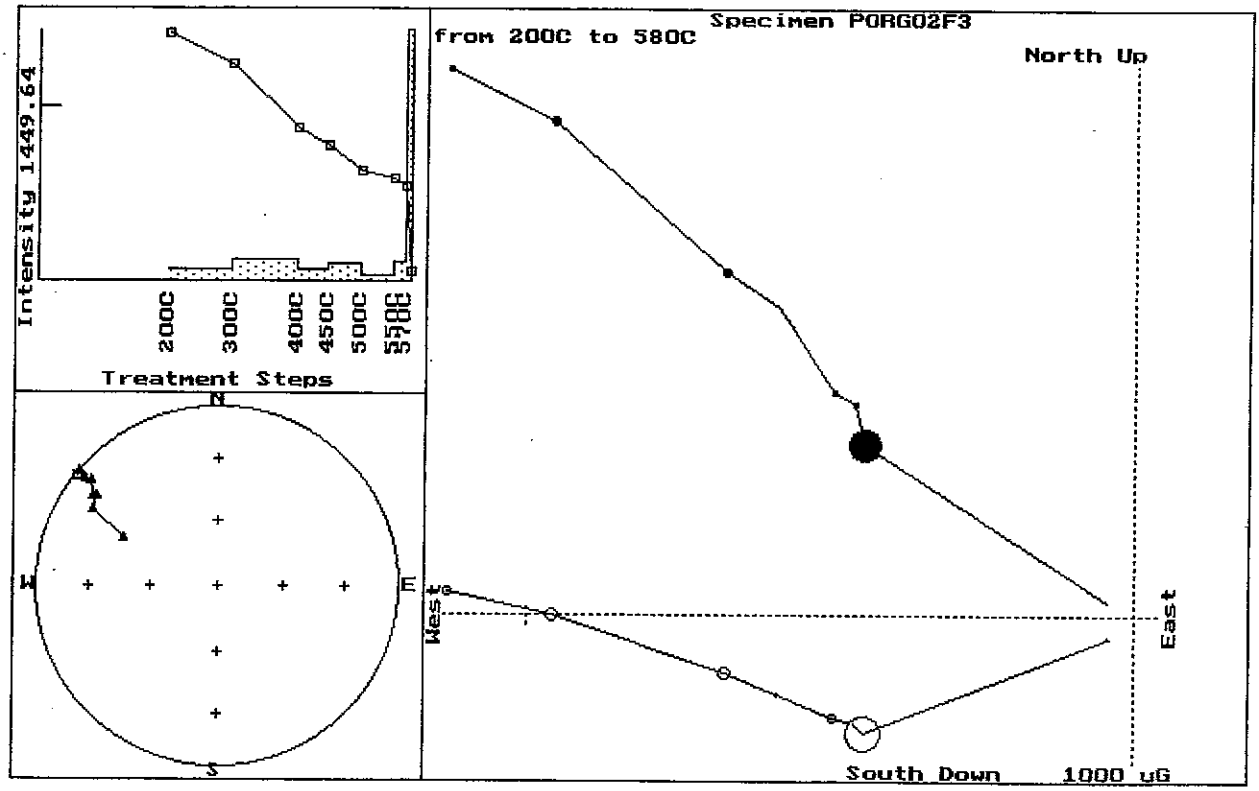
Intensity 1449.64
200C
300C
400C
450C
500C
580C
Treatment Steps
N
W
E
S
Specimen PORG02F3
from 200C to 580C
North Up
West
East
South Down
1000 uG

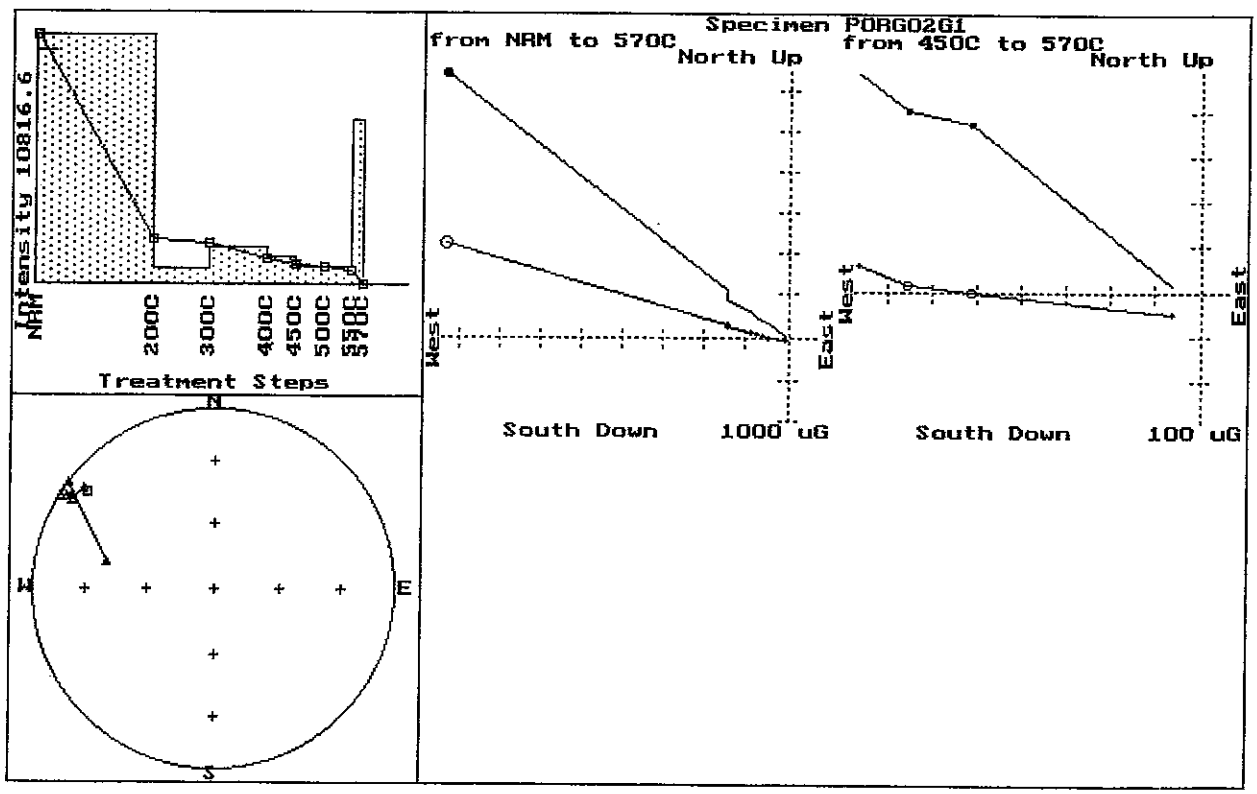
Intensity 10816.6
NRM
200C
300C
400C
450C
500C
570C
Treatment Steps
N
W
E
S
Specimen PORG02G1
from NRM to 570C
North Up
West
East
South Down
1000 uG
from 450C to 570C
North Up
West
East
South Down
100 uG

Fig.6. Zijderveld plots for the Waruwari altered hornblende diorite samples.

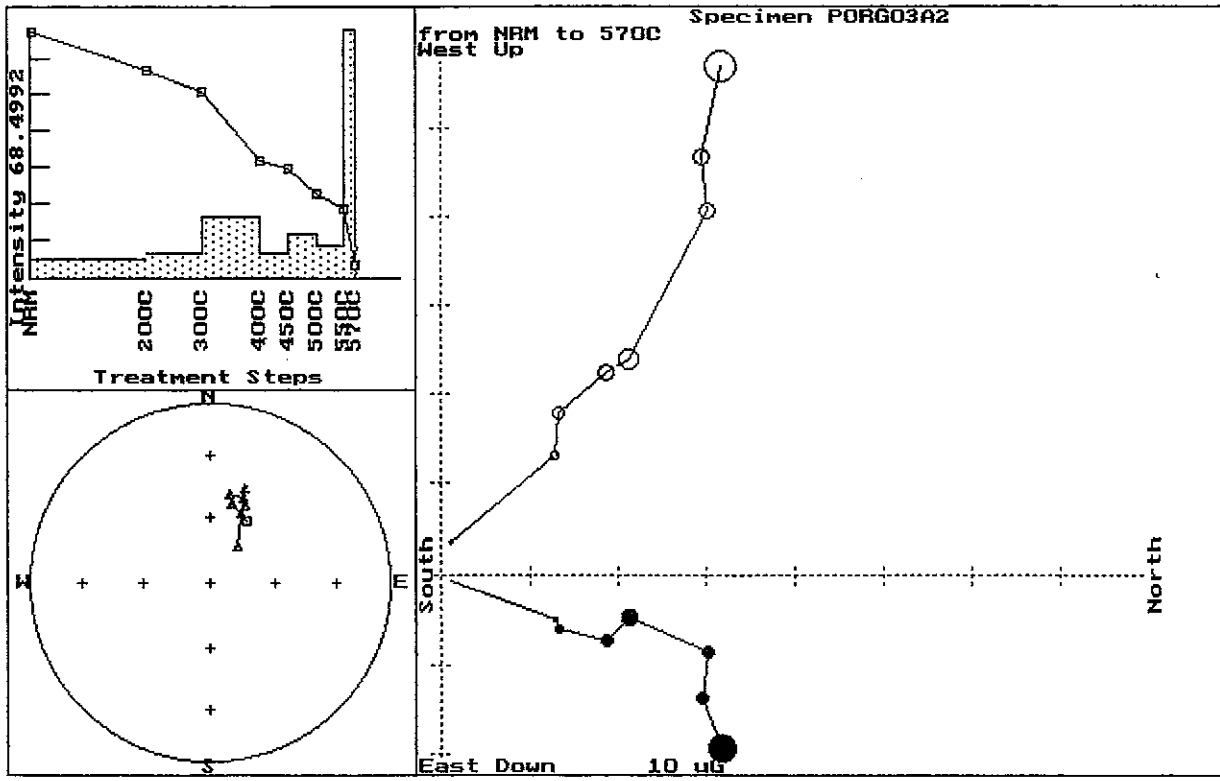
Intensity 68.4992
NRM
200C
300C
400C
450C
500C
550C
570C
Treatment Steps
N
W
E
S
Specimen PORG03A2
from NRM to 570C
West Up
South
North
East Down
10 uG

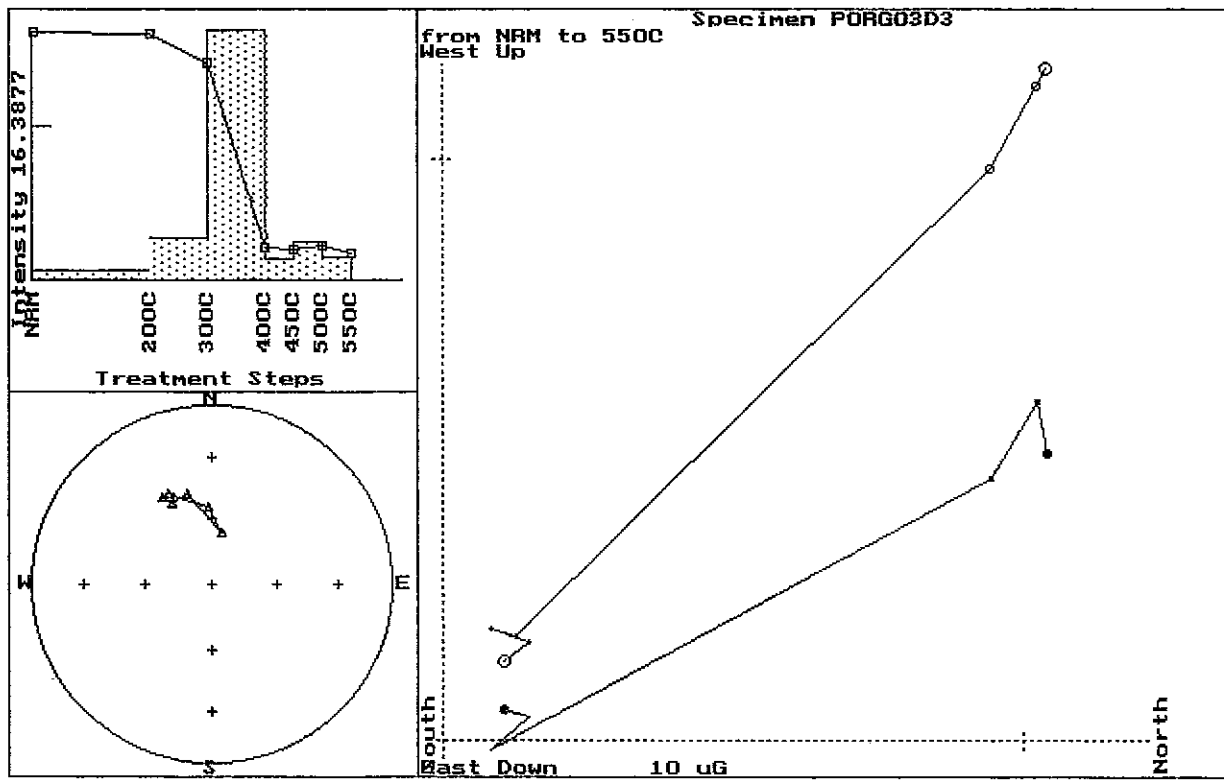
Intensity 16.3877
NRM
200C
300C
400C
450C
500C
550C
Treatment Steps
N
W
E
S
Specimen PORG03D3
from NRM to 550C
West Up
South
North
East Down
10 uG

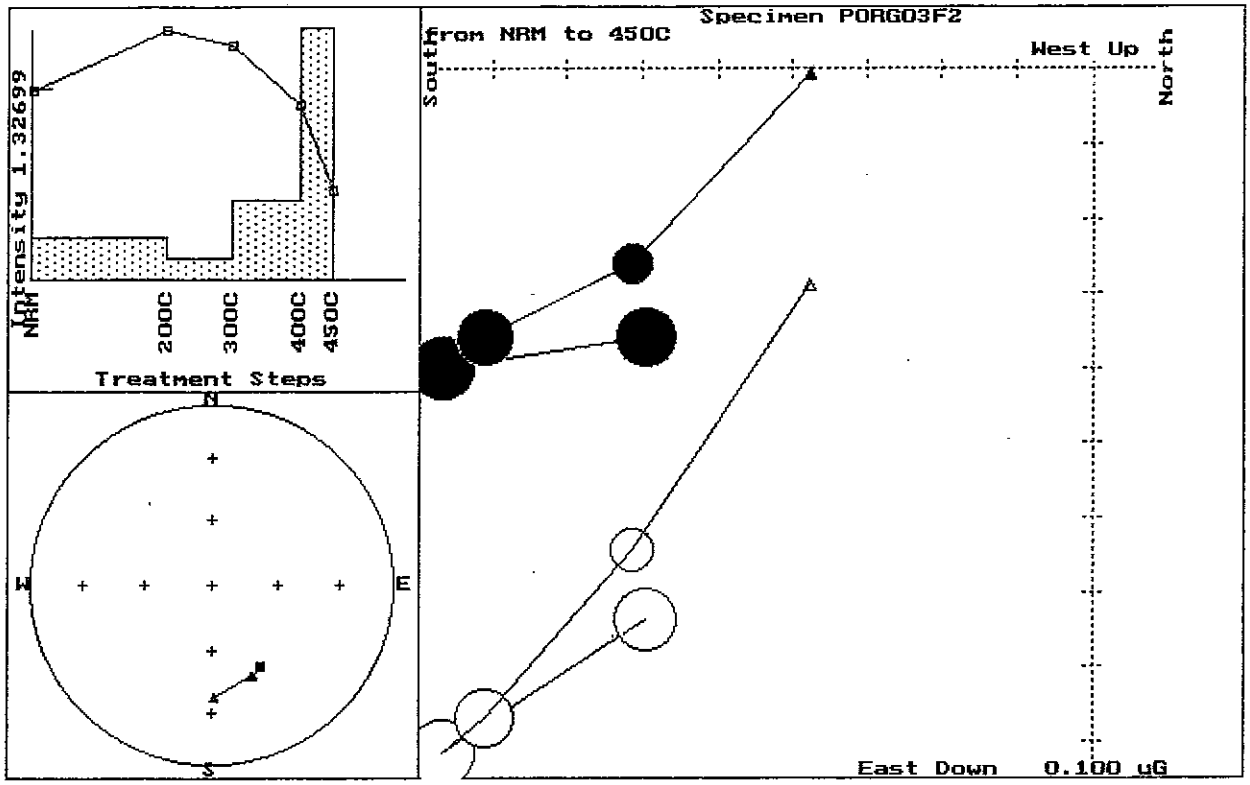
Intensity 1.32699
NRM
200C
300C
400C
450C
Treatment Steps
N
W
E
S
Specimen PORG03F2
From NRM to 450C
South
West Up
North
East Down
0.100 uG

Fig.7. Zijderveld plots for the Waruwari andesite samples.

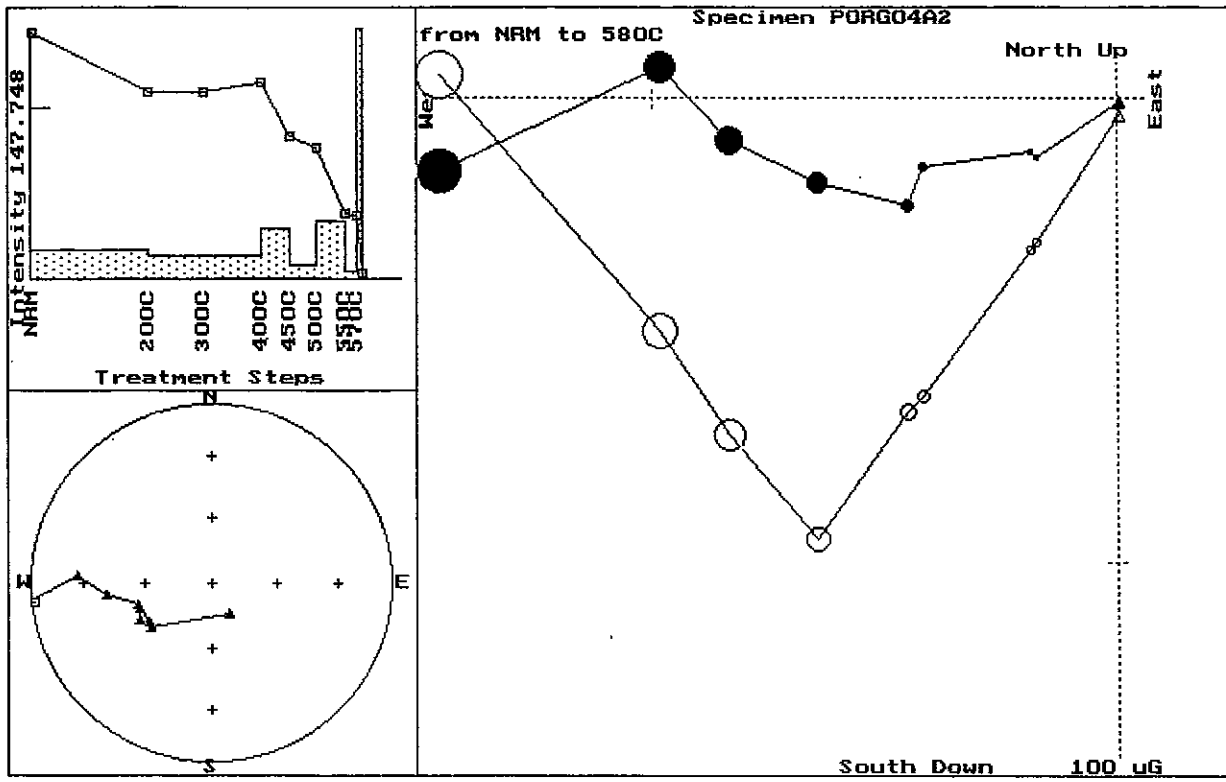
Intensity 147.748
NRM
200C
300C
400C
450C
500C
550C
580C
Treatment Steps
N
E
S
W
Specimen PORG04A2
from NRM to 580C
North Up
East
South Down
100 uG

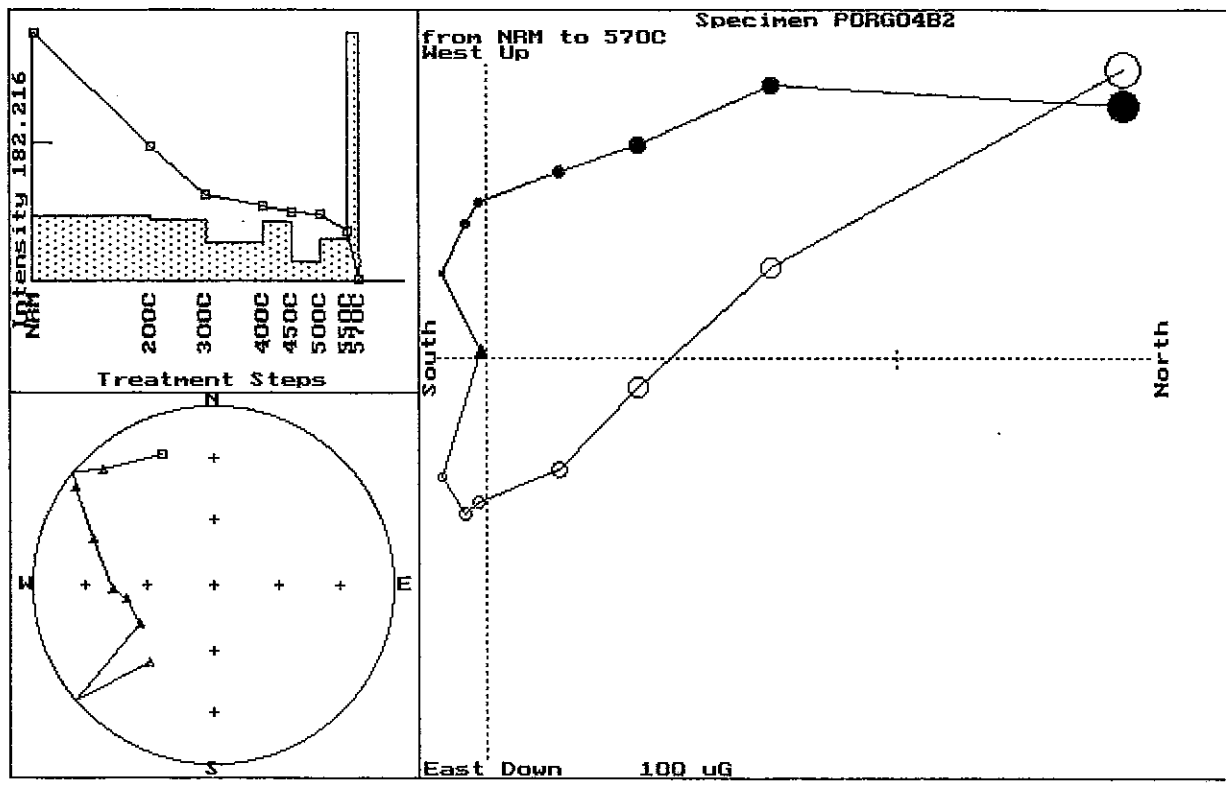
Intensity 182.216
NRM
200C
300C
400C
450C
500C
550C
570C
Treatment Steps
N
E
S
W
Specimen PORG04B2
from NRM to 570C
West Up
South
North
East Down
100 uG

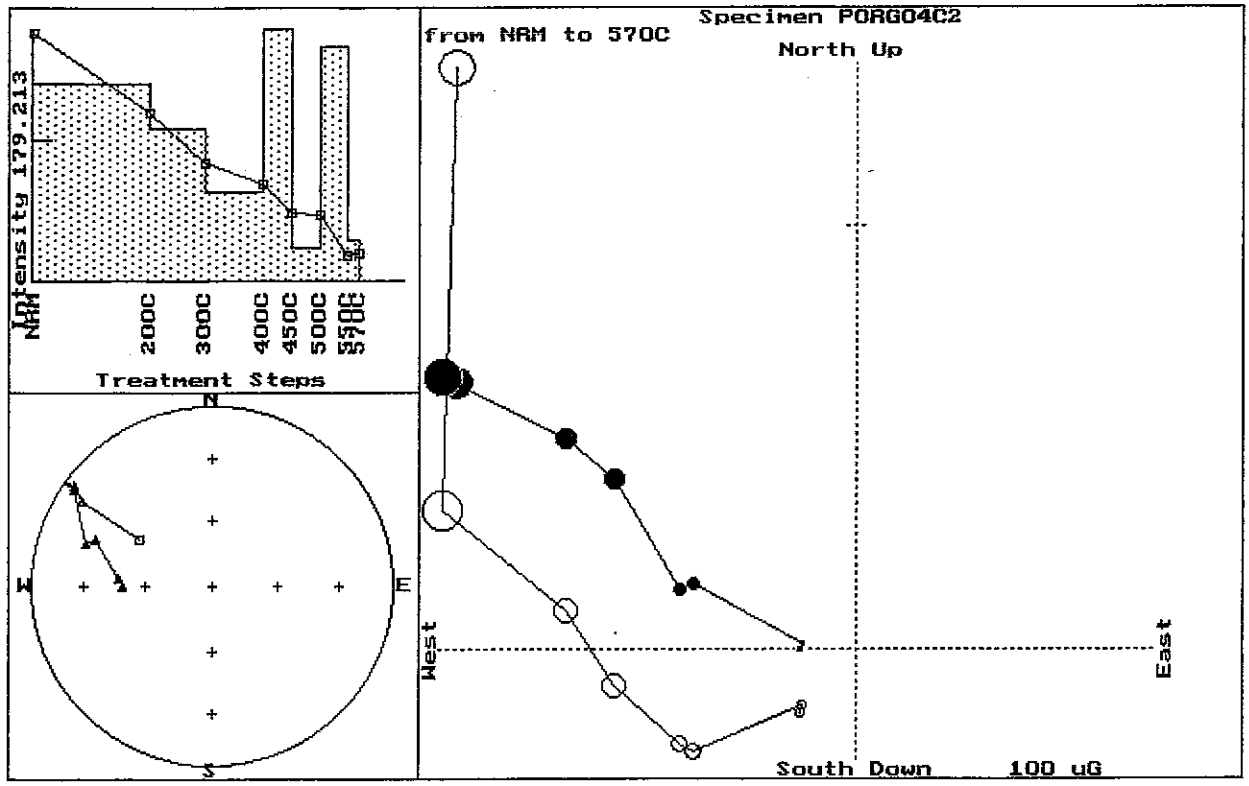
Intensity 179.213
NRM
200C
300C
400C
450C
500C
570C
Treatment Steps
N
W
E
S
Specimen PORG04C2
from NRM to 570C
North Up
West
East
South Down
100 uG

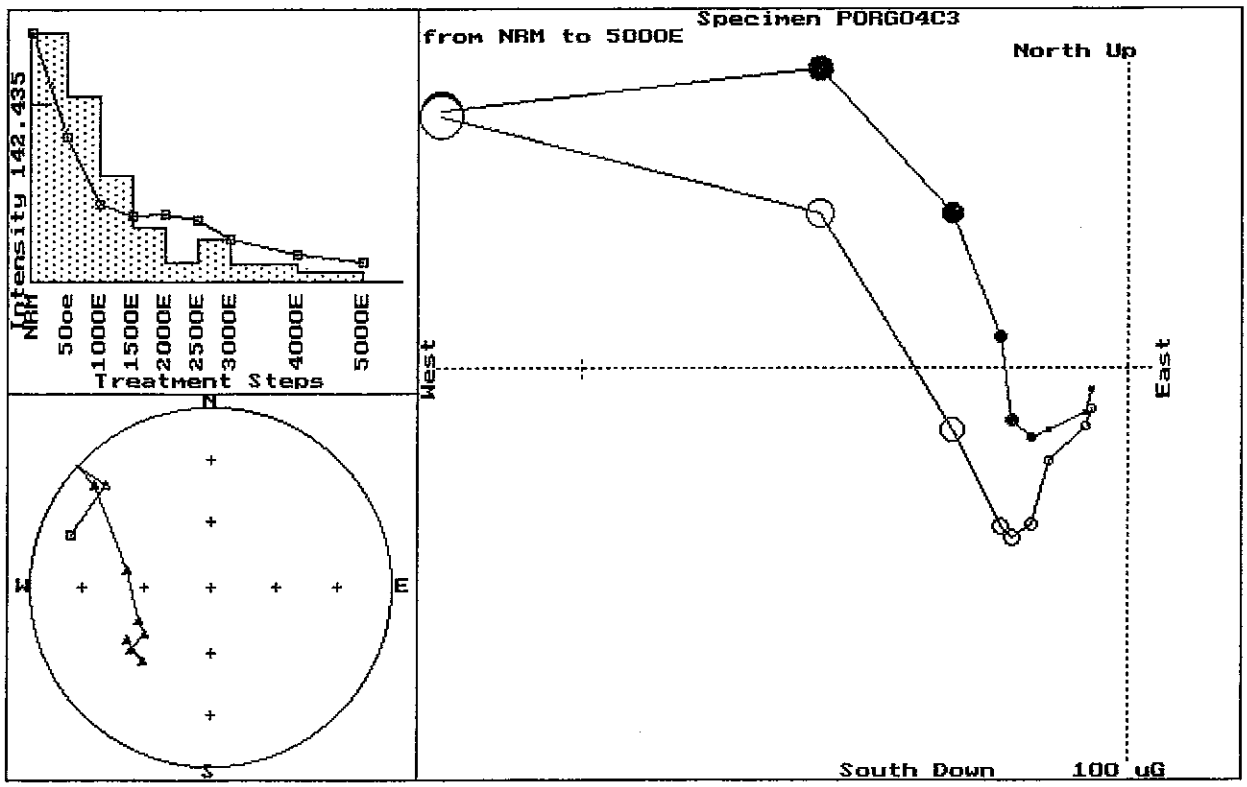
Intensity 142.435
NRM
50oe
1000E
1500E
2000E
2500E
3000E
4000E
5000E
Treatment Steps
N
W
E
S
Specimen PORG04C3
from NRM to 5000E
North Up
West
East
South Down
100 uG

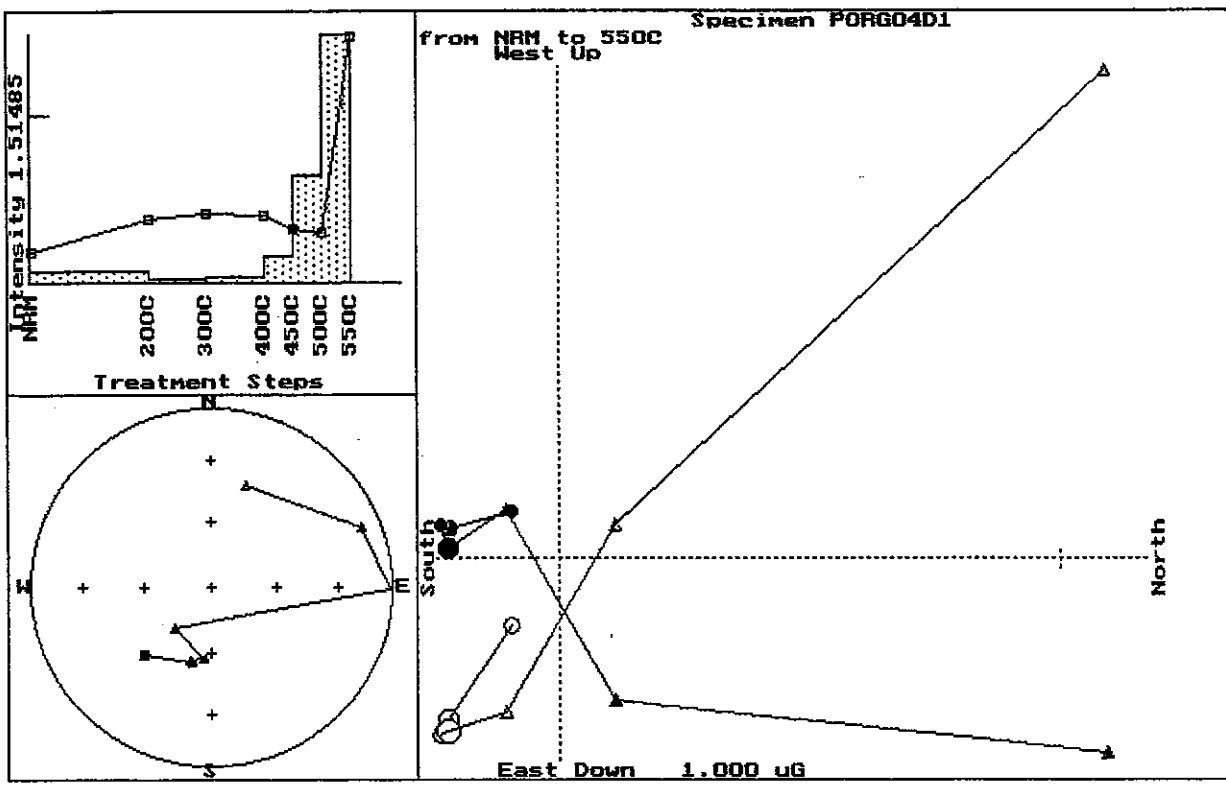
Specimen PORG04D1
from NRM to 550C
West Up
Intensity 1.51485
NRM
200C
300C
400C
450C
500C
550C
Treatment Steps
N
W
E
S
South
North
East Down 1.000 uG

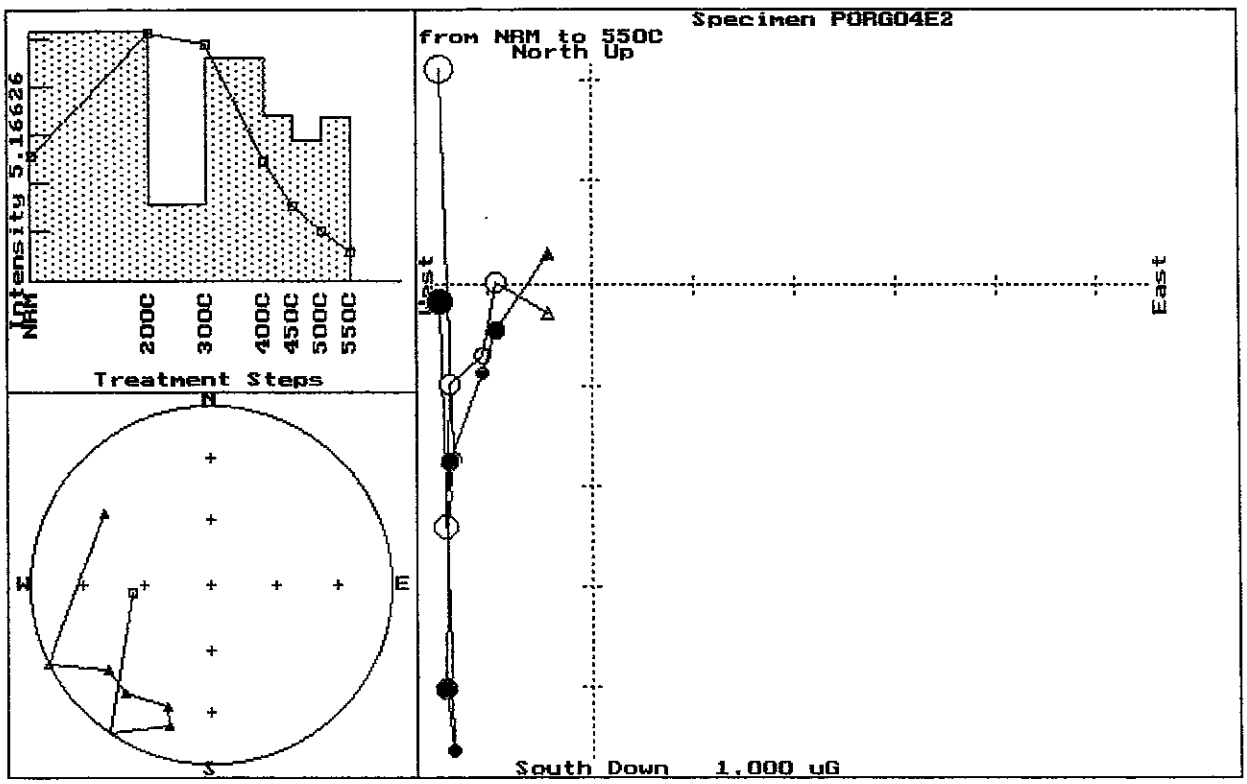
Specimen PORG04E2
from NRM to 550C
North Up
Intensity 5.16626
NRM
200C
300C
400C
450C
500C
550C
Treatment Steps
N
W
E
S
West
East
South Down 1.000 uG

Fig.8. Zijderveld plots for the Haul Road dykes samples.

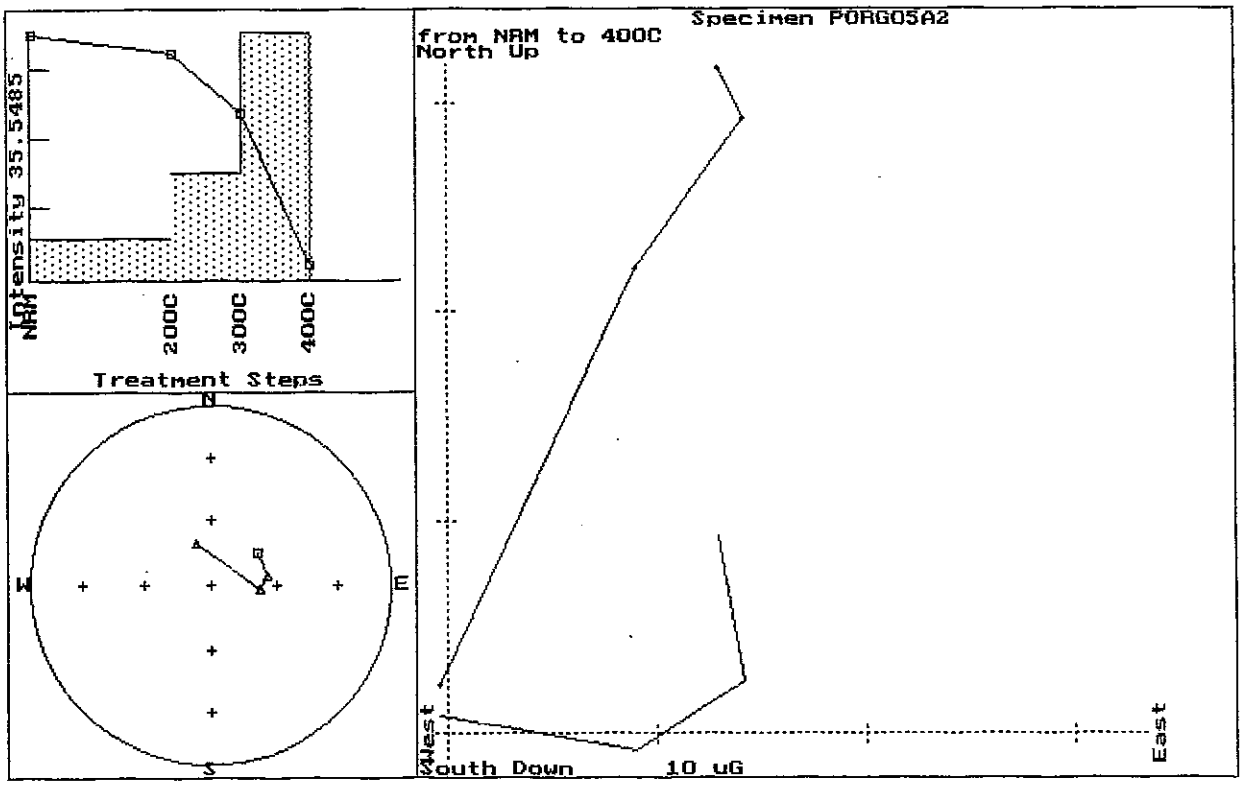
Intensity 35.5485
NRM
200C
300C
400C
Treatment Steps
N
E
S
W
Specimen PORG05A2
from NRM to 400C
North Up
West
East
South Down
10 uG

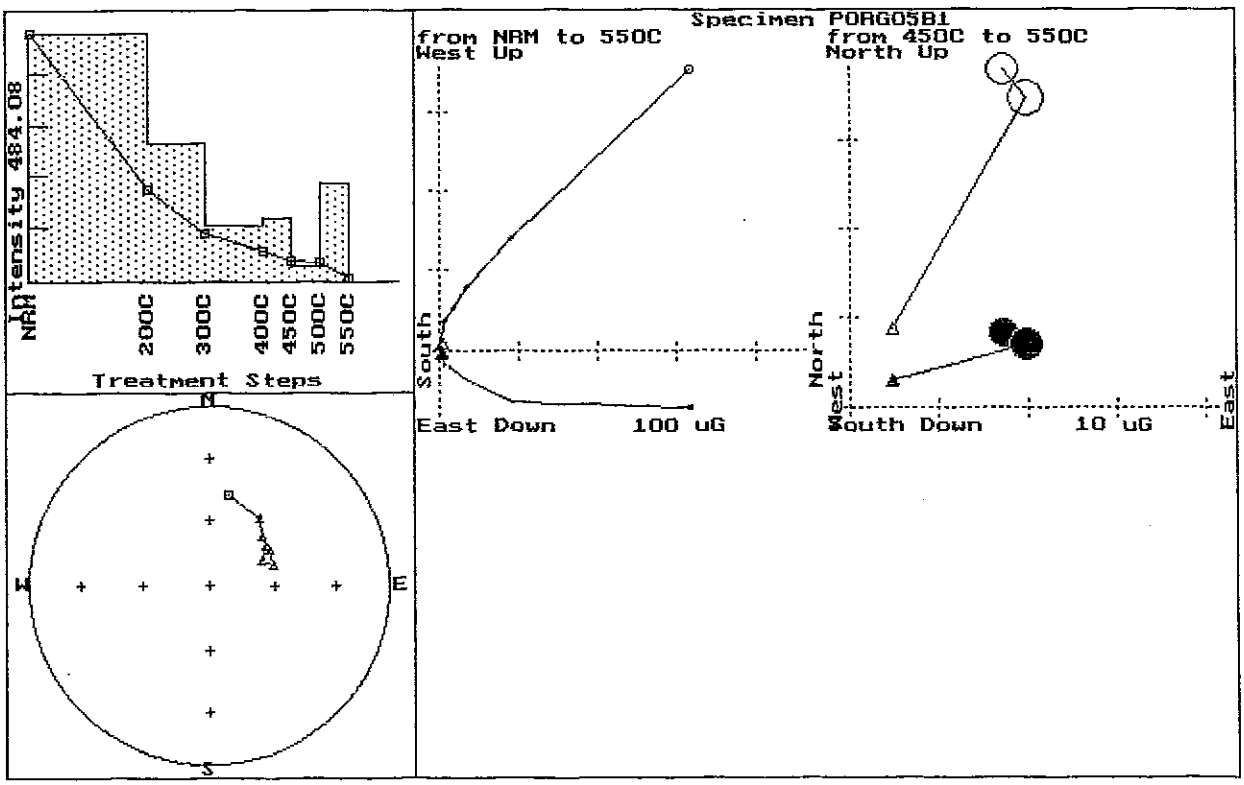
Intensity 484.08
NRM
200C
300C
400C
450C
500C
550C
Treatment Steps
N
E
S
W
Specimen PORG05B1
from NRM to 550C
West Up
South
East Down
100 uG
from 450C to 550C
North Up
North
West
South Down
10 uG
East

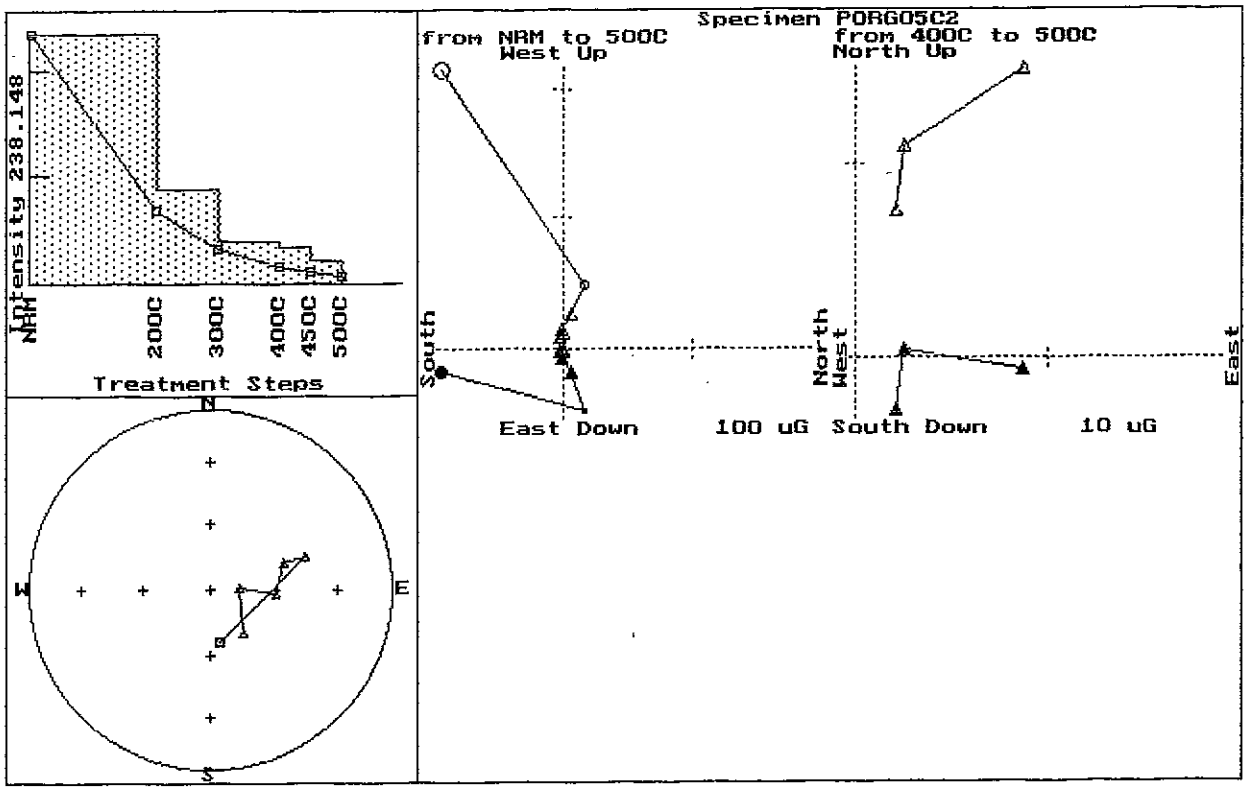
Specimen PORG05C2
from NRM to 500C
West Up
from 400C to 500C
North Up
Intensity 238.148
NRM
200C
300C
400C
450C
500C
Treatment Steps
N
W
E
S
South
East Down
100 uG
North West
South Down
10 uG
East

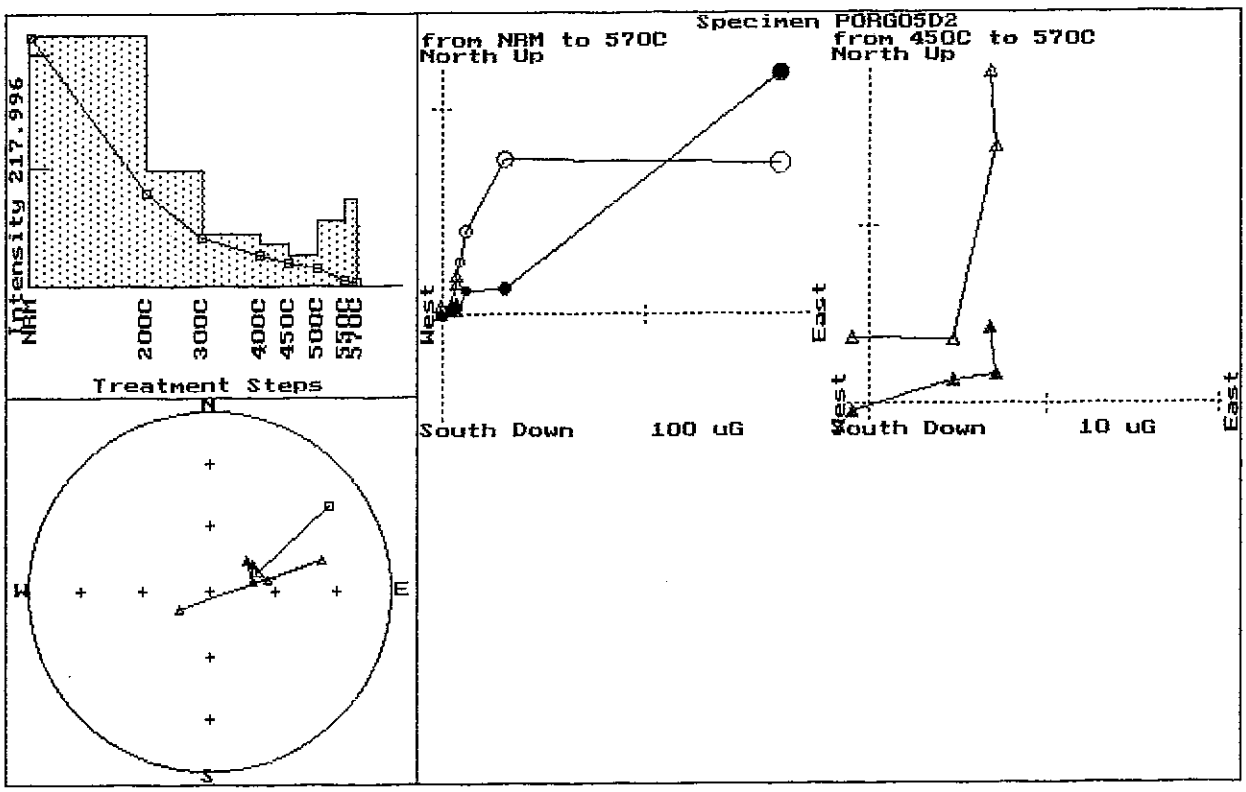
Specimen PORG05D2
from NRM to 570C
North Up
from 450C to 570C
North Up
Intensity 217.996
NRM
200C
300C
400C
450C
500C
570C
Treatment Steps
N
W
E
S
West
South Down
100 uG
East
South Down
10 uG
East

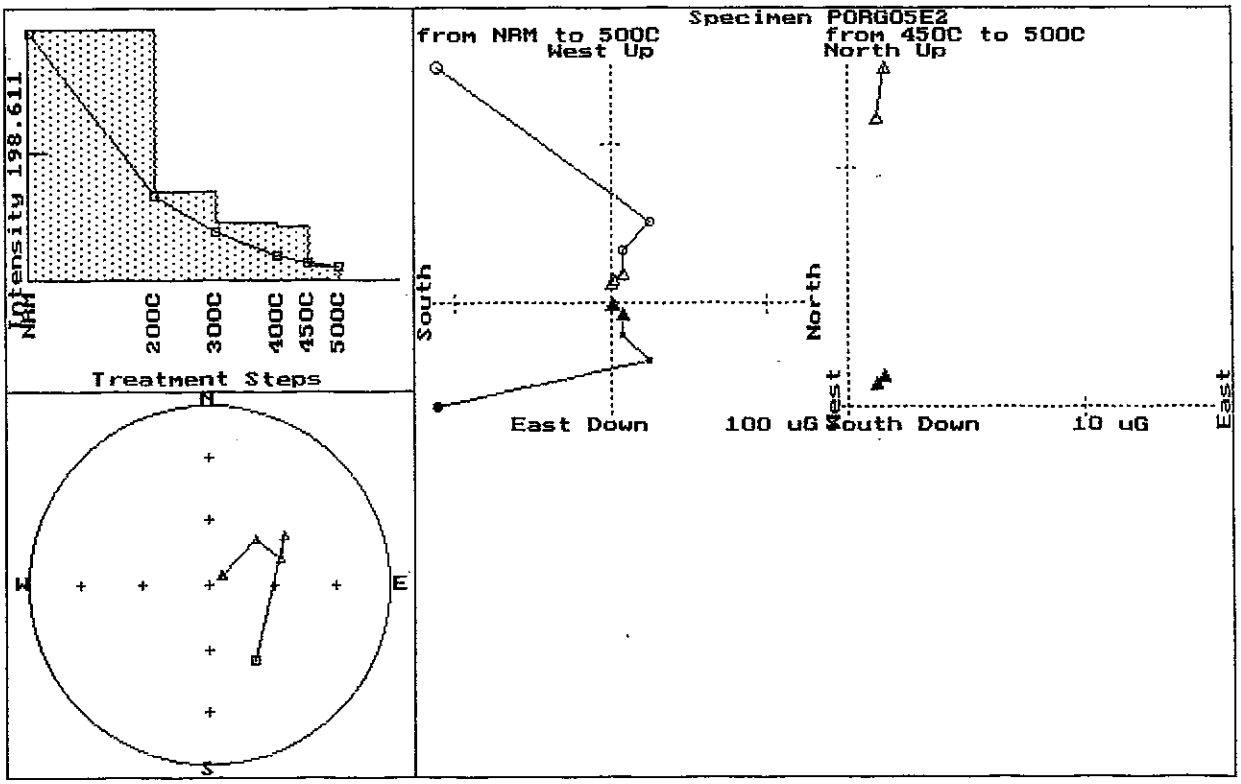
Specimen PORG05E2
from NRM to 500C
West Up
from 450C to 500C
North Up
Intensity 198.611
NRM
200C
300C
400C
450C
500C
Treatment Steps
N
W
E
S
South
North
East Down
100 uG
West
South Down
10 uG
East

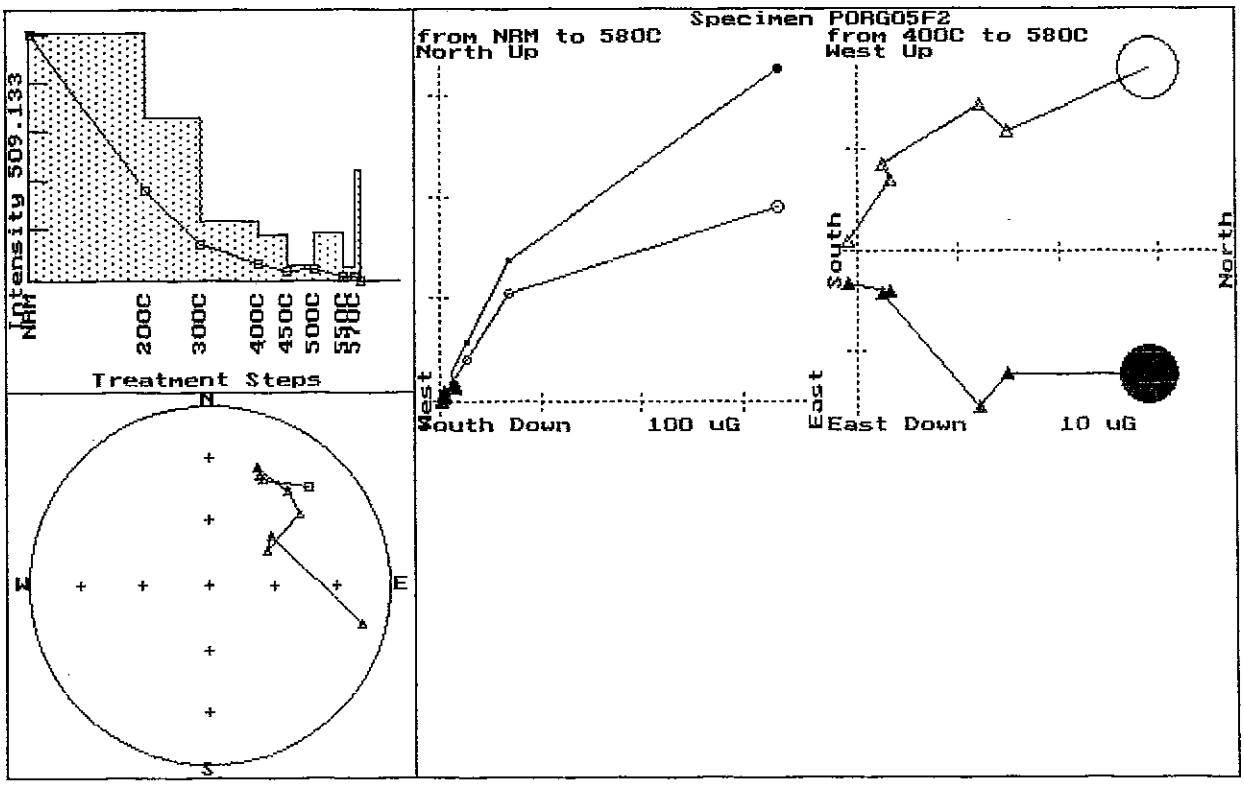
Specimen PORG05F2
from NRM to 580C
North Up
from 400C to 580C
West Up
Intensity 509.133
NRM
200C
300C
400C
450C
500C
580C
Treatment Steps
N
W
E
S
West
South Down
100 uG
East
South
North
East Down
10 uG

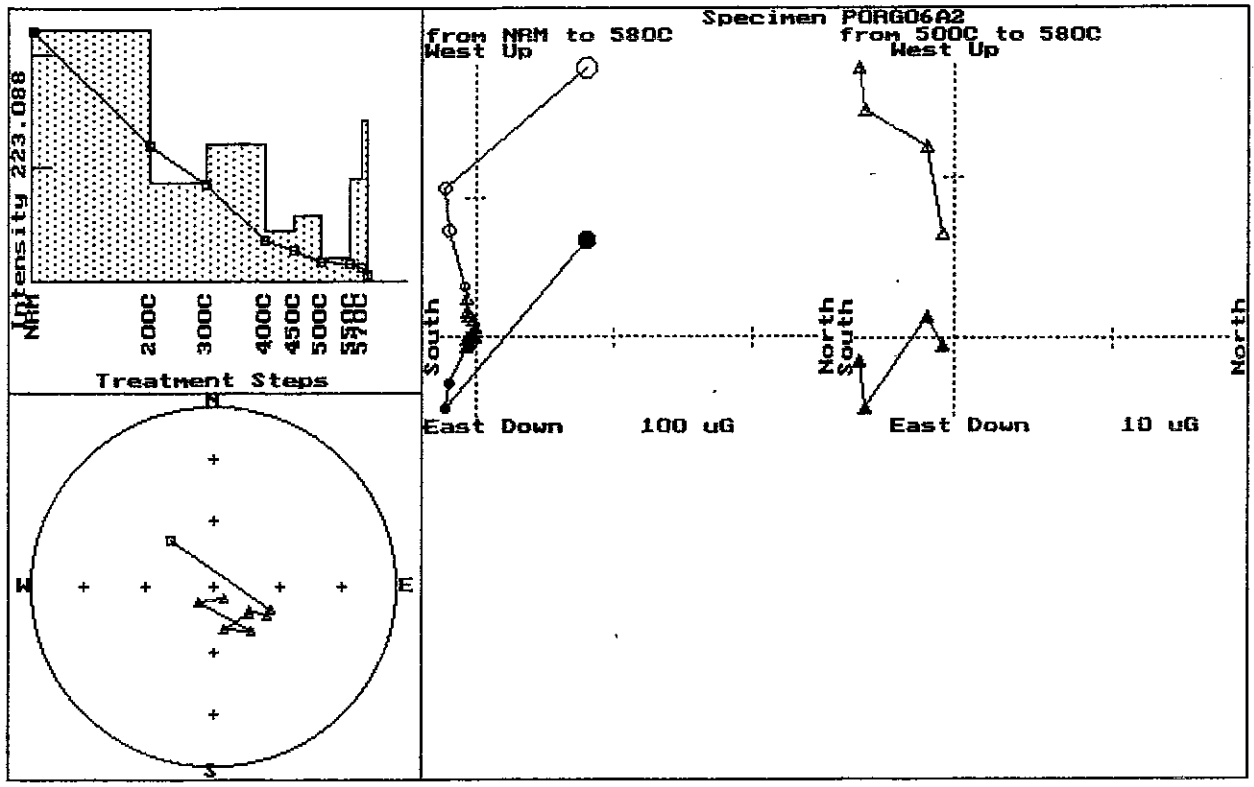
Intensity 223.088
NRM
200C
300C
400C
450C
500C
570C
580C
Treatment Steps
N
W
E
S
Specimen PORG06A2
from NRM to 580C
West Up
South
East Down
100 uG
from 500C to 580C
West Up
North
South
North
East Down
10 uG

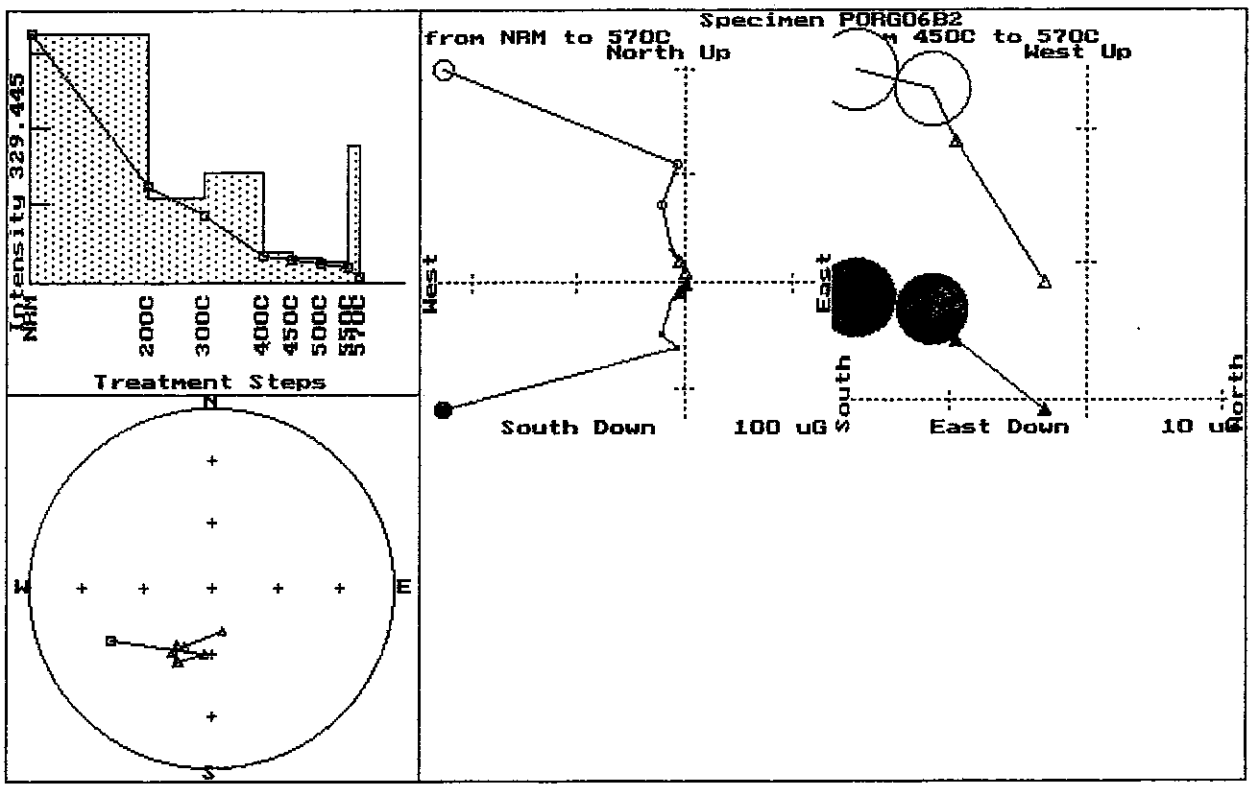
Intensity 329.445
NRM
200C
300C
400C
450C
500C
570C
Treatment Steps
N
W
E
S
Specimen PORG06B2
from NRM to 570C
North Up
West
South Down
100 uG
from 450C to 570C
West Up
East
South
East Down
10 uG
North

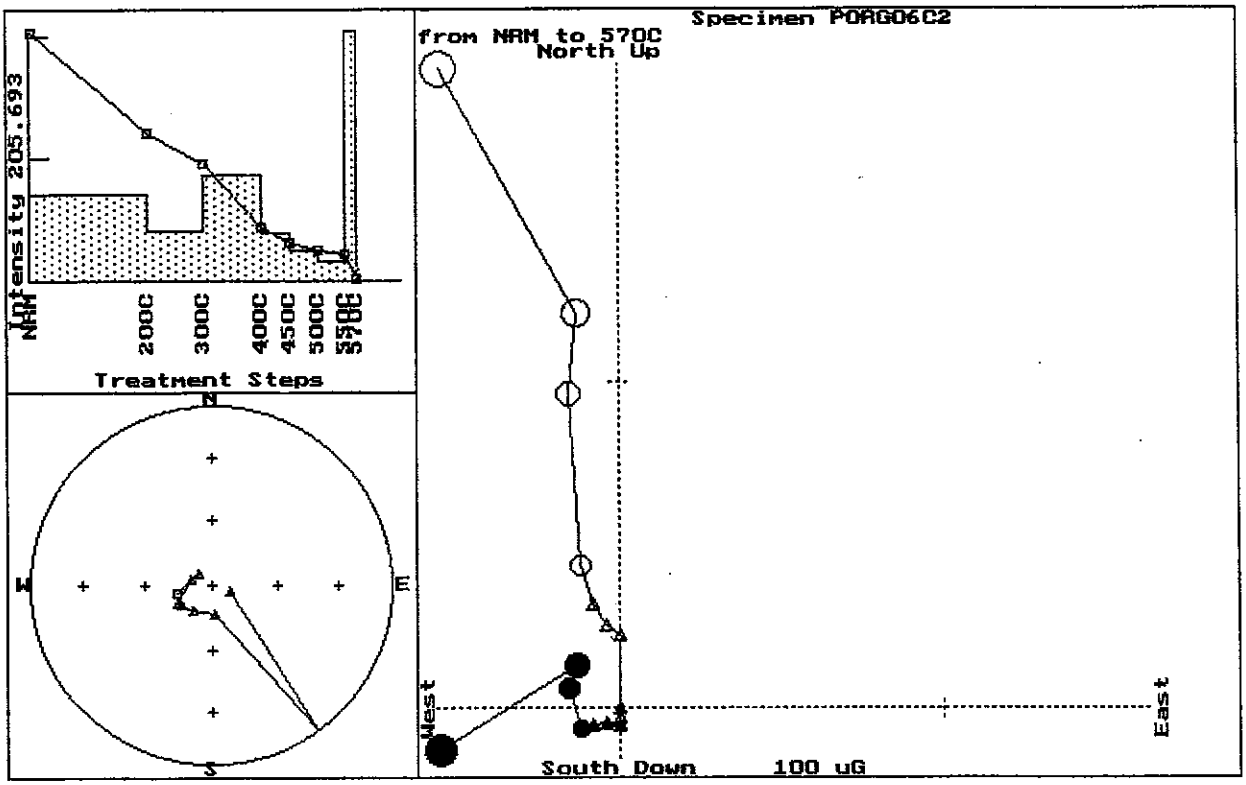
Intensity 205.693
NRM
200C
300C
400C
450C
500C
570C
Treatment Steps
N
E
W
S
Specimen PORGO6C2
from NRM to 570C
North Up
West
East
South Down
100 uG

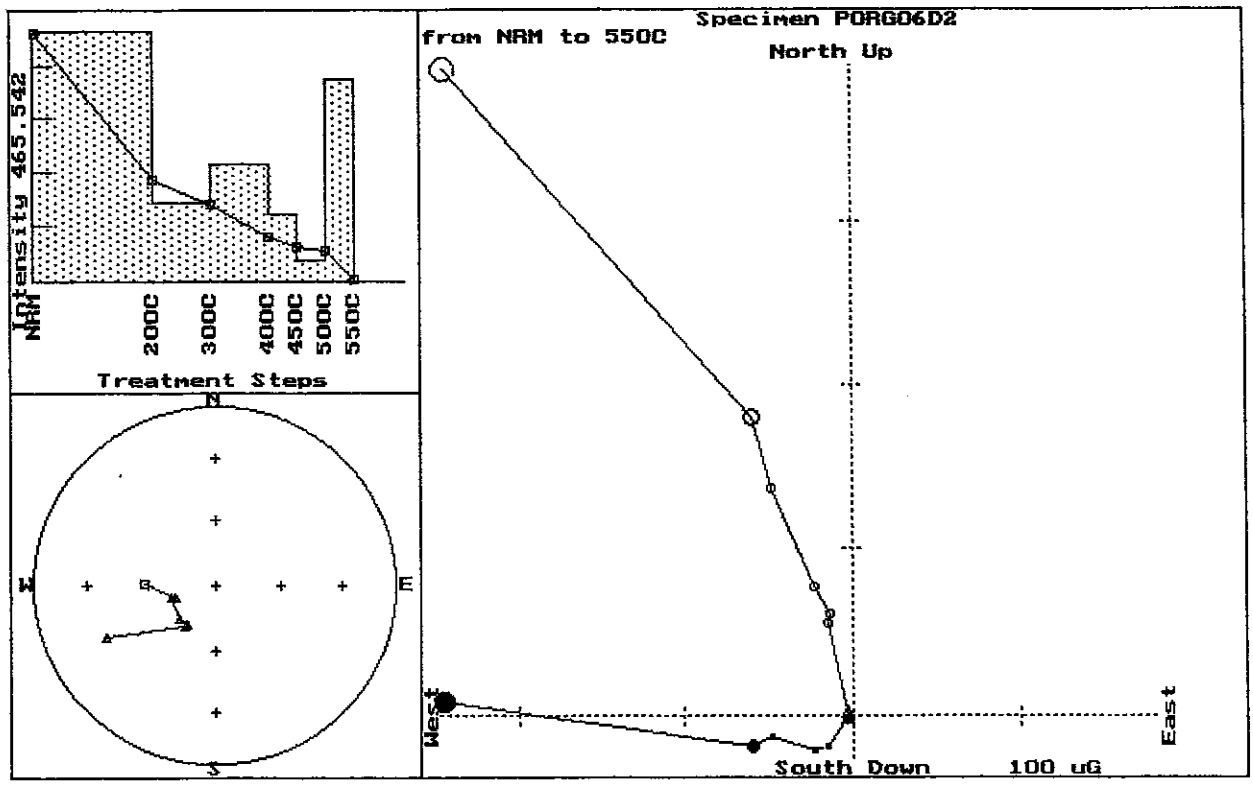
Intensity 465.542
NRM
200C
300C
400C
450C
500C
550C
Treatment Steps
N
E
W
S
Specimen PORGO6D2
from NRM to 550C
North Up
West
East
South Down
100 uG

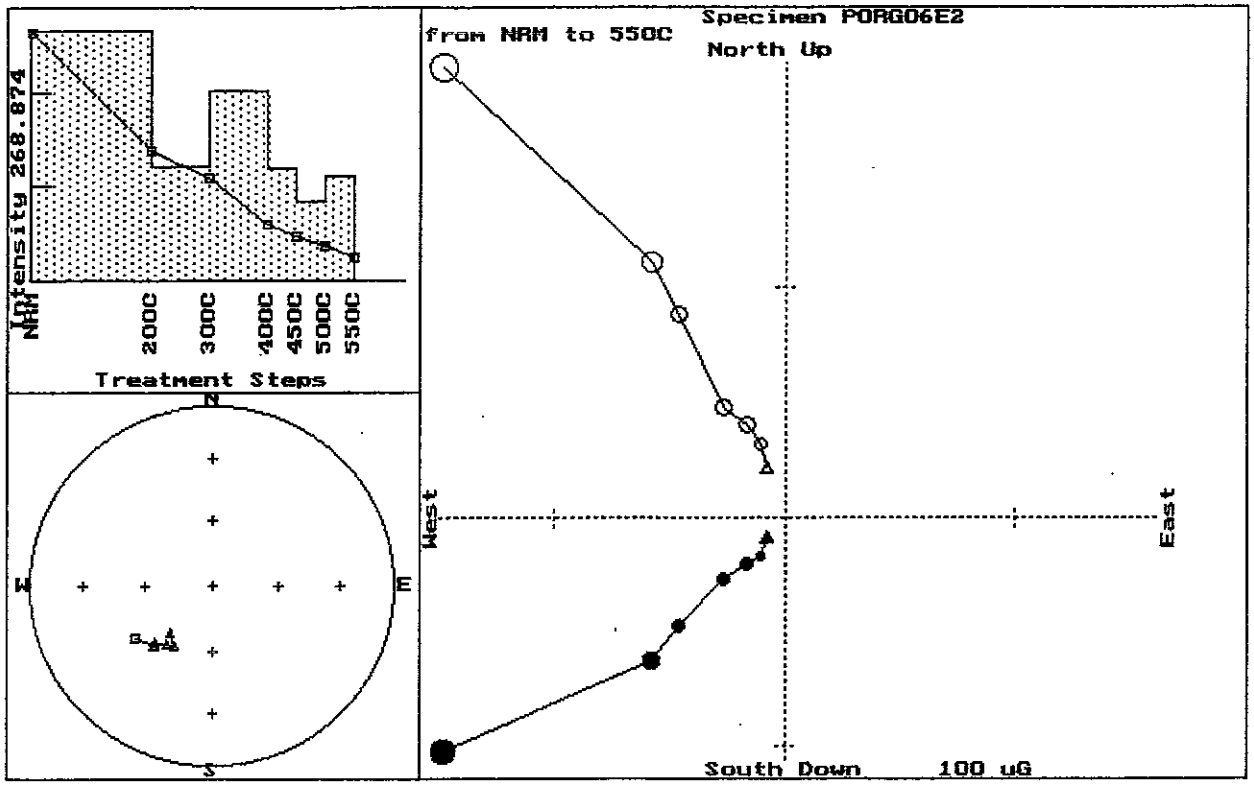
Intensity 268.874
NRM
200C
300C
400C
450C
500C
550C
Treatment Steps
N
W
E
S
from NRM to 550C
Specimen PORG06E2
North Up
West
East
South Down
100 uG

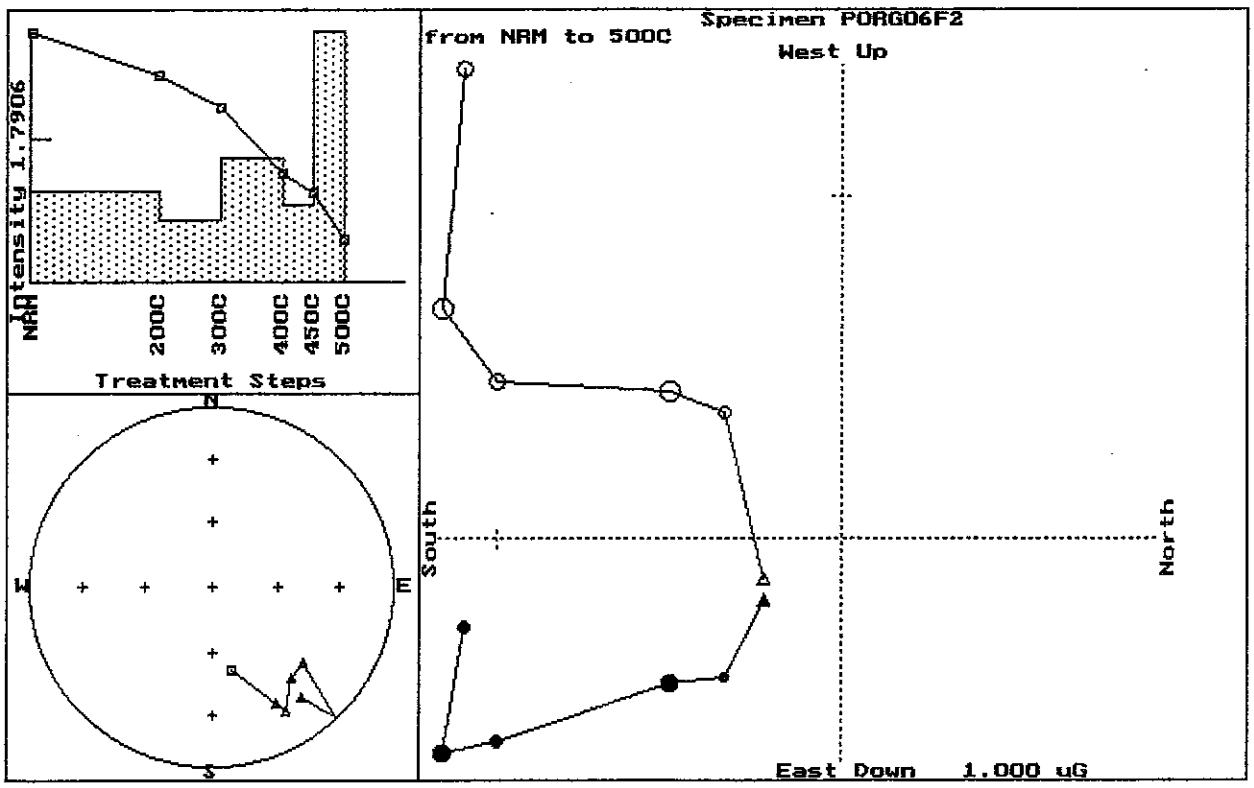
Intensity 1.7906
NRM
200C
300C
400C
450C
500C
Treatment Steps
N
W
E
S
from NRM to 500C
Specimen PORG06F2
West Up
South
North
East Down
1.000 uG

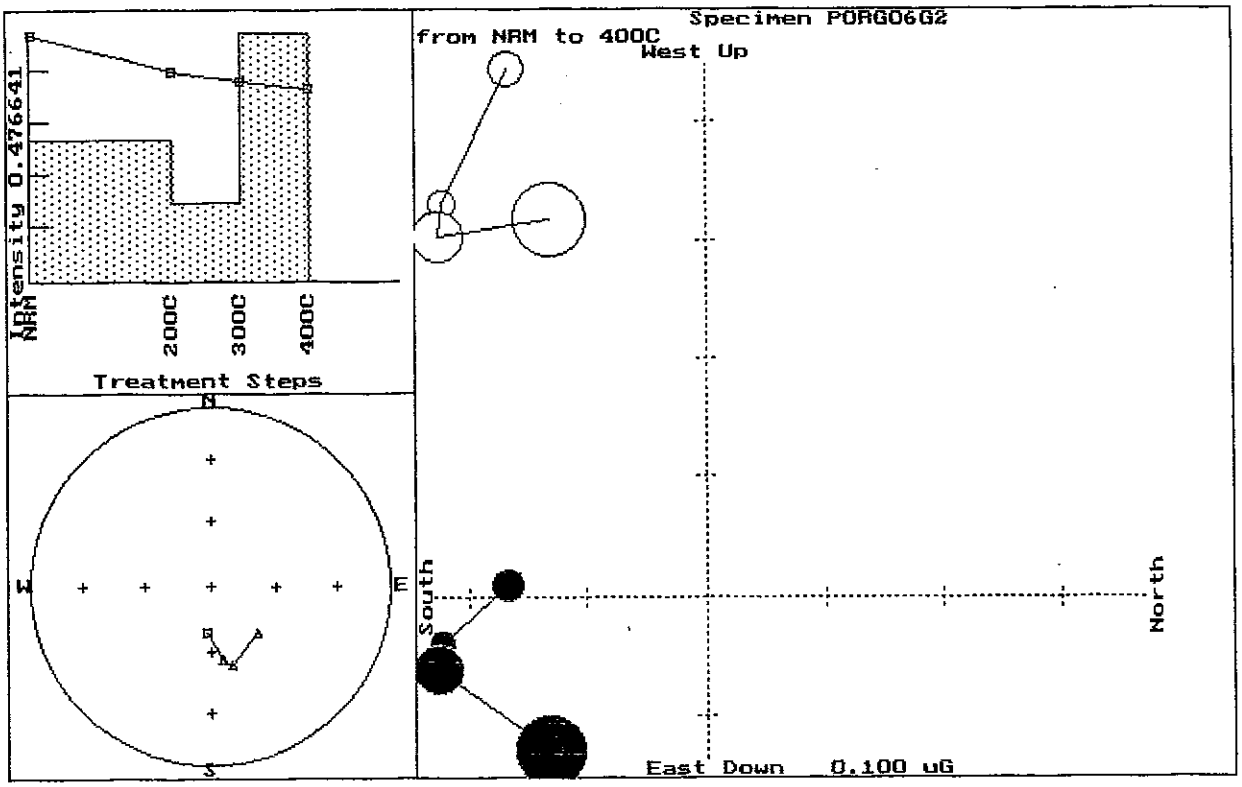
Intensity 0.476641
NRM
200C
300C
400C
Treatment Steps
N
E
S
W
Specimen PORG06G2
from NRM to 400C
West Up
South
North
East Down
0.100 uG

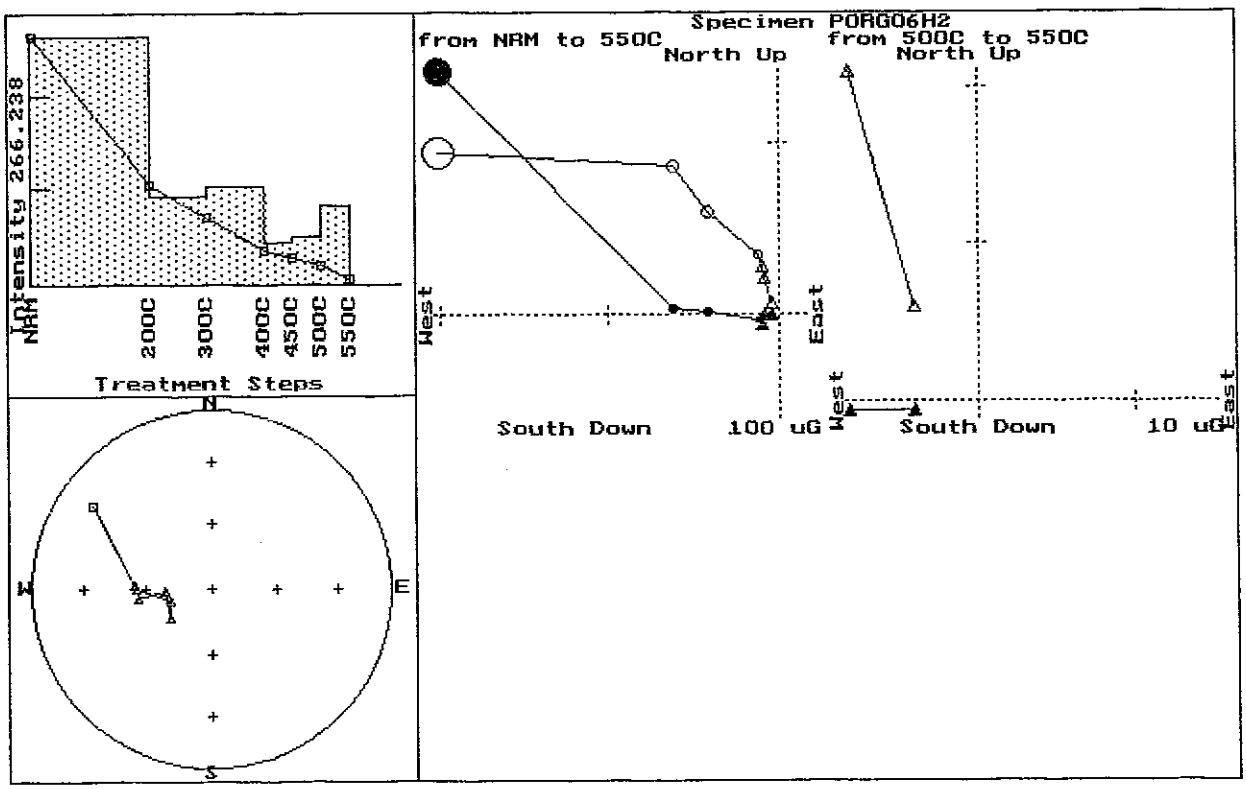
Intensity 266.238
NRM
200C
300C
400C
450C
500C
550C
Treatment Steps
N
E
S
W
Specimen PORG06H2
from NRM to 550C
North Up
from 500C to 550C
North Up
West
East
South Down
100 uG
West
East
South Down
10 uG

Fig.9. Zijderveld plots for the Tawisakale samples.

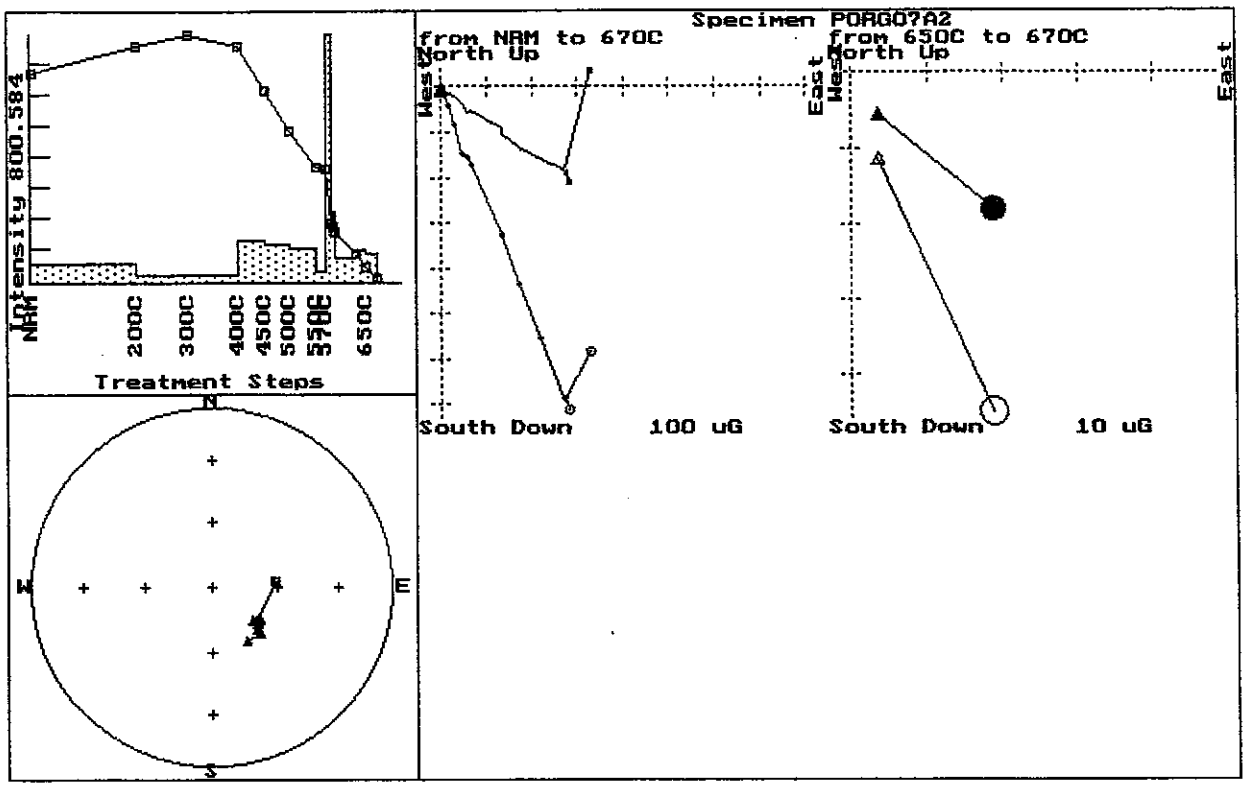
Intensity 800.584
NRM
200C
300C
400C
450C
500C
550C
650C
Treatment Steps
N
E
S
W
Specimen PORG07A2
from NRM to 670C
North Up
West
East
South Down
100 uG
from 650C to 670C
North Up
West
East
South Down
10 uG

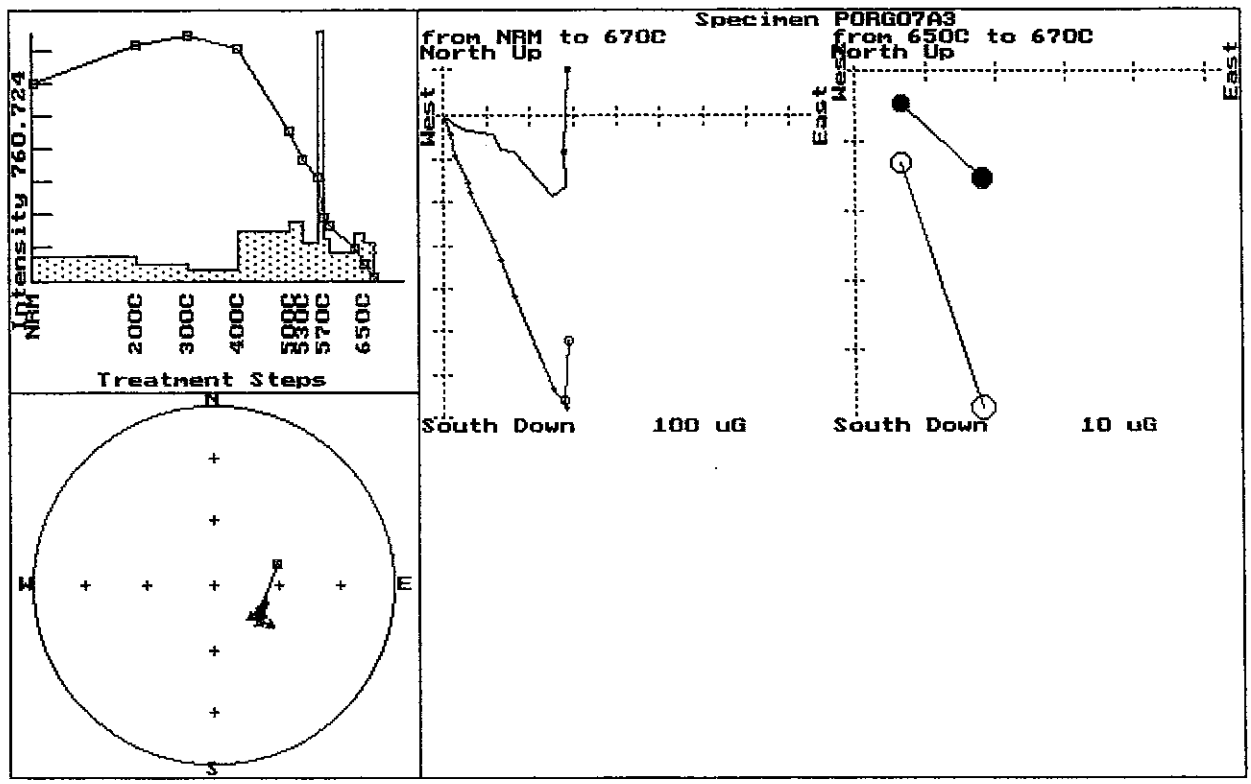
Intensity 760.724
NRM
200C
300C
400C
500C
550C
570C
650C
Treatment Steps
N
E
S
W
Specimen PORG07A3
from NRM to 670C
North Up
West
East
South Down
100 uG
from 650C to 670C
North Up
West
East
South Down
10 uG

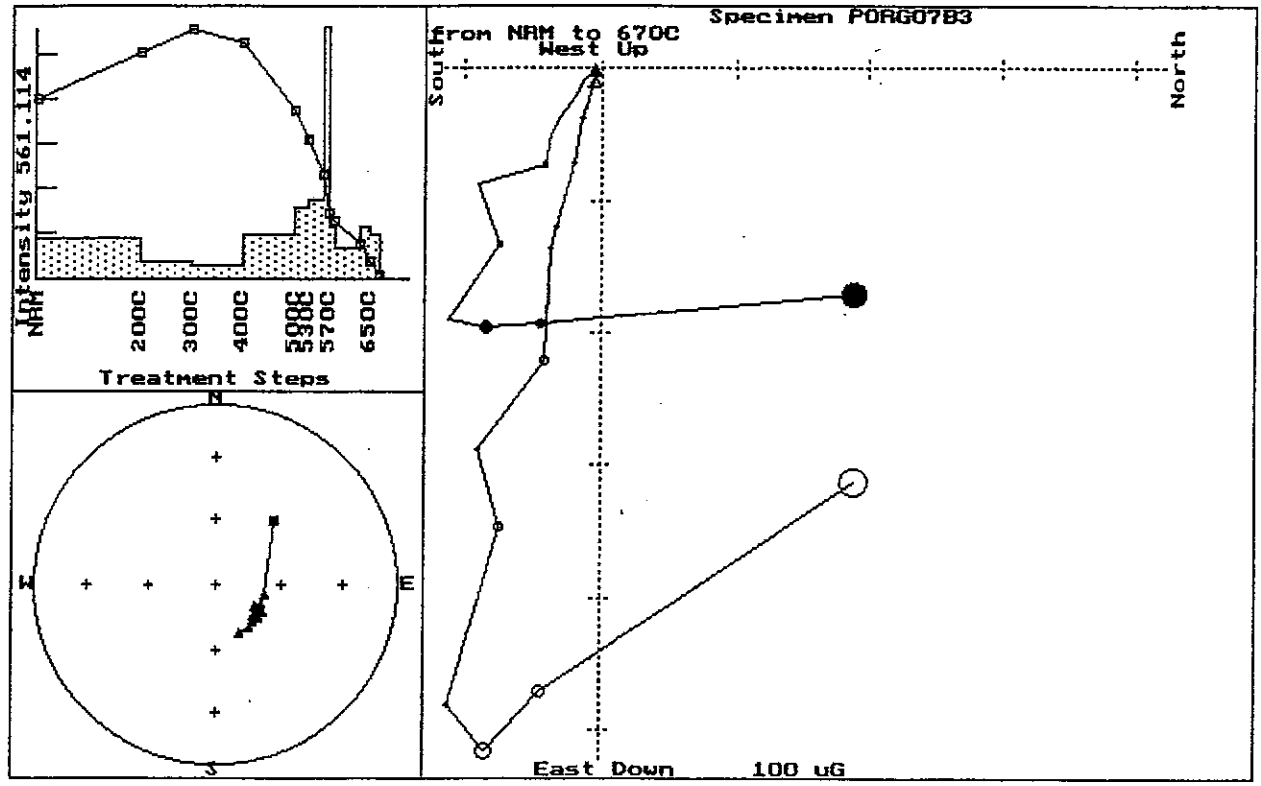
Intensity 561.114
NRM
200C
300C
400C
530C
570C
650C
Treatment Steps
N
E
S
W
Specimen PORG07B3
from NRM to 670C
West Up
South
North
East Down
100 uG

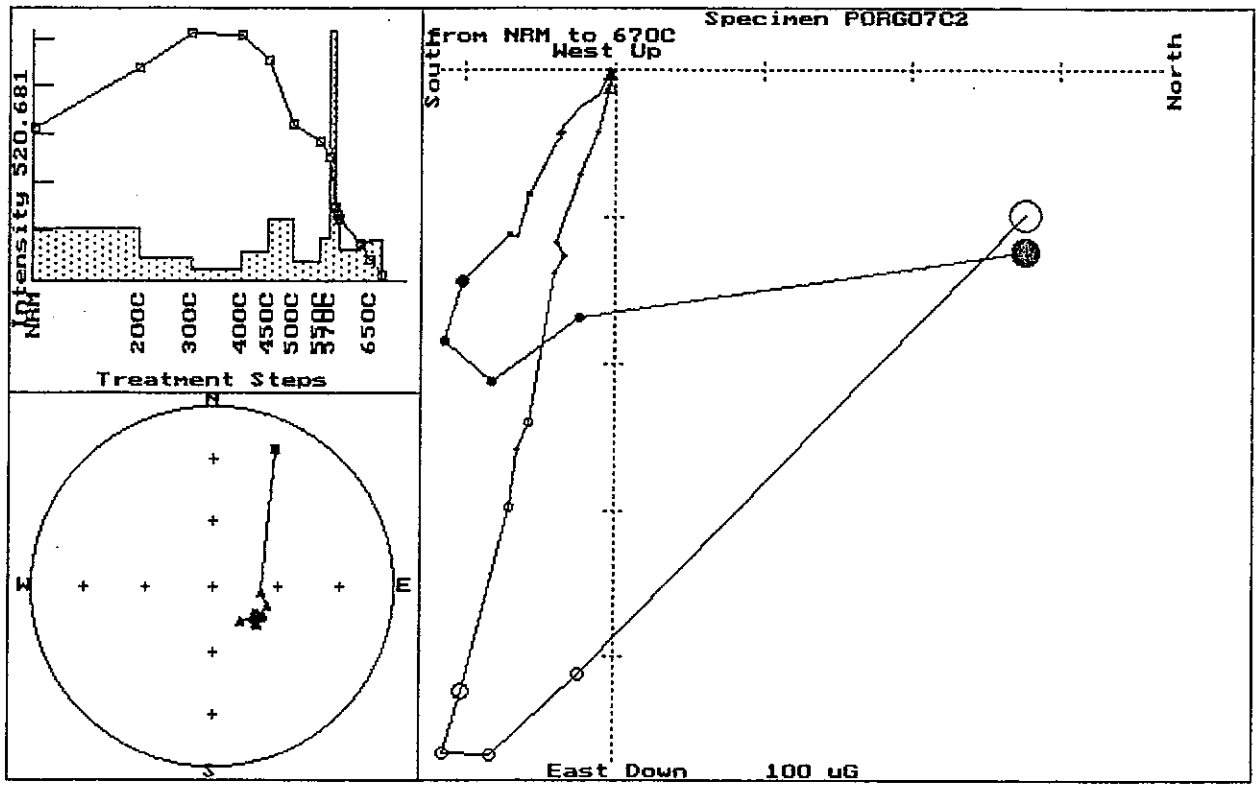
Intensity 520.681
NRM
200C
300C
400C
450C
500C
570C
650C
Treatment Steps
N
E
S
W
Specimen PORG07C2
from NRM to 670C
West Up
South
North
East Down
100 uG

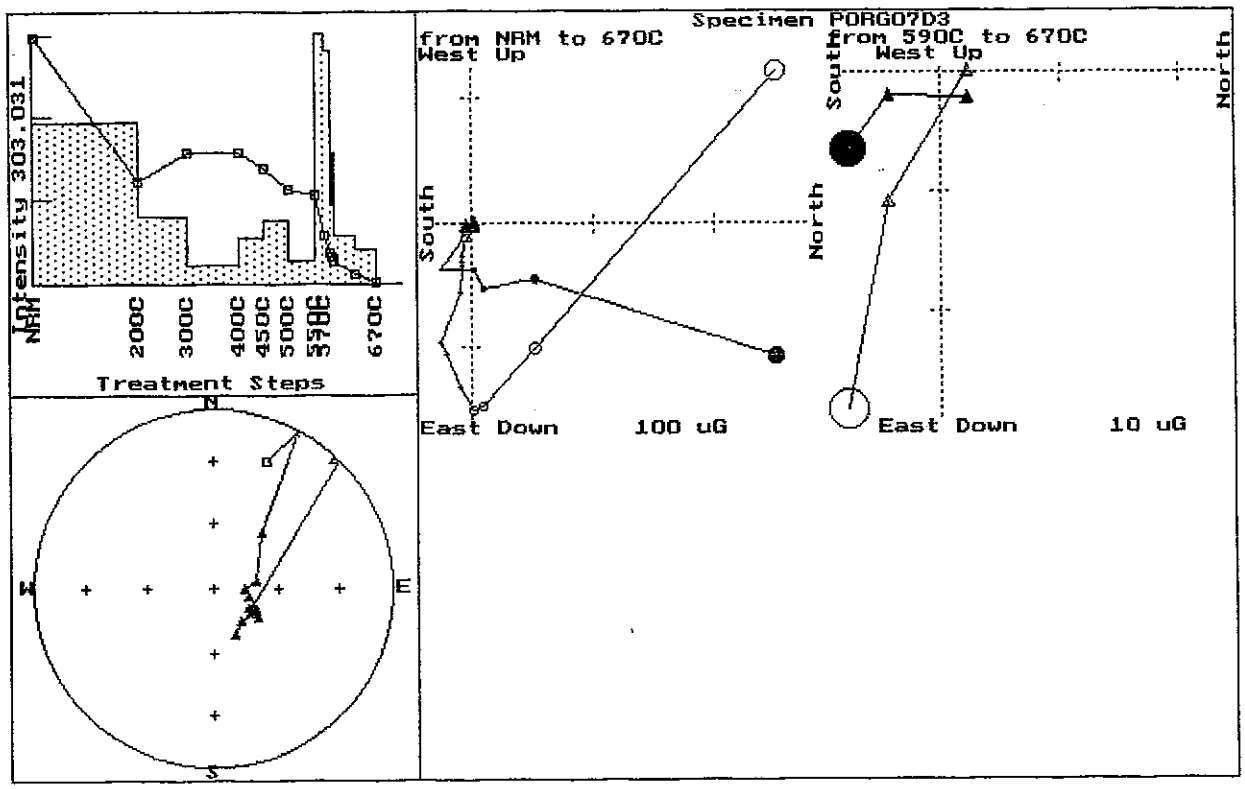
Intensity 303.031
NRM
200C
300C
400C
450C
500C
570C
670C
Treatment Steps
N
E
S
W
Specimen PORG07D3
from NRM to 670C
West Up
South
North
East Down
100 uG
from 590C to 670C
West Up
South
North
East Down
10 uG

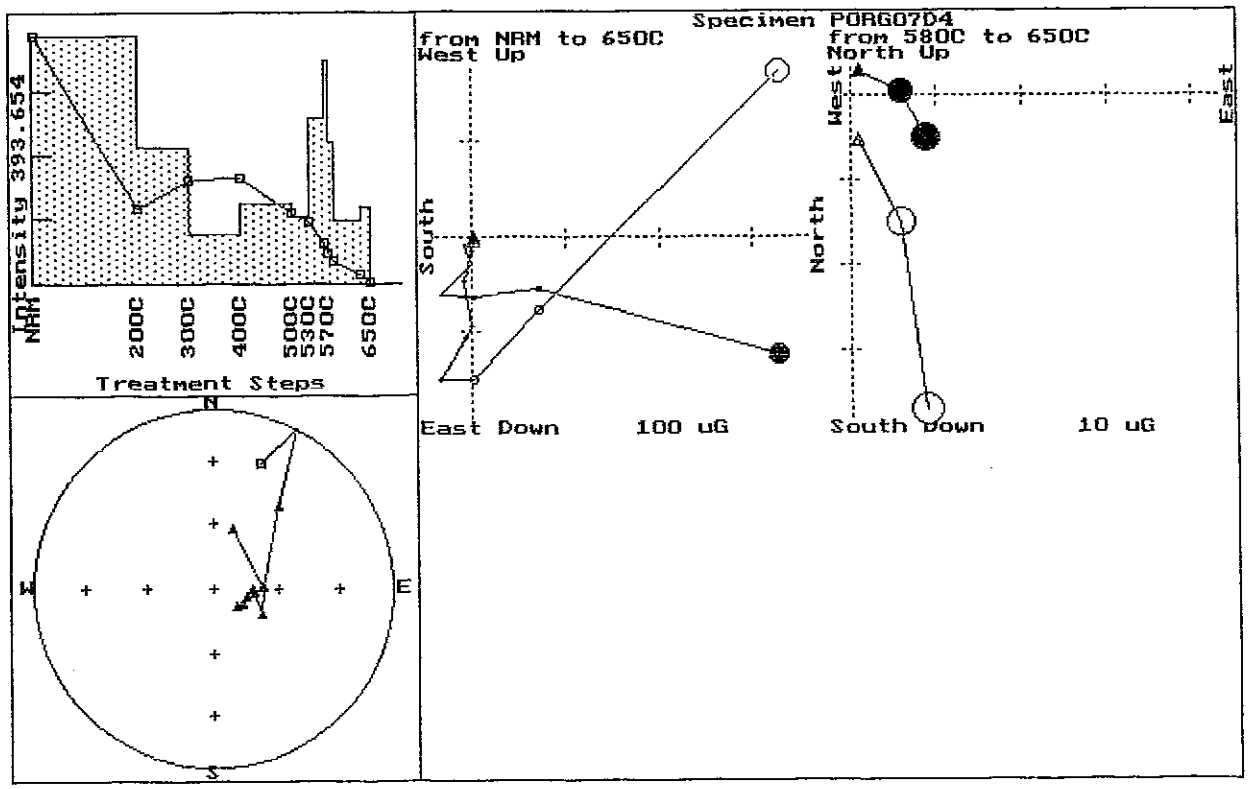
Intensity 393.654
NRM
200C
300C
400C
500C
530C
570C
650C
Treatment Steps
N
E
S
W
Specimen PORG07D4
from NRM to 650C
West Up
South
North
East Down
100 uG
from 580C to 650C
North Up
West
East
South
North
South Down
10 uG

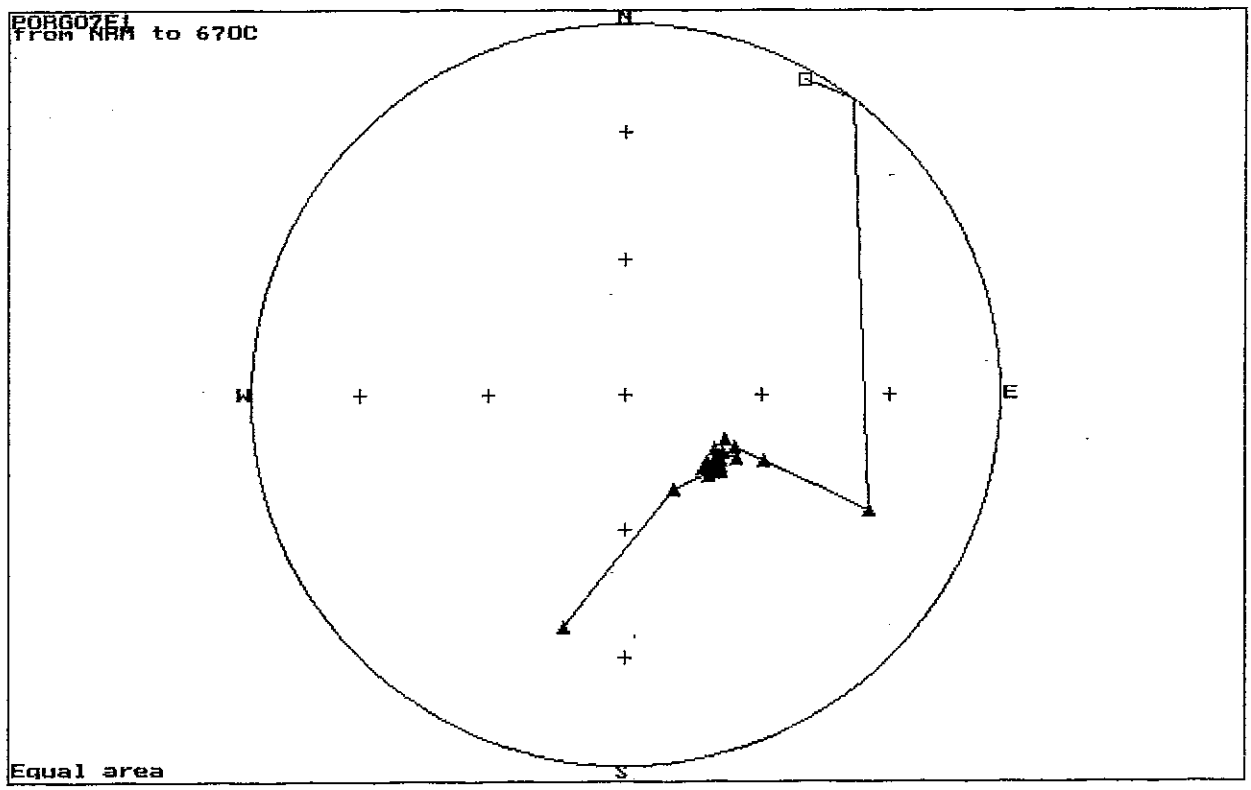
PORG07E1
from NRM to 670C
N
W
E
S
Equal area

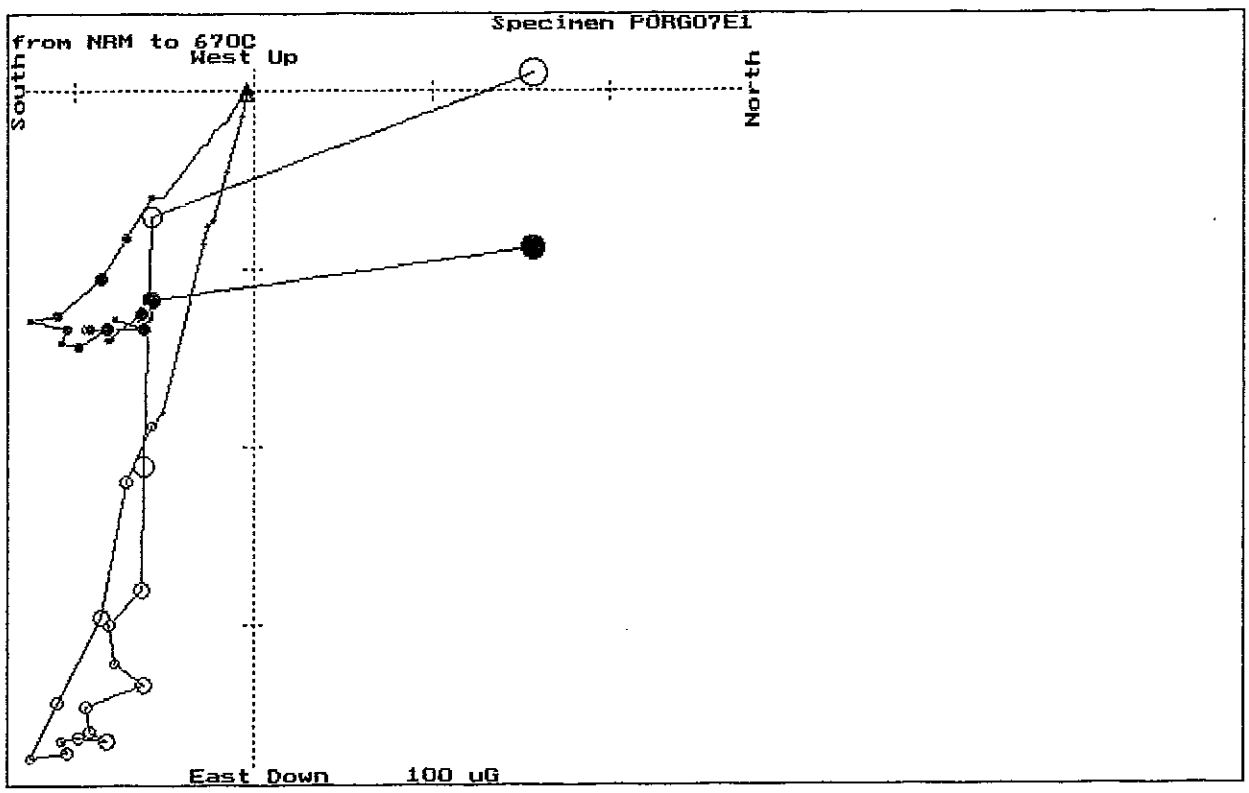
Specimen PORG07E1
from NRM to 670C
West Up
South
North
East Down
100 uG

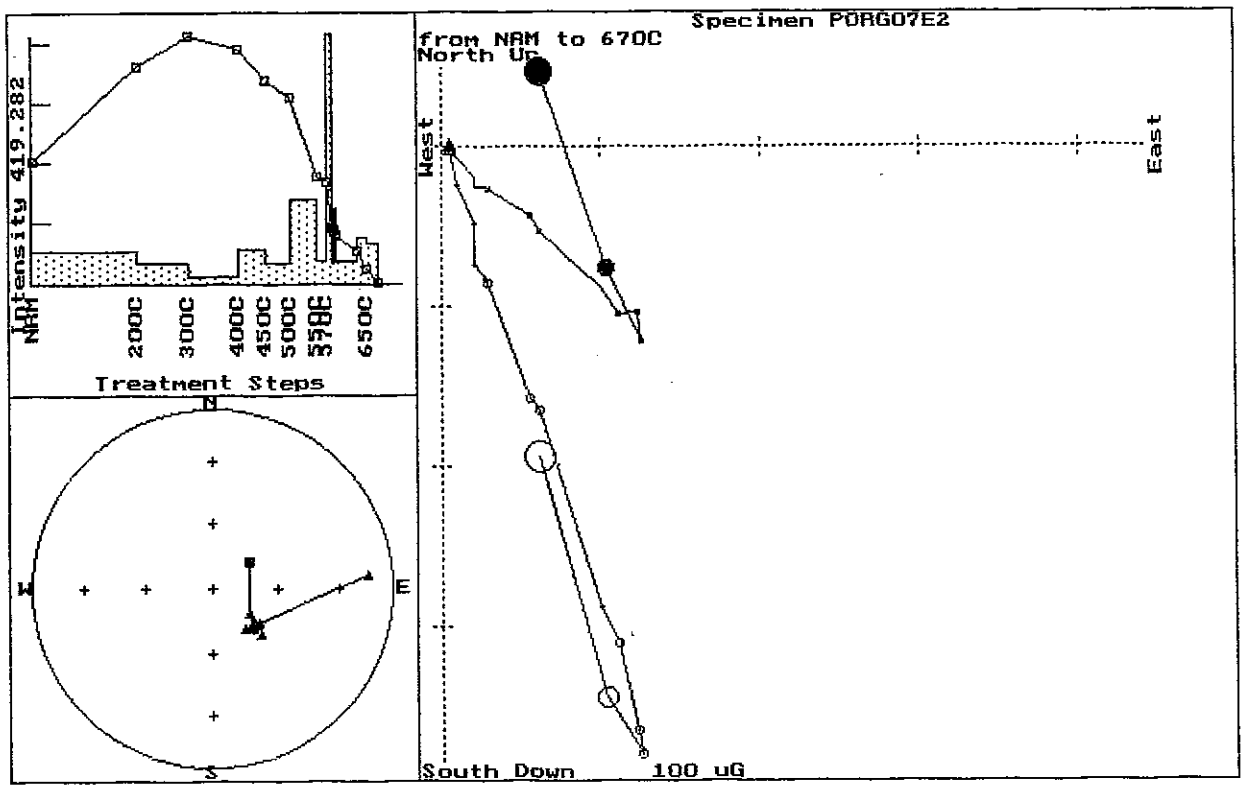
Intensity 419.282
NRM
200C
300C
400C
450C
500C
570C
650C
Treatment Steps
N
E
S
W
Specimen PORG07E2
from NRM to 670C
North Up
West
East
South Down
100 uG

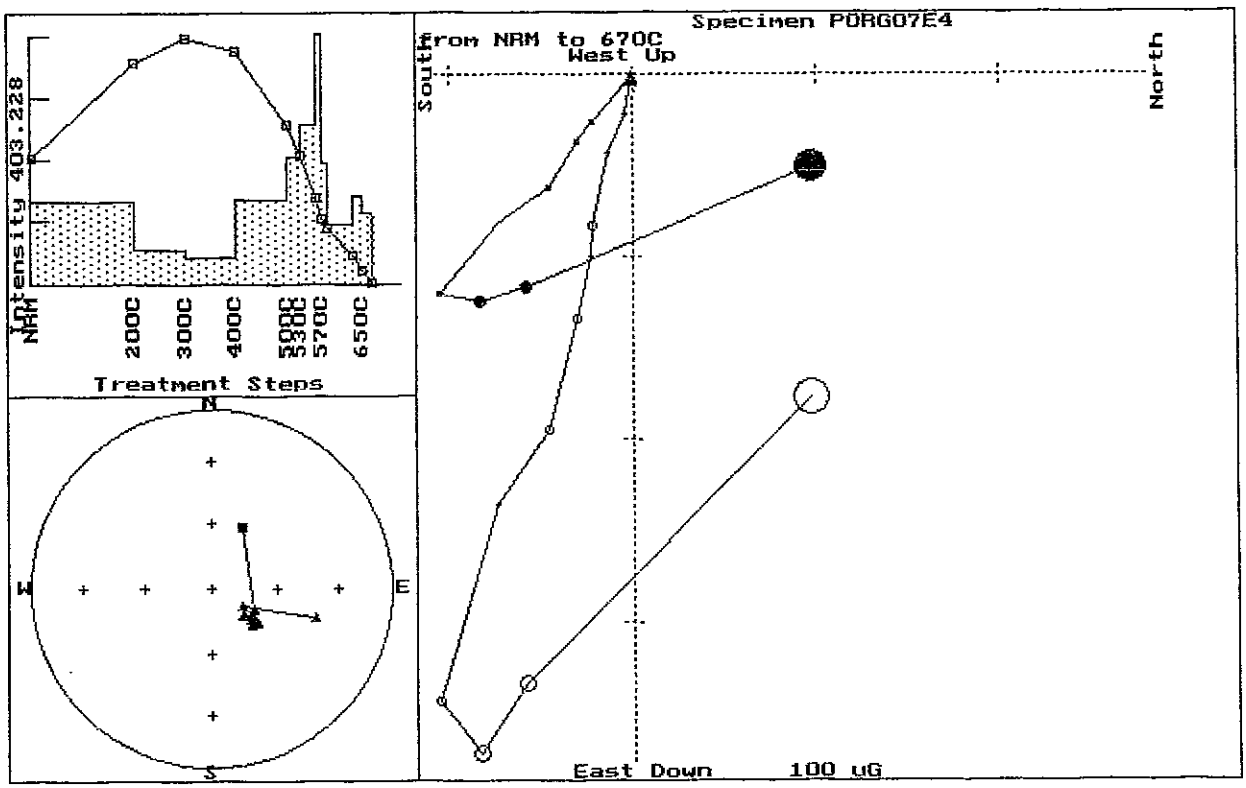
Intensity 403.228
NRM
200C
300C
400C
530C
570C
650C
Treatment Steps
N
E
S
W
Specimen PORG07E4
from NRM to 670C
West Up
South
North
East Down
100 uG

Fig.10. Zijderveld plots for the Mount Kare samples.

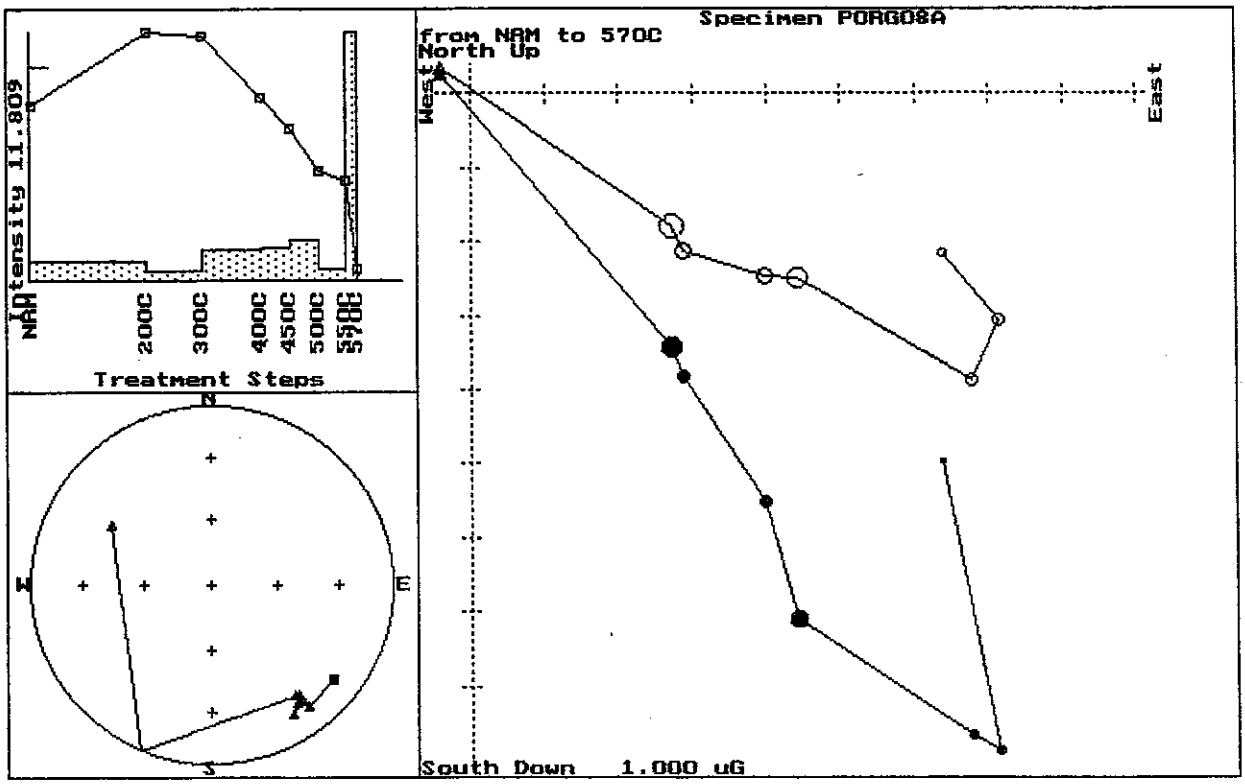
Intensity 11.809
NRM
200C
300C
400C
450C
500C
570C
Treatment Steps
N
W
E
S
Specimen PORGO8A
from NRM to 570C
North Up
West
East
South Down 1.000 uG

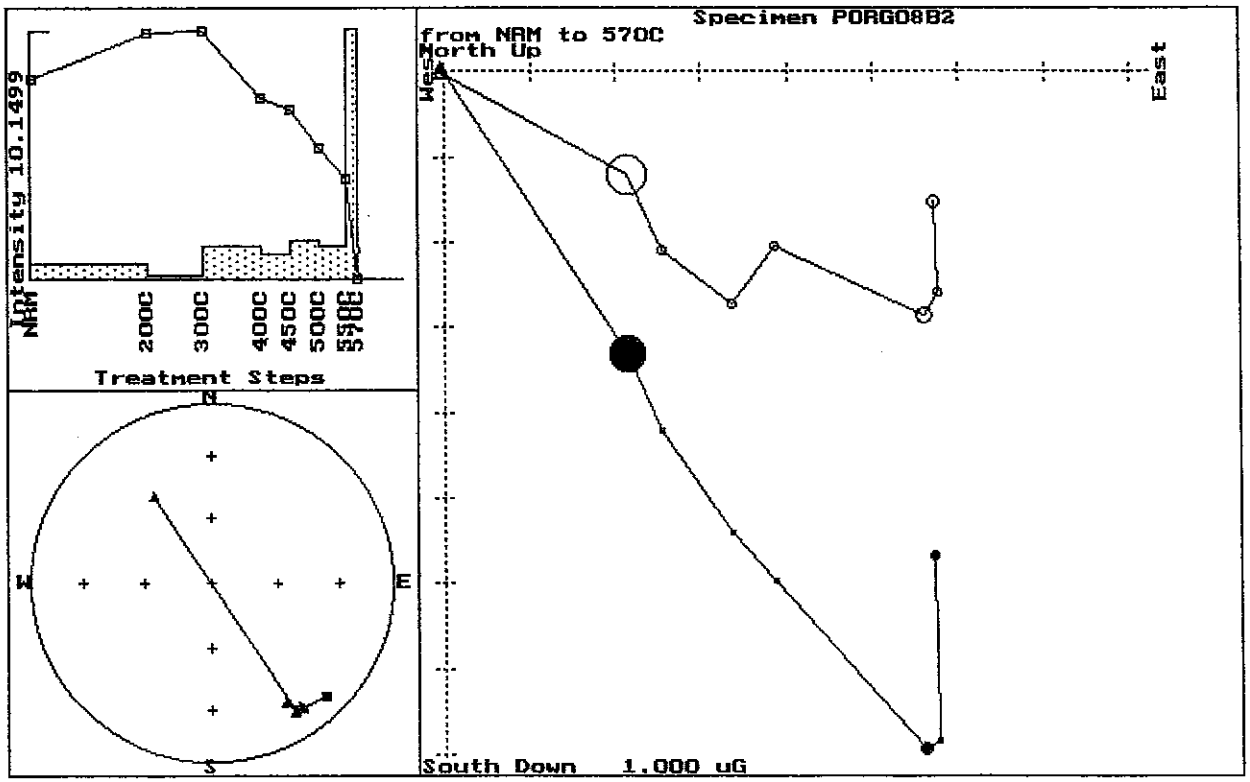
Intensity 10.1499
NRM
200C
300C
400C
450C
500C
570C
Treatment Steps
N
W
E
S
Specimen PORGO8B2
from NRM to 570C
North Up
West
East
South Down 1.000 uG

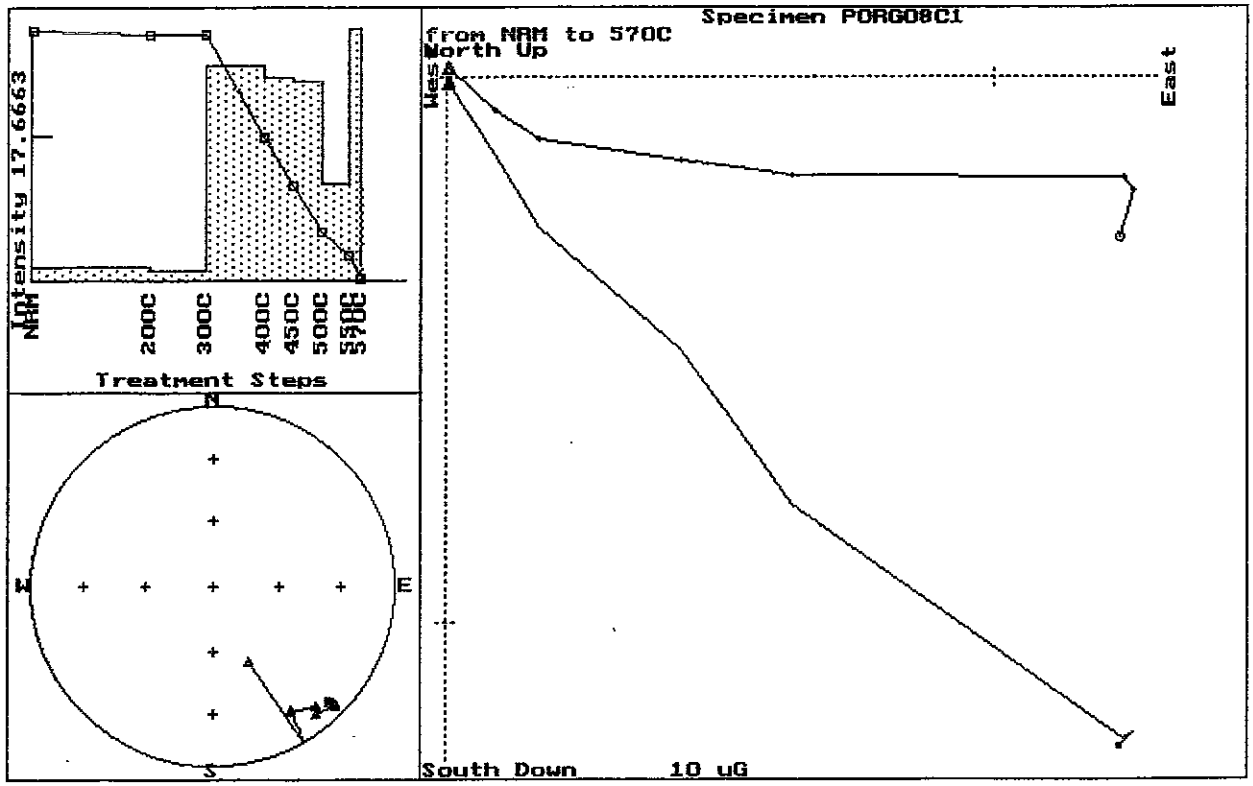
Specimen PORG08C1
from NRM to 570C
North Up
West
East
Intensity 17.6663
NRM
200C
300C
400C
450C
500C
570C
Treatment Steps
N
E
S
W
South Down
10 uG

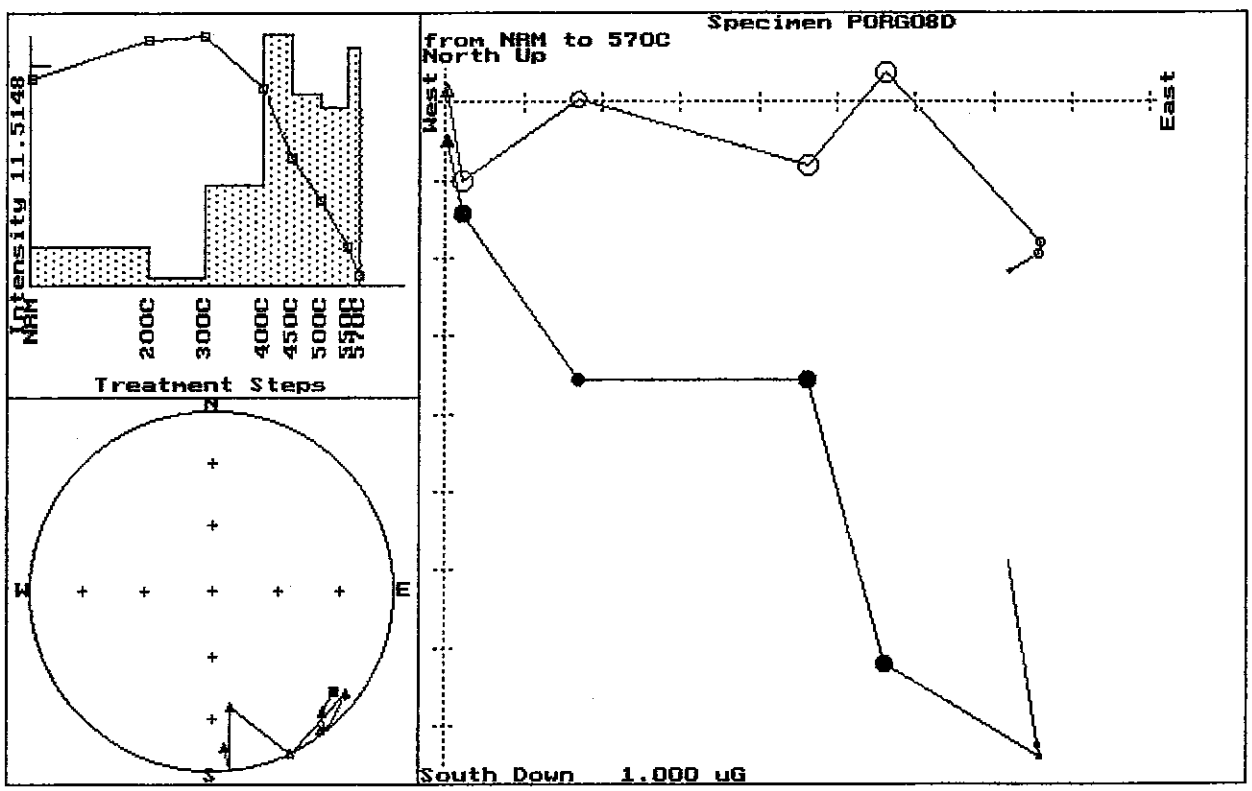
Specimen PORG08D
from NRM to 570C
North Up
West
East
Intensity 11.5148
NRM
200C
300C
400C
450C
500C
570C
Treatment Steps
N
E
S
W
South Down
1.000 uG

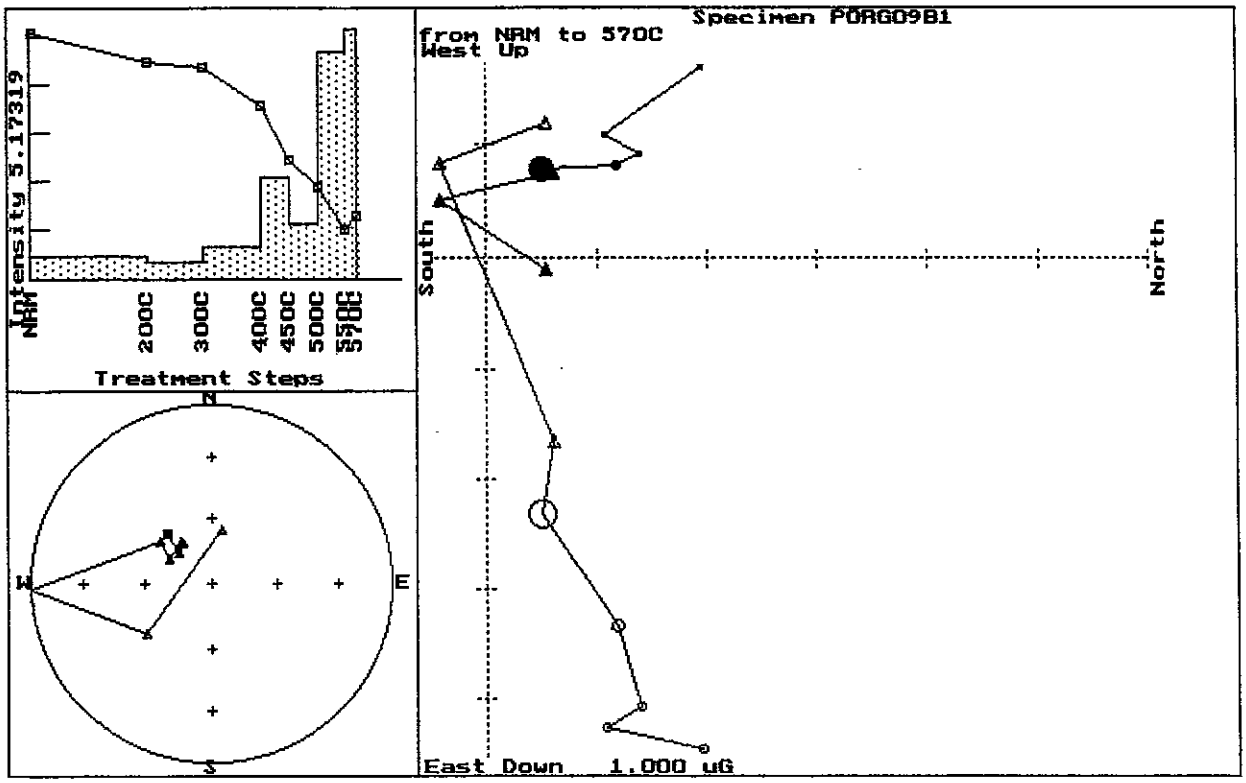
Specimen PORGO9B1
from NRM to 570C
West Up
South
North
East Down 1.000 uG
Intensity 5.17319
NRM
200C
300C
400C
450C
500C
570C
Treatment Steps
N
W
E
S

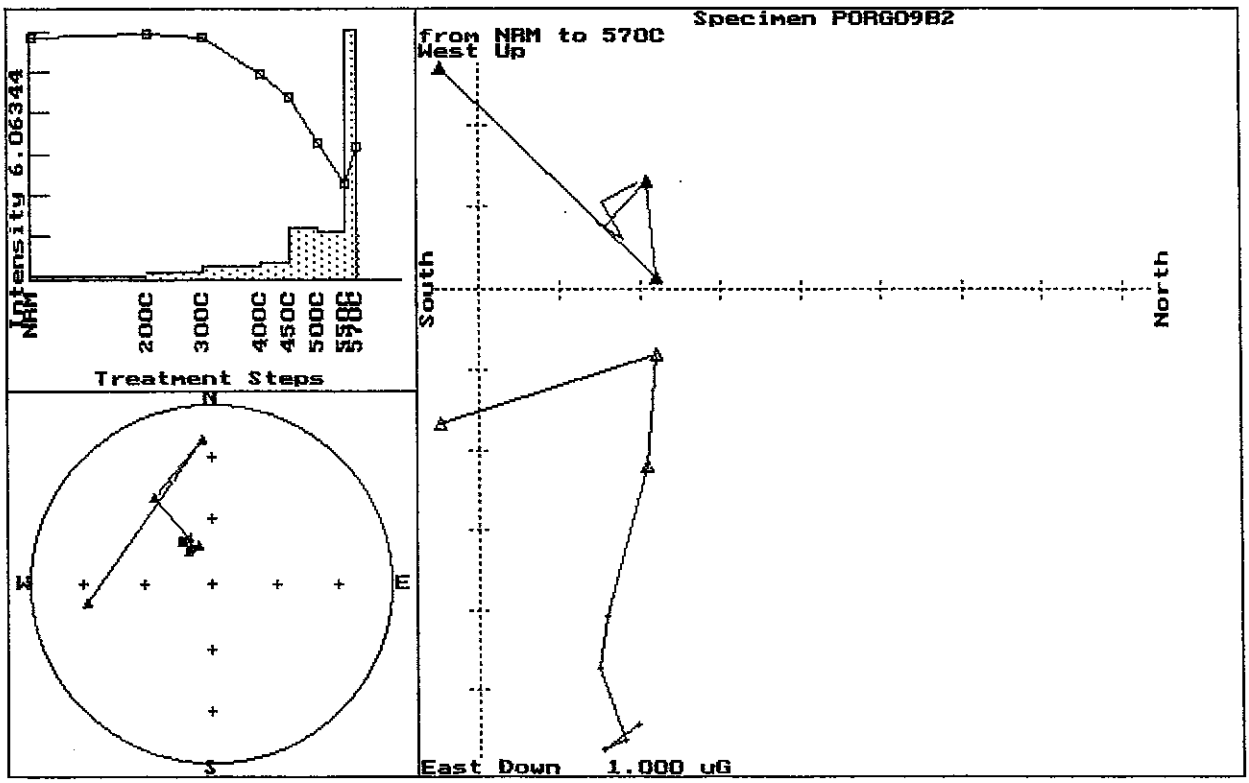
Specimen PORGO9B2
from NRM to 570C
West Up
South
North
East Down 1.000 uG
Intensity 6.06344
NRM
200C
300C
400C
450C
500C
570C
Treatment Steps
N
W
E
S

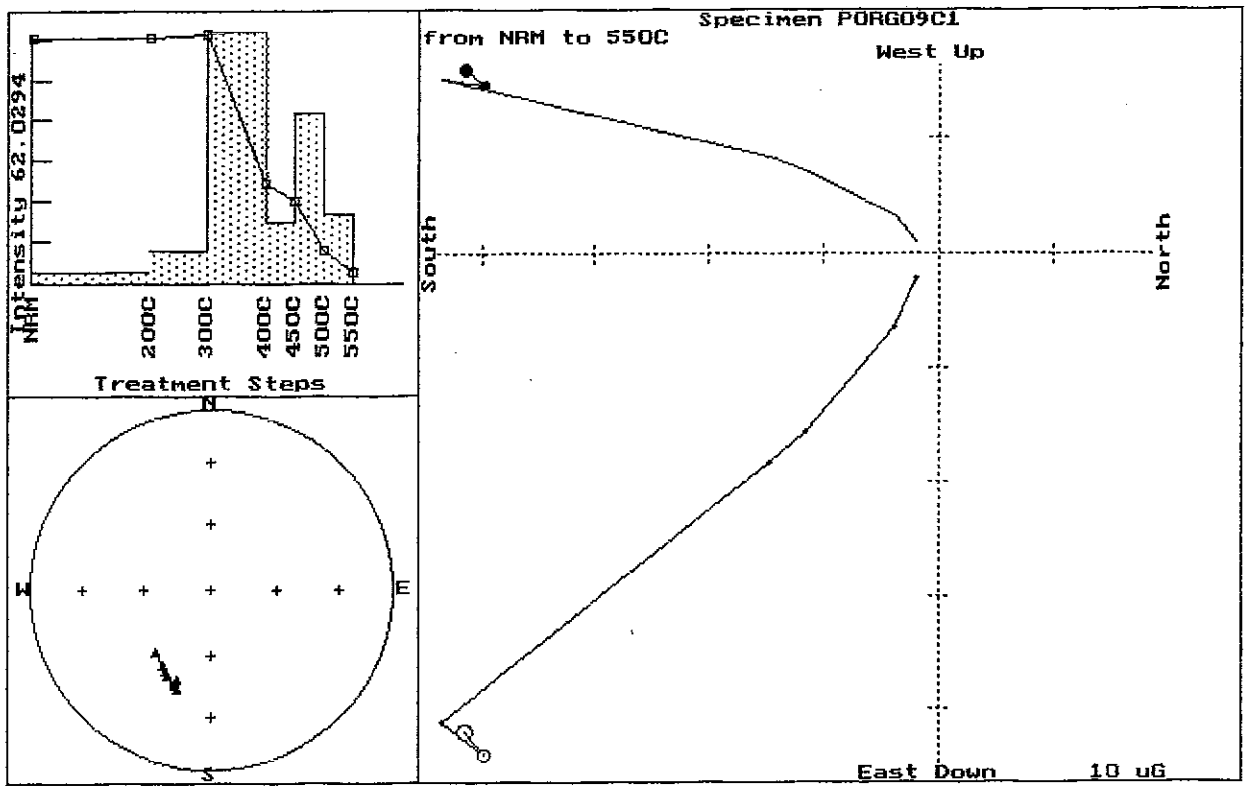
Intensity 62.0294
NRM
200C
300C
400C
450C
500C
550C
Treatment Steps
N
W
E
S
Specimen PORG09C1
from NRM to 550C
West Up
South
North
East Down
10 uG

Fig.11. Zijderveld plots for the NE Porgera Complex samples.

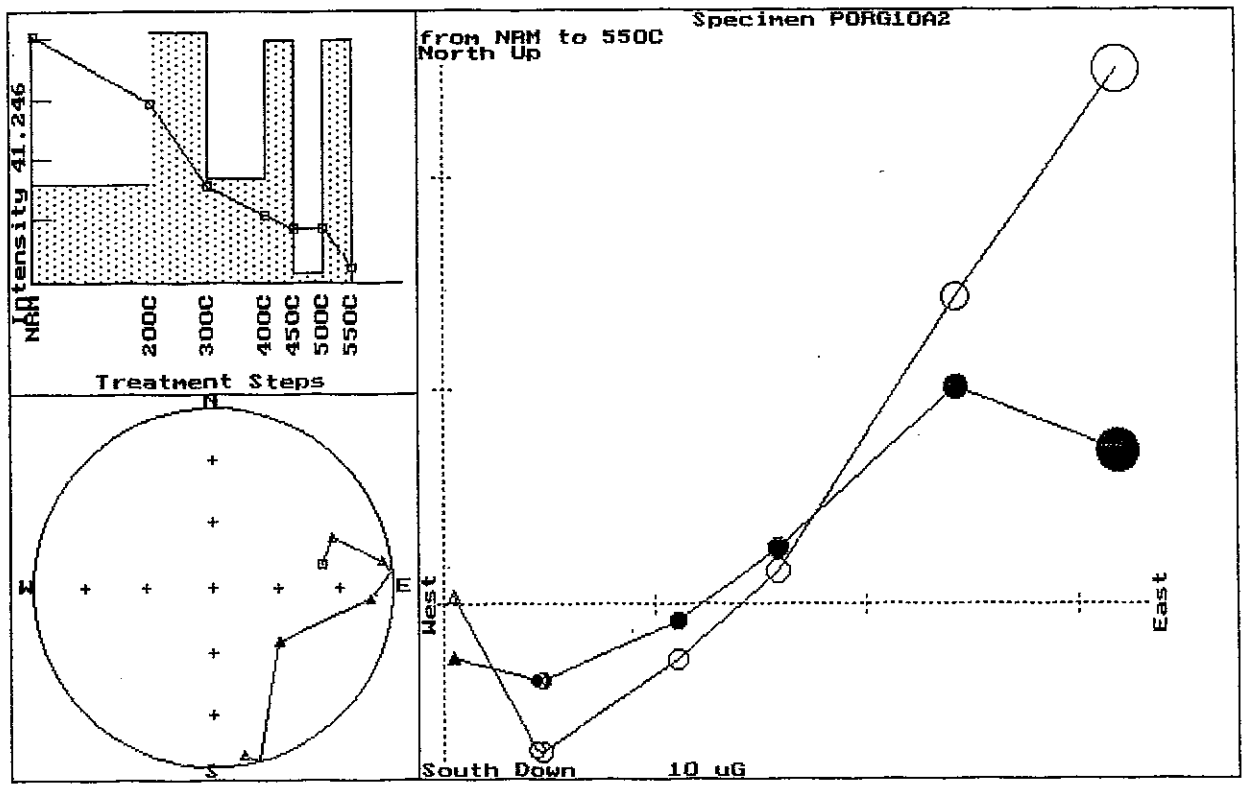
Specimen PORG10A2
from NRM to 550C
North Up
Intensity 41.246
NRM
200C
300C
400C
450C
500C
550C
Treatment Steps
N
E
S
West
East
South Down
10 uG

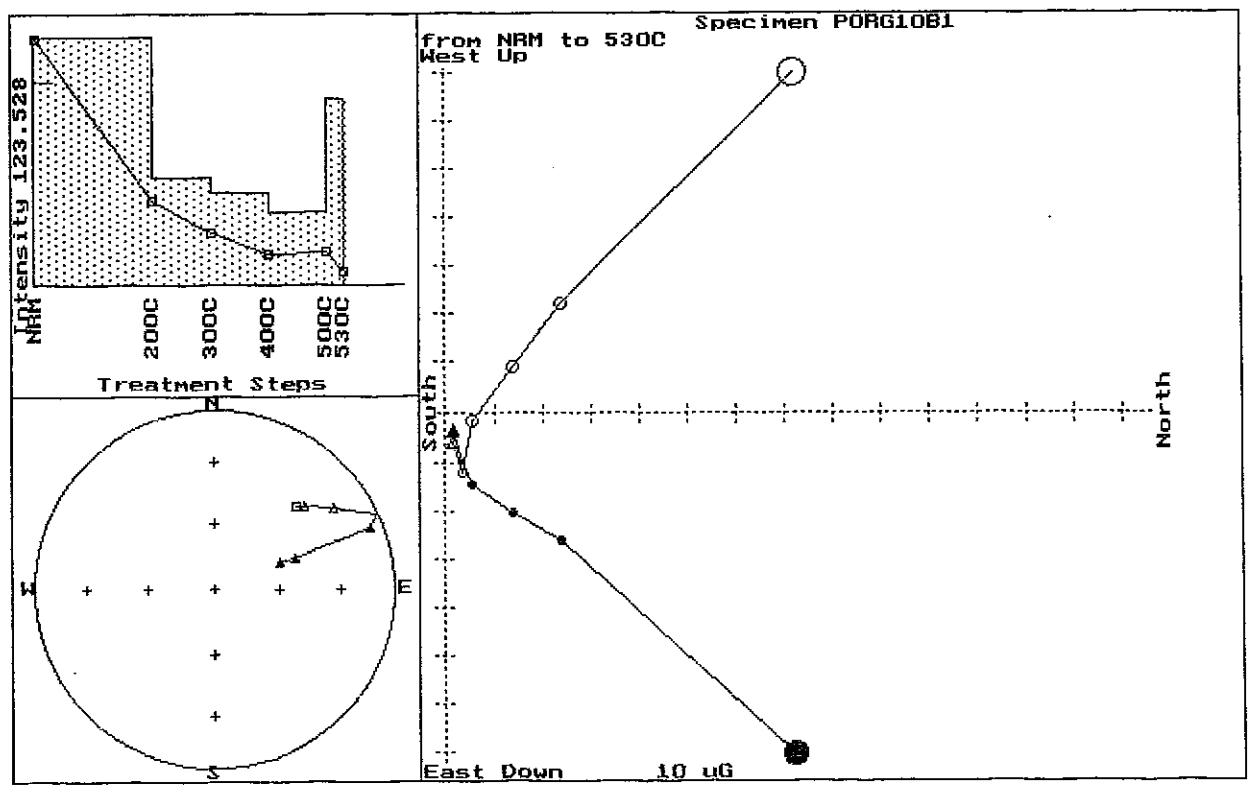
Specimen PORG10B1
from NRM to 530C
West Up
Intensity 123.528
NRM
200C
300C
400C
500C
530C
Treatment Steps
N
E
S
South
North
East Down
10 uG

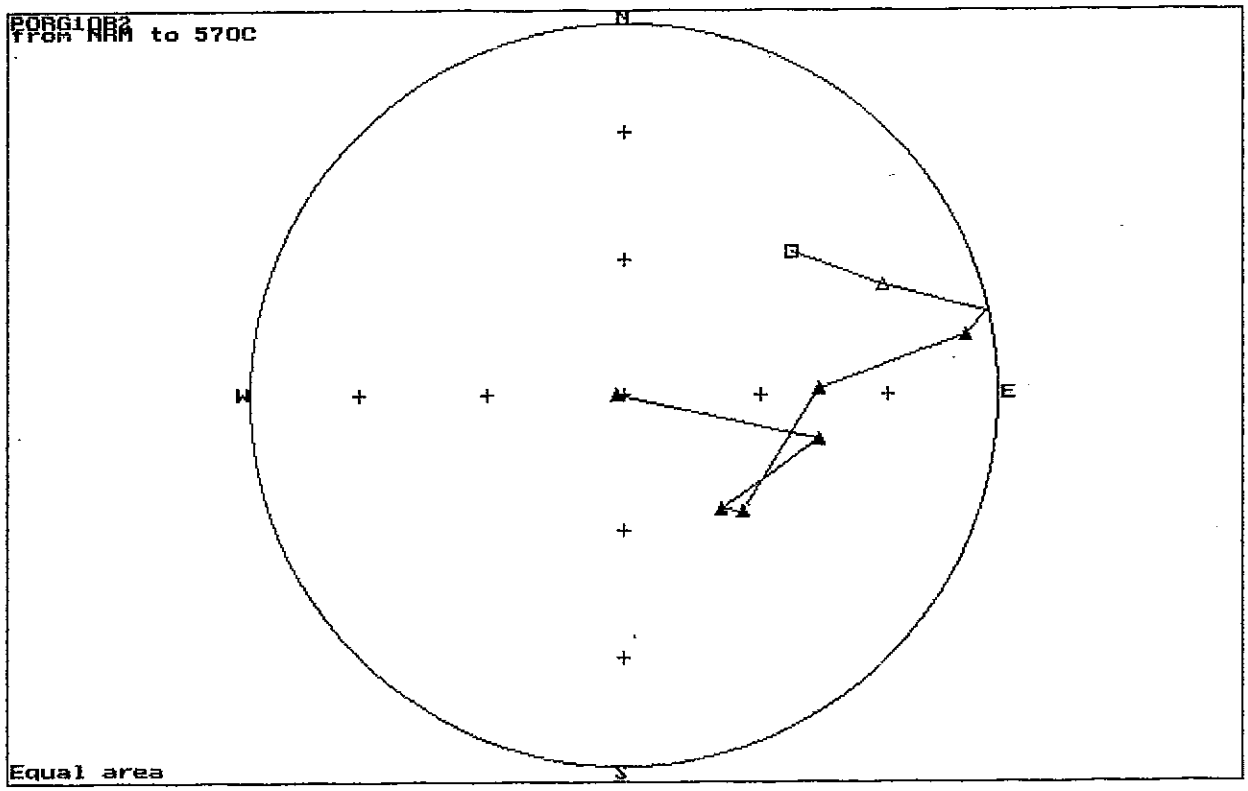
PORG1OB2
from NRM to 570C
N
W
E
S
Equal area

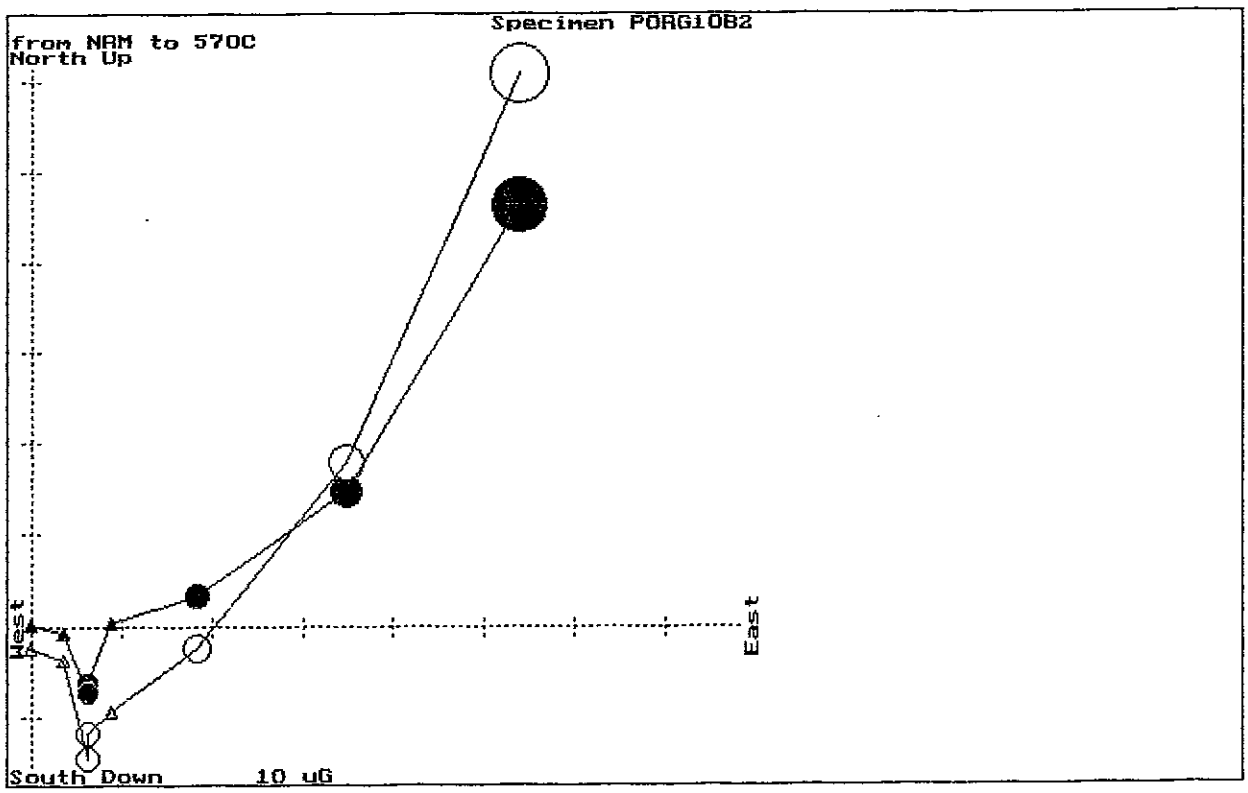
Specimen PORG1OB2
from NRM to 570C
North Up
West
East
South Down
10 uG

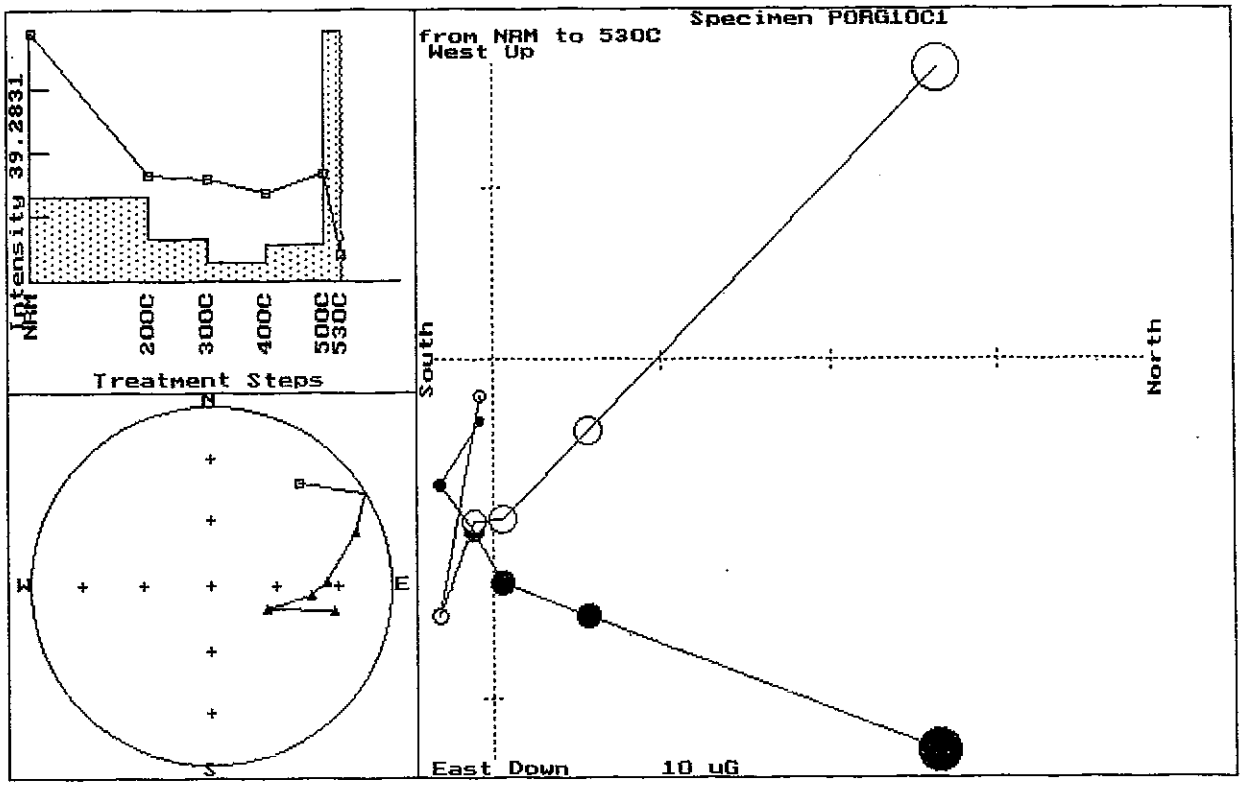
Specimen PORG10C1
from NRM to 530C
West Up
Intensity 39.2831
NRM
200C
300C
400C
500C
530C
Treatment Steps
N
W
E
S
South
North
East Down
10 uG

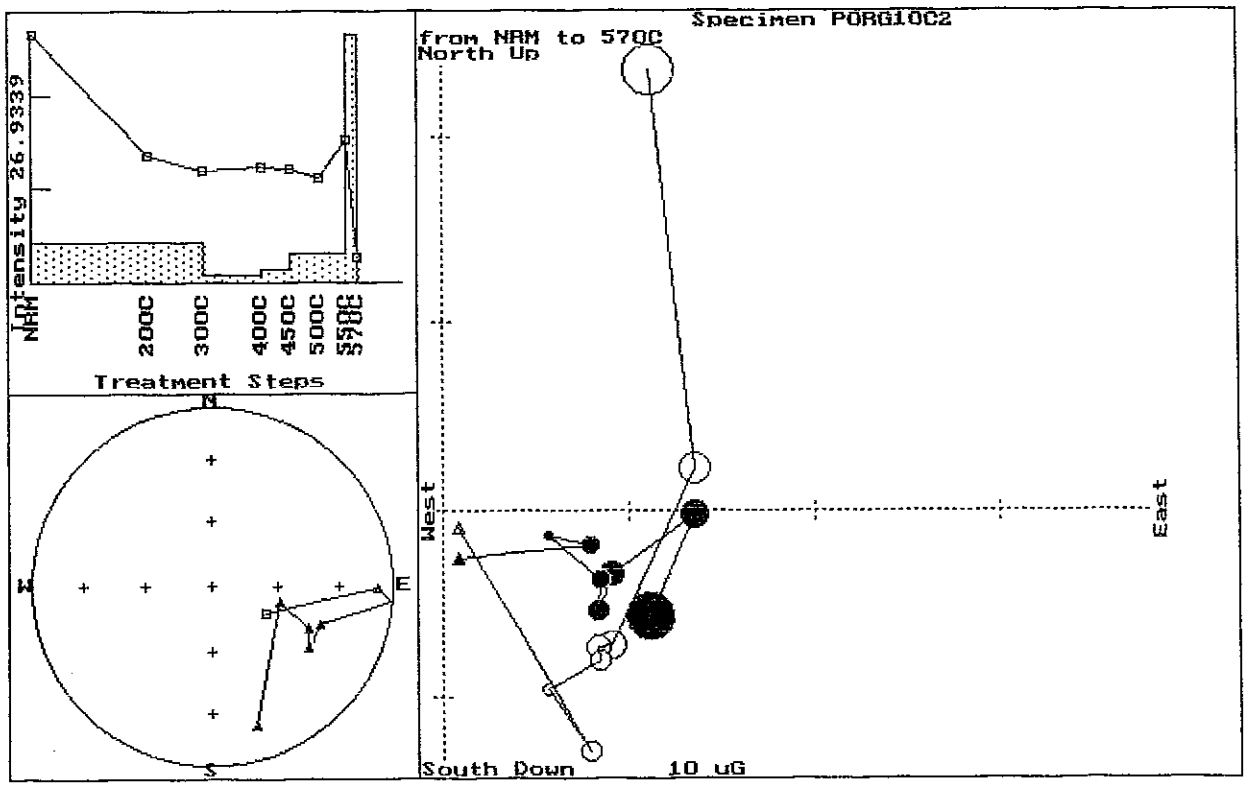
Specimen PORG10C2
from NRM to 570C
North Up
Intensity 26.9339
NRM
200C
300C
400C
450C
500C
570C
Treatment Steps
N
W
E
S
West
East
South Down
10 uG

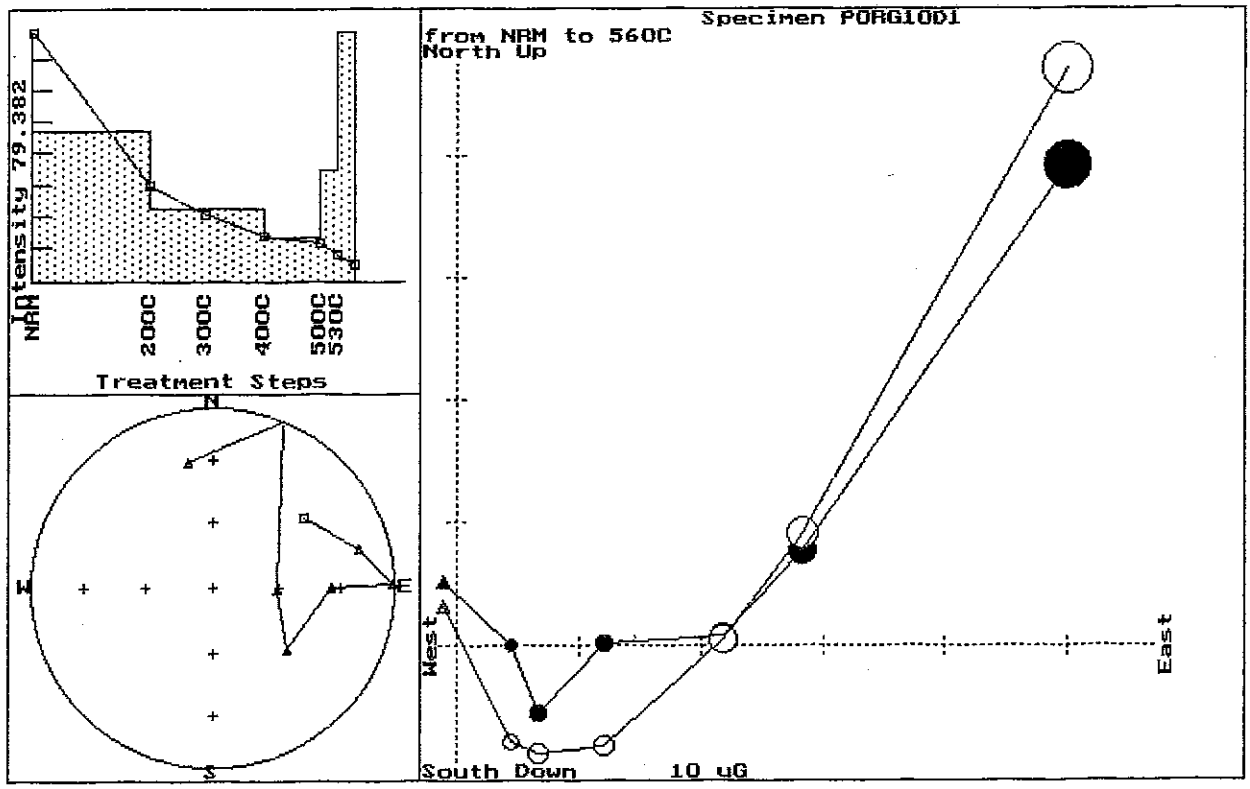
Intensity 79.382
NRM
200C
300C
400C
500C
530C
Treatment Steps
N
W
E
S
Specimen PORG10D1
from NRM to 560C
North Up
West
East
South Down
10 uG

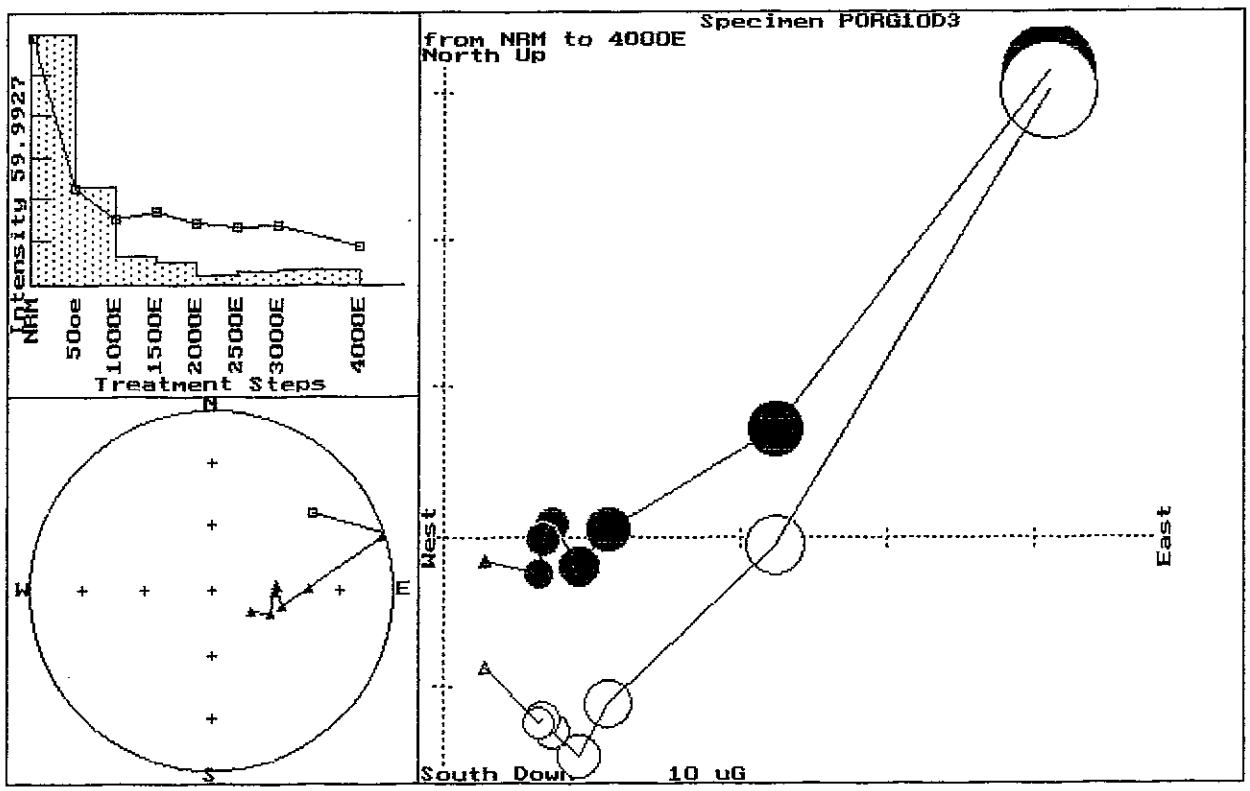
Intensity 59.9927
NRM
50oe
1000E
1500E
2000E
2500E
3000E
4000E
Treatment Steps
N
W
E
S
Specimen PORG10D3
from NRM to 4000E
North Up
West
East
South Down
10 uG

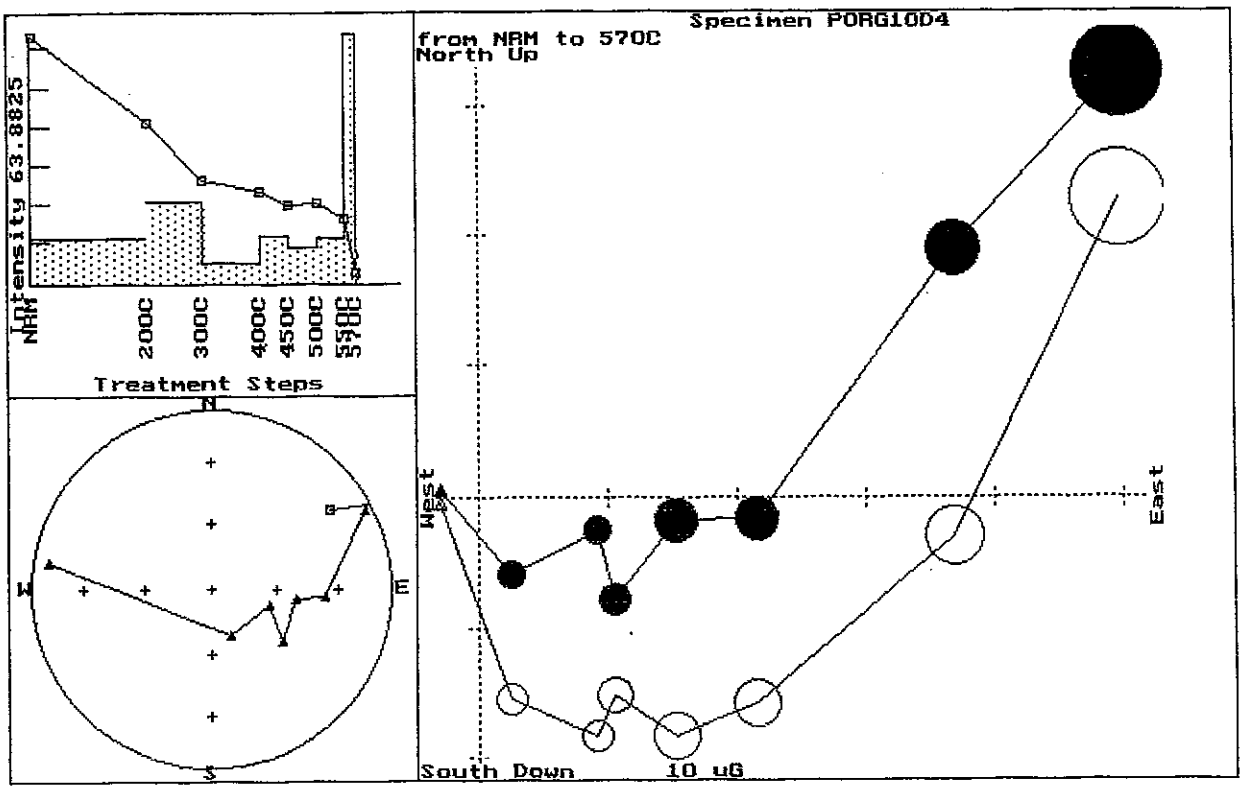
Intensity 63.8825
NRM
200C
300C
400C
450C
500C
570C
Treatment Steps
N
W
E
S
Specimen PORG10D4
from NRM to 570C
North Up
West
East
South Down
10 uG

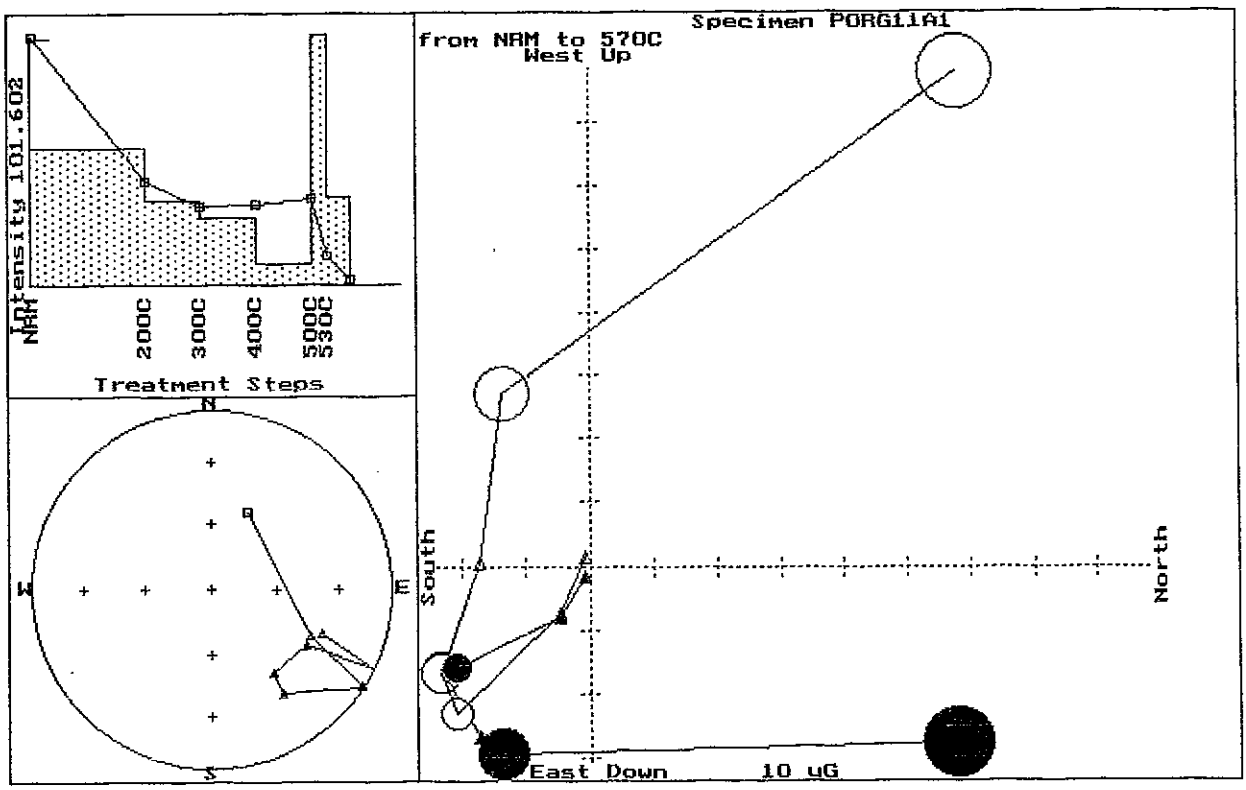
Intensity 101.602
NRM
200C
300C
400C
500C
530C
Treatment Steps
N
W
E
S
Specimen PORG11A1
from NRM to 570C
West Up
South
North
East Down
10 uG

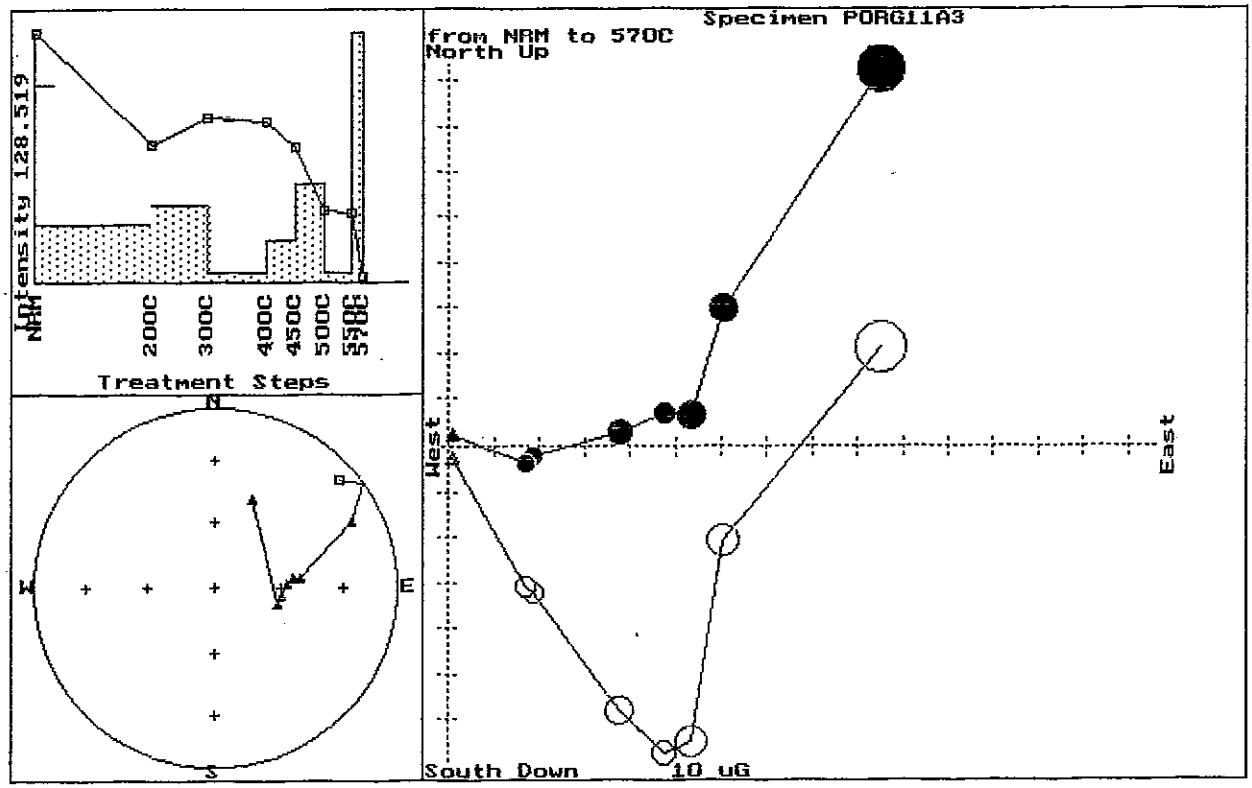
Specimen PORG11A3
from NRM to 570C
North Up
Intensity 128.519
NRM
200C
300C
400C
450C
500C
570C
Treatment Steps
N
W
E
S
West
East
South Down
10 uG

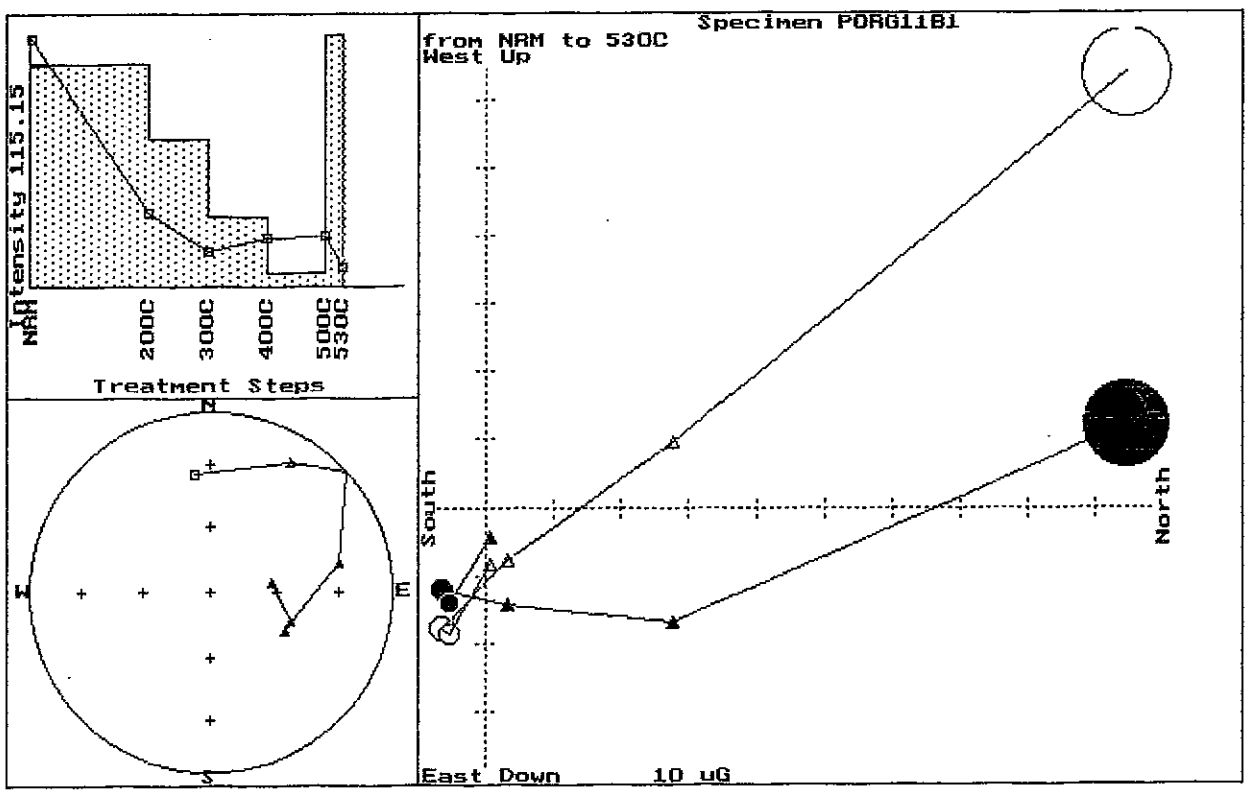
Specimen PORG11B1
from NRM to 530C
West Up
Intensity 115.15
NRM
200C
300C
400C
500C
530C
Treatment Steps
N
W
E
S
South
North
East Down
10 uG

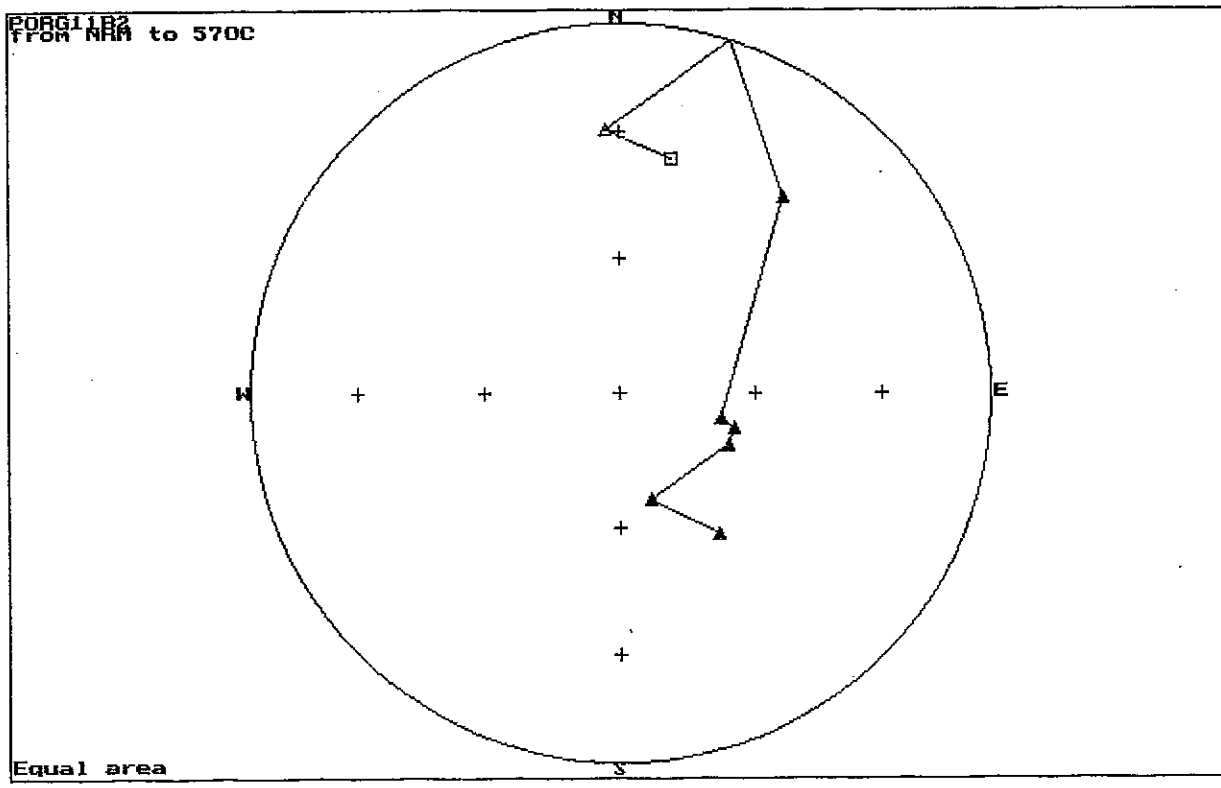
PORG11B2
from NRM to 570C
N
W
E
S
Equal area

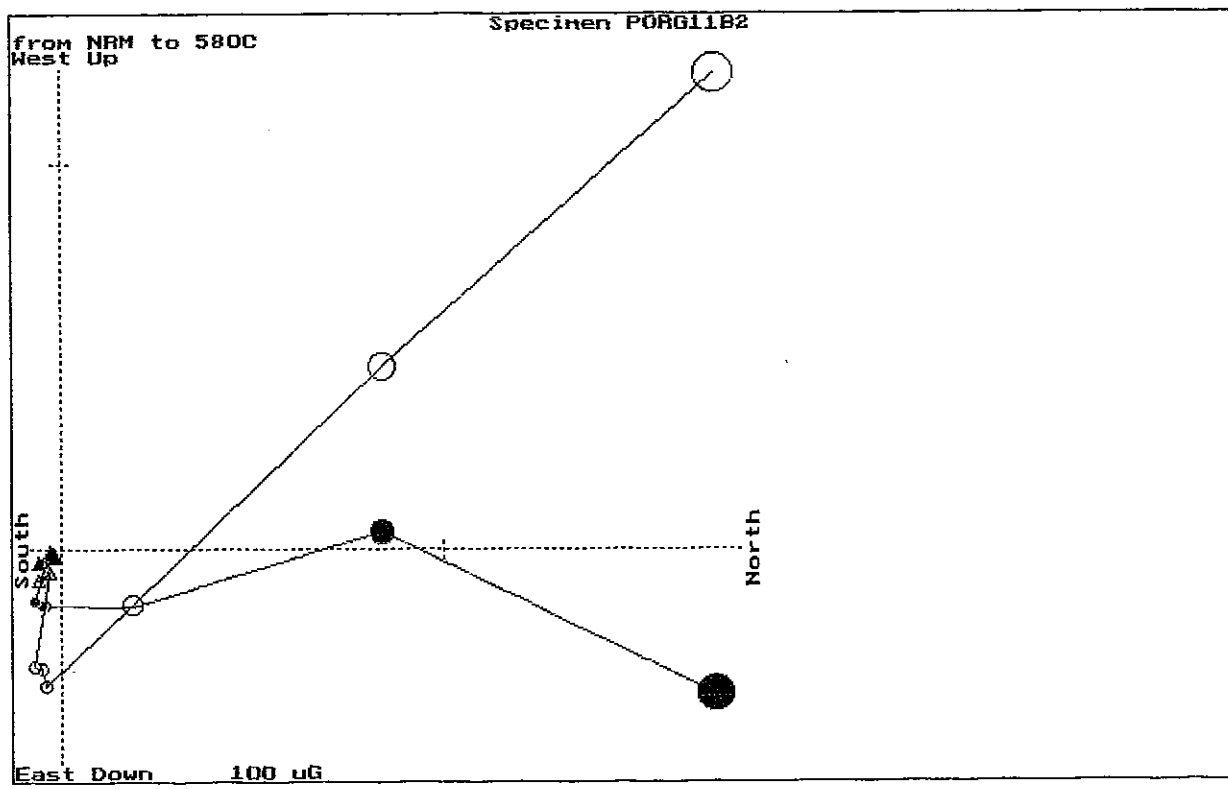
Specimen PORG11B2
from NRM to 580C
West Up
South
North
East Down
100 uG

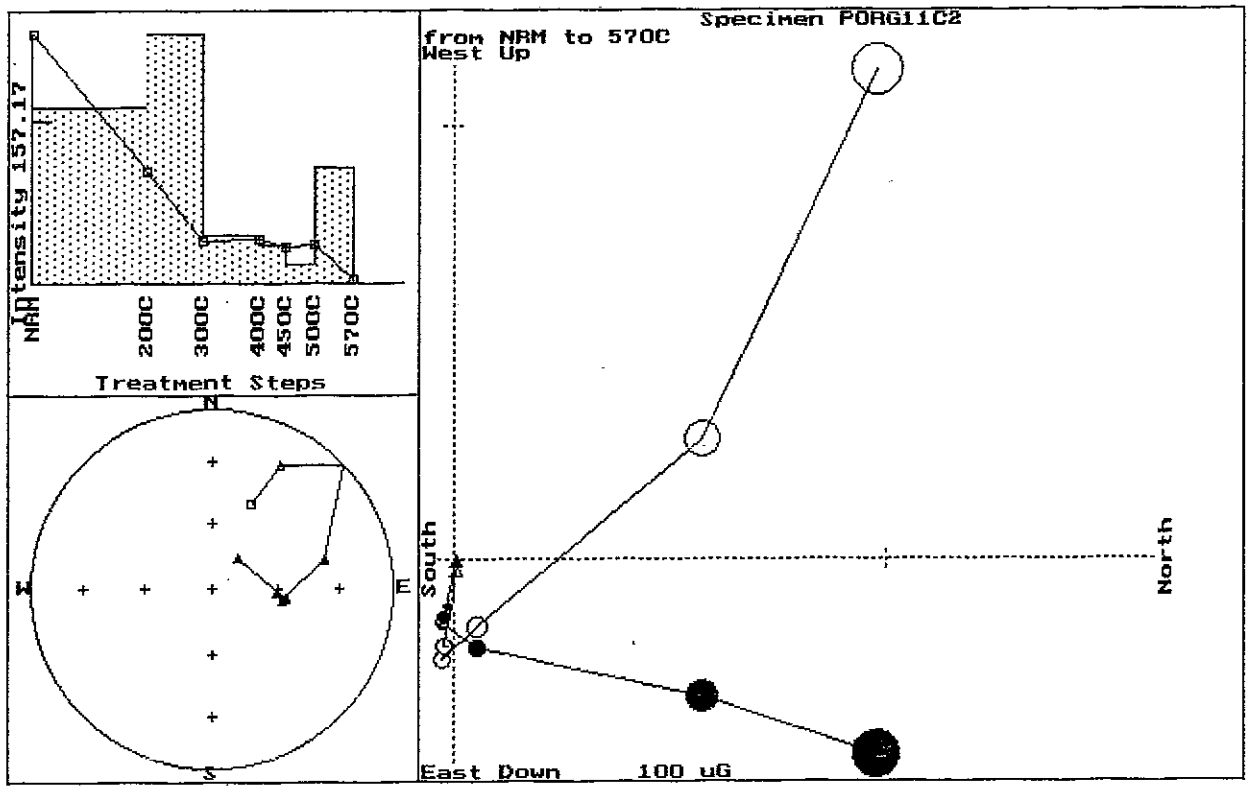
Specimen PORG11C2
from NRM to 570C
West Up
Intensity 157.17
NRM
200C
300C
400C
450C
500C
570C
Treatment Steps
N
E
S
W
South
North
East Down
100 uG

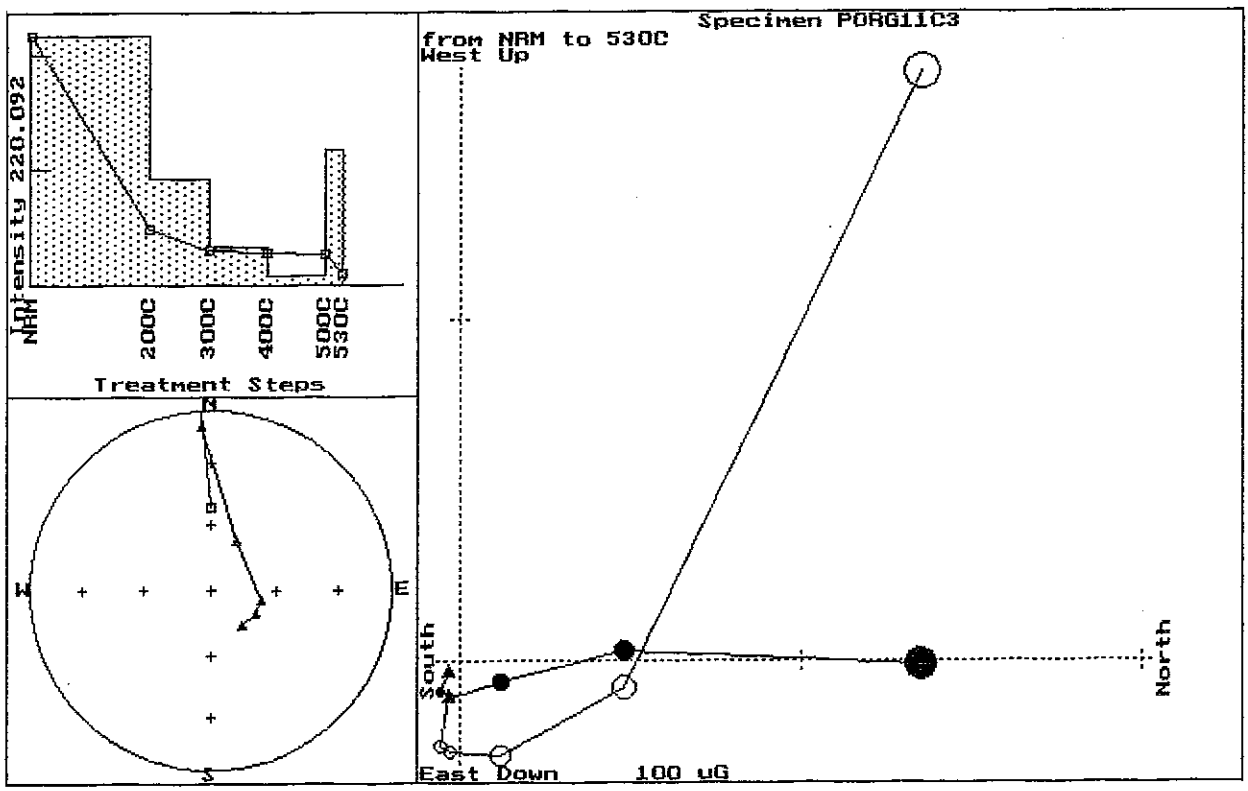
Specimen PORG11C3
from NRM to 530C
West Up
Intensity 220.092
NRM
200C
300C
400C
500C
530C
Treatment Steps
N
E
S
W
South
North
East Down
100 uG

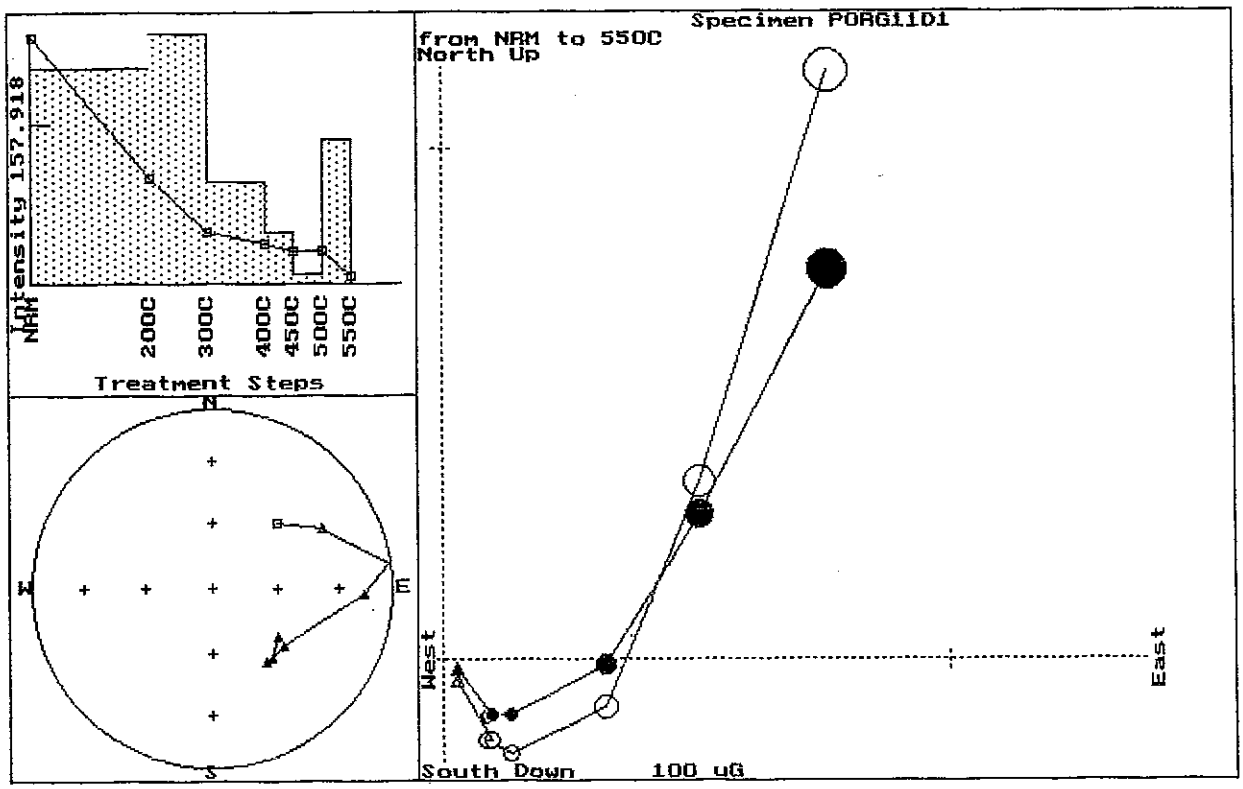
Specimen PORG11D1
from NRM to 550C
North Up
Intensity 157.918
NRM
200C
300C
400C
450C
500C
550C
Treatment Steps
N
E
S
West
East
South Down
100 uG

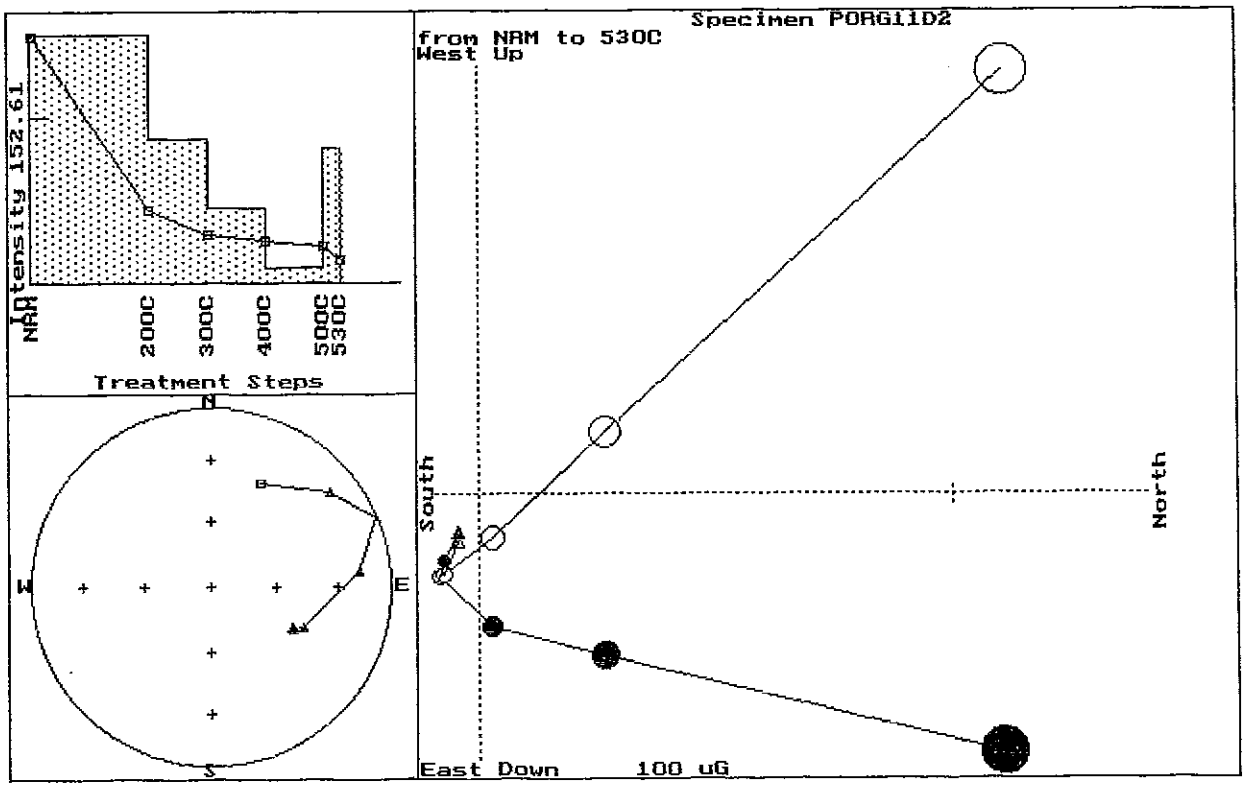
Specimen PORG11D2
from NRM to 530C
West Up
Intensity 152.61
NRM
200C
300C
400C
500C
530C
Treatment Steps
N
E
S
South
North
East Down
100 uG

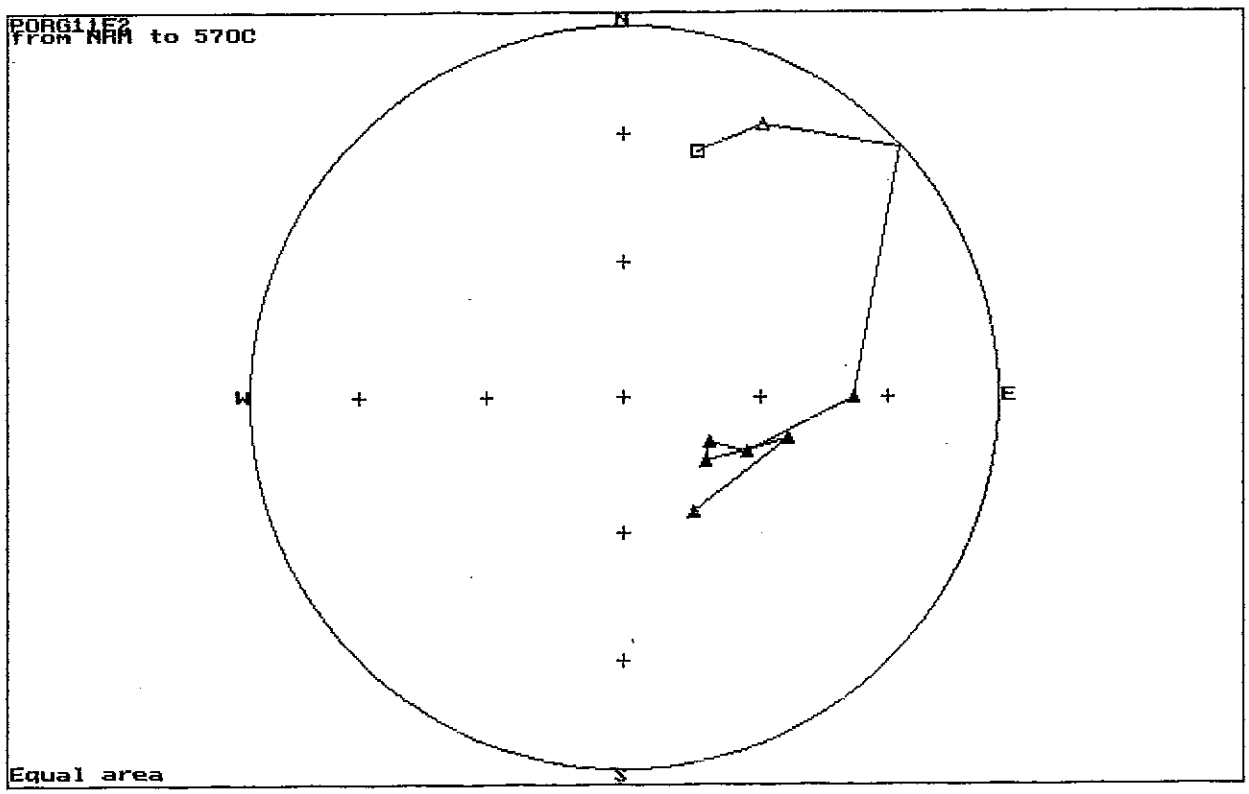
PORG11E2
from NRM to 570C
N
W
E
S
Equal area

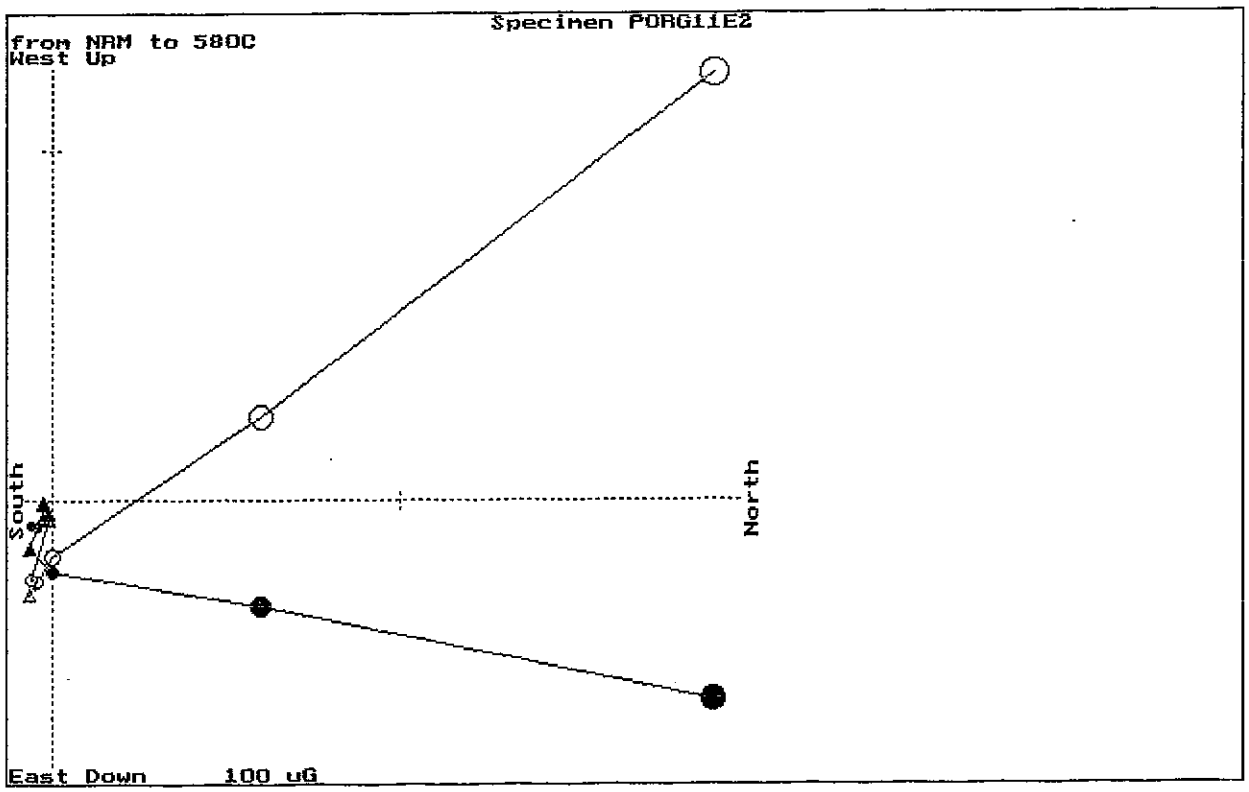
Specimen PORG11E2
from NRM to 580C
West Up
South
North
East Down
100 uG

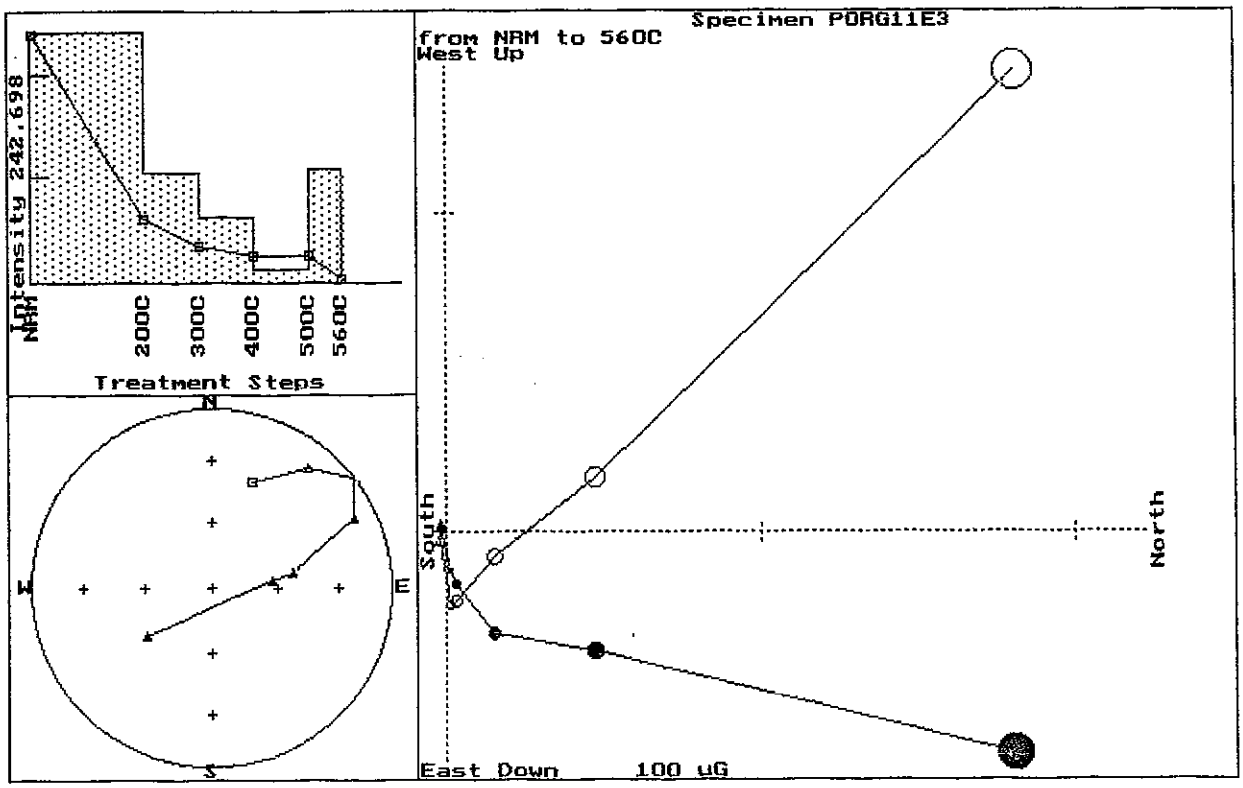
Specimen PORG11E3
from NRM to 560C
West Up
Intensity 242.698
NRM
200C
300C
400C
500C
560C
Treatment Steps
N
E
S
W
South
North
East Down
100 uG

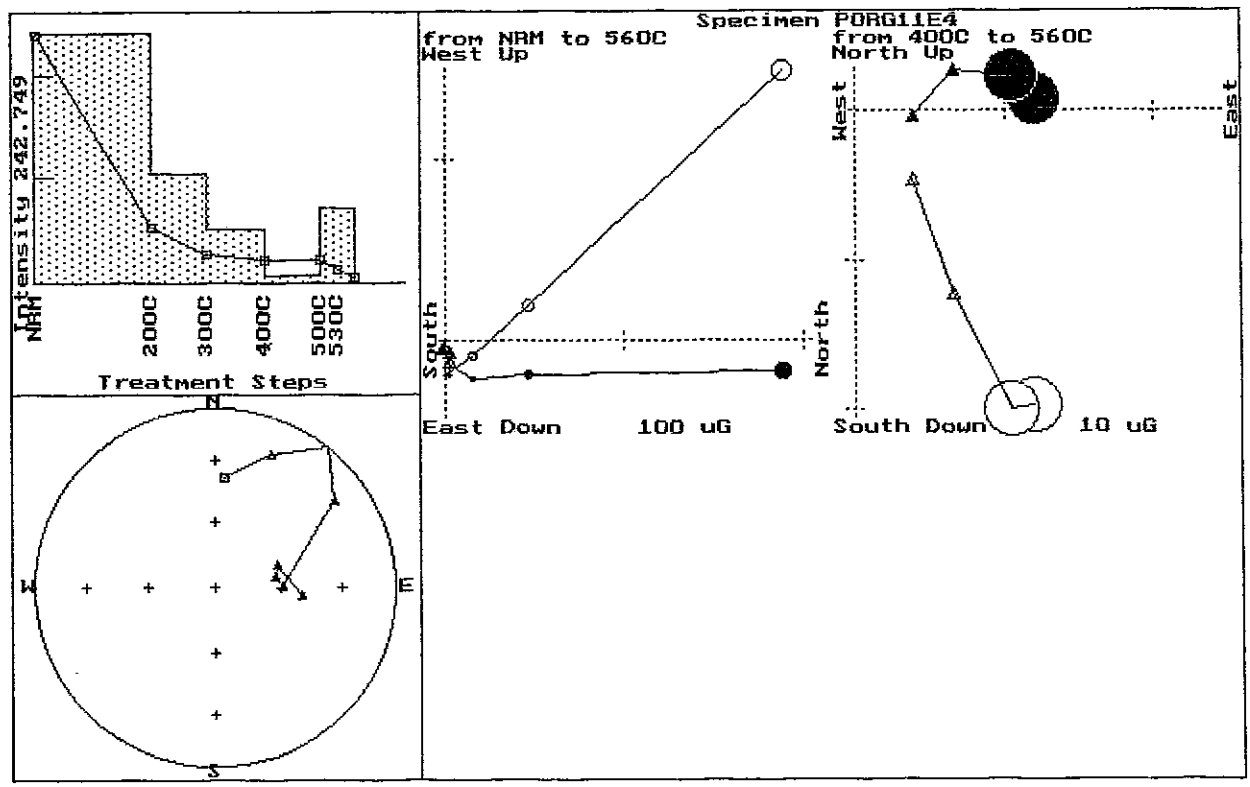
Specimen PORG11E4
from NRM to 560C
West Up
from 400C to 560C
North Up
Intensity 242.749
NRM
200C
300C
400C
500C
530C
Treatment Steps
N
E
S
W
South
North
West
East
East Down
100 uG
South Down
10 uG

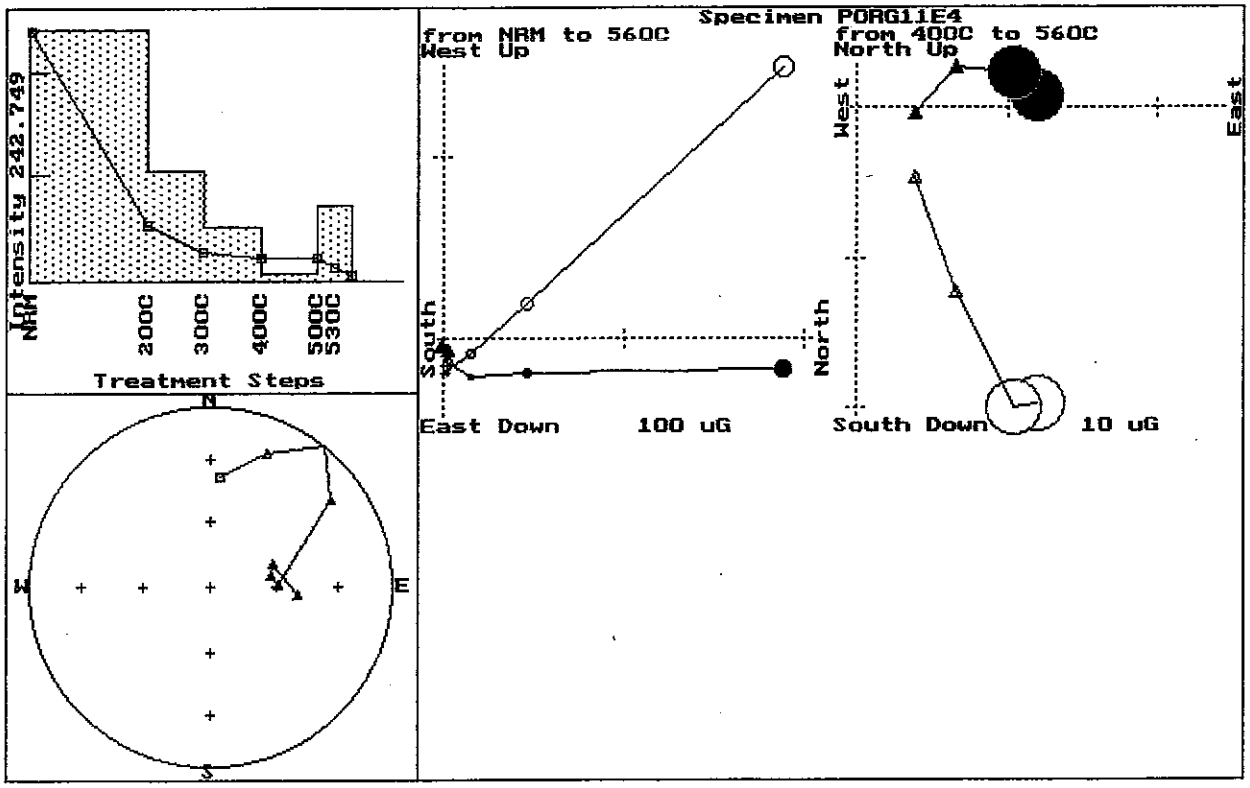
Intensity 242.749
NRM
200C
300C
400C
500C
530C
Treatment Steps
N
E
S
W
Specimen PORG11E4
from NRM to 560C
West Up
South
North
East Down
100 uG
from 400C to 560C
North Up
West
East
South Down
10 uG

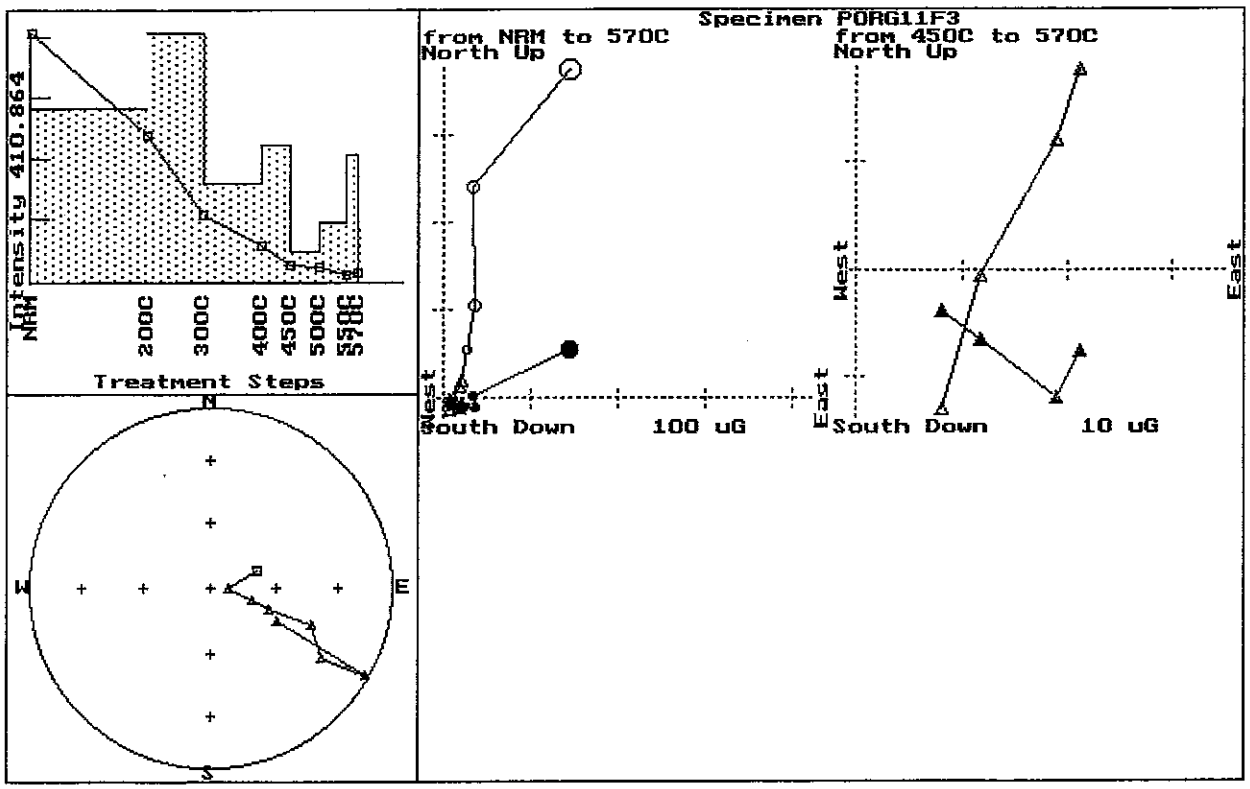
Intensity 410.864
NRM
200C
300C
400C
450C
500C
570C
Treatment Steps
N
E
S
W
Specimen PORG11F3
from NRM to 570C
North Up
West
East
South Down
100 uG
from 450C to 570C
North Up
West
East
South Down
10 uG

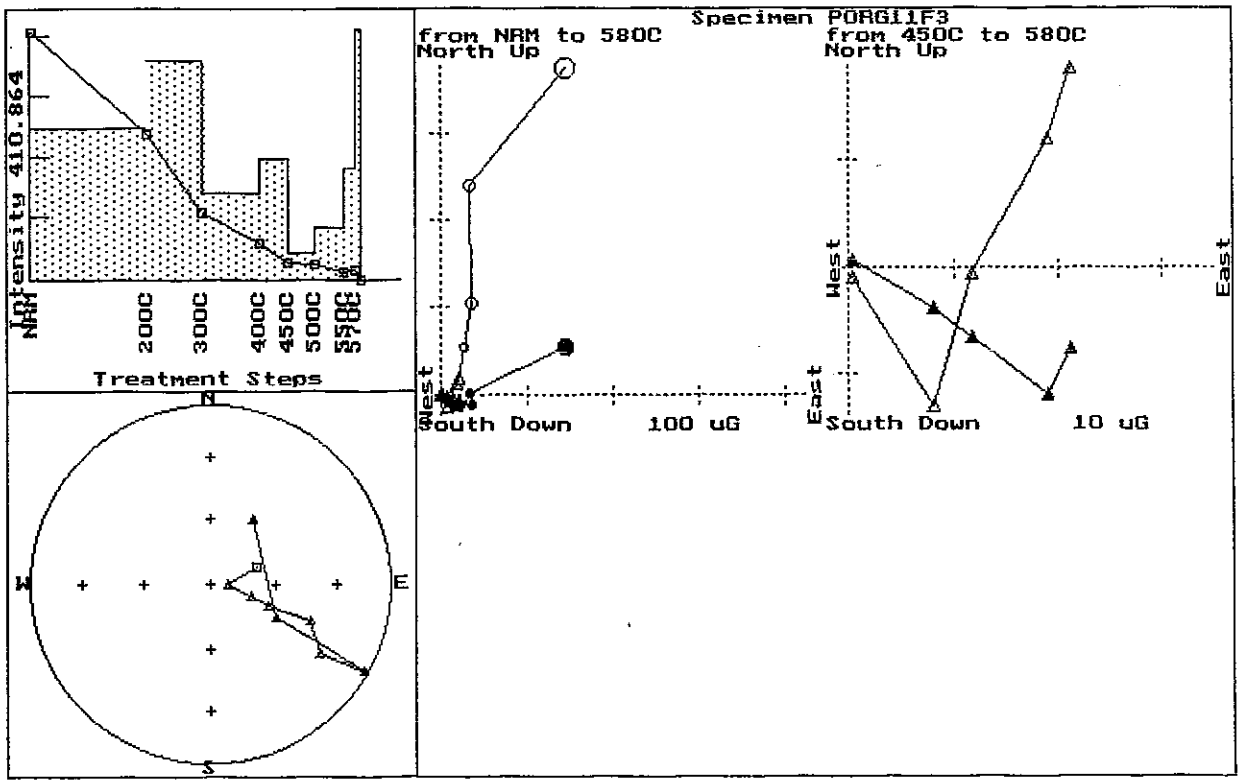
Specimen PORG11F3
from NRM to 580C
North Up
from 450C to 580C
North Up
Intensity 410.864
NRM
200C
300C
400C
450C
500C
580C
Treatment Steps
N
E
S
W
West
East
South Down
100 uG
10 uG

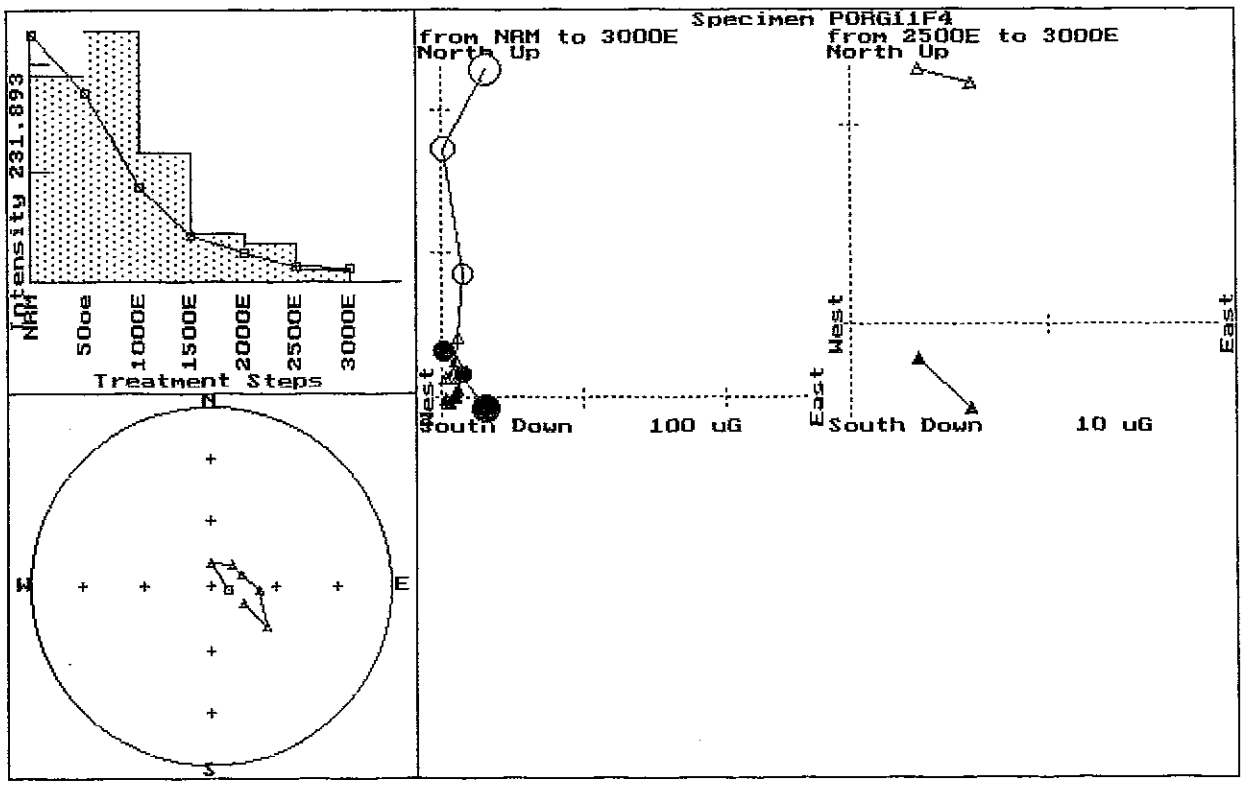
Specimen PORG11F4
from NRM to 3000E
North Up
from 2500E to 3000E
North Up
Intensity 231.893
NRM
500e
1000E
1500E
2000E
2500E
3000E
Treatment Steps
N
E
S
W
West
East
South Down
100 uG
10 uG

Fig.12 Zijderveld plots for the Roamane hornblende diorite samples.

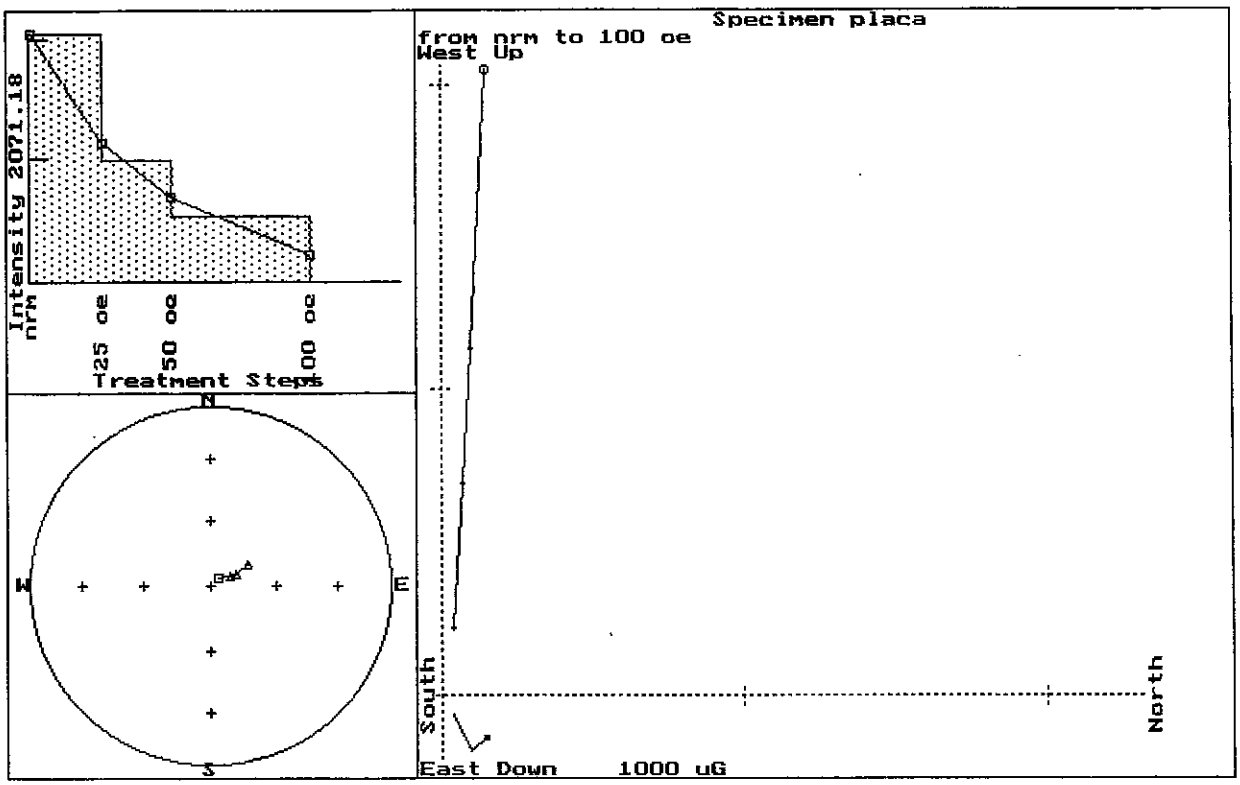
Intensity 2071.18
nrm
25 oe
50 oe
00 oe
Treatment Steps
N
E
S
Specimen placa
from nrm to 100 oe
West Up
South
North
East Down
1000 uG

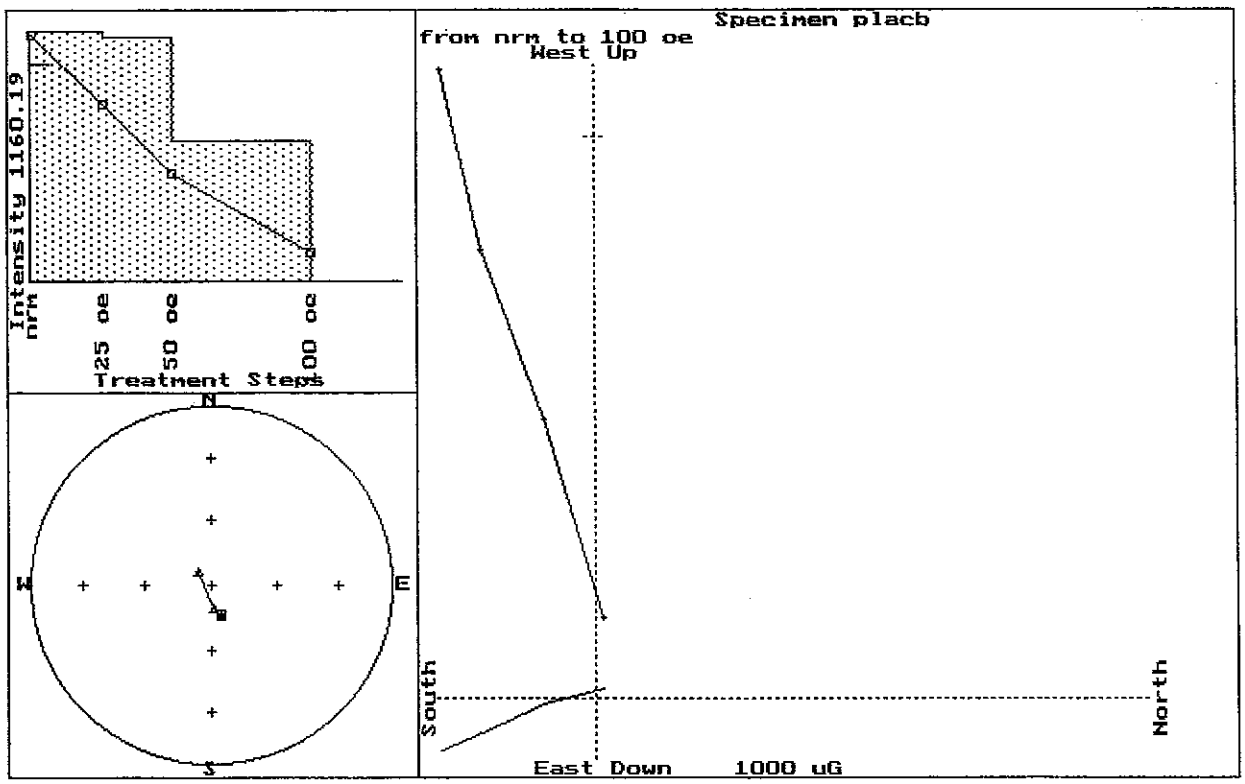
Intensity 1160.19
nrm
25 oe
50 oe
00 oe
Treatment Steps
N
E
S
Specimen placb
from nrm to 100 oe
West Up
South
North
East Down
1000 uG

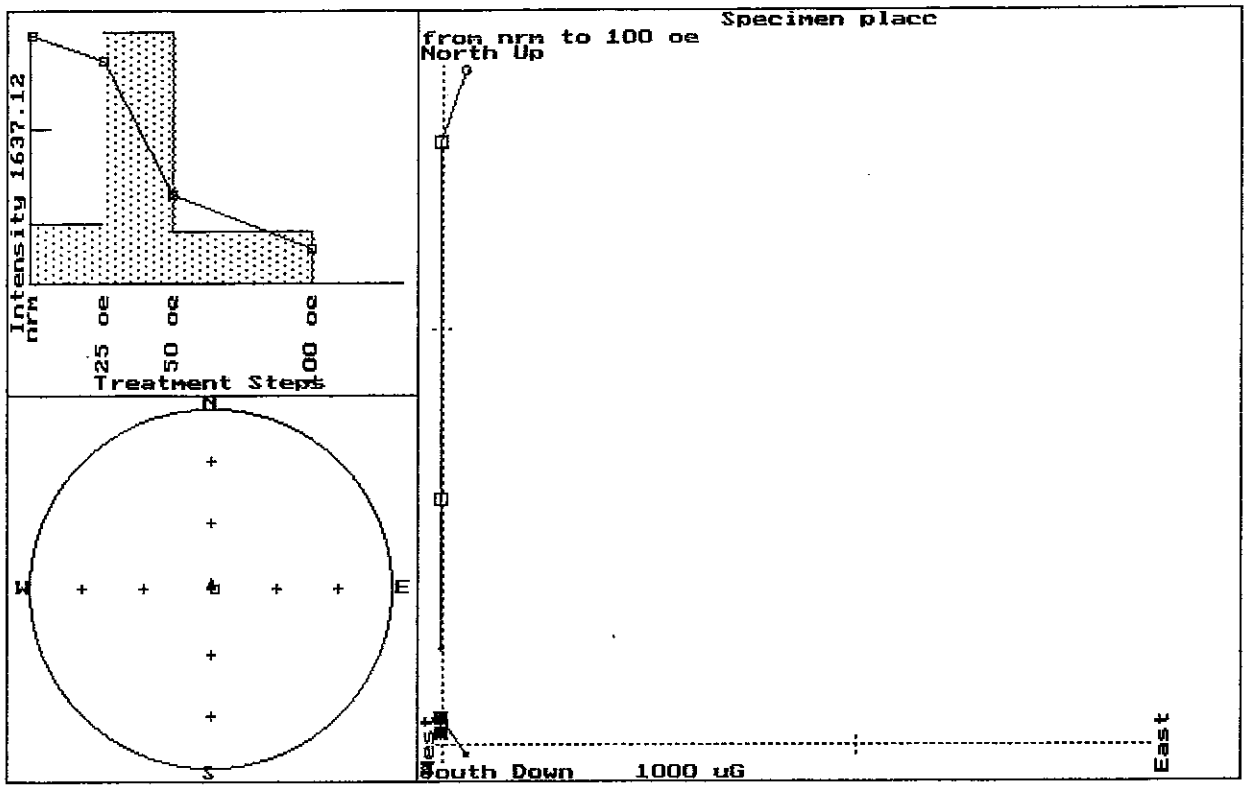
Intensity 1637.12
nrm
25 oe
50 oe
00 oe
Treatment Steps
N
W
E
S
Specimen placc
from nrm to 100 oe
North Up
West
East
South Down
1000 uG

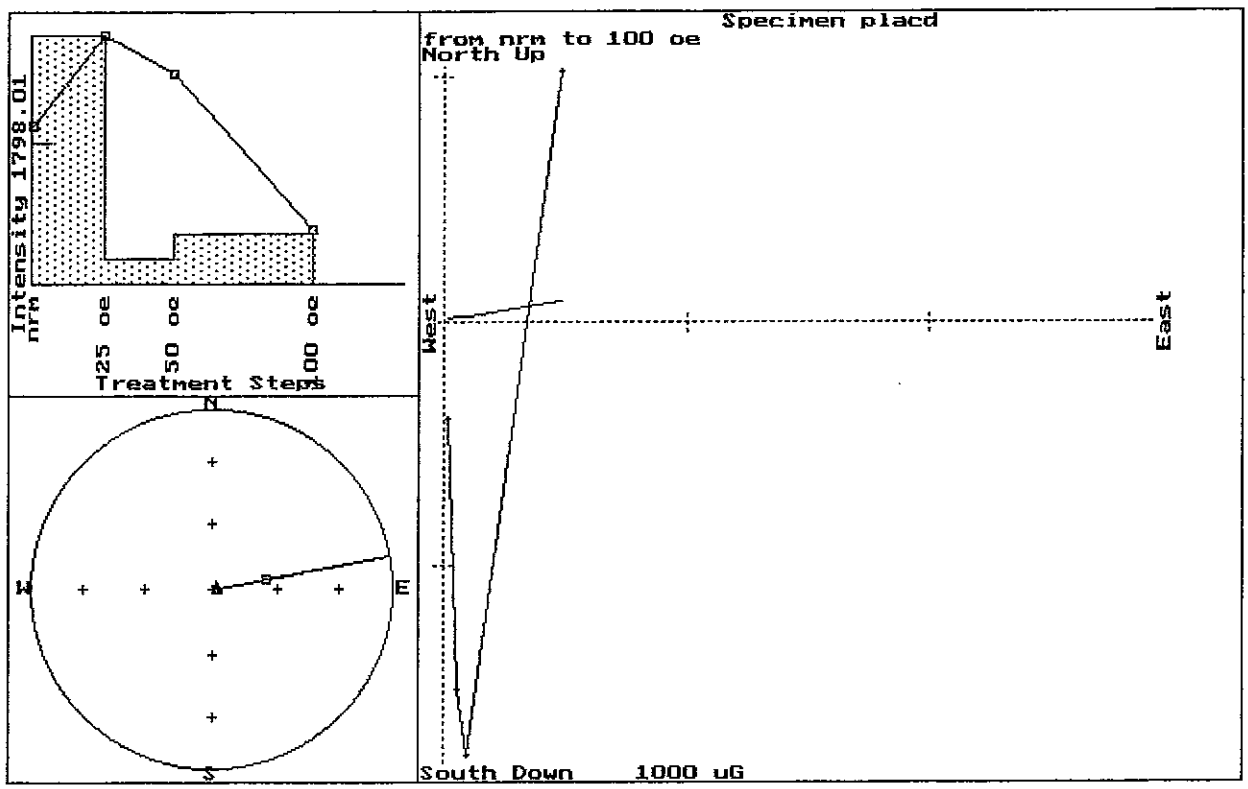
Intensity 1798.01
nrm
25 oe
50 oe
00 oe
Treatment Steps
N
W
E
S
Specimen placd
from nrm to 100 oe
North Up
West
East
South Down
1000 uG

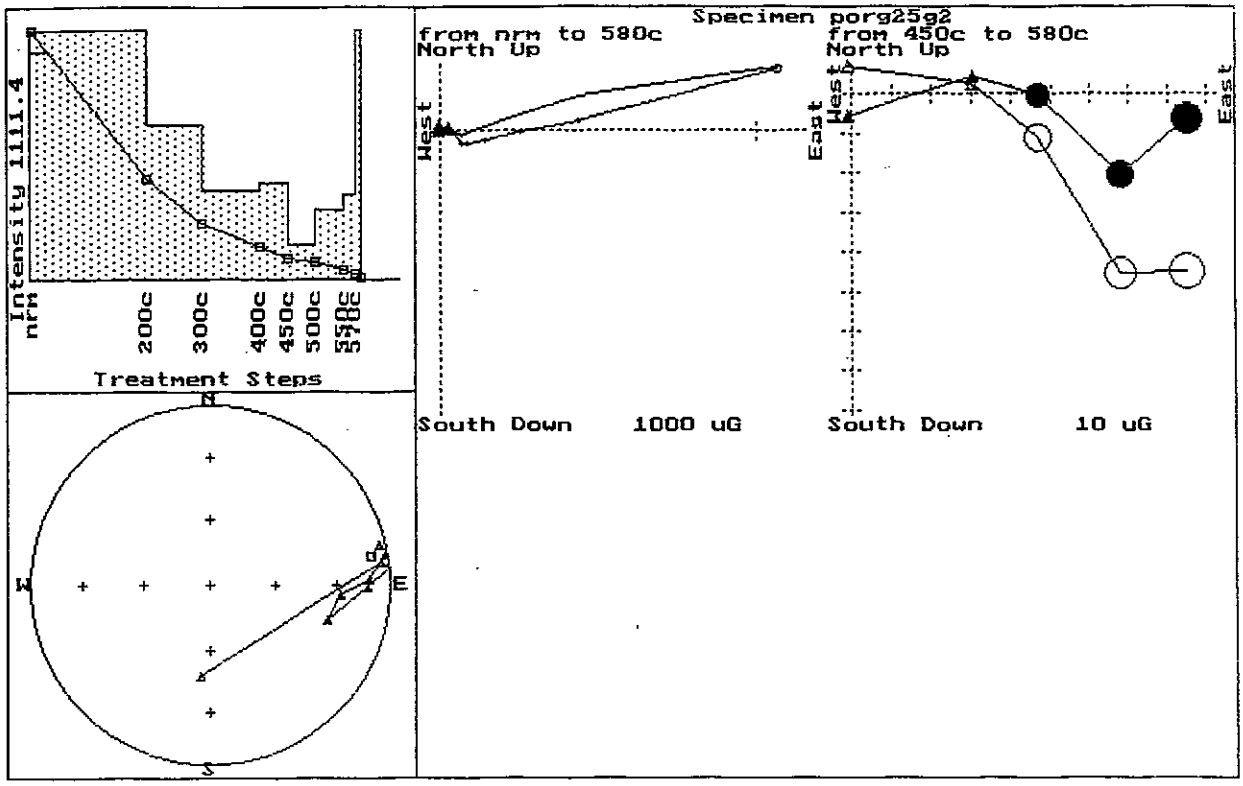
Specimen porg25g2
from nrm to 580c
North Up
from 450c to 580c
North Up
Intensity 1111.4
nrm
200c
300c
400c
450c
500c
580c
Treatment Steps
West
East
South Down
1000 uG
South Down
10 uG

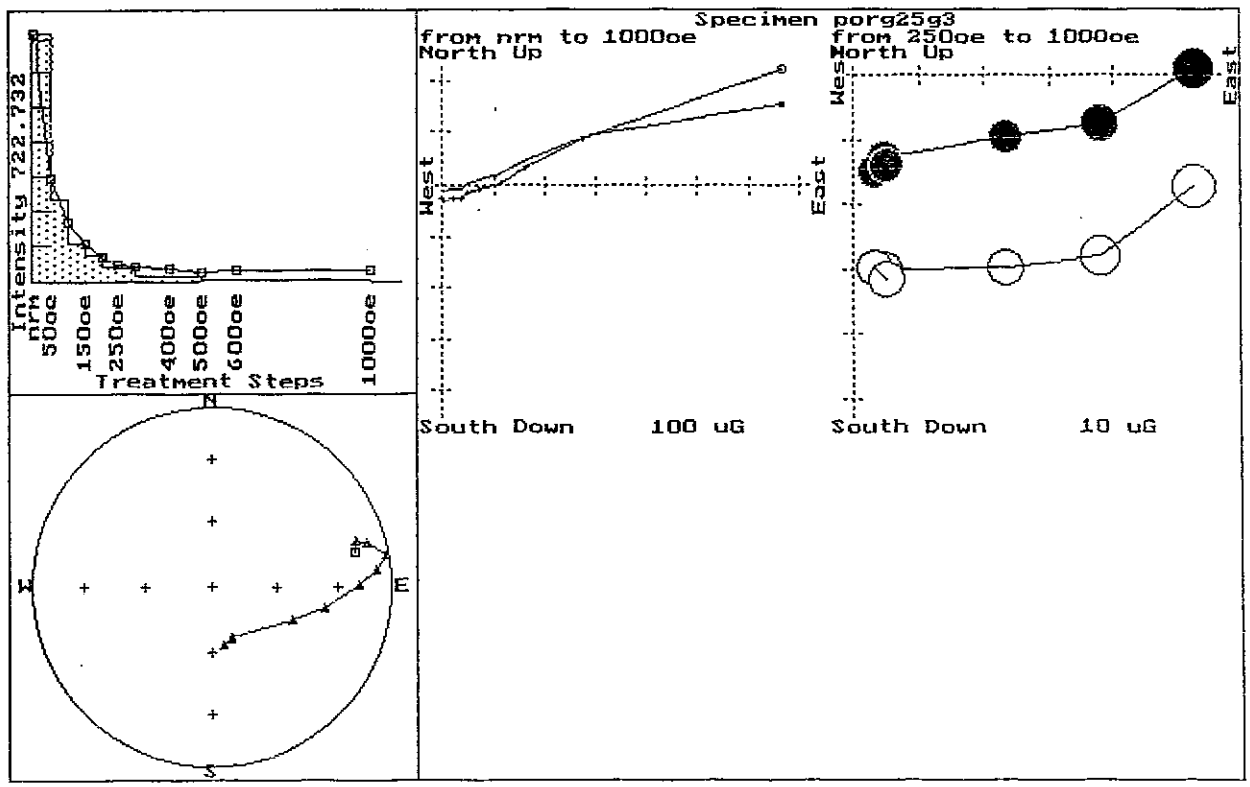
Specimen porg25g3
from nrm to 1000oe
North Up
from 250oe to 1000oe
North Up
Intensity 722.732
nrm
50oe
150oe
250oe
400oe
500oe
600oe
1000oe
Treatment Steps
West
East
South Down
100 uG
South Down
10 uG

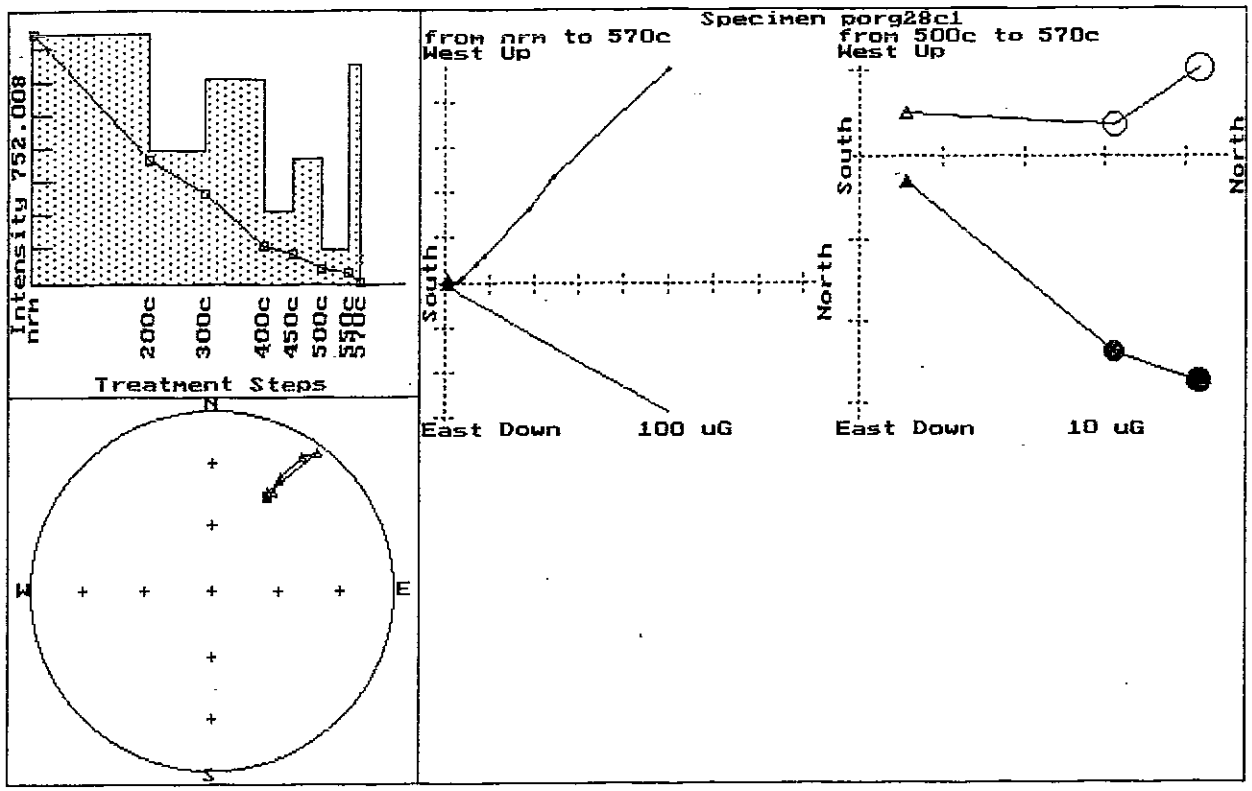
Specimen porg28c1
from nrm to 570c
West Up
South
North
East Down
100 uG
from 500c to 570c
West Up
South
North
East Down
10 uG
Intensity 752.008
nrm
200c
300c
400c
450c
500c
550c
Treatment Steps
N
E
S
W

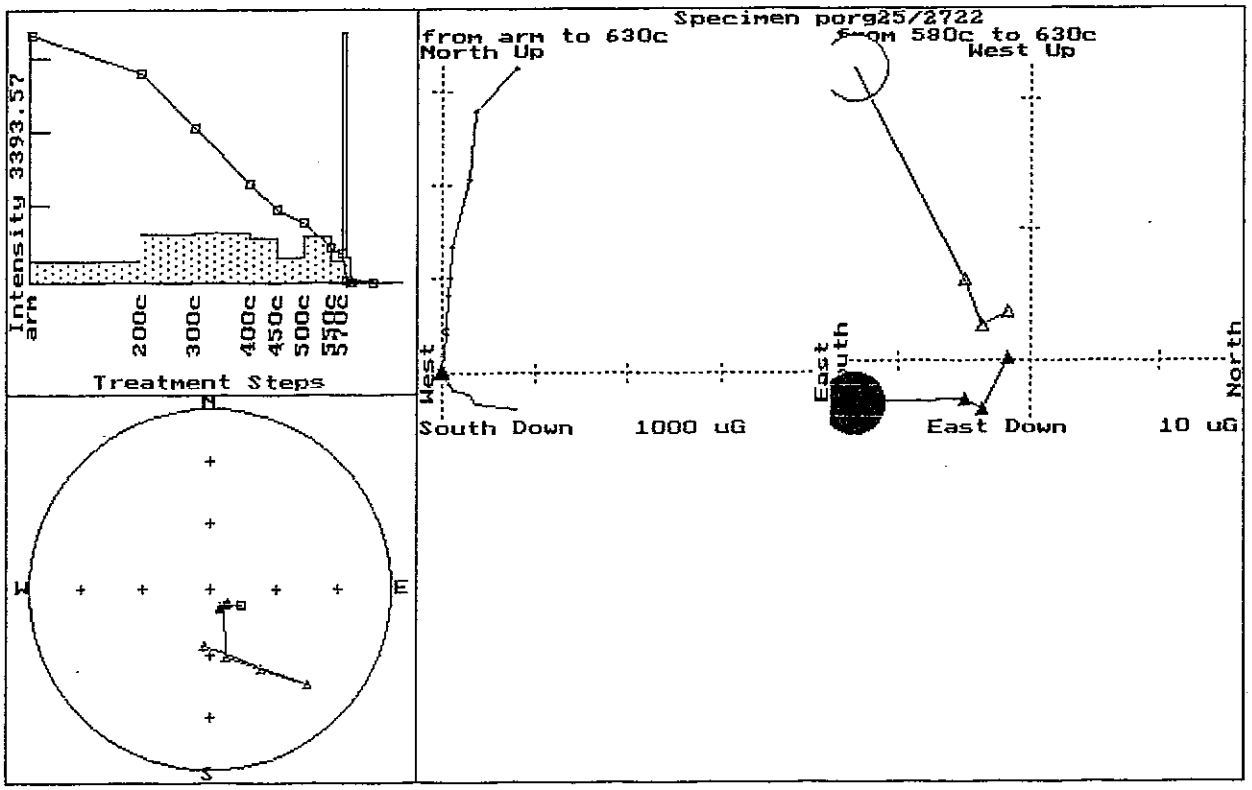
Specimen porg25/2722
from arm to 630c
North Up
West
East
South
North
South Down
1000 uG
from 580c to 630c
West Up
East Down
10 uG
Intensity 3393.57
arm
200c
300c
400c
450c
500c
550c
Treatment Steps
N
E
S
W

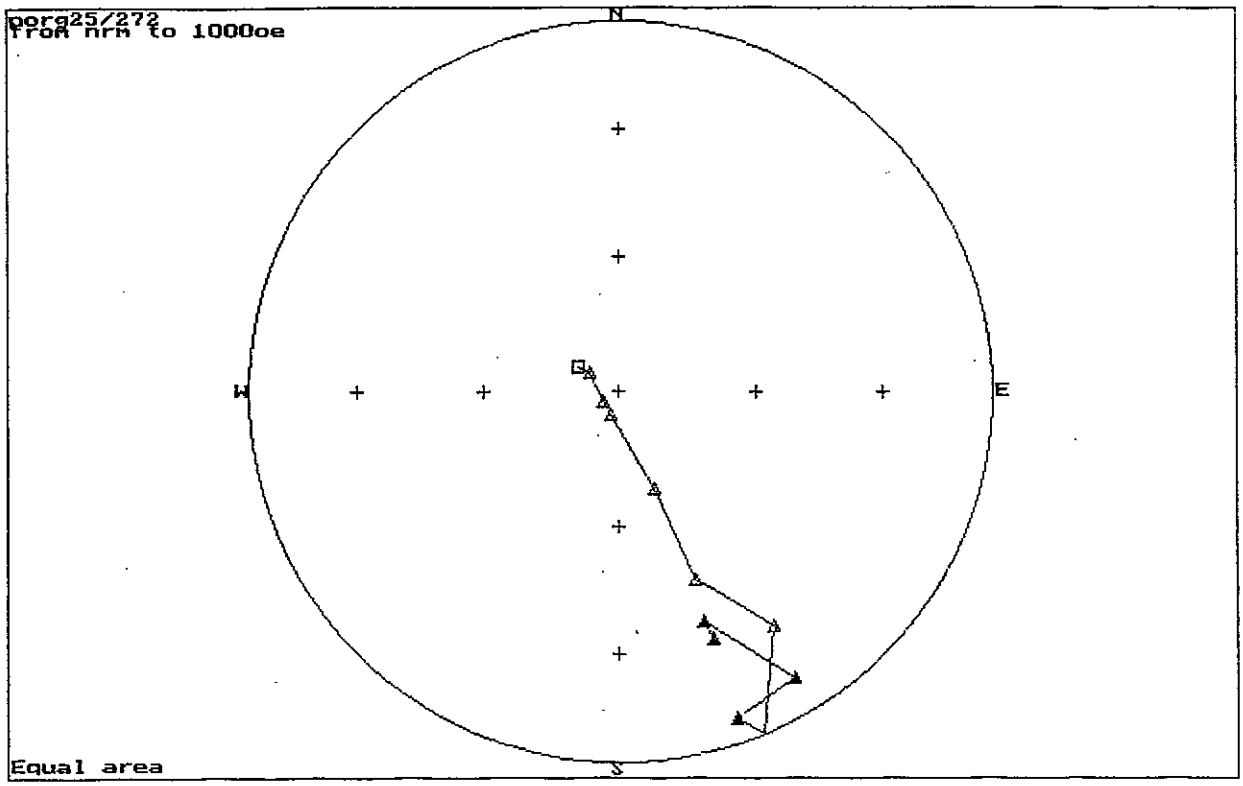
porg25/272
from nrm to 1000oe
N
W
E
S
Equal area

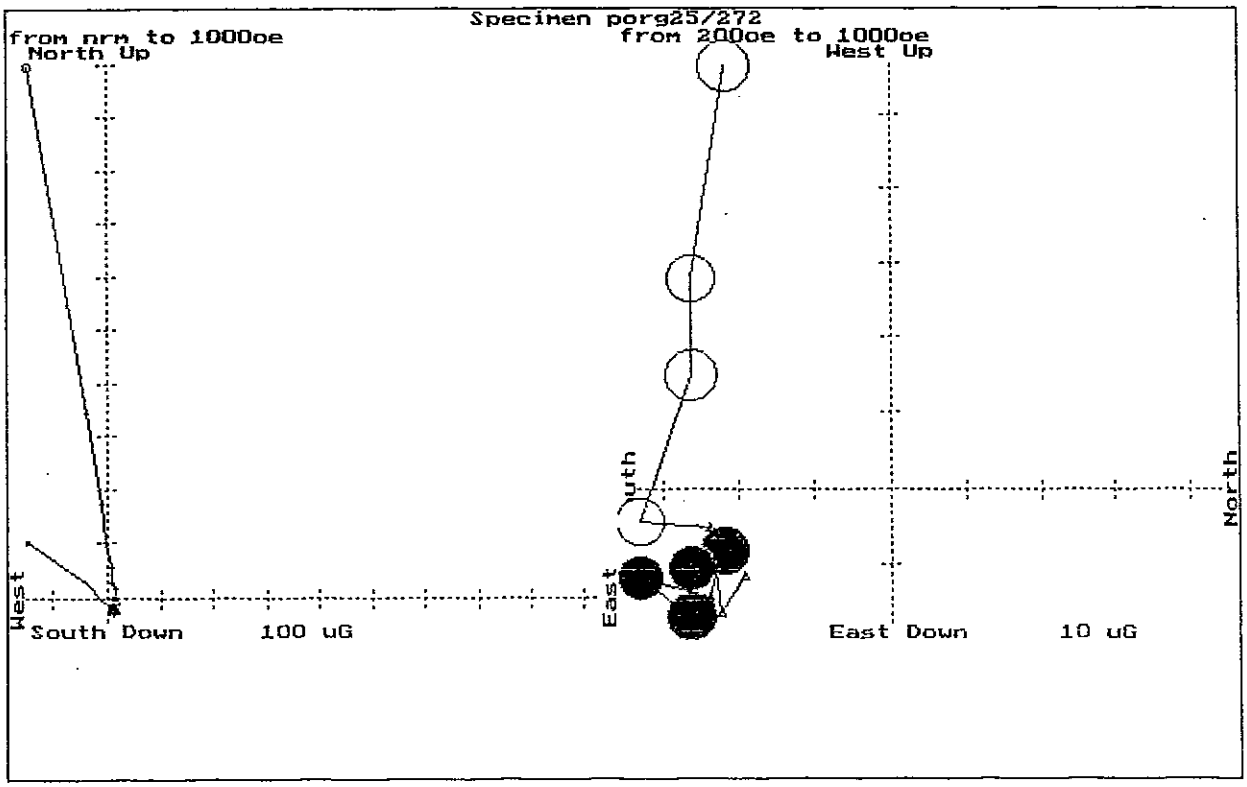
Specimen porg25/272
from nrm to 1000oe
North Up
from 200oe to 1000oe
West Up
West
South Down
100 uG
East
East Down
10 uG
North

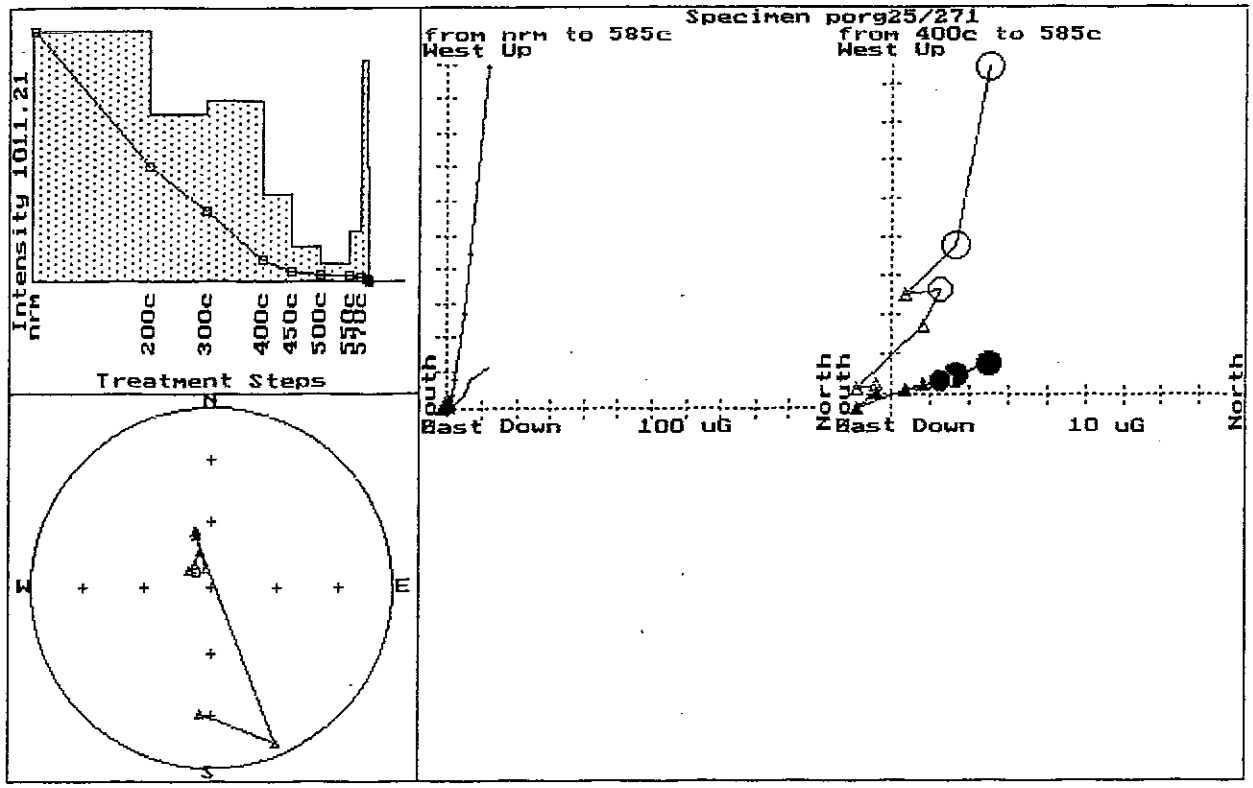
Specimen porg25/271
from nrm to 585c
West Up
from 400c to 585c
West Up
Intensity 1011.21
nrm
200c
300c
400c
450c
500c
550c
Treatment Steps
N
E
S
W
South
North
East Down
100 uG
10 uG

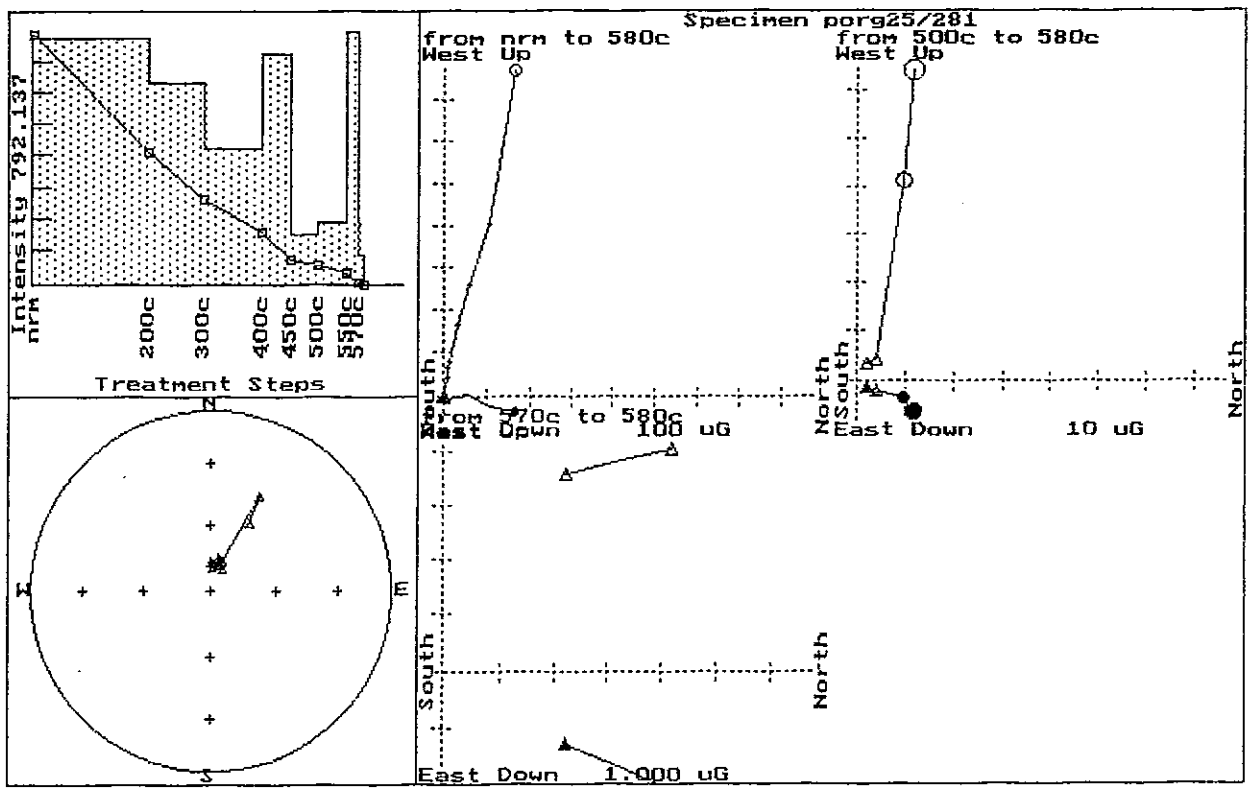
Specimen porg25/281
from nrm to 580c
West Up
from 500c to 580c
West Up
Intensity 792.137
nrm
200c
300c
400c
450c
500c
550c
Treatment Steps
N
E
S
W
South
North
East Down
100 uG
10 uG
1,000 uG

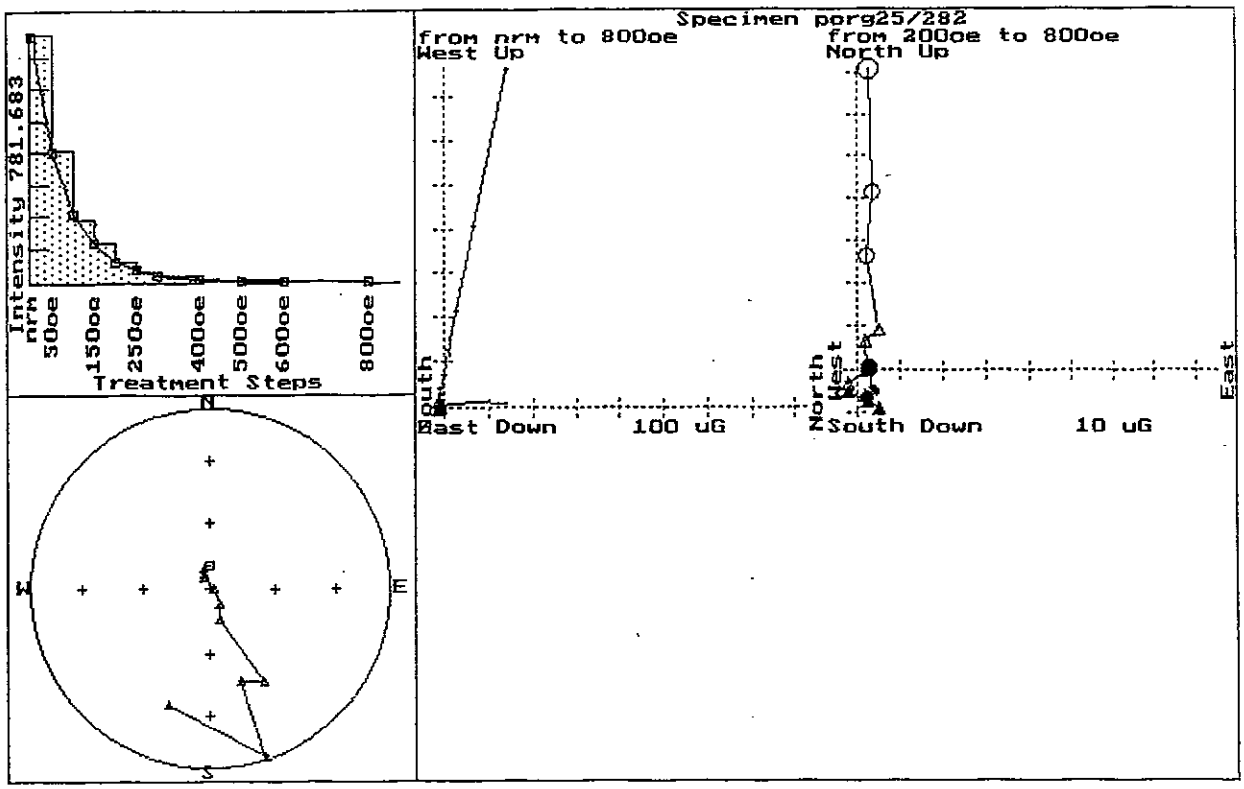
Intensity 781.683
nrm
50oe
150oe
250oe
400oe
500oe
600oe
800oe
Treatment Steps
N
W
E
S
Specimen porg25/282
from nrm to 800oe
West Up
from 200oe to 800oe
North Up
South
East Down
100 uG
North
West
South Down
10 uG
East

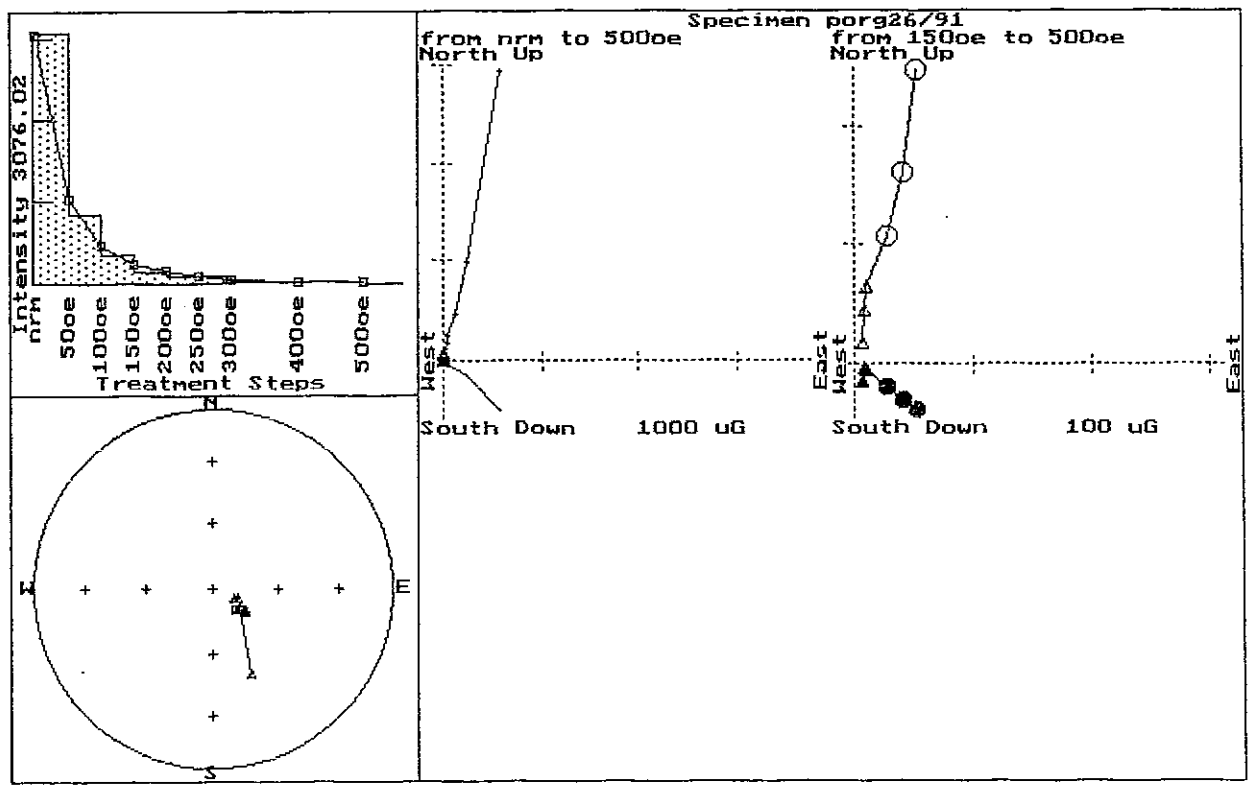
Intensity 3076.02
nrm
50oe
100oe
150oe
200oe
250oe
300oe
400oe
500oe
Treatment Steps
N
W
E
S
Specimen porg26/91
from nrm to 500oe
North Up
from 150oe to 500oe
North Up
West
South Down
1000 uG
East
West
South Down
100 uG
East

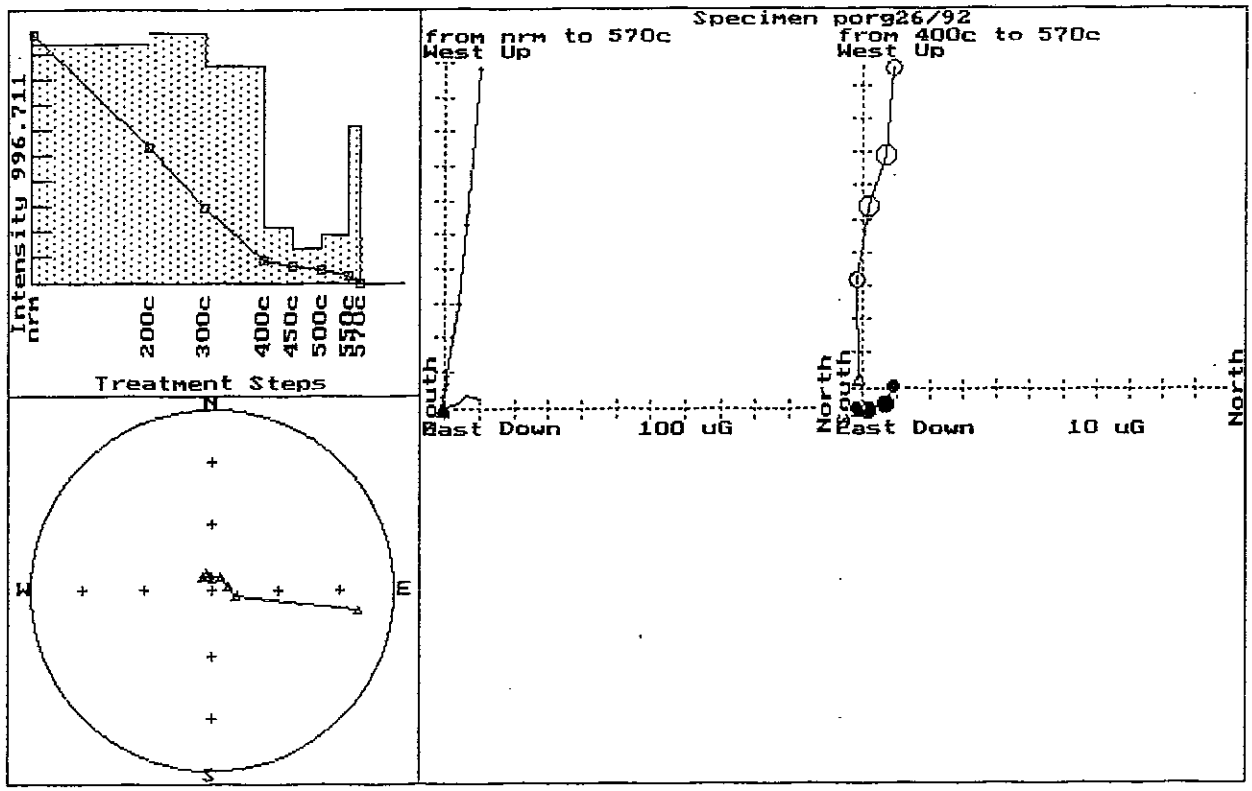
Specimen porg26/92
from nrm to 570c
West Up
from 400c to 570c
West Up
Intensity 996.711
nrm
200c
300c
400c
450c
500c
570c
Treatment Steps
N
W
E
S
South
East Down
100 uG
North
South
East Down
10 uG
North

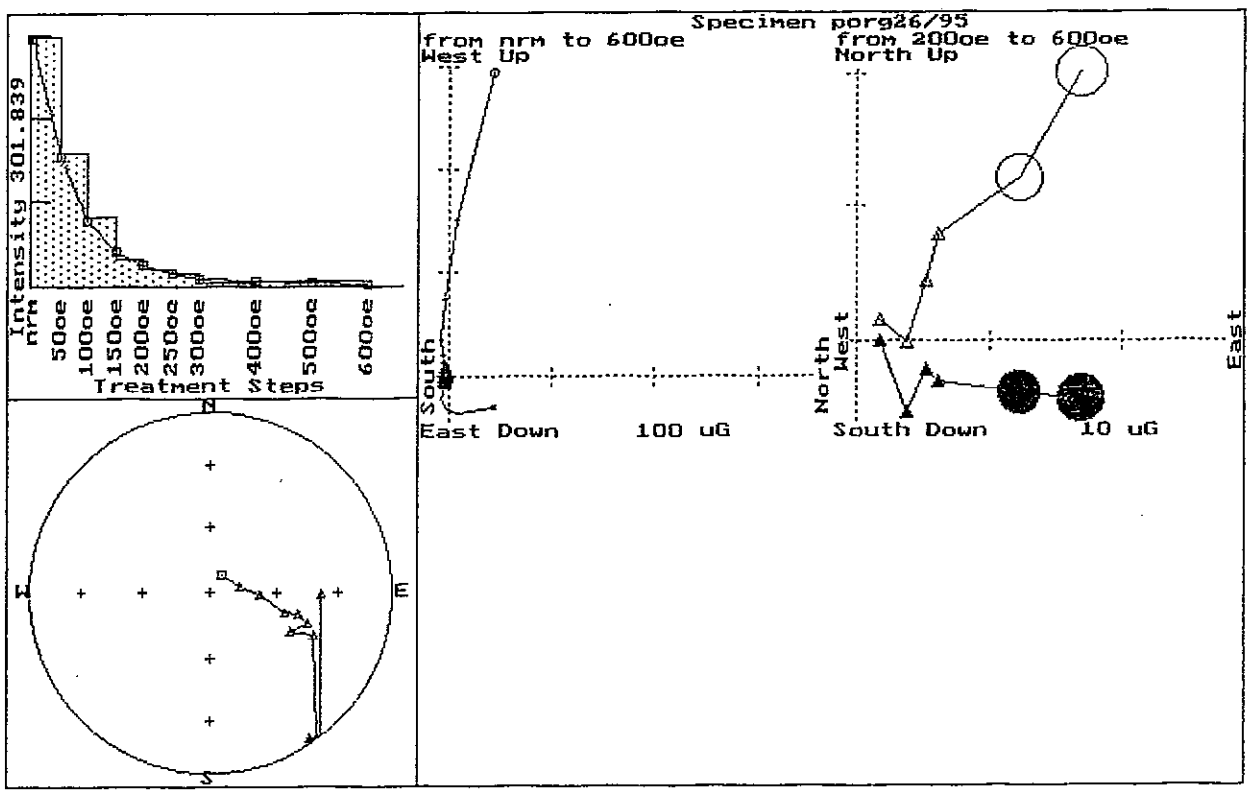
Specimen porg26/95
from nrm to 600oe
West Up
from 200oe to 600oe
North Up
Intensity 301.839
nrm
50oe
100oe
150oe
200oe
250oe
300oe
400oe
500oe
600oe
Treatment Steps
N
W
E
S
South
East Down
100 uG
North
West
South Down
10 uG
East

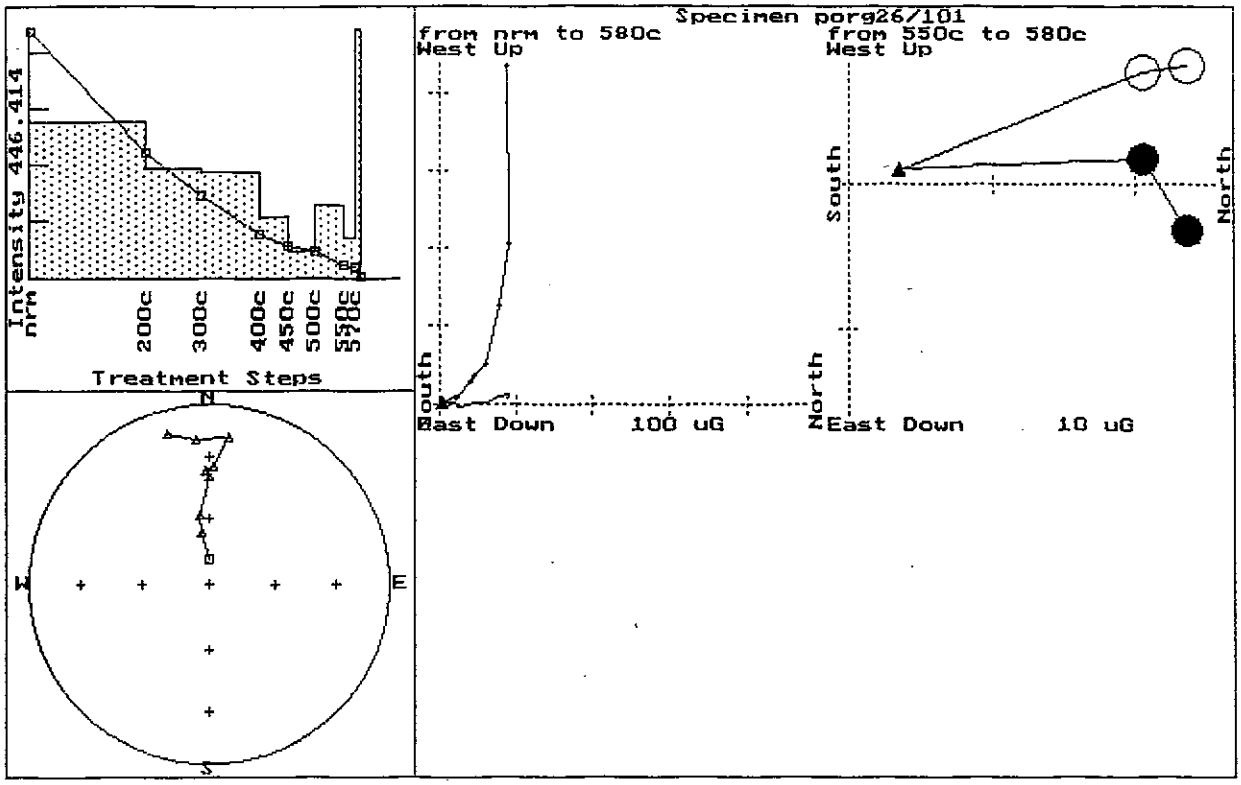
Specimen porg26/101
from nrm to 580c
West Up
from 550c to 580c
West Up
Intensity 446.414
nrm
200c
300c
400c
450c
500c
580c
Treatment Steps
N
W
E
S
South
North
East Down
100 uG
East Down
10 uG

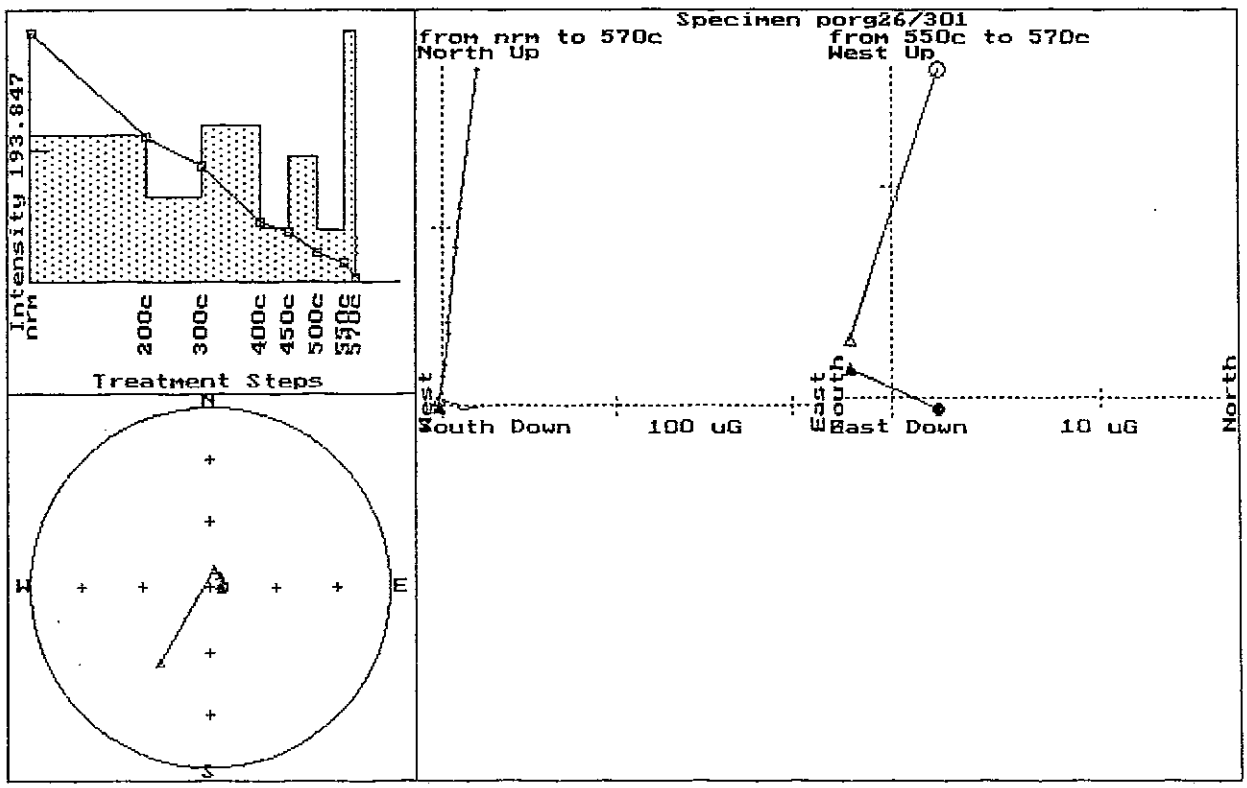
Specimen porg26/301
from nrm to 570c
North Up
from 550c to 570c
West Up
Intensity 193.847
nrm
200c
300c
400c
450c
500c
570c
Treatment Steps
N
W
E
S
West
East
South Down
100 uG
East Down
10 uG
North

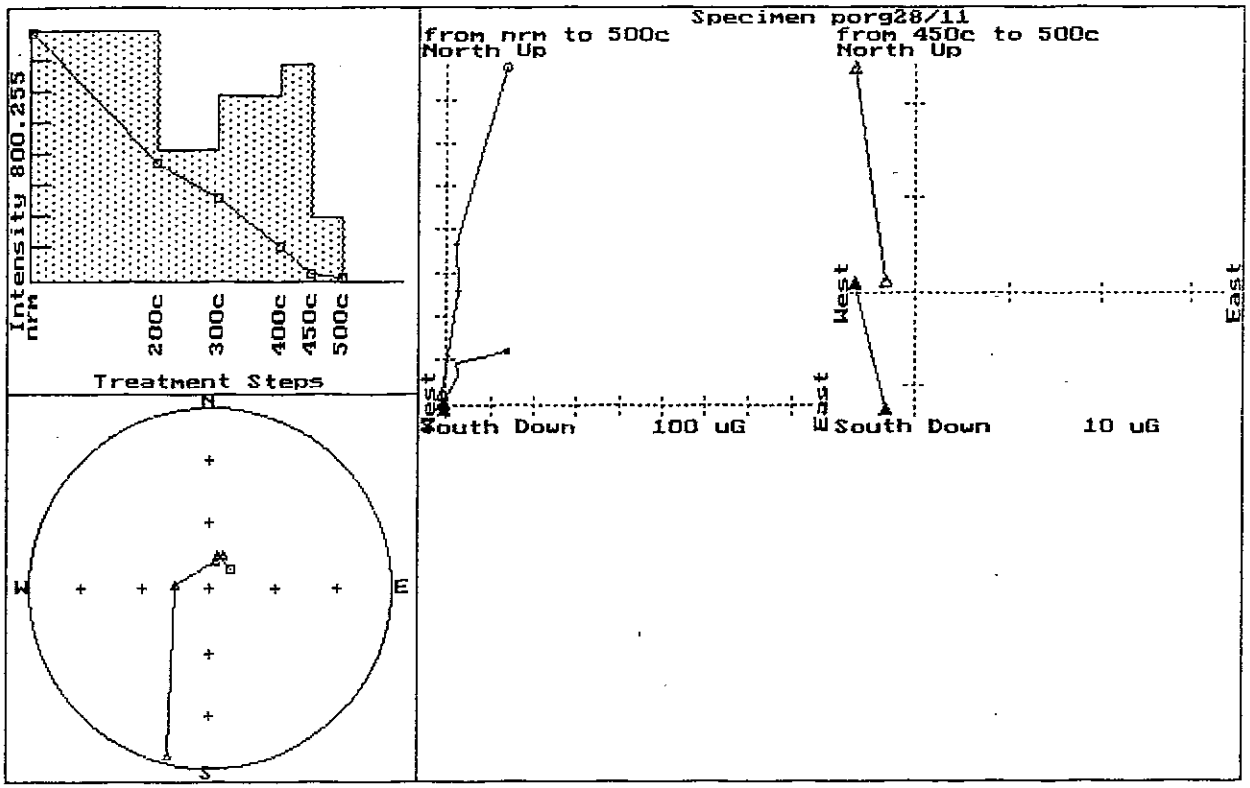
Specimen porg28/11
from nrm to 500c
North Up
from 450c to 500c
North Up
Intensity 800.255
nrm
200c
300c
400c
450c
500c
Treatment Steps
West
East
South Down
100 uG
South Down
10 uG
N
W
E
S

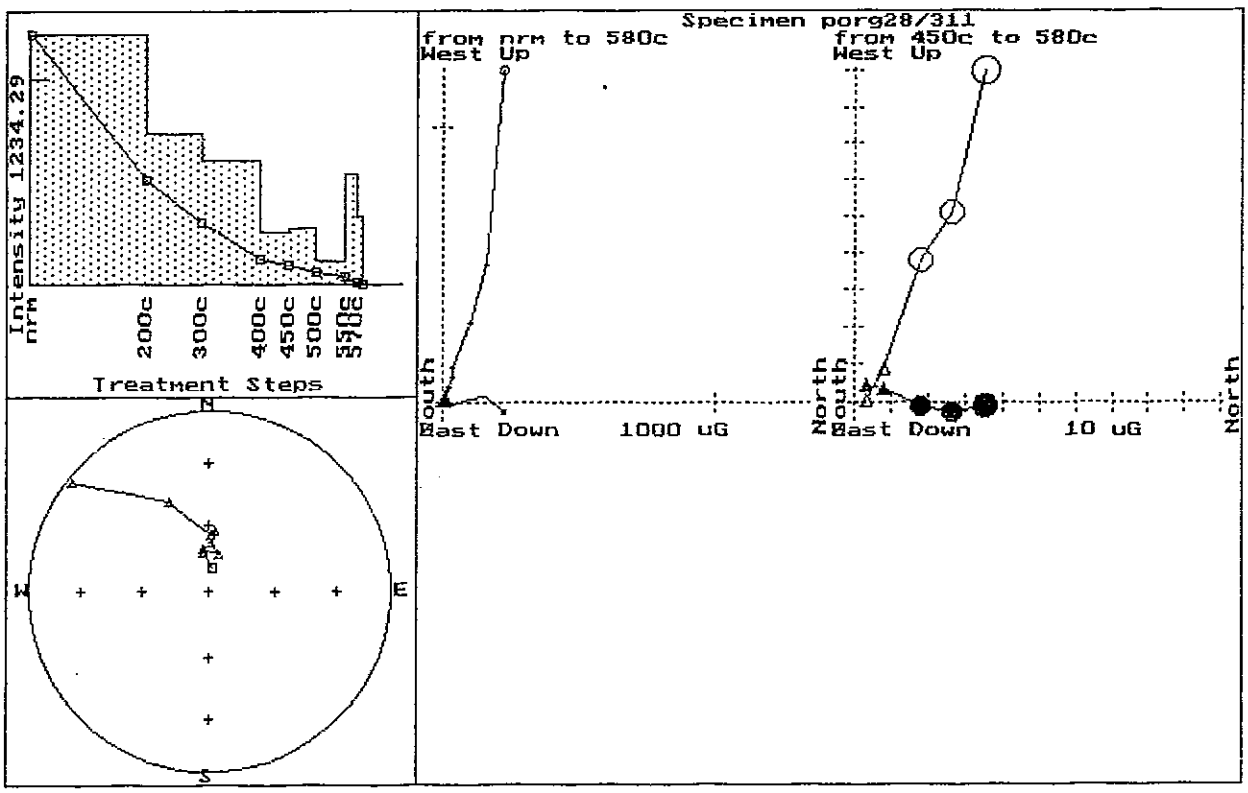
Specimen porg28/311
from nrm to 580c
West Up
from 450c to 580c
West Up
Intensity 1234.29
nrm
200c
300c
400c
450c
500c
580c
Treatment Steps
East Down
1000 uG
East Down
10 uG
N
W
E
S

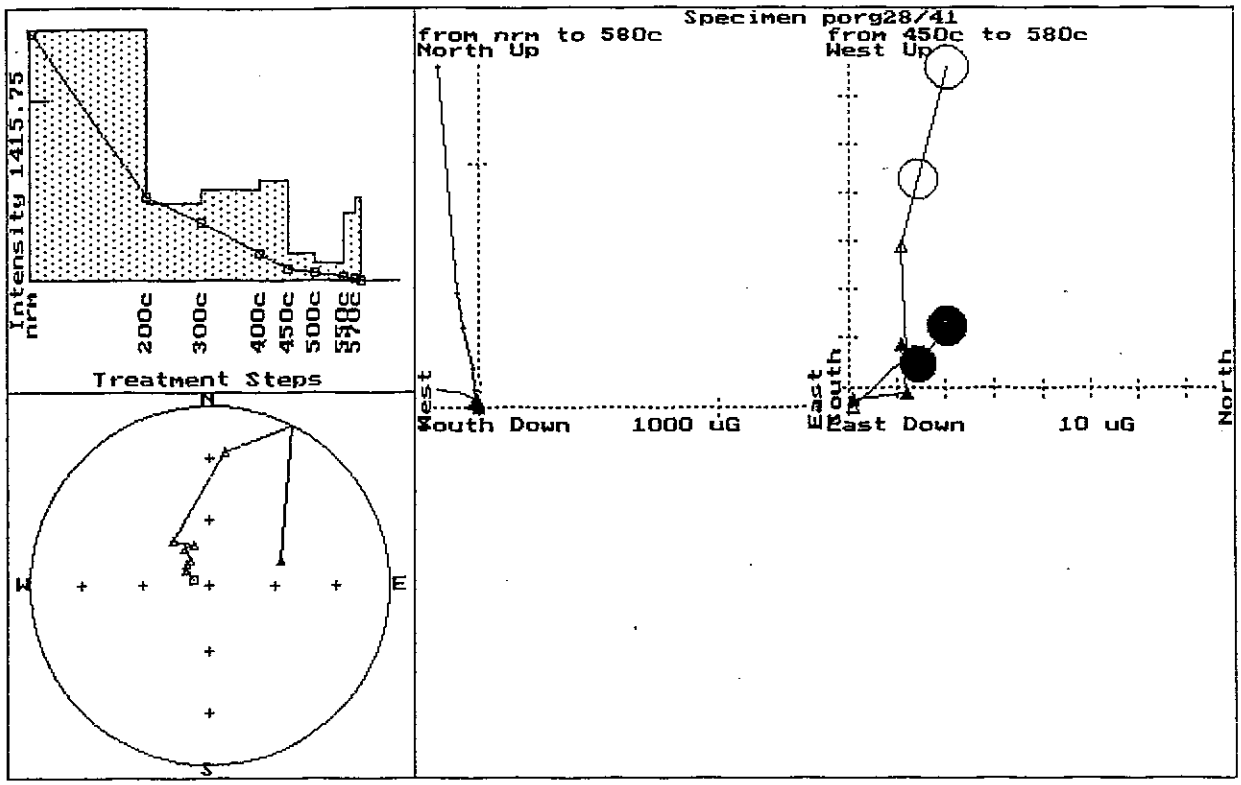
Specimen porg28/41
from nrm to 580c
North Up
from 450c to 580c
West Up
Intensity 1415.75
nrm
200c
300c
400c
450c
500c
580c
Treatment Steps
N
W
E
S
West
South Down
1000 uG
East
South
East Down
10 uG
North

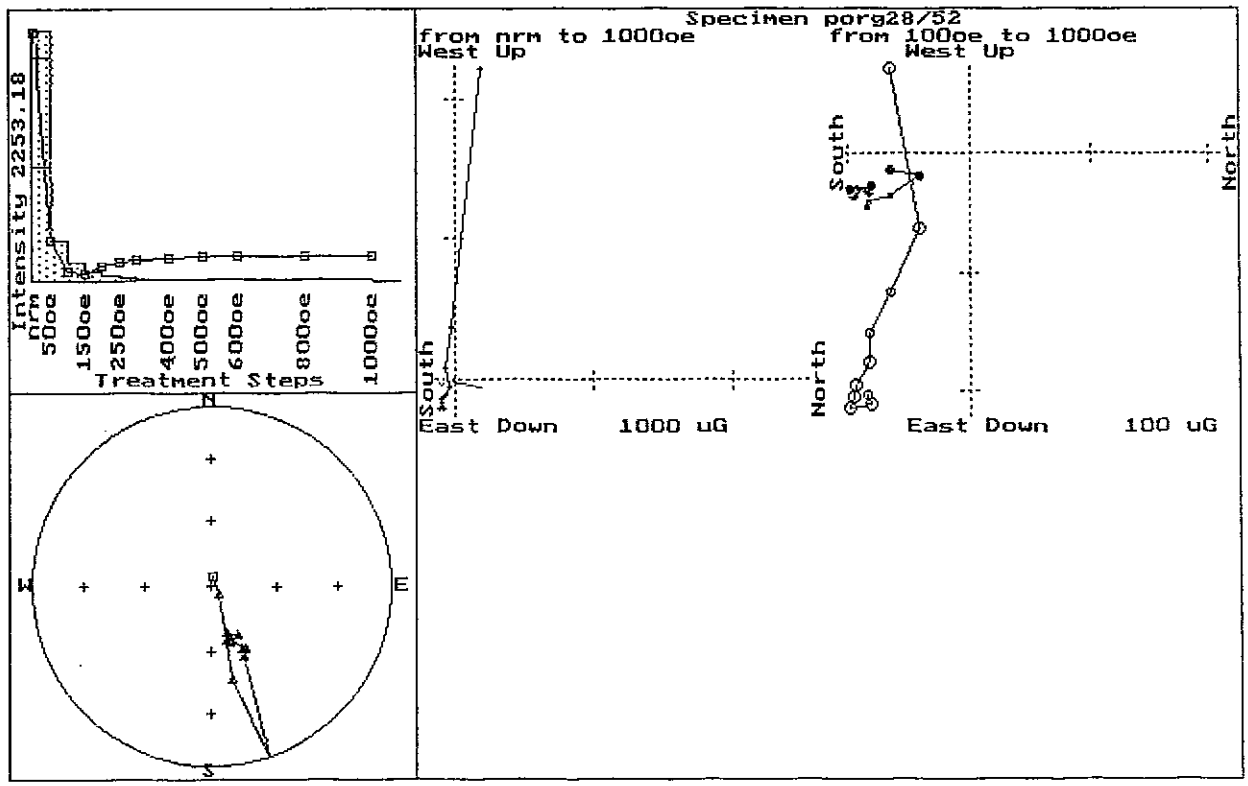
Specimen porg28/52
from nrm to 1000oe
West Up
from 100oe to 1000oe
West Up
Intensity 2253.18
nrm
50oe
150oe
250oe
400oe
500oe
600oe
800oe
1000oe
Treatment Steps
N
W
E
S
South
East Down
1000 uG
South
North
East Down
100 uG
North

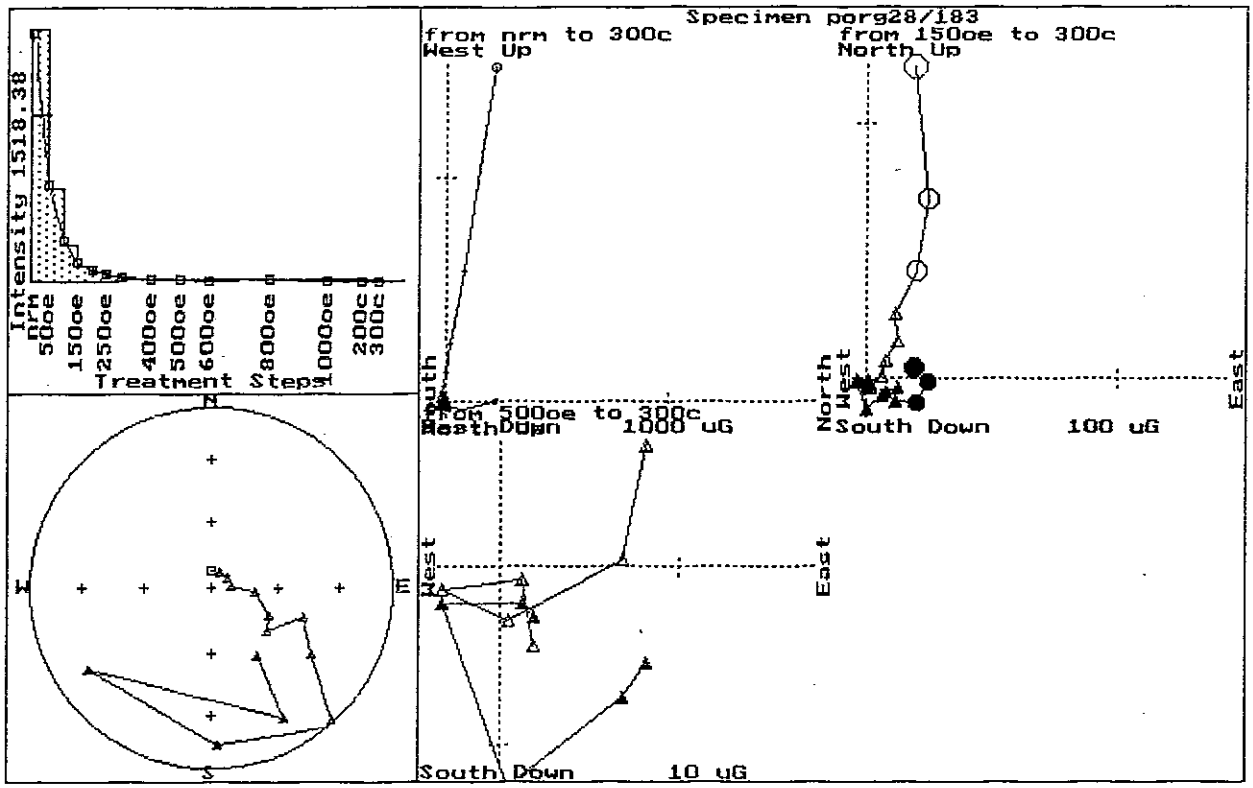
Specimen porg28/183
Intensity 1518.38
nrm
50Oe
150Oe
250Oe
400Oe
500Oe
600Oe
800Oe
1000Oe
200c
300c
Treatment Steps
from nrm to 300c
West Up
from 150oe to 300c
North Up
South
North
West
East
from 500oe to 300c
South Down 1000 uG
North West
South Down 100 uG
West
East
South Down 10 uG
N
W
E
S

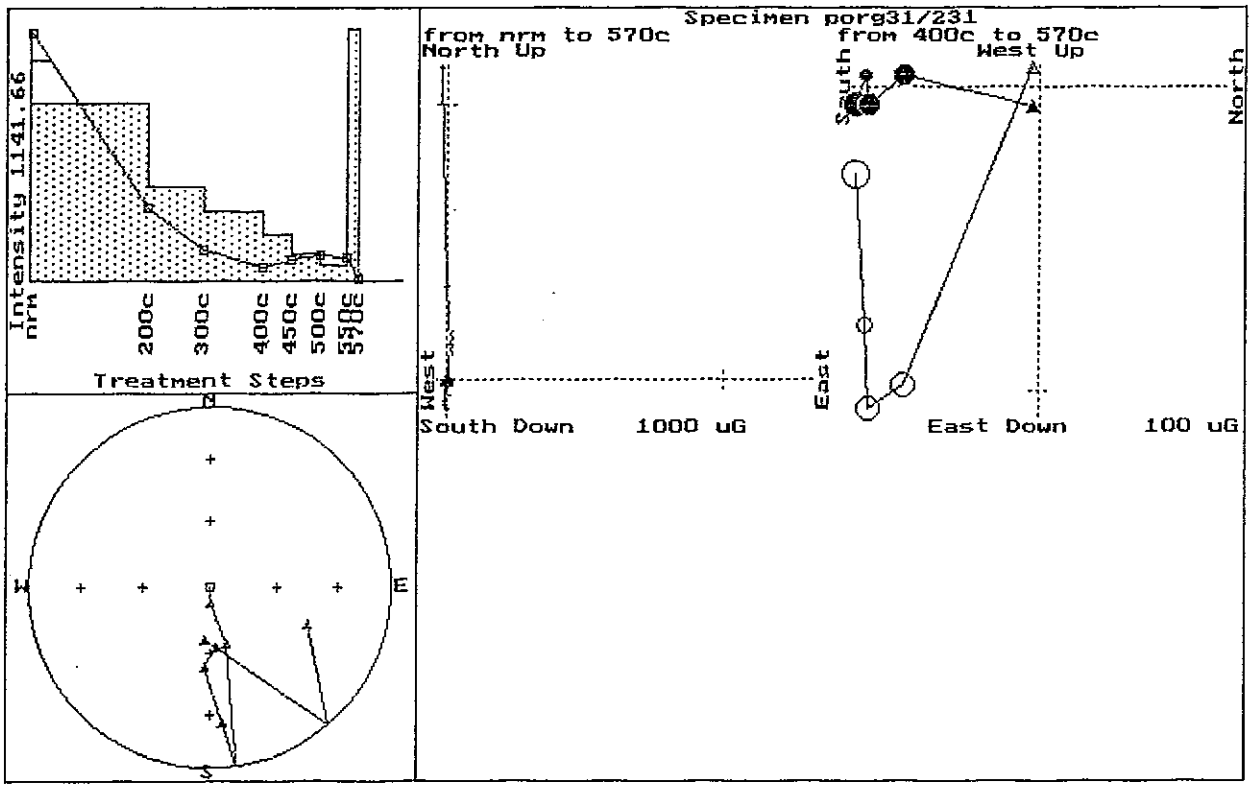
Specimen porg31/231
Intensity 1141.66
nrm
200c
300c
400c
450c
500c
550c
570c
Treatment Steps
from nrm to 570c
North Up
from 400c to 570c
West Up
South
North
West
East
South Down 1000 uG
East Down 100 uG
N
W
E
S

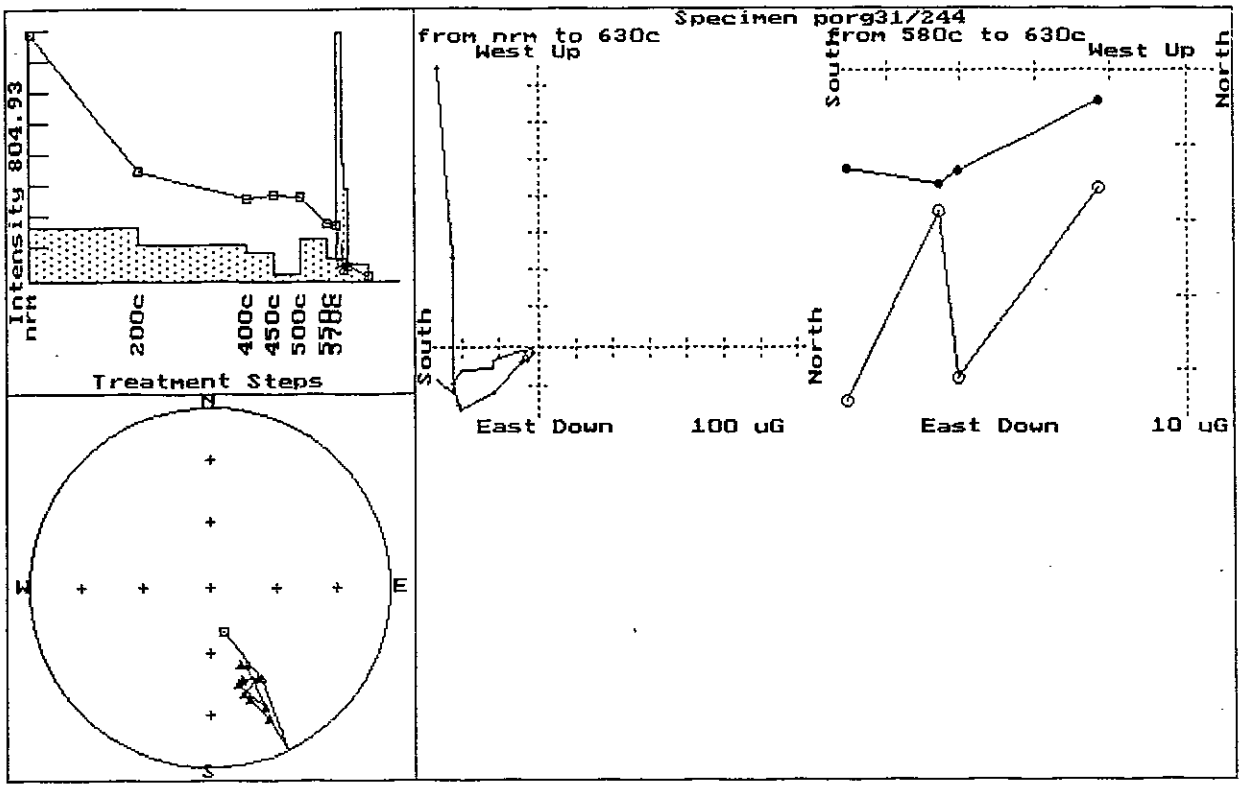
Specimen porg31/244
from nrm to 630c
West Up
South
North
East Down
100 uG
from 580c to 630c
West Up
South
North
East Down
10 uG
Intensity 804.93
nrm
200c
400c
450c
500c
570c
Treatment Steps
N
E
S

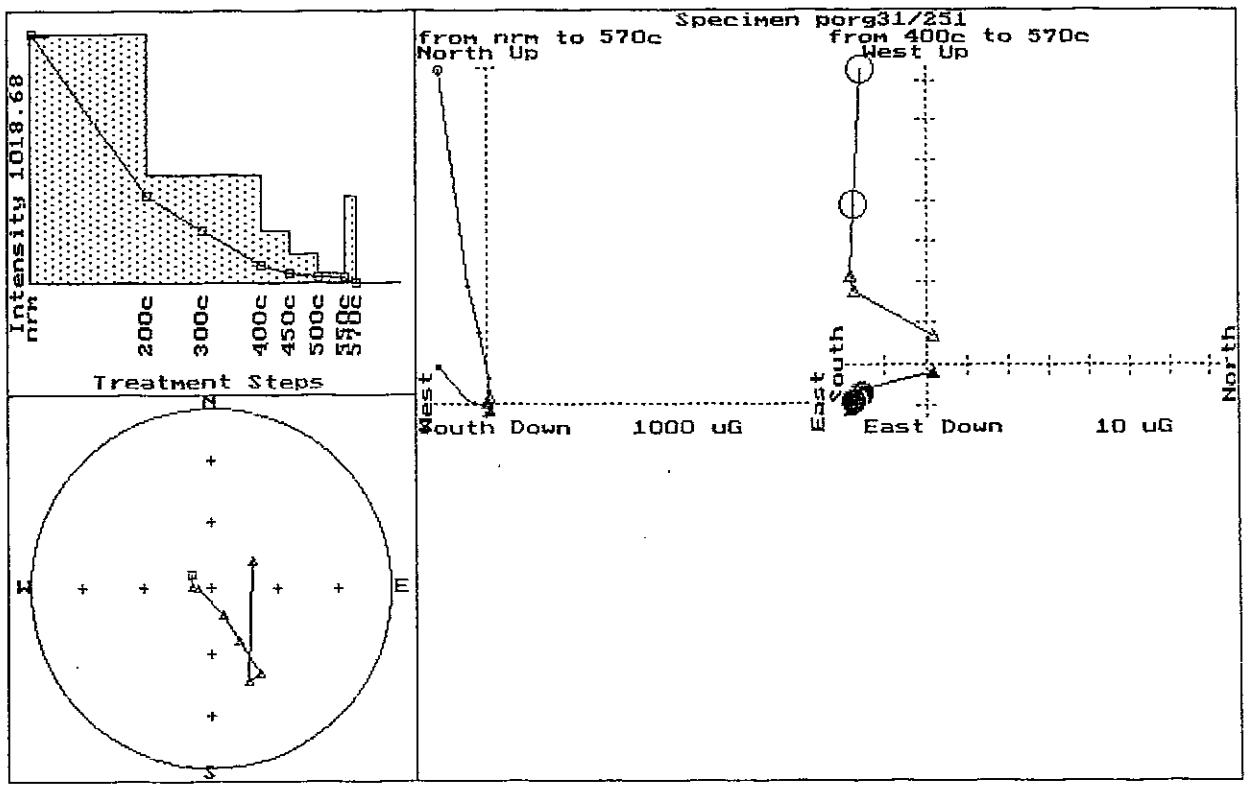
Specimen porg31/251
from nrm to 570c
North Up
West
South Down
1000 uG
from 400c to 570c
West Up
East
South
North
East Down
10 uG
Intensity 1018.68
nrm
200c
300c
400c
450c
500c
570c
Treatment Steps
N
E
S

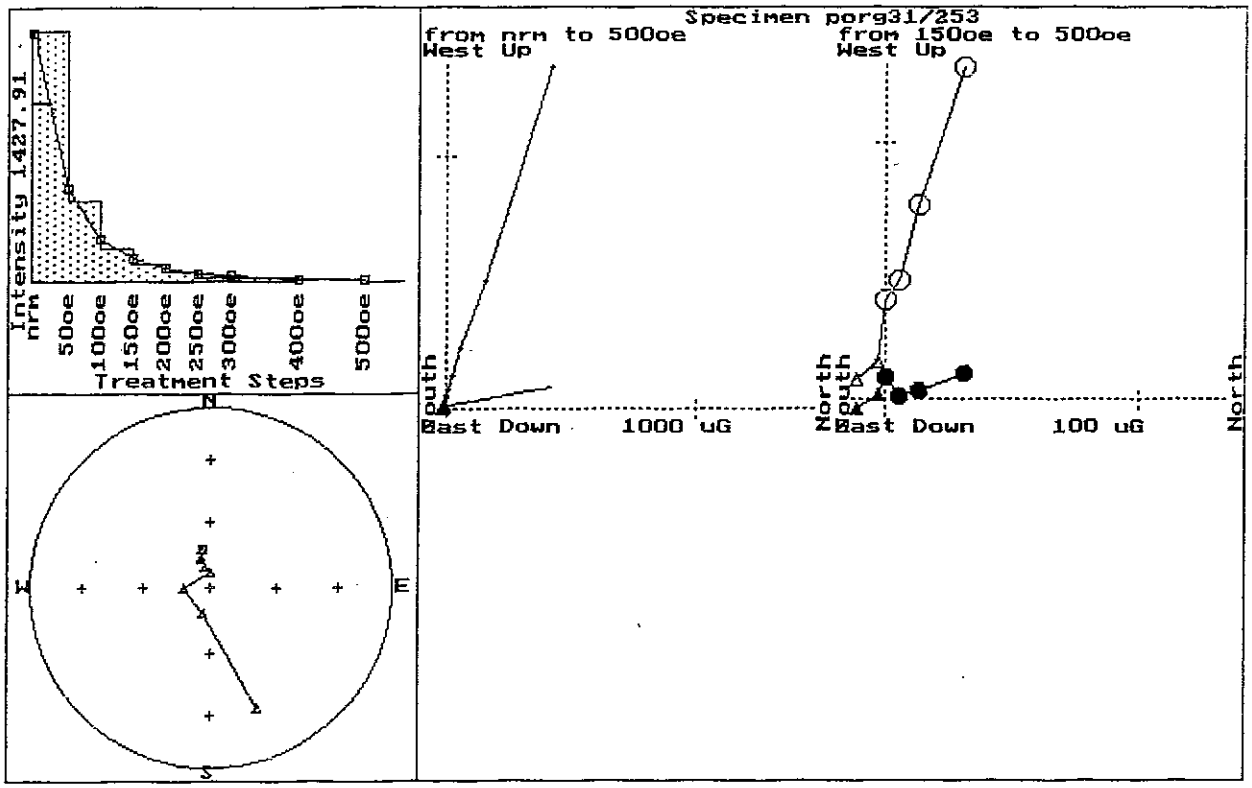
Specimen porg31/253
from nrm to 500oe
West Up
from 150oe to 500oe
West Up
Intensity 1427.91
nrm
50oe
100oe
150oe
200oe
250oe
300oe
400oe
500oe
Treatment Steps
N
W
E
S
South
East Down
1000 uG
North
South
East Down
100 uG
North

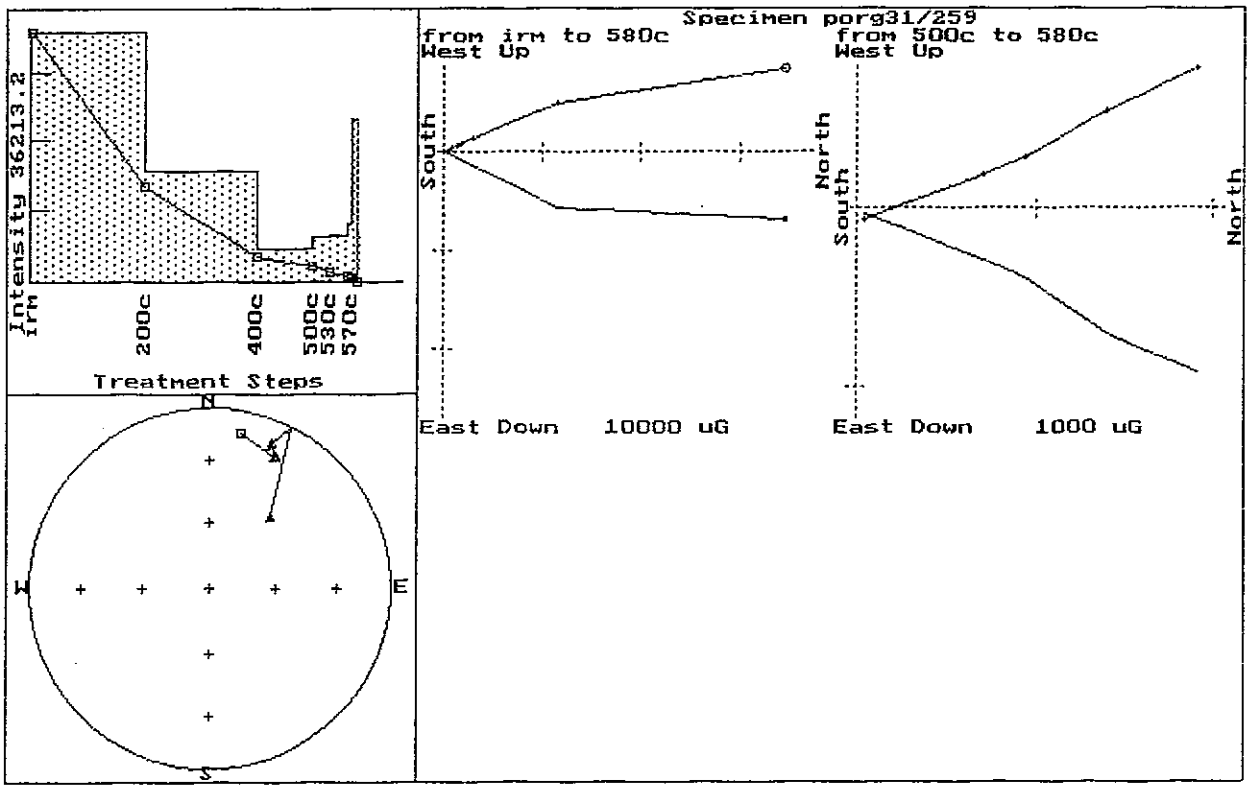
Specimen porg31/259
from irm to 580c
West Up
from 500c to 580c
West Up
Intensity 36213.2
irm
200c
400c
500c
530c
570c
Treatment Steps
N
W
E
S
South
East Down
10000 uG
North
South
East Down
1000 uG
North

Fig.13. Zijderveld plots for the Rambari/Roamane augite hornblende diorite samples.

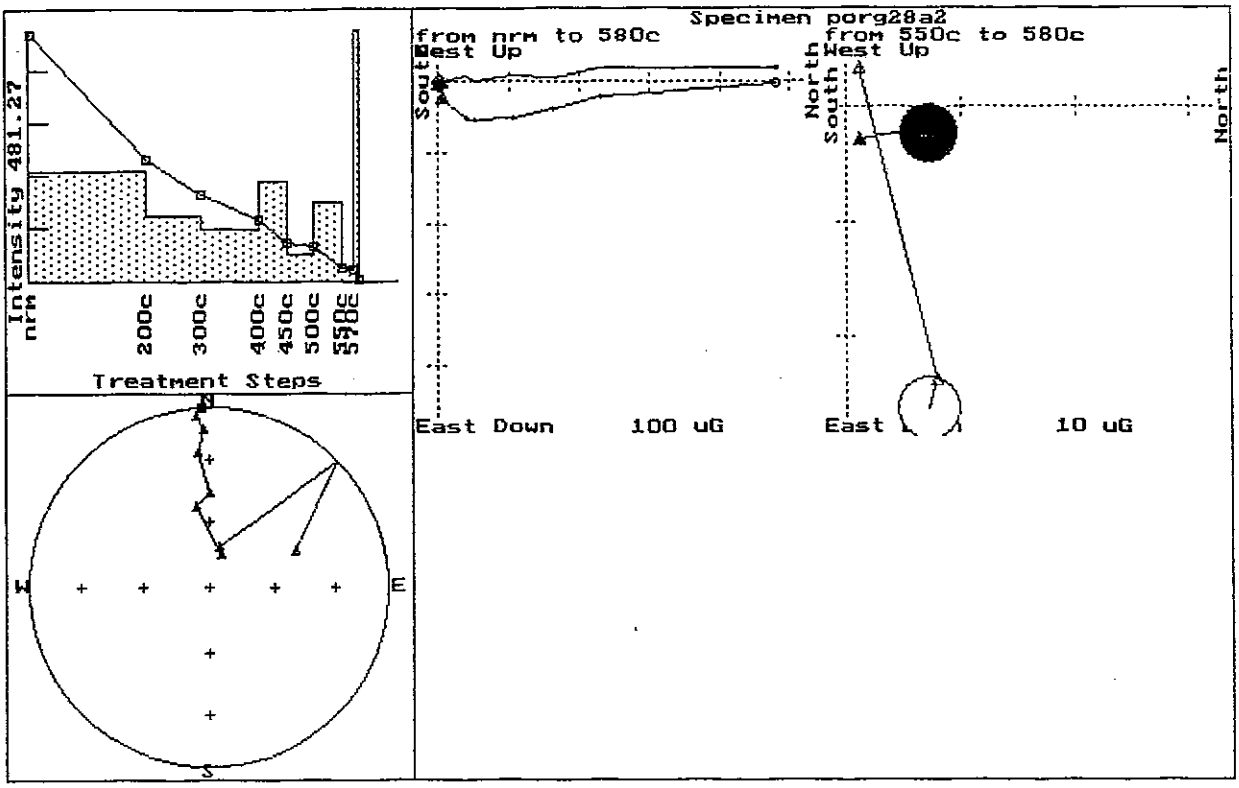
Specimen porg28a2
from nrm to 580c
from 550c to 580c
West Up
West Up
South
North
South
North
Intensity 481.27
nrm
200c
300c
400c
450c
500c
550c
580c
Treatment Steps
N
W
E
S
East Down
100 uG
East
10 uG

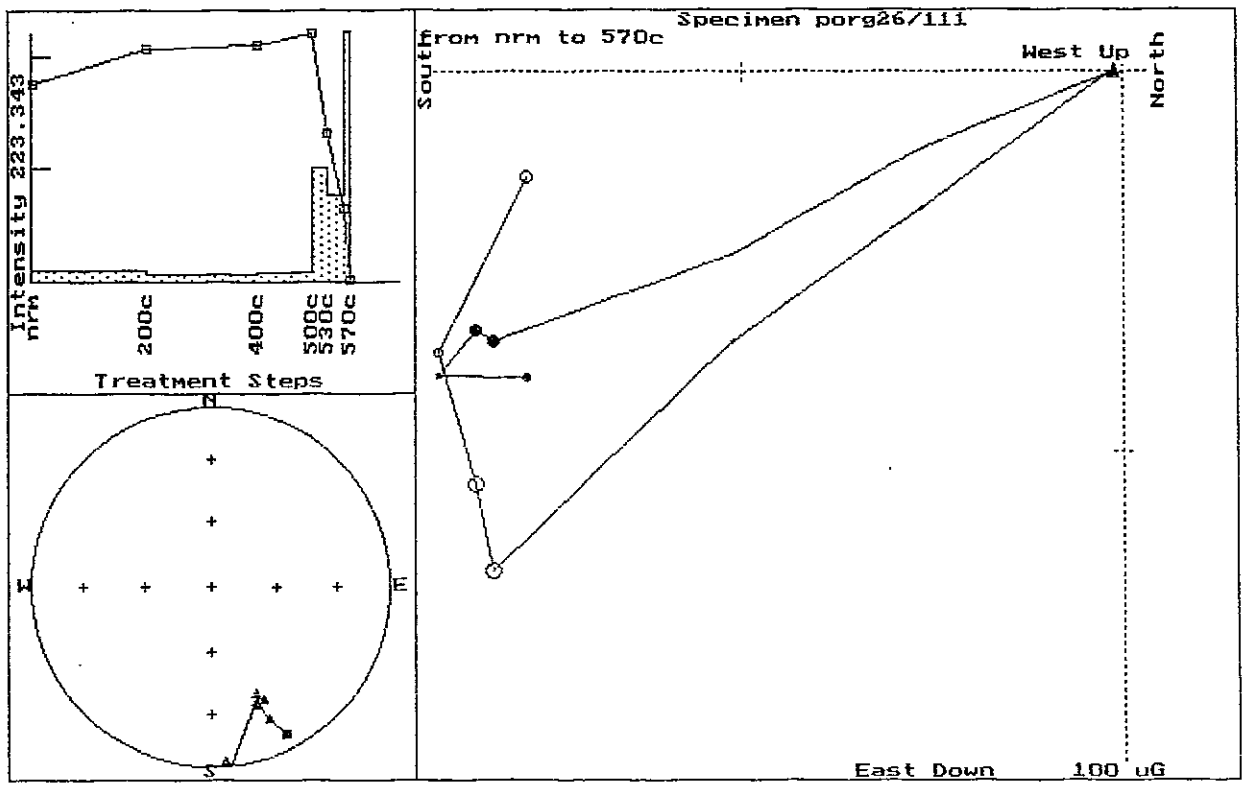
Specimen porg26/111
from nrm to 570c
South
West Up
North
Intensity 223.343
nrm
200c
400c
500c
530c
570c
Treatment Steps
N
W
E
S
East Down
100 uG

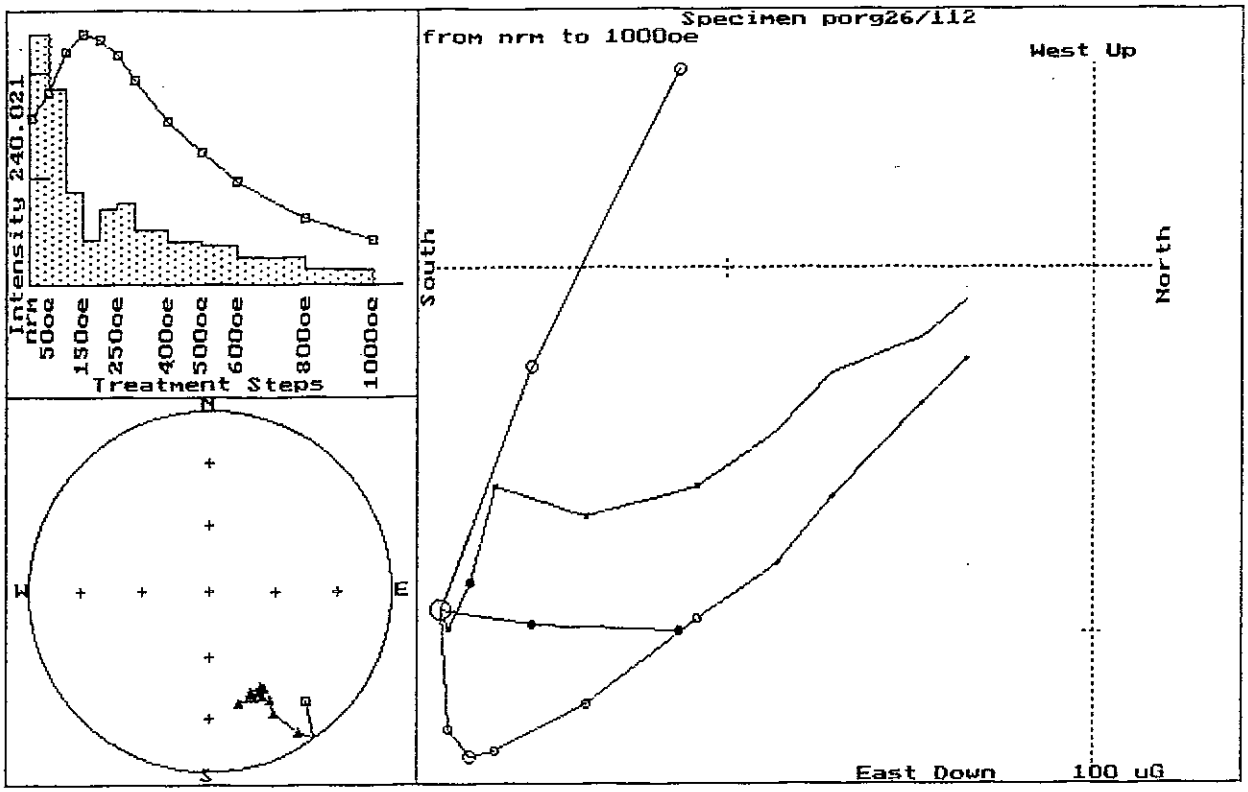
Specimen porg26/112
from nrm to 1000oe
West Up
South
North
East Down
100 uG
Intensity 240.021
nrm
50oe
150oe
250oe
400oe
500oe
600oe
800oe
1000oe
Treatment Steps
N
E
S
W

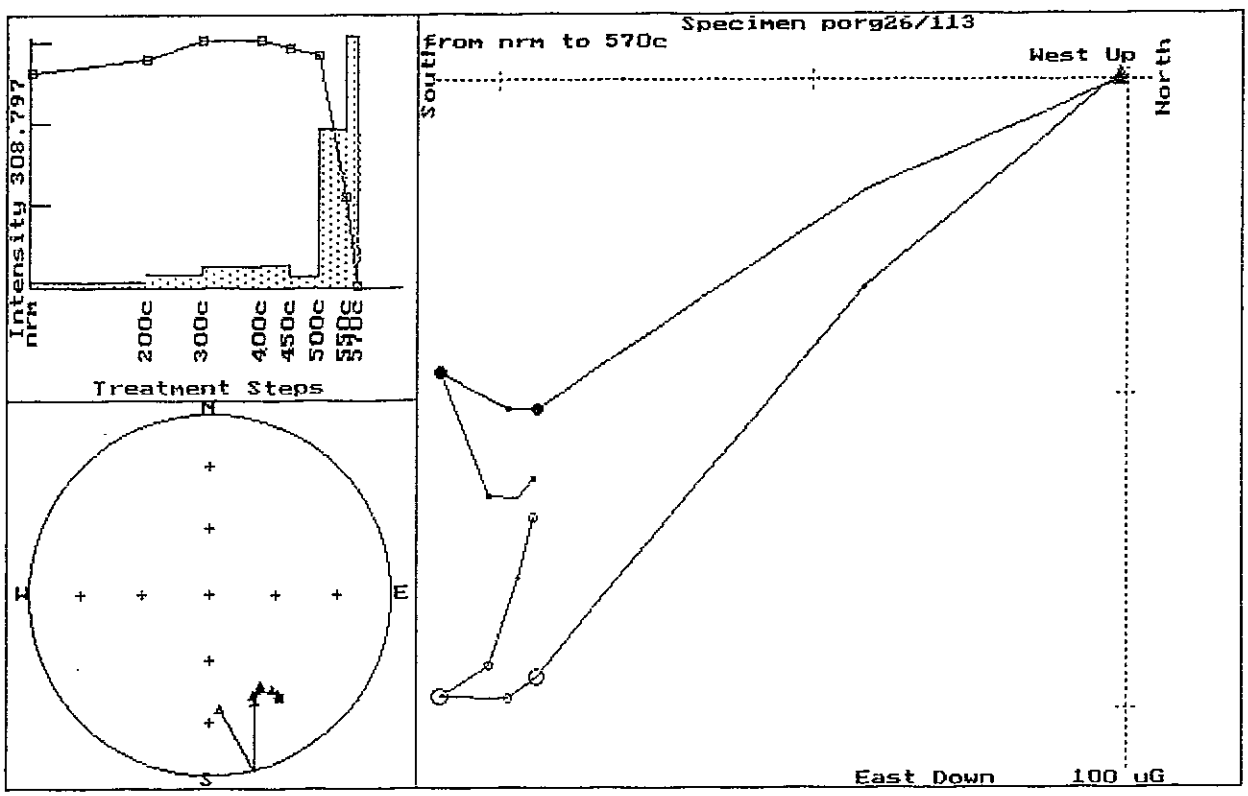
Specimen porg26/113
from nrm to 570c
West Up
South
North
East Down
100 uG
Intensity 308.797
nrm
200c
300c
400c
450c
500c
570c
Treatment Steps
N
E
S
W

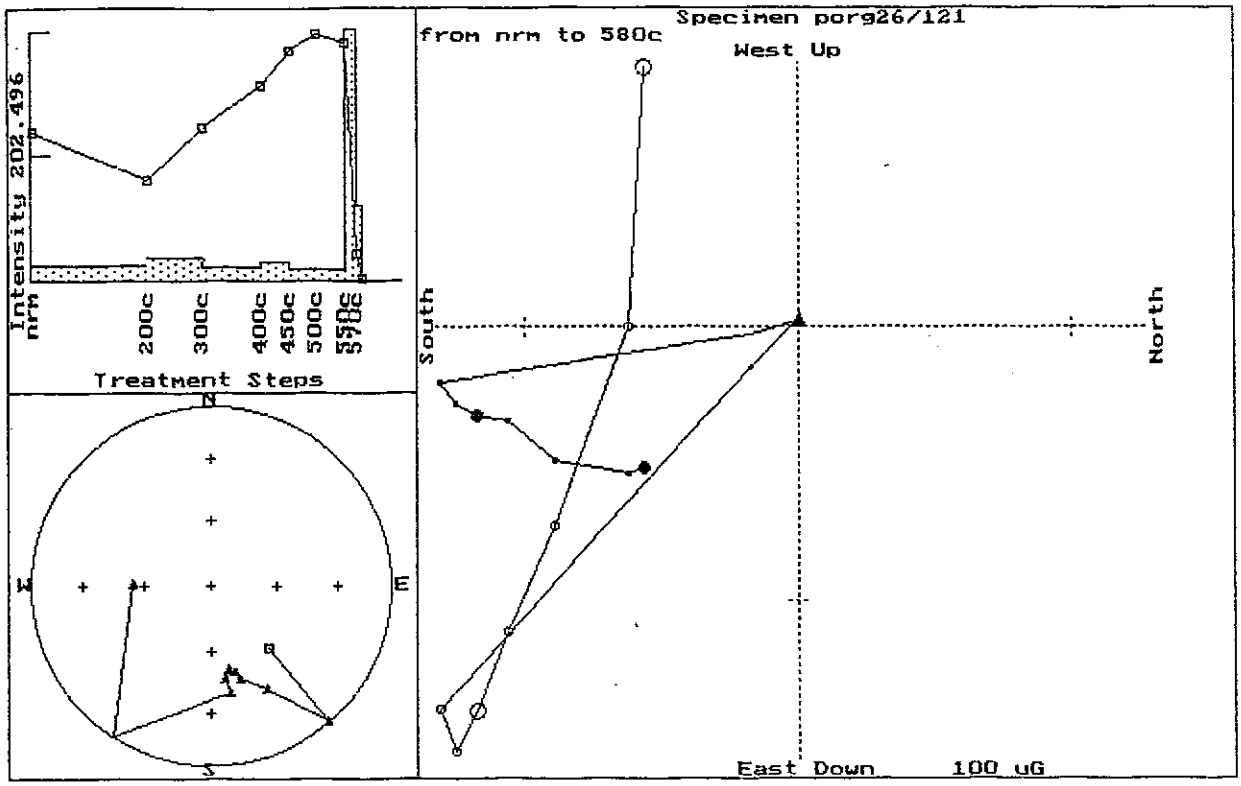
Specimen porg26/121
from nrm to 580c
West Up
Intensity 202.496
nrm
200c
300c
400c
450c
500c
580c
Treatment Steps
South
North
East Down
100 uG

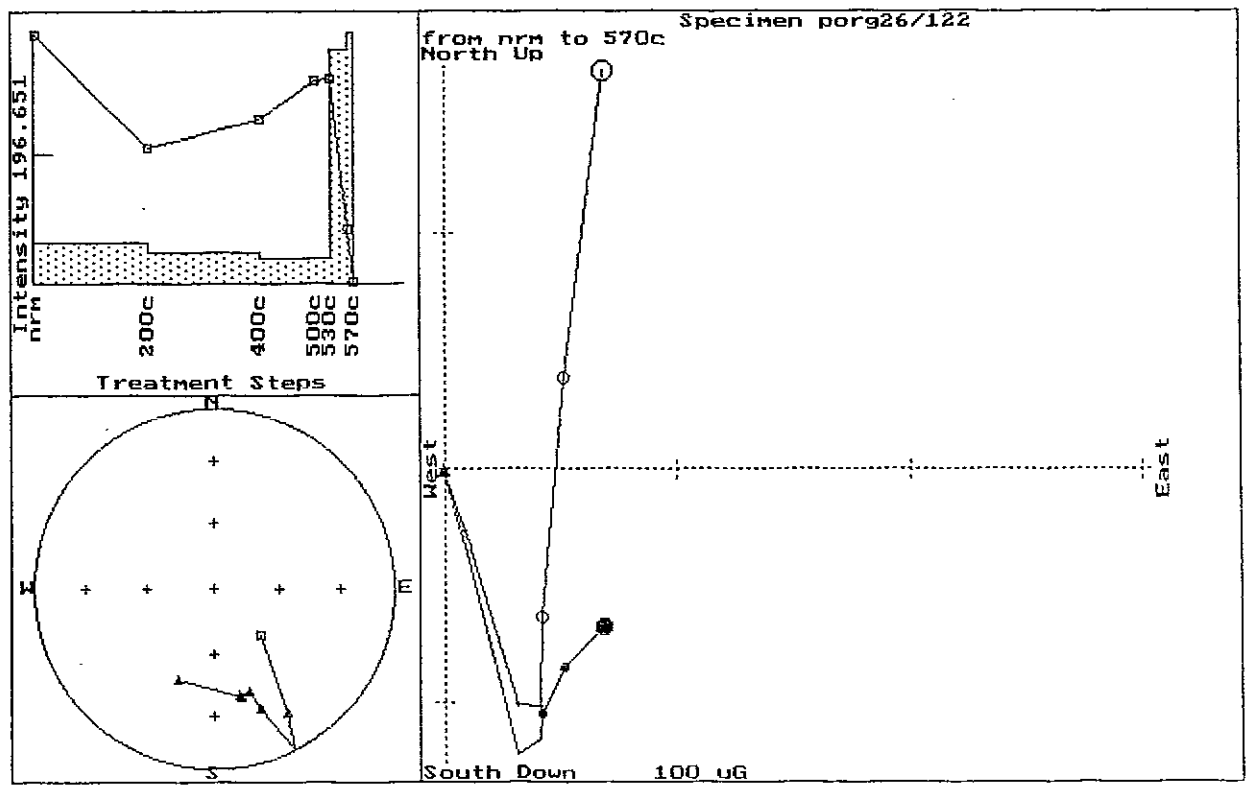
Specimen porg26/122
from nrm to 570c
North Up
Intensity 196.651
nrm
200c
400c
500c
530c
570c
Treatment Steps
West
East
South Down
100 uG

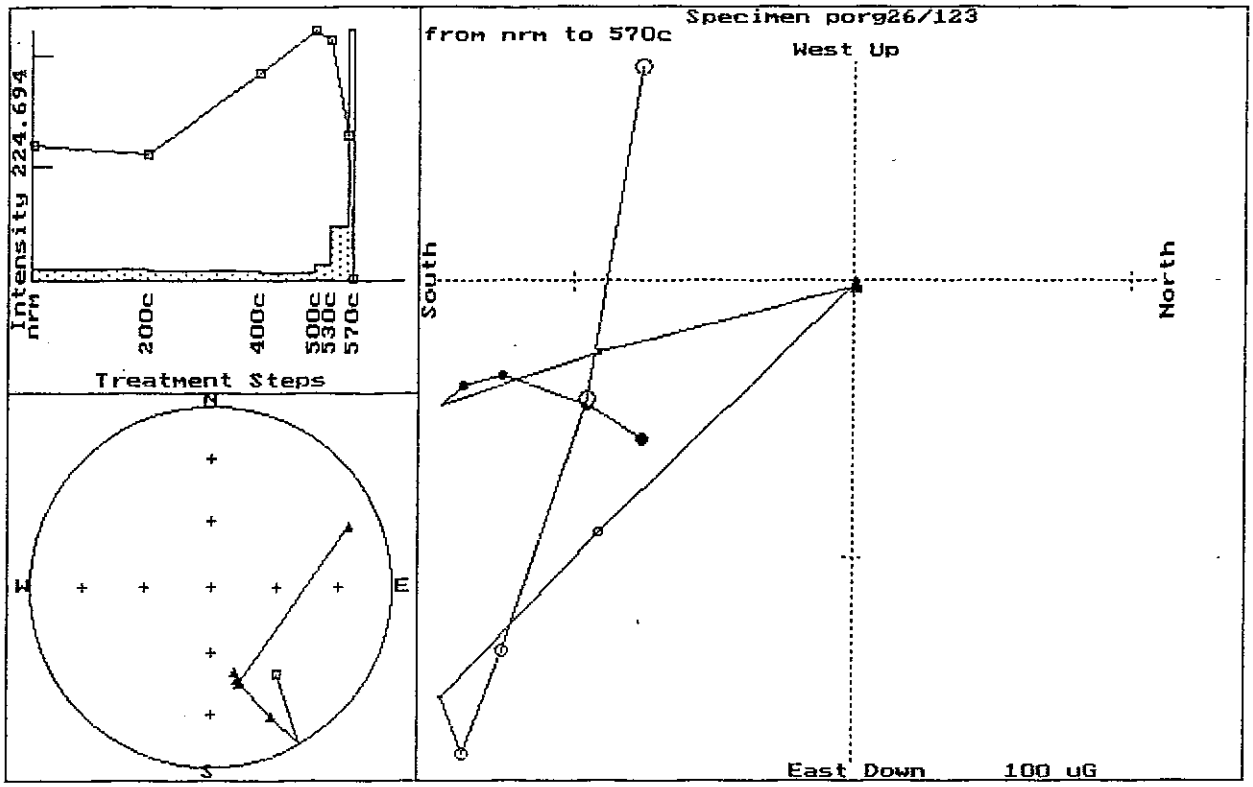
Intensity 224.694
nrm
200c
400c
500c
530c
570c
Treatment Steps
N
W
E
S
Specimen porg26/123
from nrm to 570c
West Up
South
North
East Down
100 uG

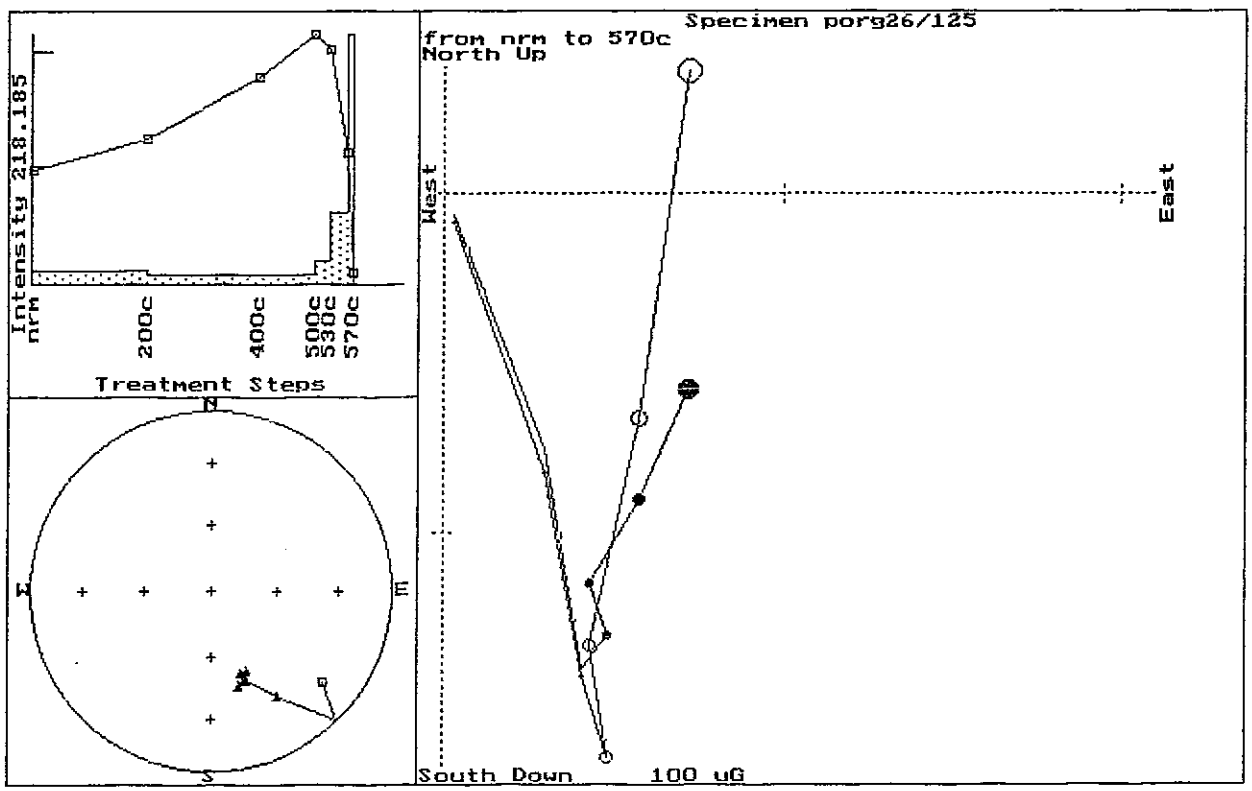
Intensity 218.185
nrm
200c
400c
500c
530c
570c
Treatment Steps
N
W
E
S
Specimen porg26/125
from nrm to 570c
North Up
West
East
South Down
100 uG

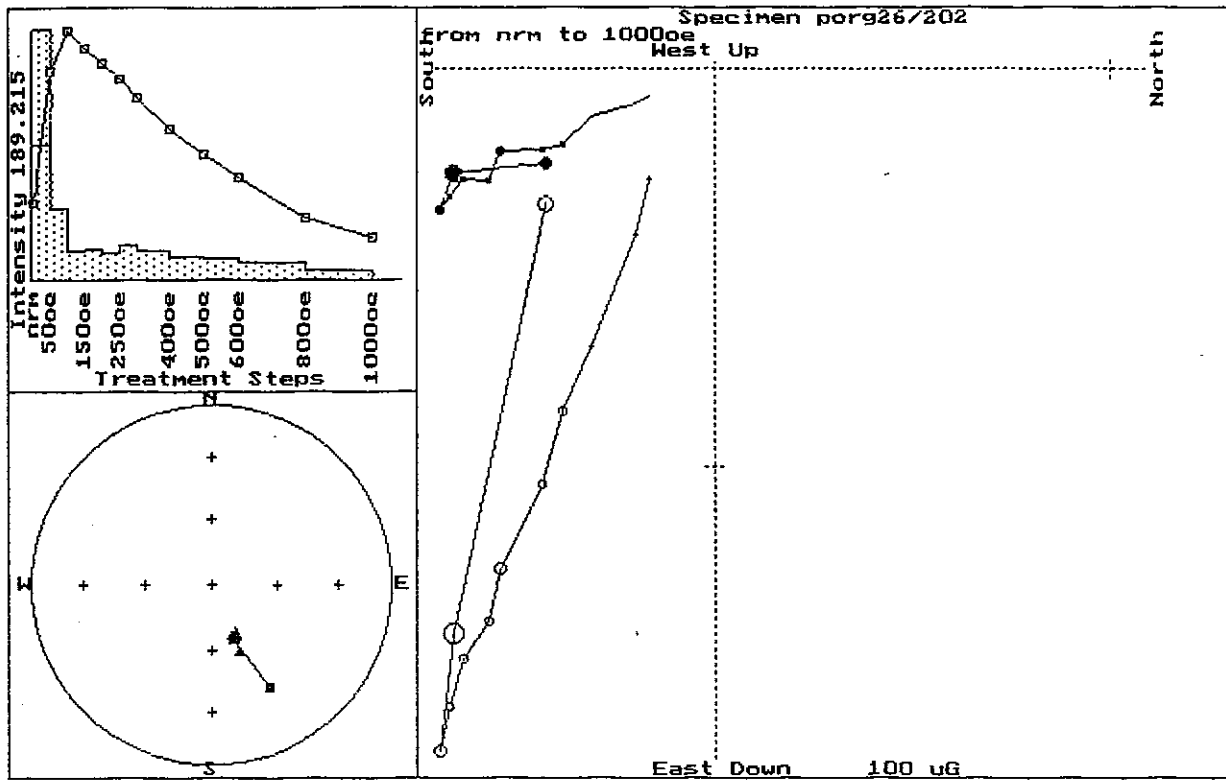
Intensity 189.215
nrm
50oe
150oe
250oe
400oe
500oe
600oe
800oe
1000oe
Treatment Steps
N
W
E
S
Specimen porg26/202
from nrm to 1000oe
West Up
South
North
East Down
100 uG

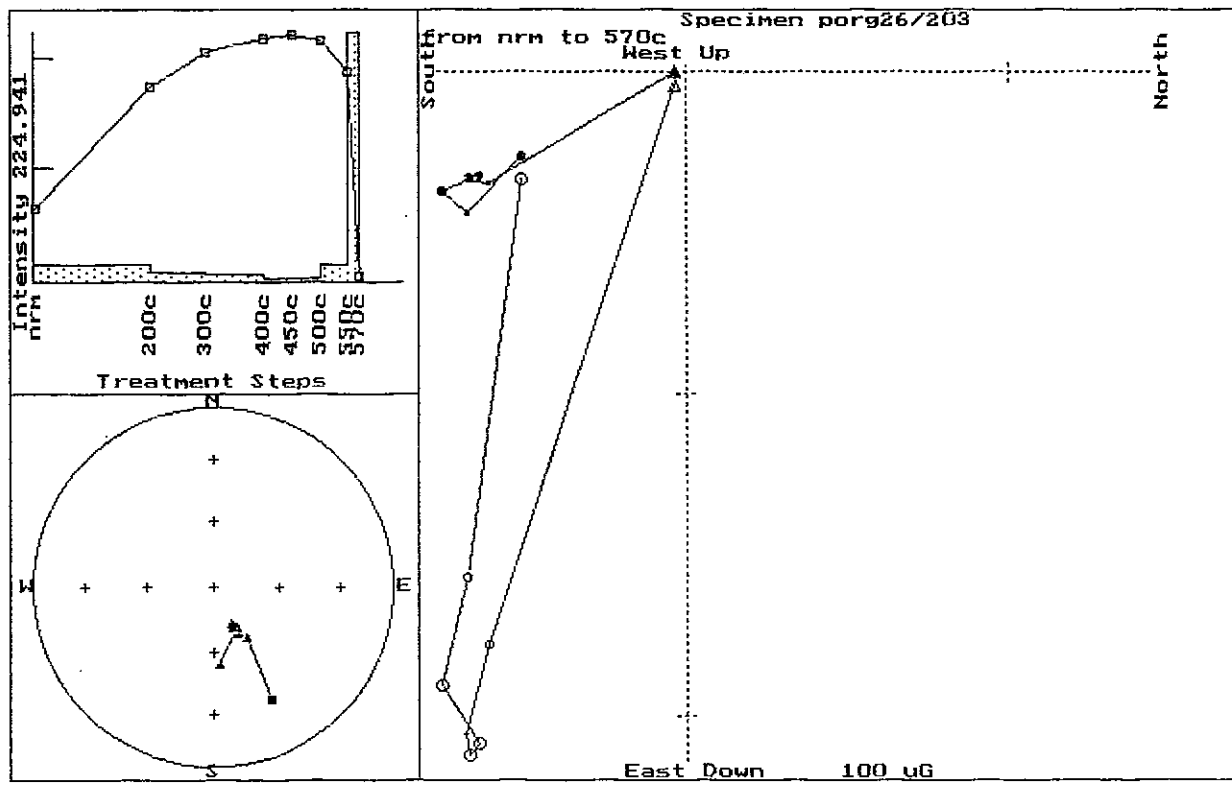
Intensity 224.941
nrm
200c
300c
400c
450c
500c
550c
570c
Treatment Steps
N
W
E
S
Specimen porg26/203
from nrm to 570c
West Up
South
North
East Down
100 uG

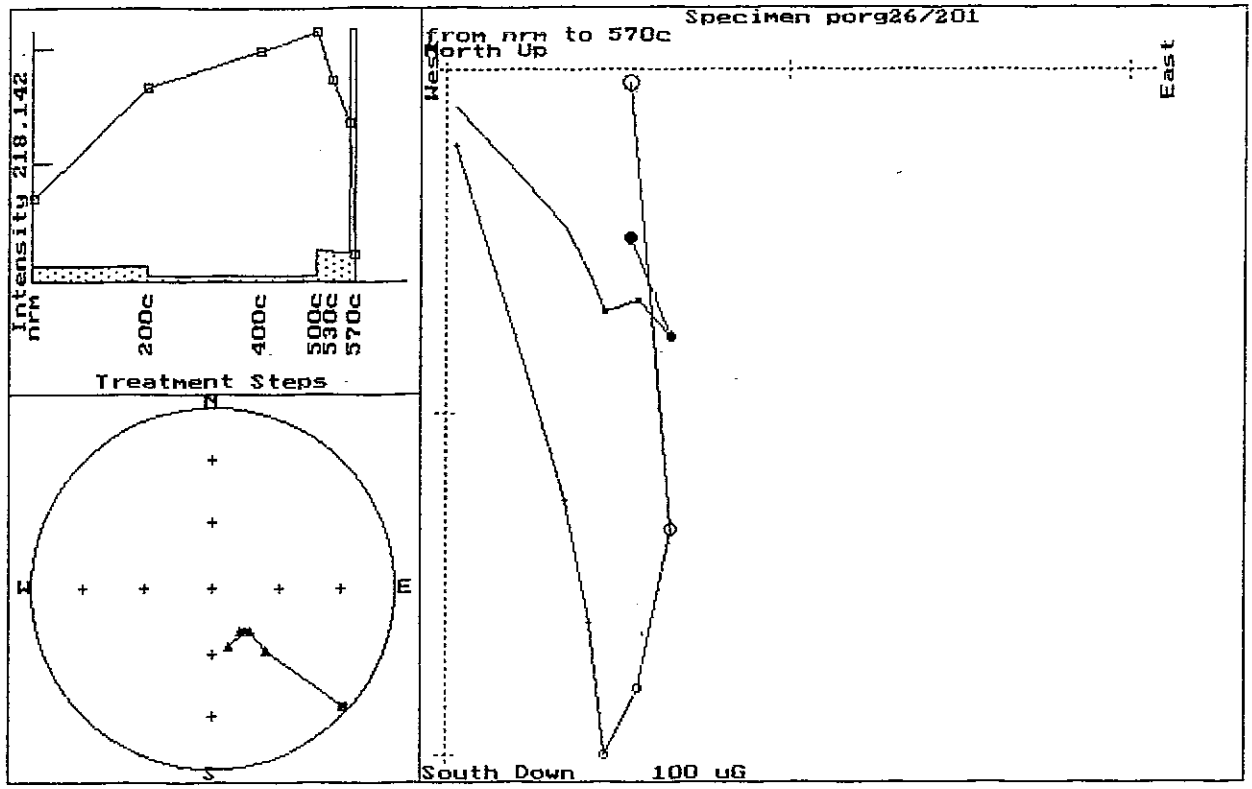
Specimen porg26/201
from nrm to 570c
North Up
West
East
Intensity 218.142
nrm
200c
400c
500c
530c
570c
Treatment Steps
N
E
S
W
South Down
100 uG

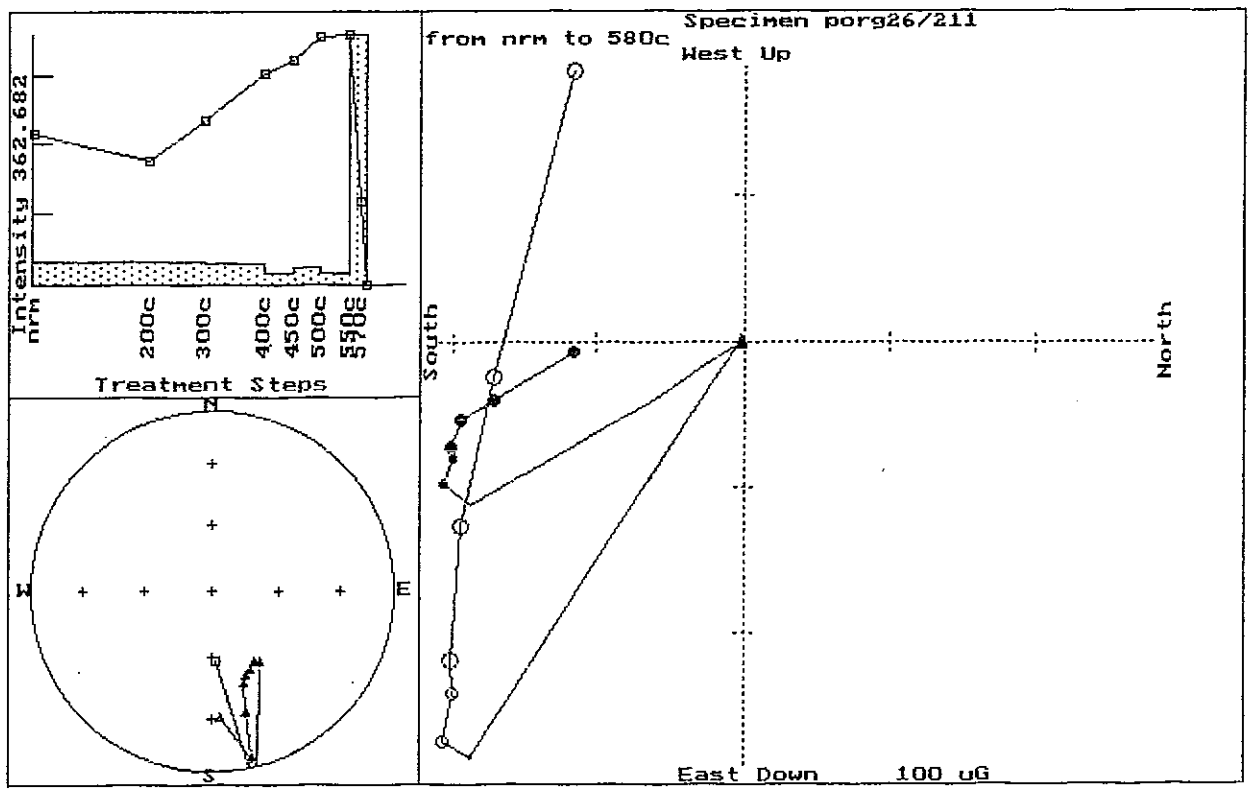
Specimen porg26/211
from nrm to 580c
West Up
South
North
Intensity 362.682
nrm
200c
300c
400c
450c
500c
550c
580c
Treatment Steps
N
E
S
W
East Down
100 uG

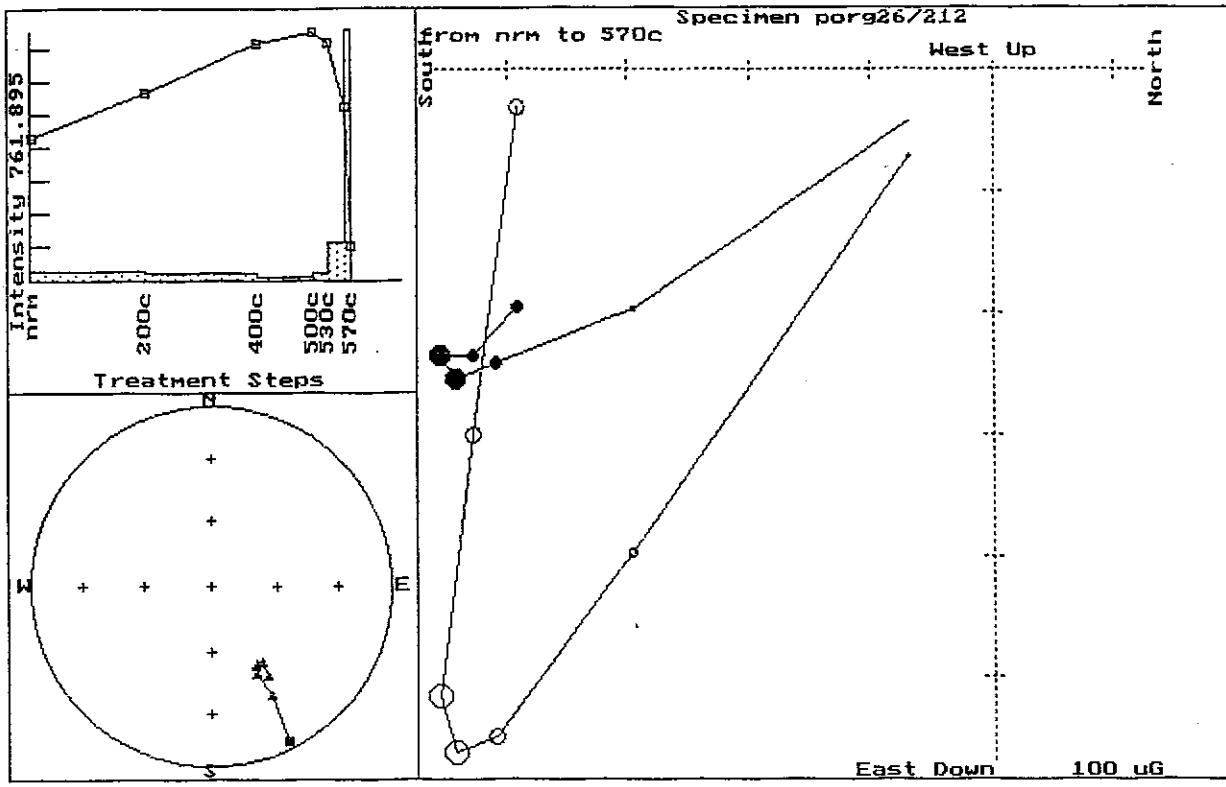
Specimen porg26/212
from nrm to 570c
West Up
South
North
Intensity 761.895
nrm
200c
400c
500c
530c
570c
Treatment Steps
N
E
S
East Down
100 uG

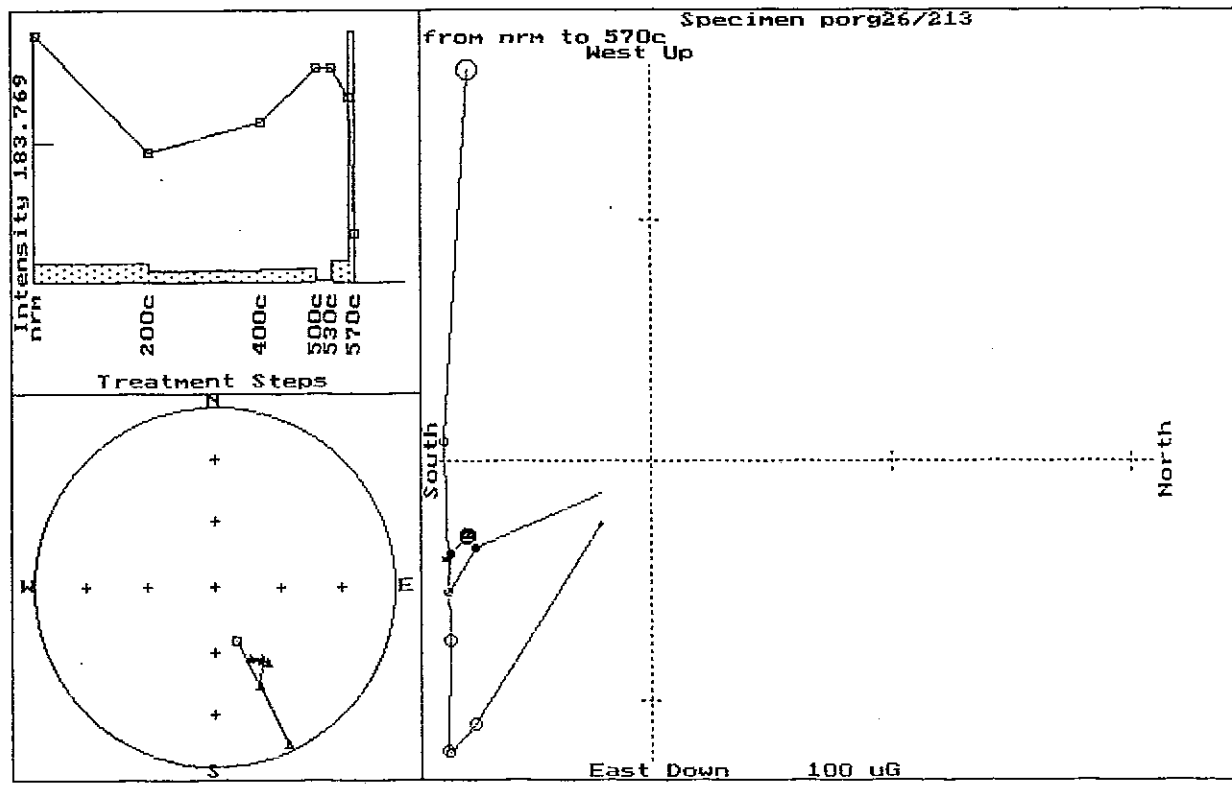
Specimen porg26/213
from nrm to 570c
West Up
South
North
Intensity 183.769
nrm
200c
400c
500c
530c
570c
Treatment Steps
N
E
S
East Down
100 uG

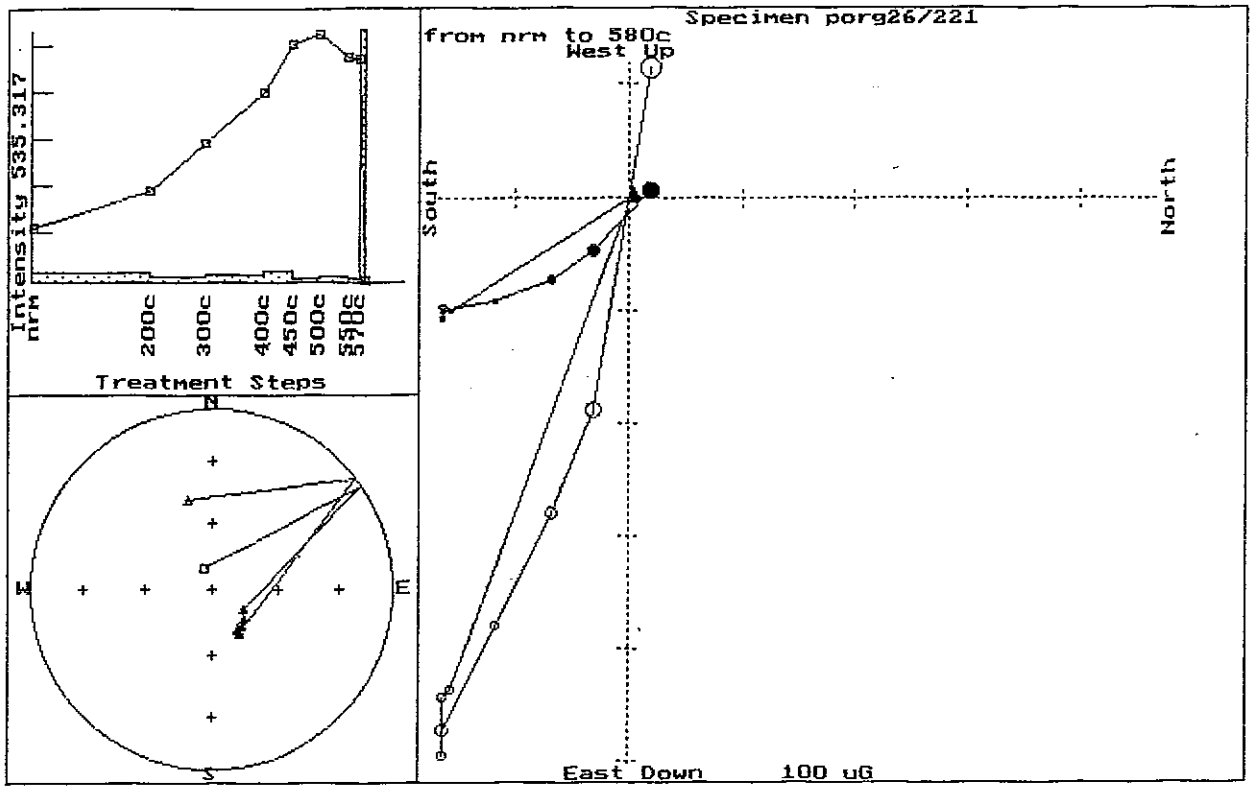
Intensity 535.317
nrm
200c
300c
400c
450c
500c
550c
570c
Treatment Steps
N
E
S
W
Specimen porg26/221
from nrm to 580c
West Up
South
North
East Down
100 uG

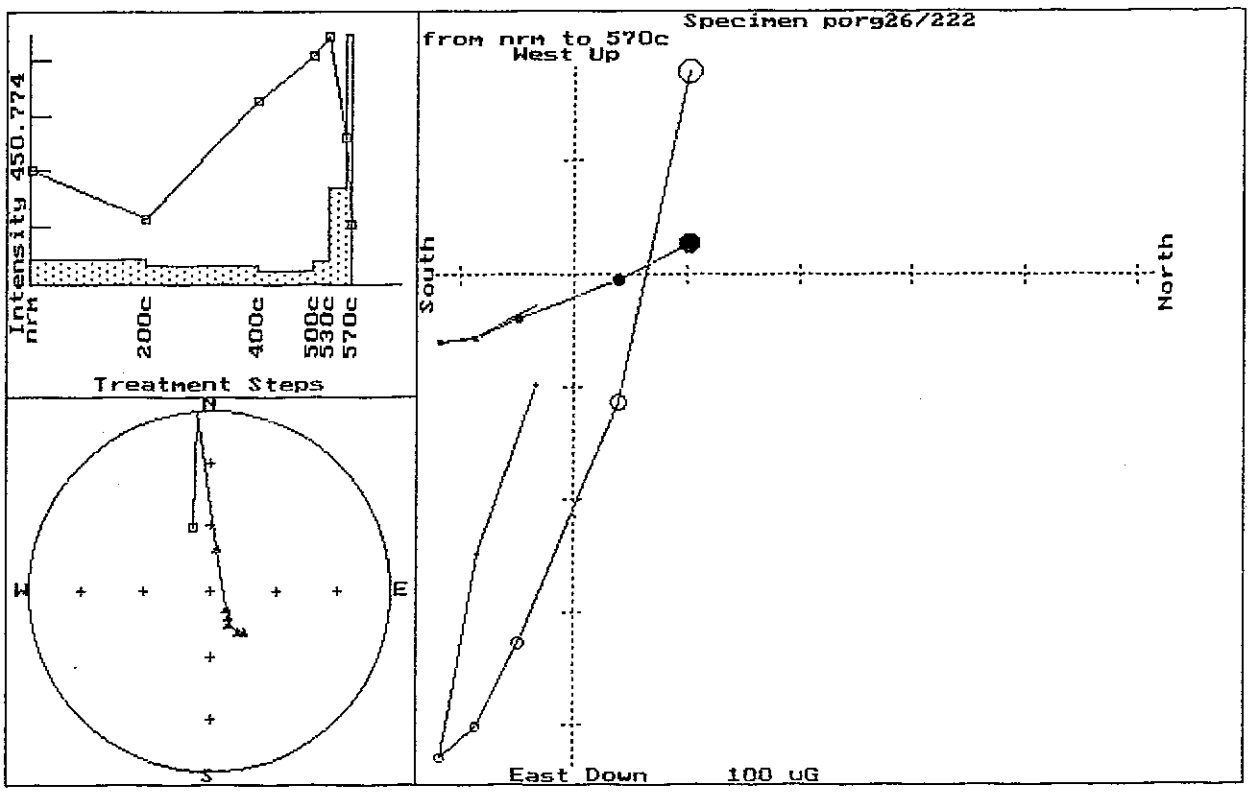
Intensity 450.774
nrm
200c
400c
500c
530c
570c
Treatment Steps
N
E
S
W
Specimen porg26/222
from nrm to 570c
West Up
South
North
East Down
100 uG

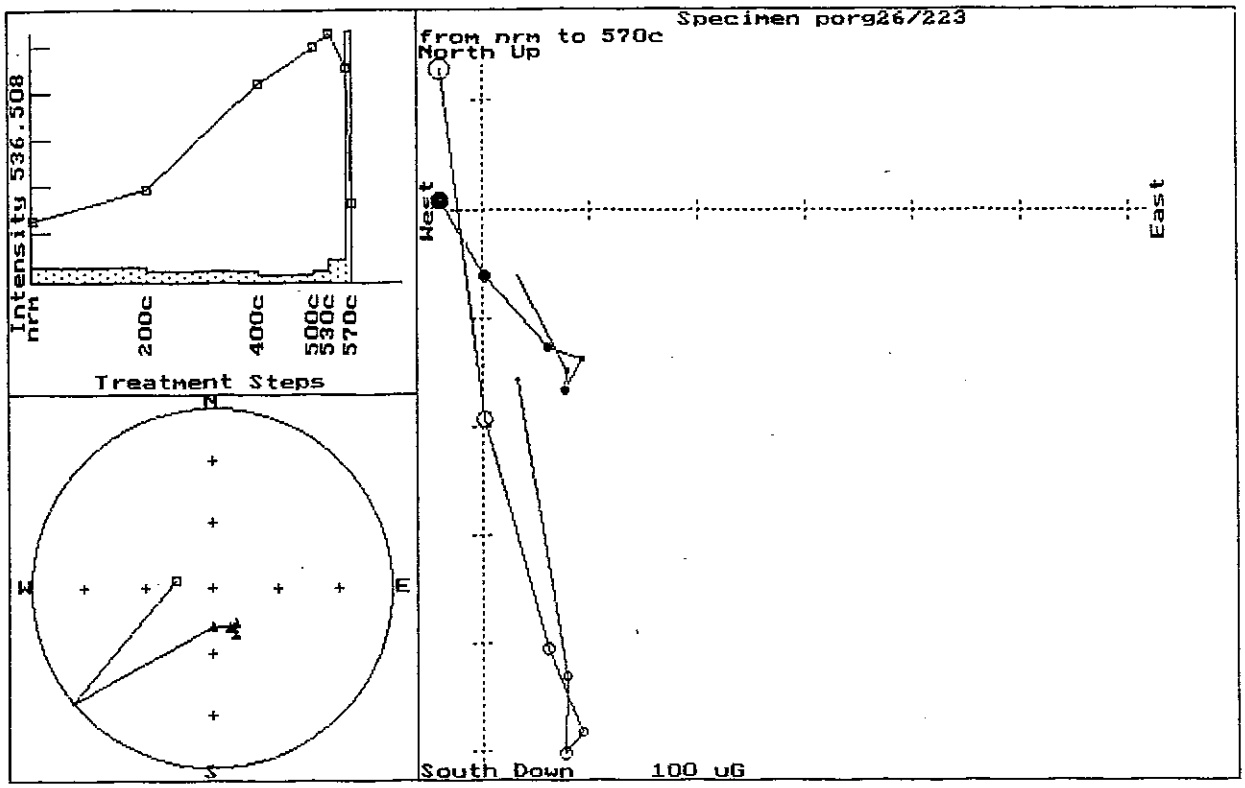
Intensity 536.508
nrm
200c
400c
500c
530c
570c
Treatment Steps
N
W
E
S
Specimen porg26/223
from nrm to 570c
North Up
West
East
South Down
100 uG

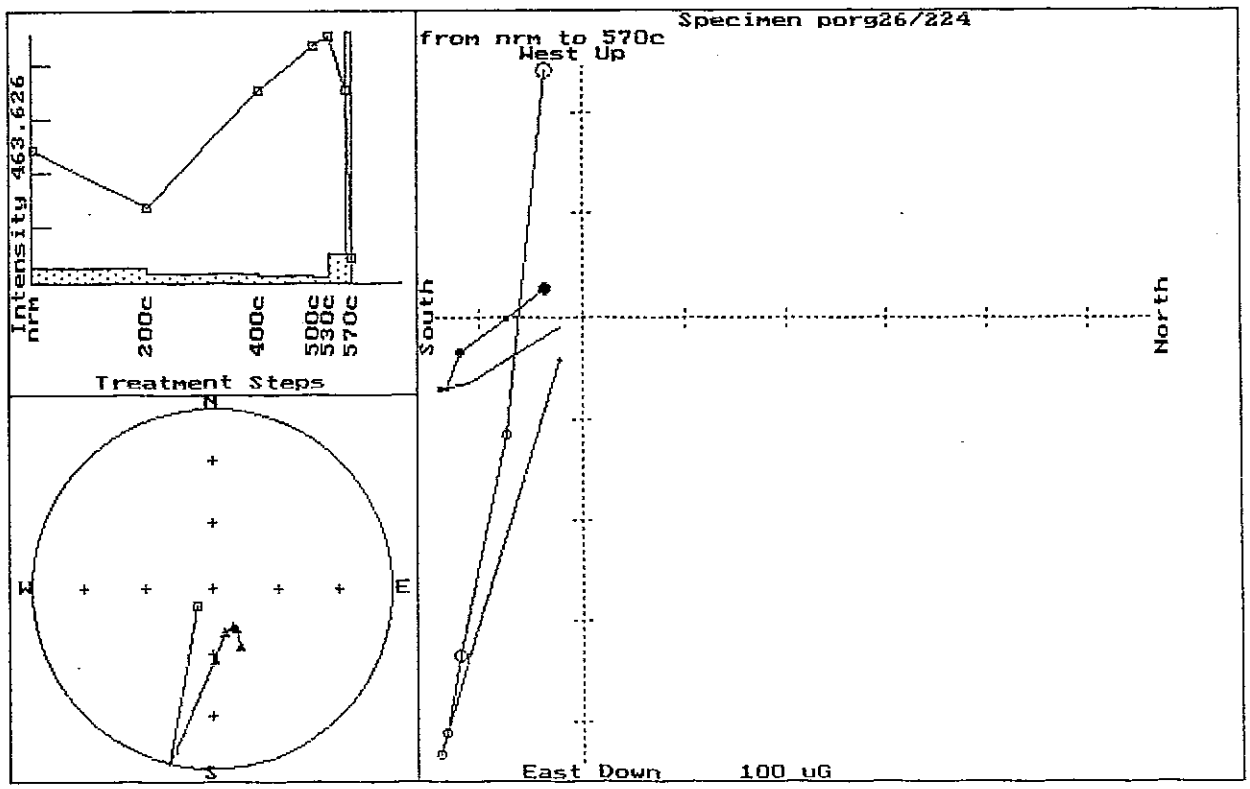
Intensity 463.626
nrm
200c
400c
500c
530c
570c
Treatment Steps
N
W
E
S
Specimen porg26/224
from nrm to 570c
West Up
South
North
East Down
100 uG

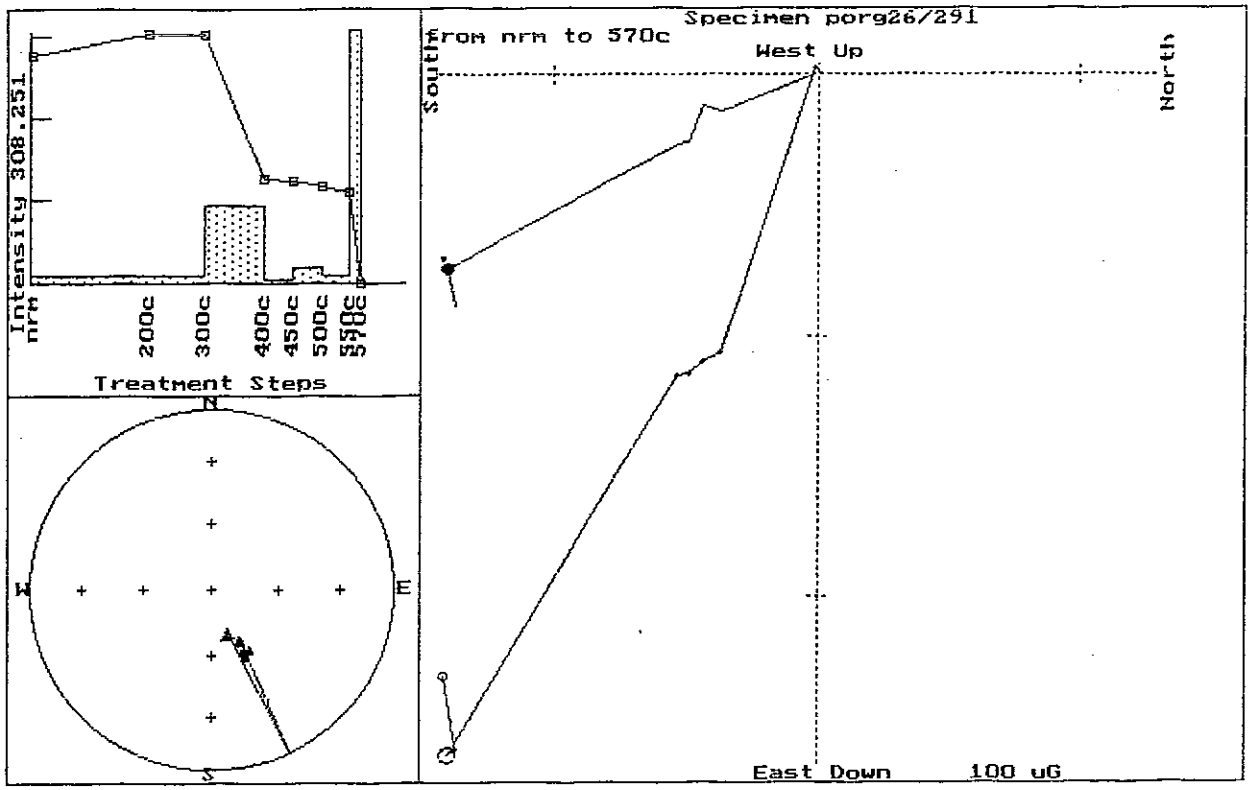
Intensity 308.251
nrm
200c
300c
400c
450c
500c
550c
570c
Treatment Steps
N
E
S
W
Specimen porg26/291
from nrm to 570c
West Up
South
North
East Down
100 uG

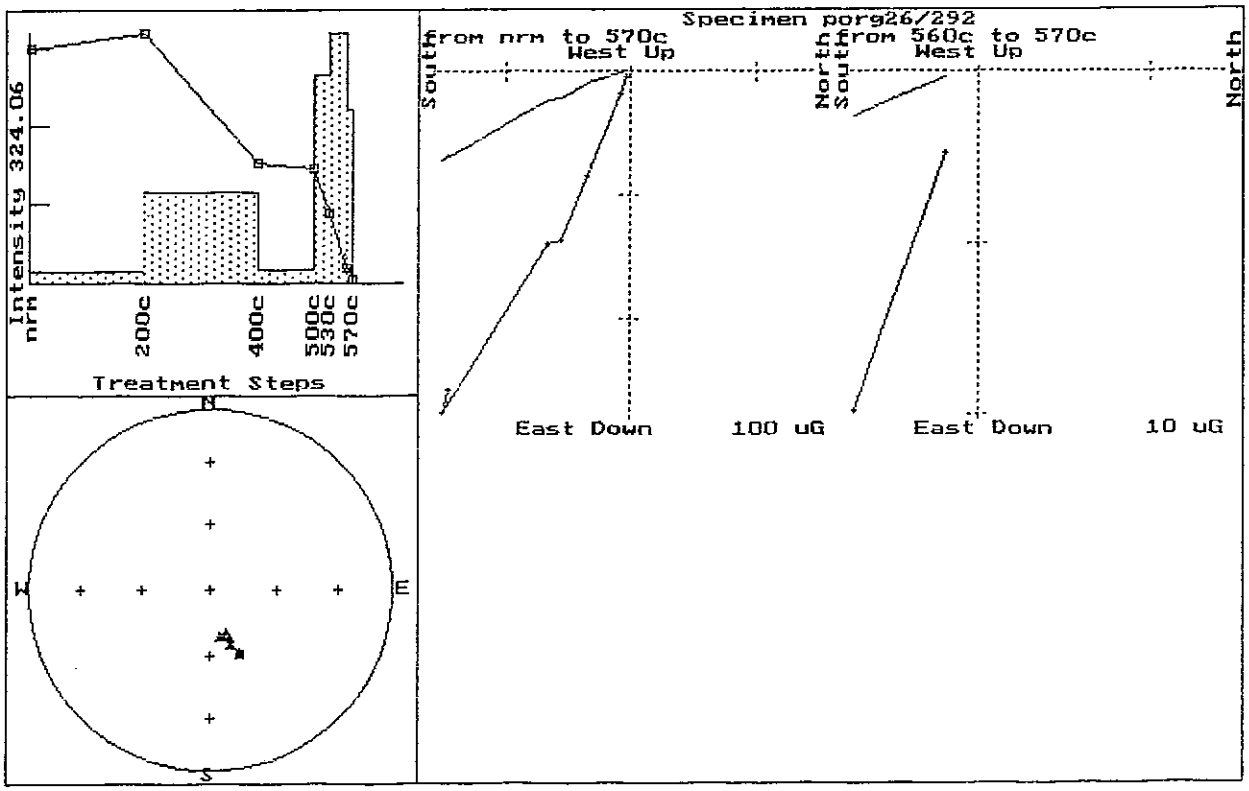
Intensity 324.06
nrm
200c
400c
500c
530c
570c
Treatment Steps
N
E
S
W
Specimen porg26/292
from nrm to 570c
West Up
South
North
from 560c to 570c
West Up
South
North
East Down
100 uG
East Down
10 uG

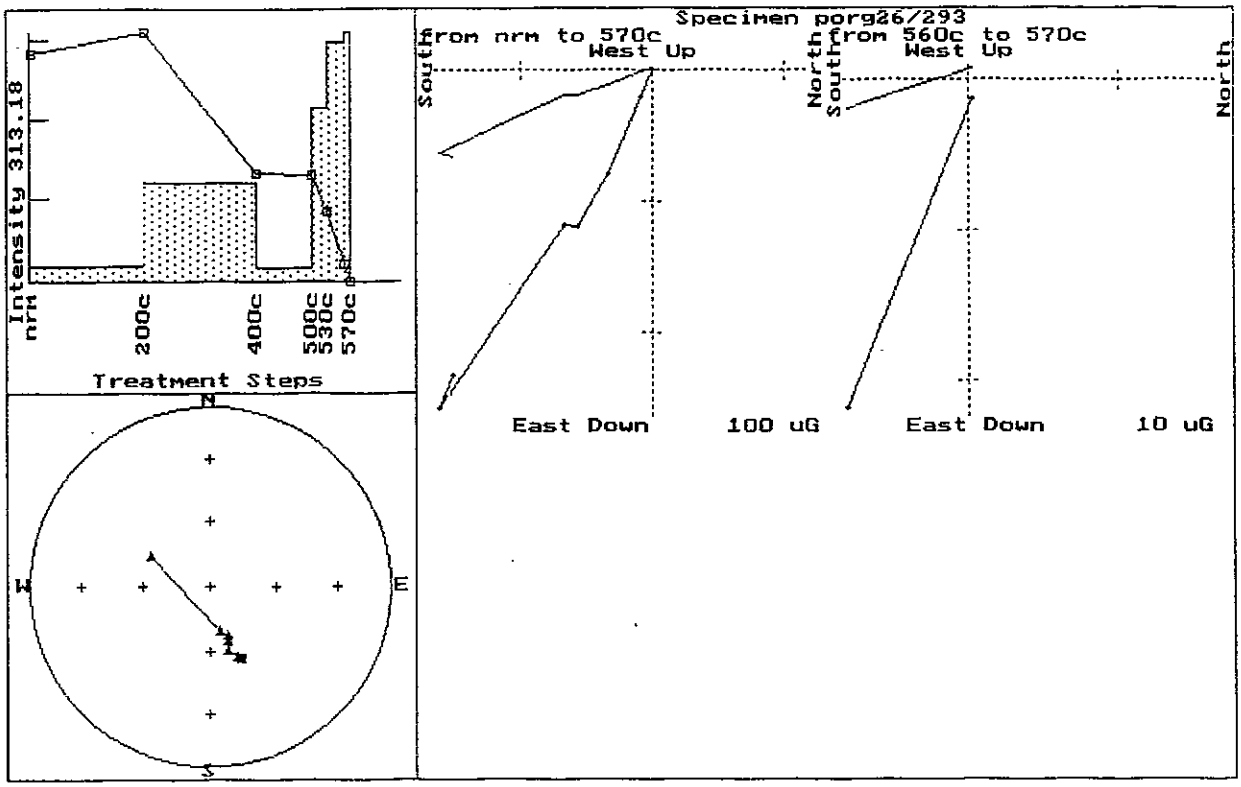
Specimen porg26/293
from nrm to 570c
West Up
South
North
from 560c to 570c
West Up
South
North
Intensity 313.18
nrm
200c
400c
500c
530c
570c
Treatment Steps
W
E
East Down
100 uG
East Down
10 uG

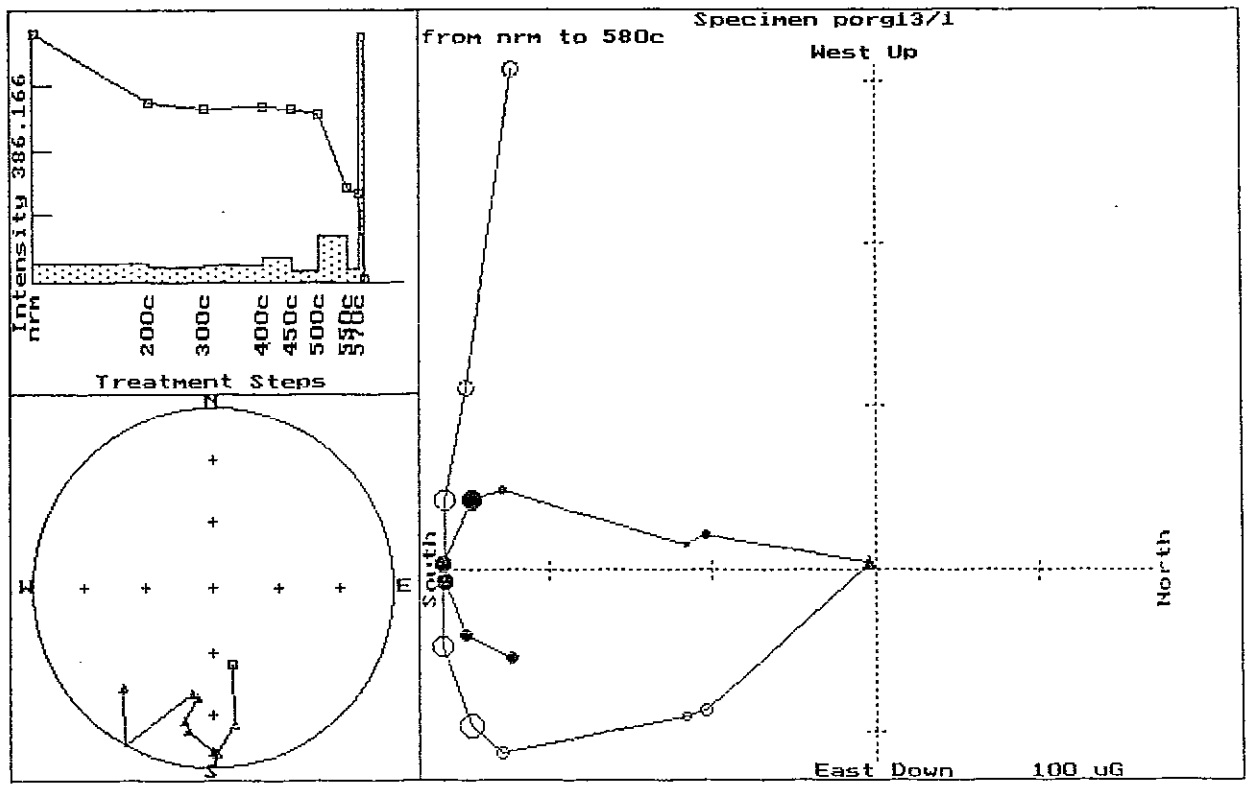
Specimen porgi3/1
from nrm to 580c
West Up
Intensity 386.166
nrm
200c
300c
400c
450c
500c
550c
580c
Treatment Steps
W
E
South
North
East Down
100 uG

Fig.14. Zijderveld plots for the fresh and altered andesite samples from the underground mine.

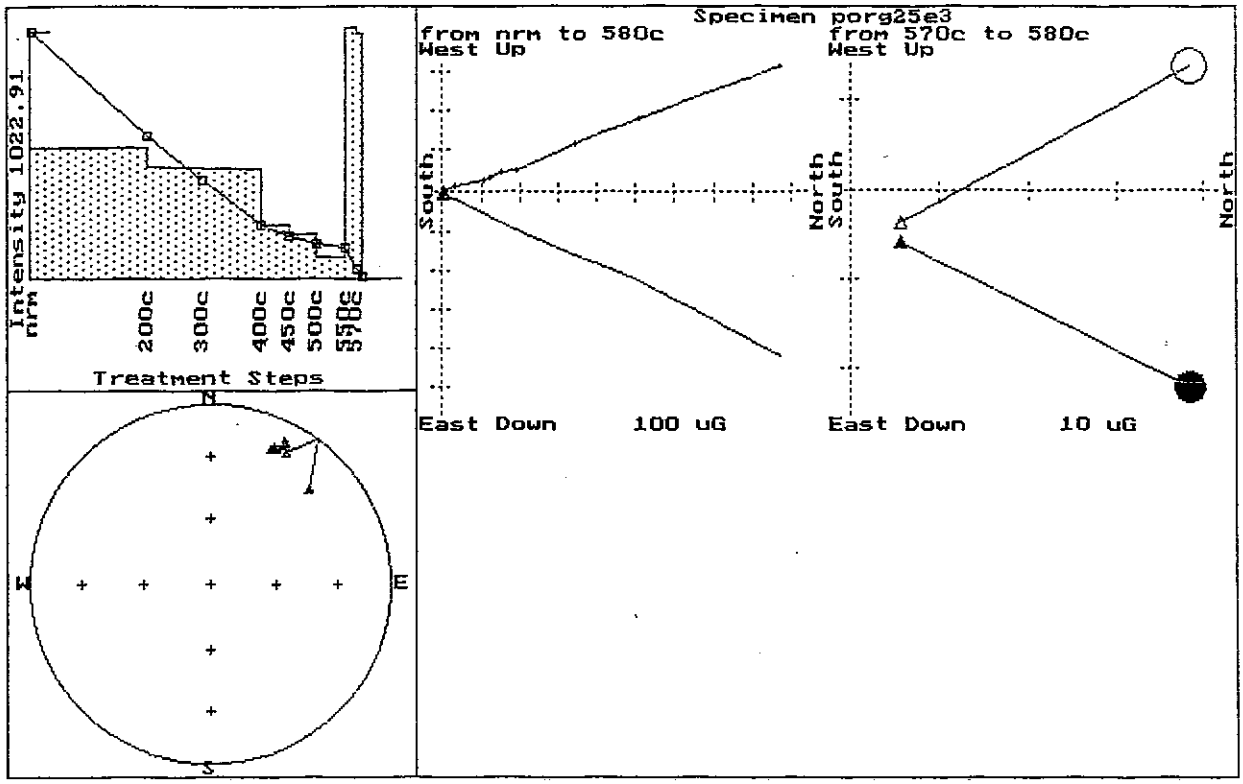
Intensity 1022.91
nrm
200c
300c
400c
450c
500c
550c
580c
Treatment Steps
N
E
S
W
Specimen porg25e3
from nrm to 580c
West Up
South
East Down
100 uG
from 570c to 580c
West Up
North
South
North
East Down
10 uG

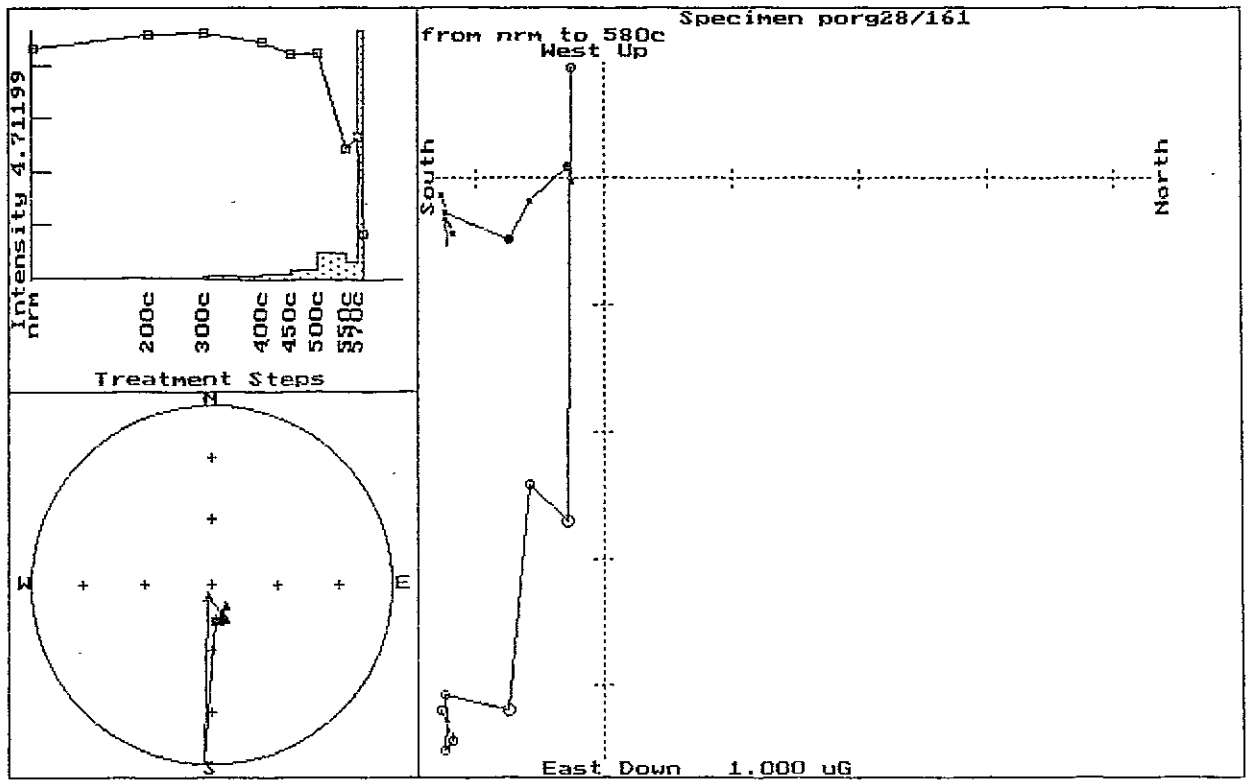
Intensity 4.71199
nrm
200c
300c
400c
450c
500c
550c
580c
Treatment Steps
N
E
S
W
Specimen porg28/161
from nrm to 580c
West Up
South
North
East Down
1.000 uG

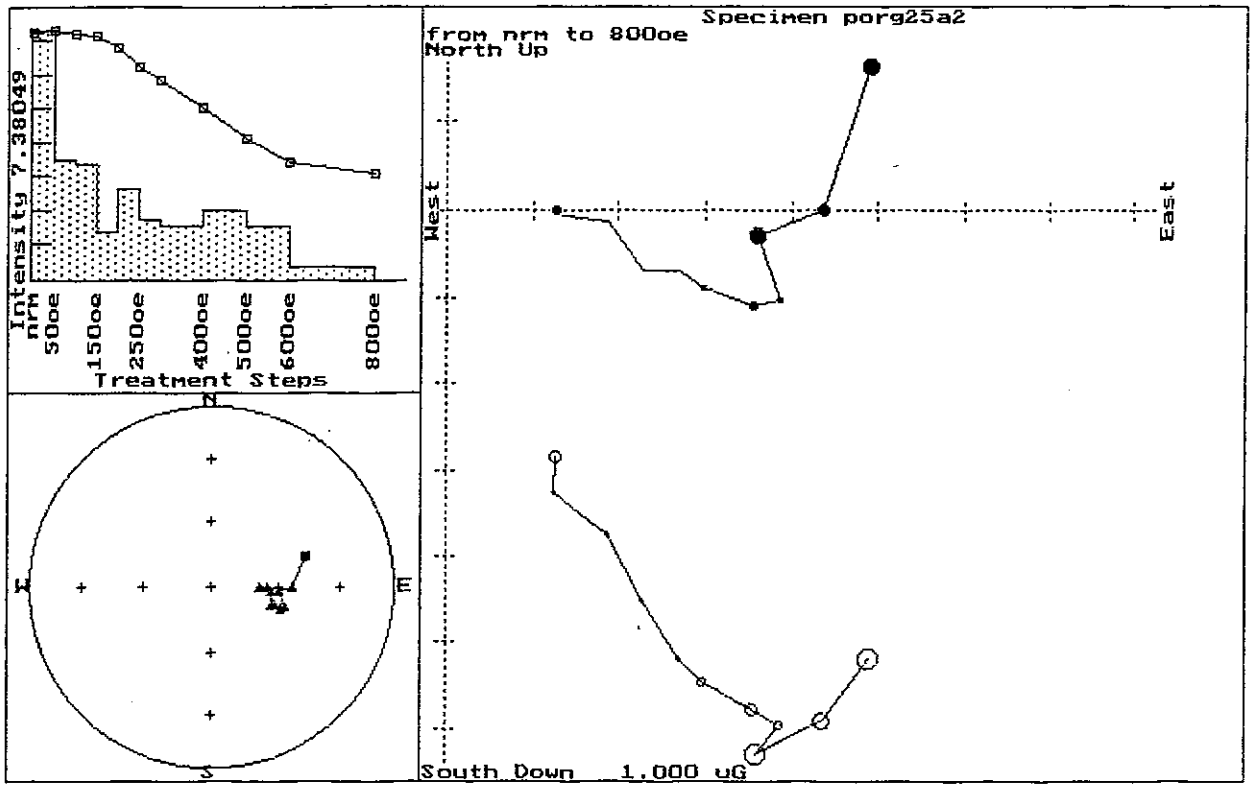
Intensity 7.38049
nrm
50oe
150oe
250oe
400oe
500oe
600oe
800oe
Treatment Steps
N
E
S
Specimen porg25a2
from nrm to 800oe
North Up
West
East
South Down 1.000 uG

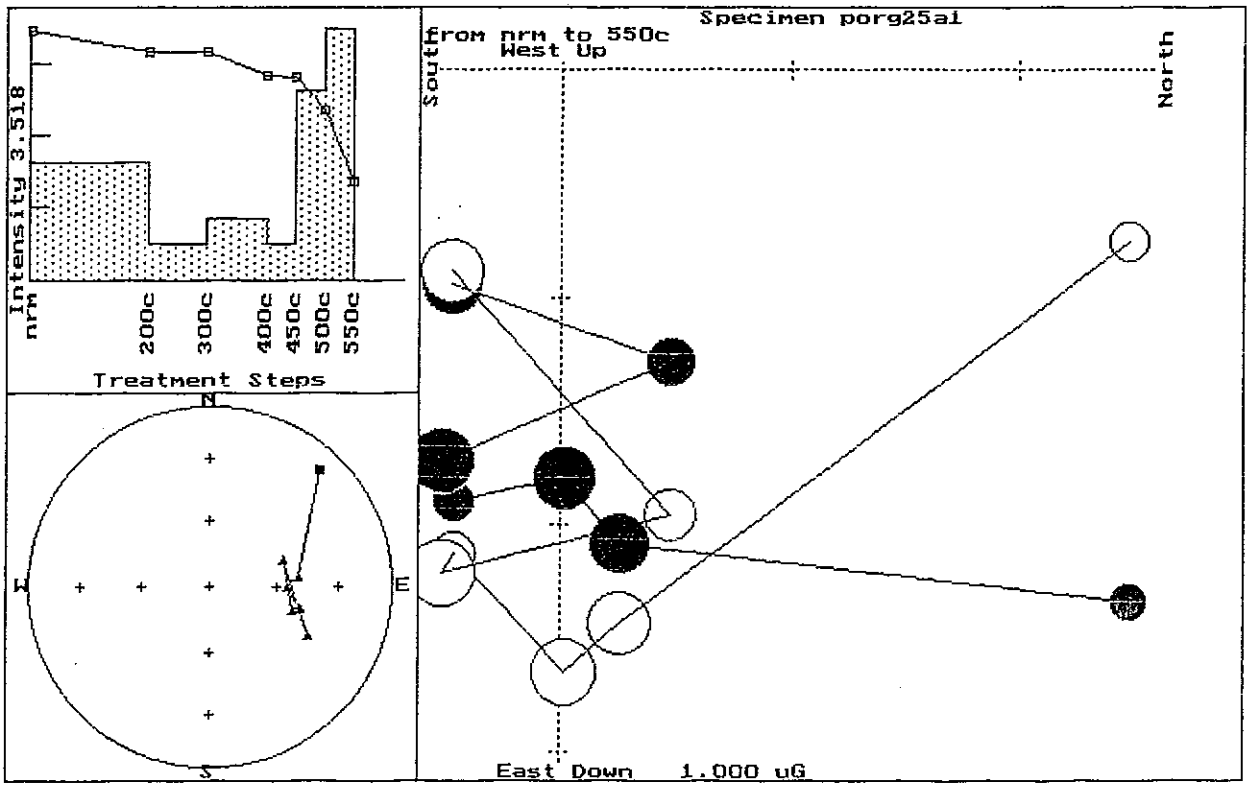
Intensity 3.518
nrm
200c
300c
400c
450c
500c
550c
Treatment Steps
N
E
S
Specimen porg25a1
from nrm to 550c
West Up
South
North
East Down 1.000 uG

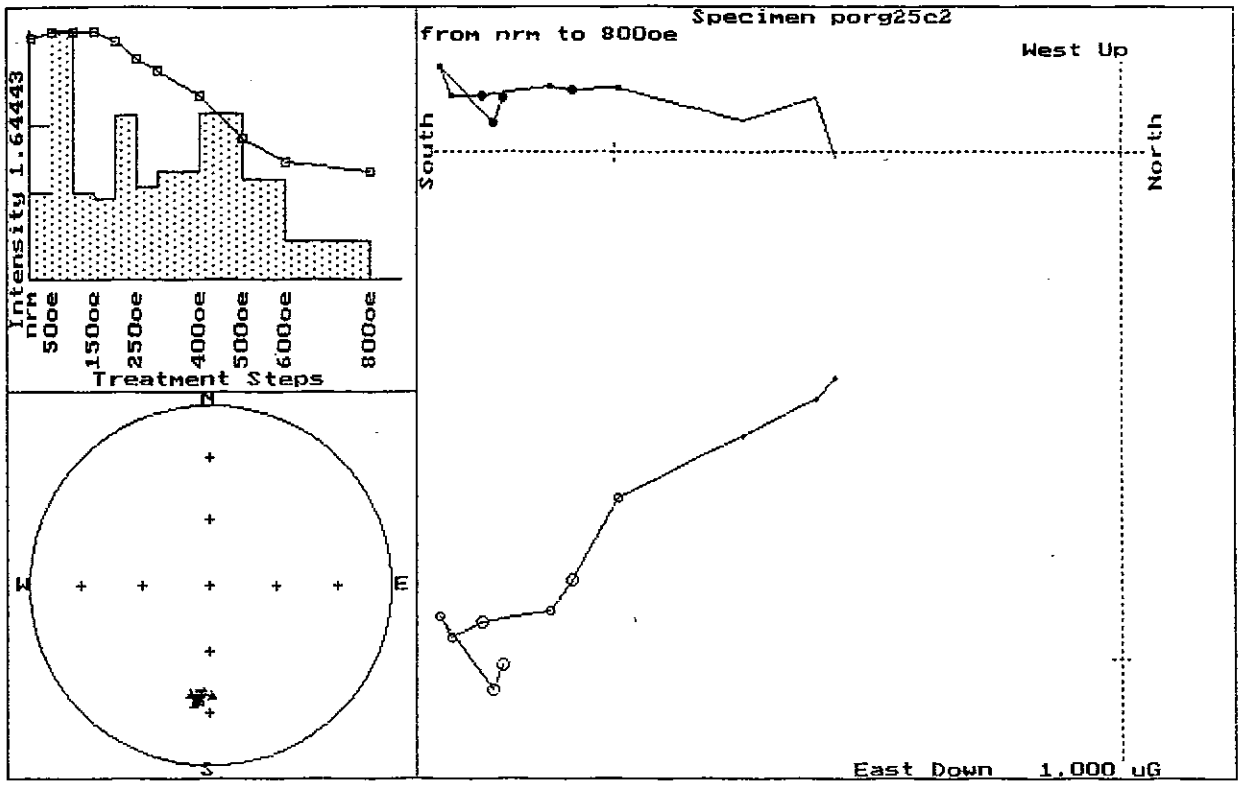
Intensity 1.64443
nrm
50oe
150oe
250oe
400oe
500oe
600oe
800oe
Treatment Steps
N
W
E
S
Specimen porg25c2
from nrm to 800oe
West Up
South
North
East Down 1.000 uG

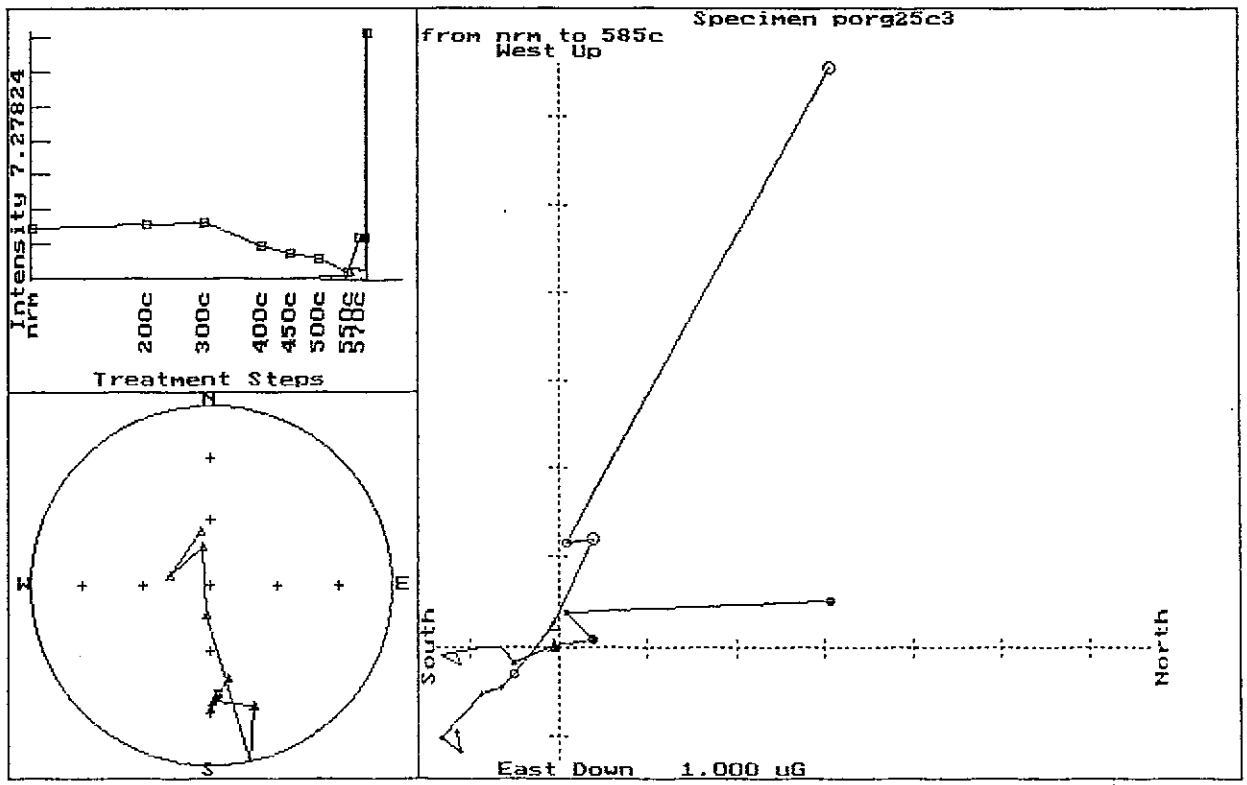
Intensity 7.27824
nrm
200c
300c
400c
450c
500c
550c
Treatment Steps
N
W
E
S
Specimen porg25c3
from nrm to 585c
West Up
South
North
East Down 1.000 uG

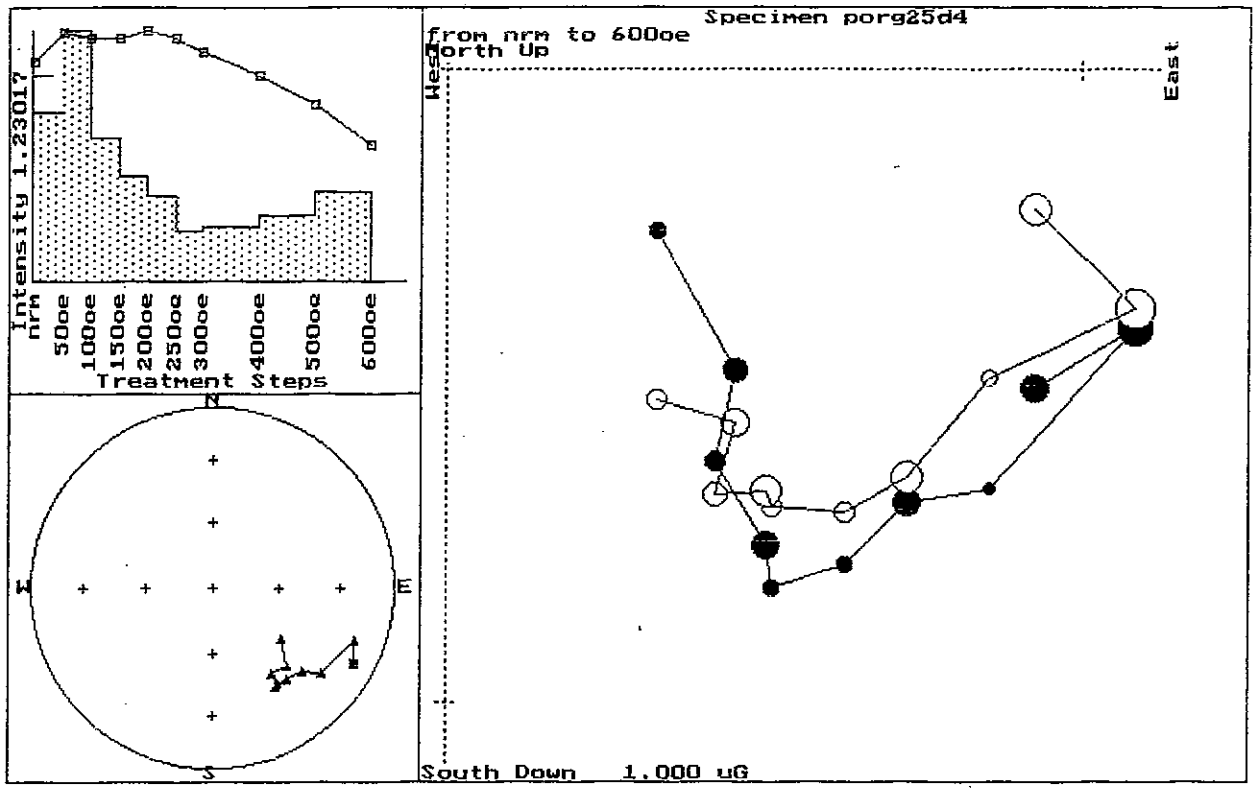
Intensity 1.23017
nrm
50oe
100oe
150oe
200oe
250oa
300oe
400oe
500oa
600oe
Treatment Steps
N
W
E
S
Specimen porg25d4
from nrm to 600oe
North Up
West
East
South Down 1.000 uG

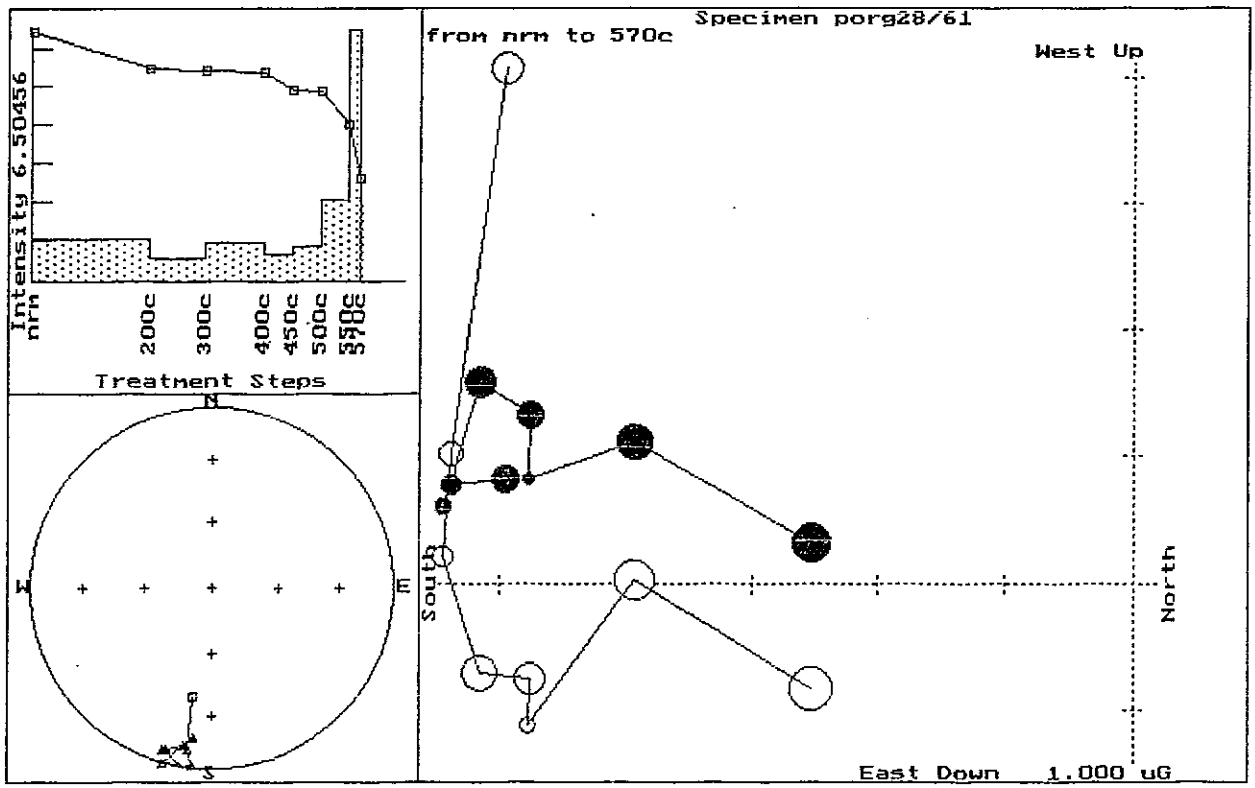
Intensity 6.50456
nrm
200c
300c
400c
450c
500c
570c
Treatment Steps
N
W
E
S
Specimen porg28/61
from nrm to 570c
West Up
South
North
East Down 1.000 uG

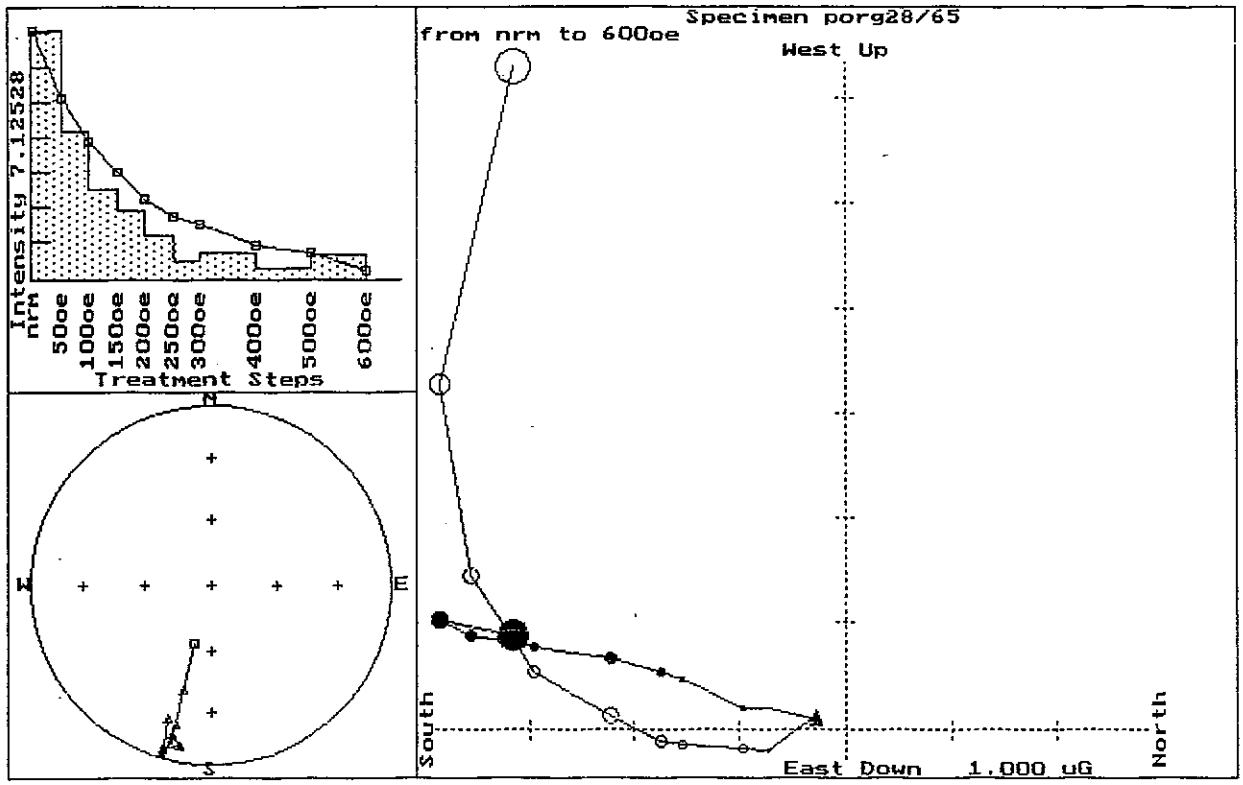
Intensity 7.12528
nrm
50oe
100oe
150oe
200oe
250oe
300oe
400oe
500oe
600oe
Treatment Steps
N
W
E
S
Specimen porg28/65
from nrm to 600oe
West Up
South
North
East Down
1.000 uG

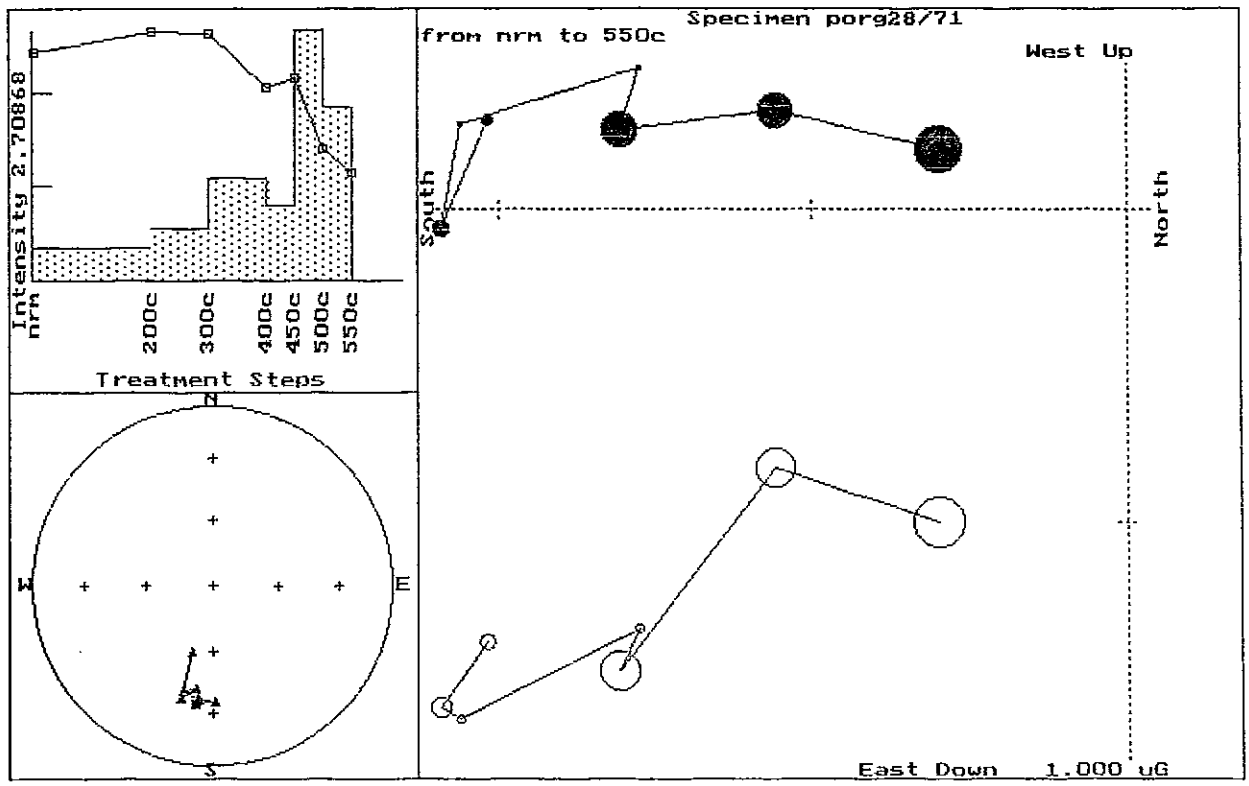
Intensity 2.70868
nrm
200c
300c
400c
450c
500c
550c
Treatment Steps
N
W
E
S
Specimen porg28/71
from nrm to 550c
West Up
South
North
East Down
1.000 uG

Fig.15. Zijderveld plots for samples of altered host sediments and sulphide mineralisation.

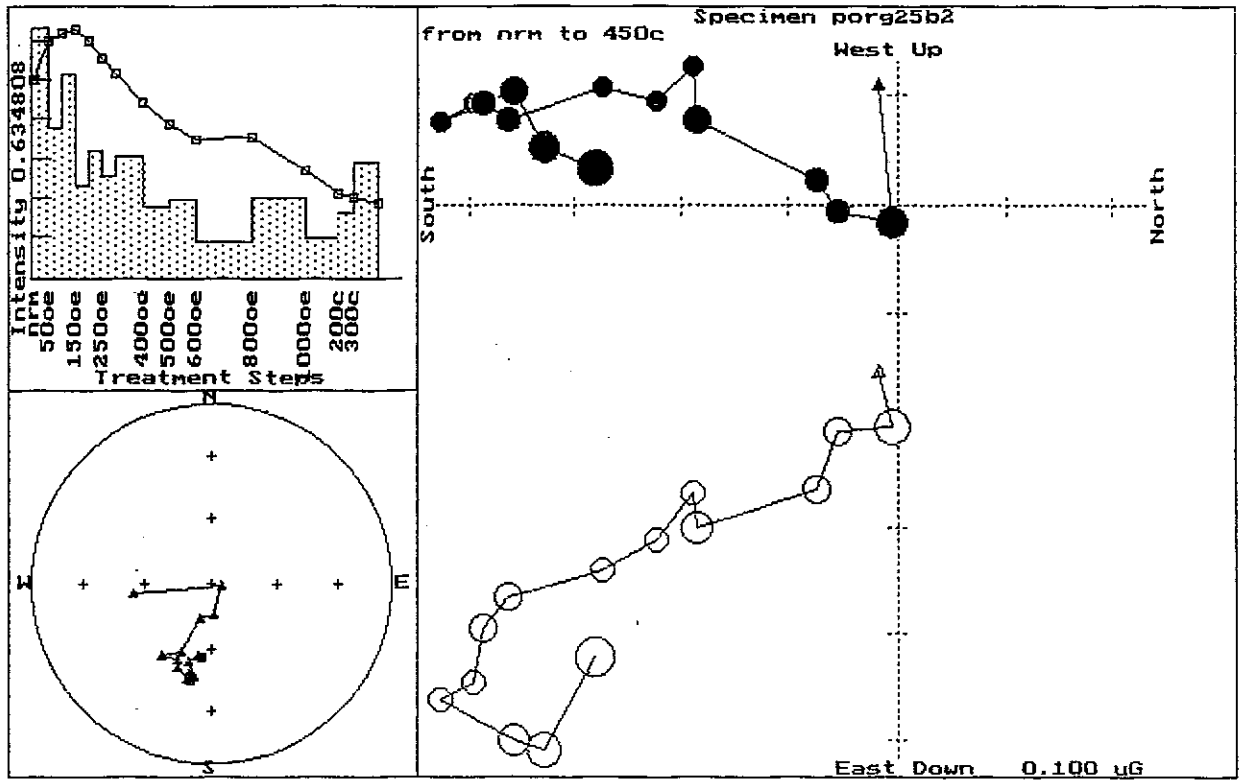
Specimen porg25b2
from nrm to 450c
West Up
South
North
East Down 0.100 uG
Intensity 0.634808
nrm
50oe
150oe
250oe
400oe
500oe
600oe
800oe
000oe
200c
300c
Treatment Steps
N
E
S
W

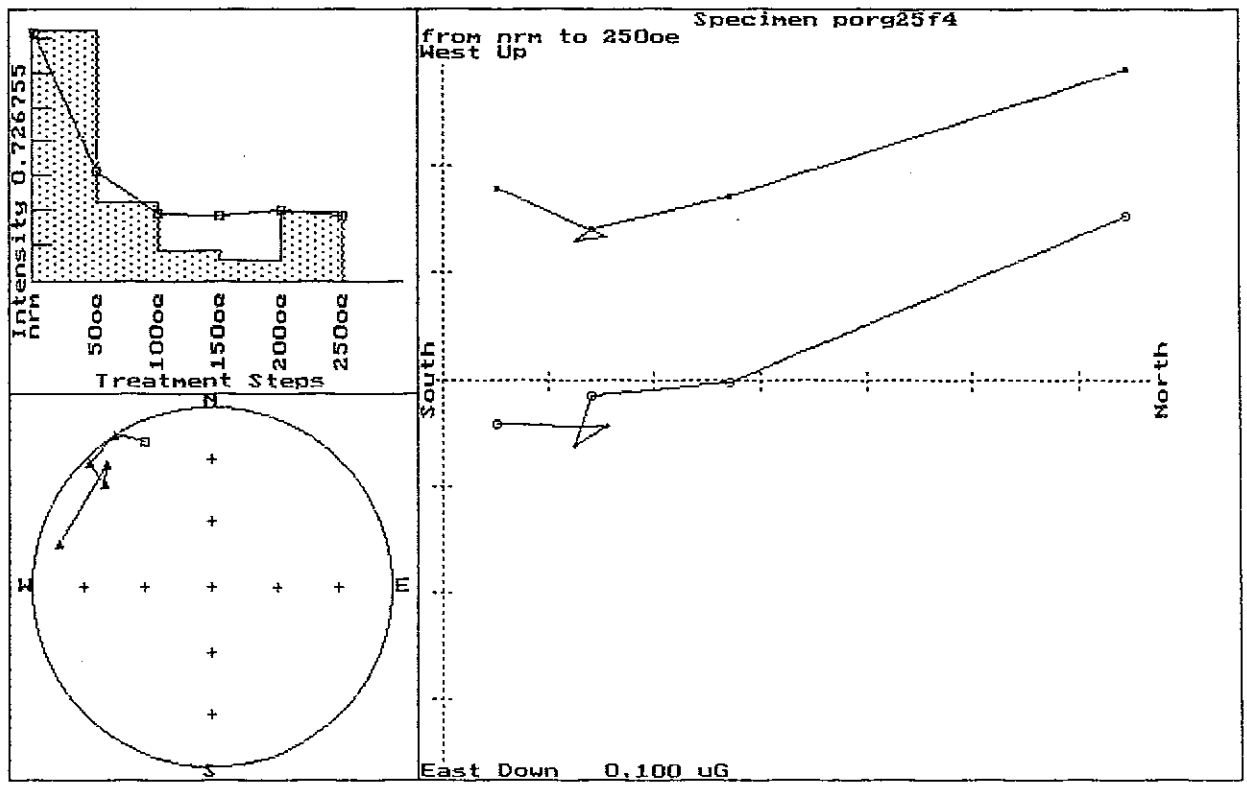
Specimen porg25f4
from nrm to 250oe
West Up
South
North
East Down 0,100 uG
Intensity 0.726755
nrm
50oe
100oe
150oe
200oe
250oe
Treatment Steps
N
E
S
W

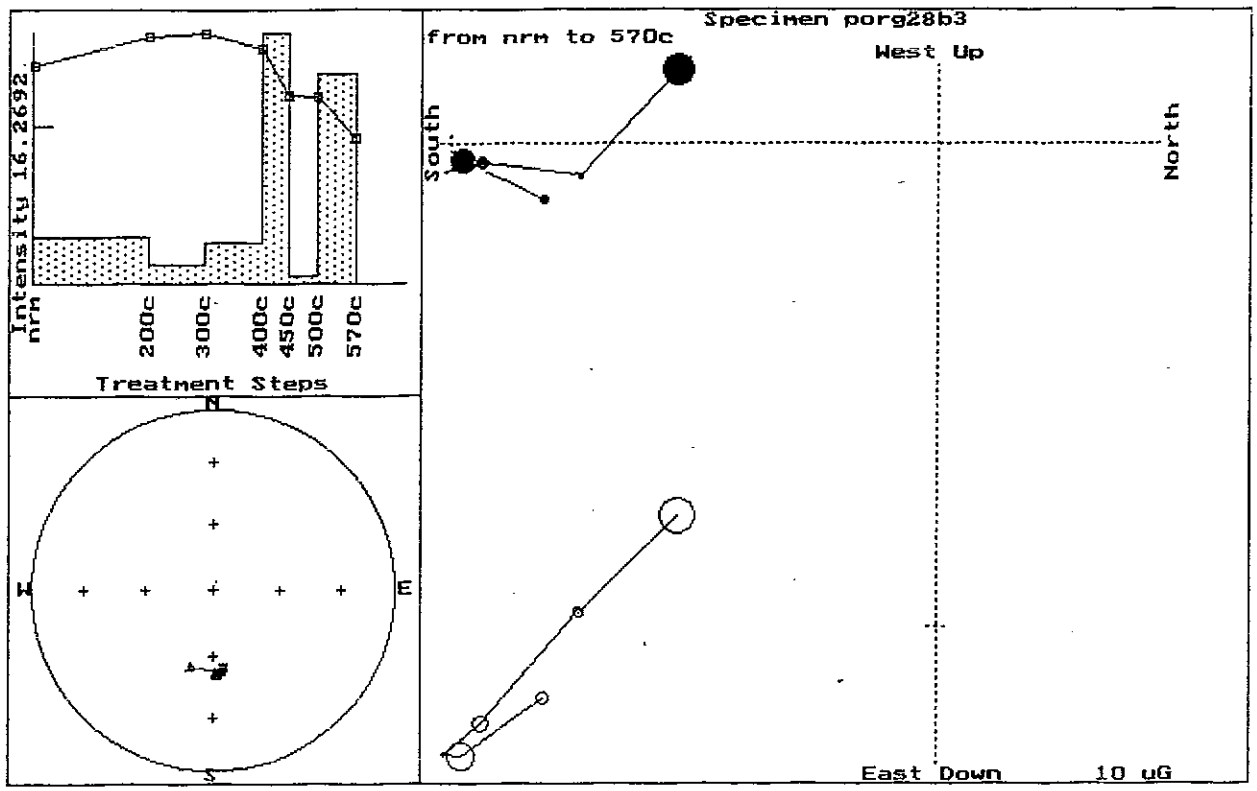
Intensity 16.2692
nrm
200c
300c
400c
450c
500c
570c
Treatment Steps
N
E
S
W
Specimen porg28b3
from nrm to 570c
West Up
South
North
East Down
10 uG

Fig.16. Low and high temperature remanence components from the Tawisakale intrusion.

Low temp

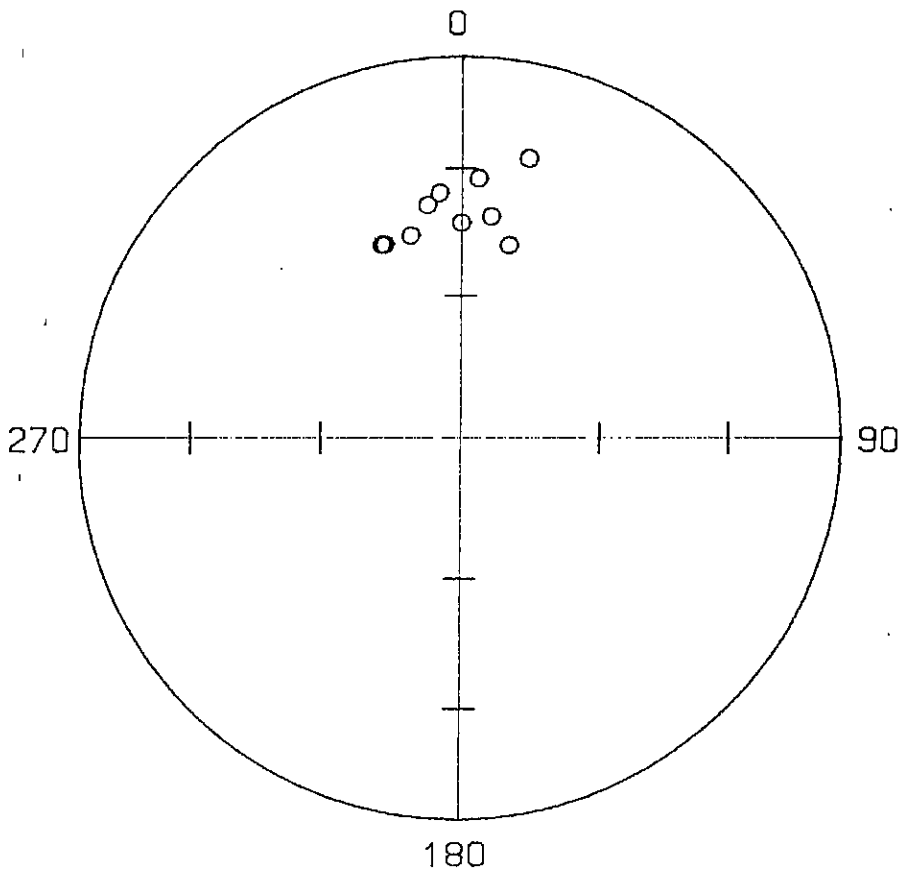

High temp

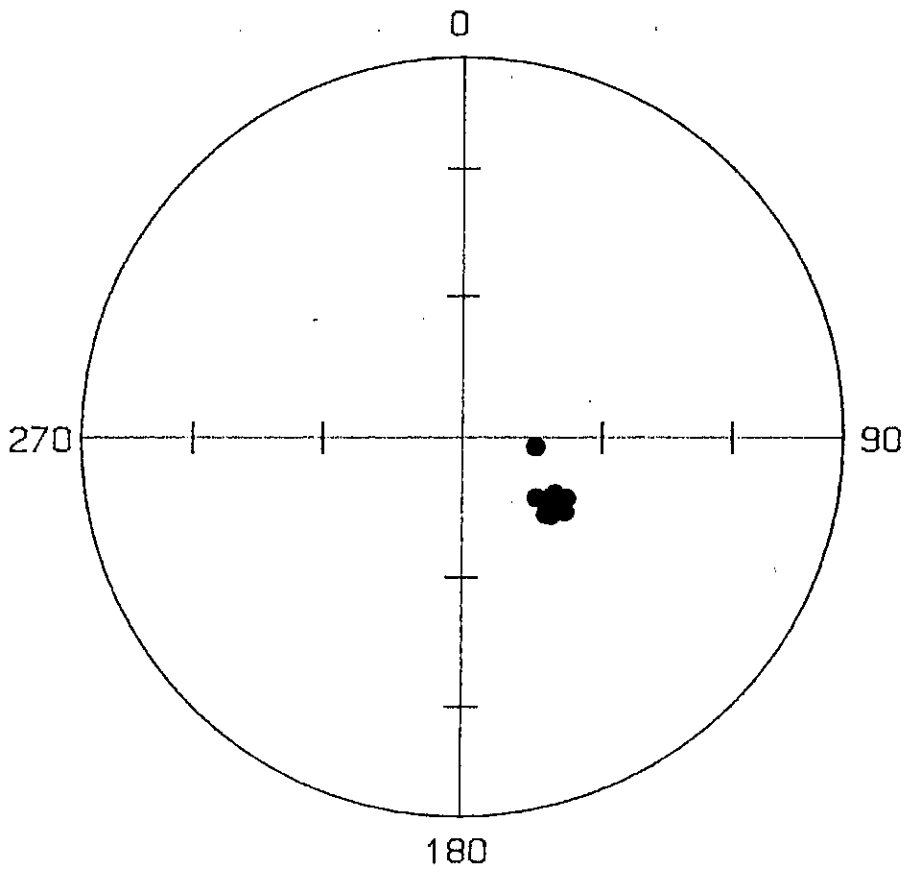

Fig.17. Low and high temperature remanence components from the NE Porgera Complex gabbros.

Gabbro
Low temp

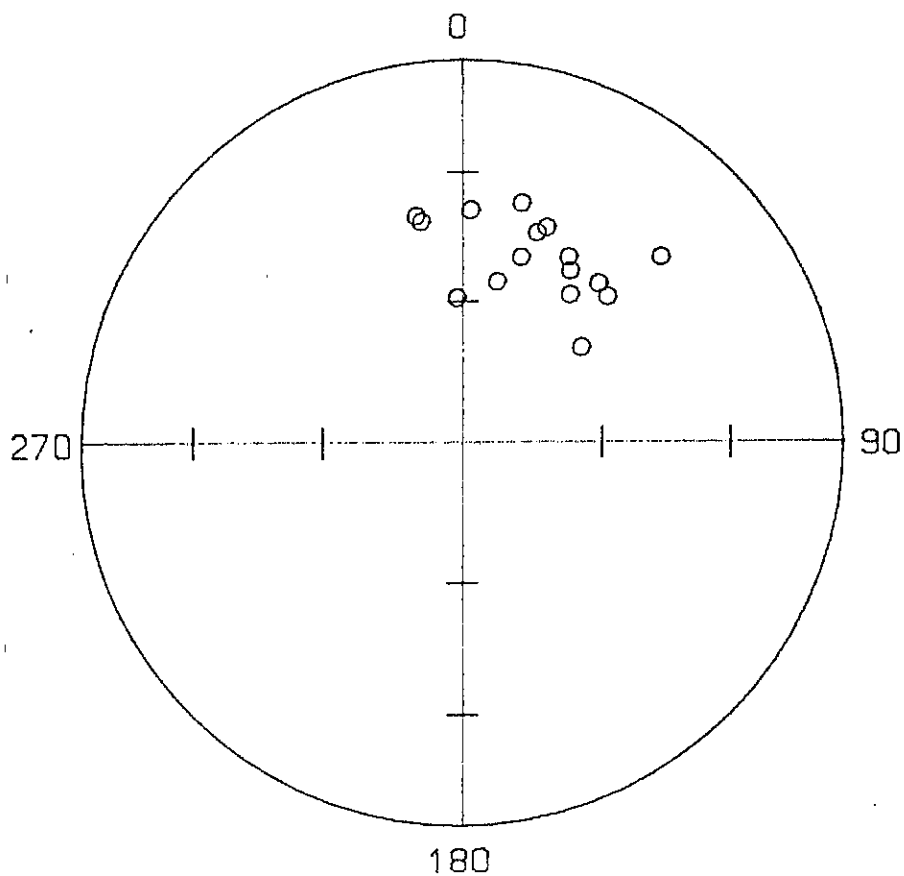

High temp

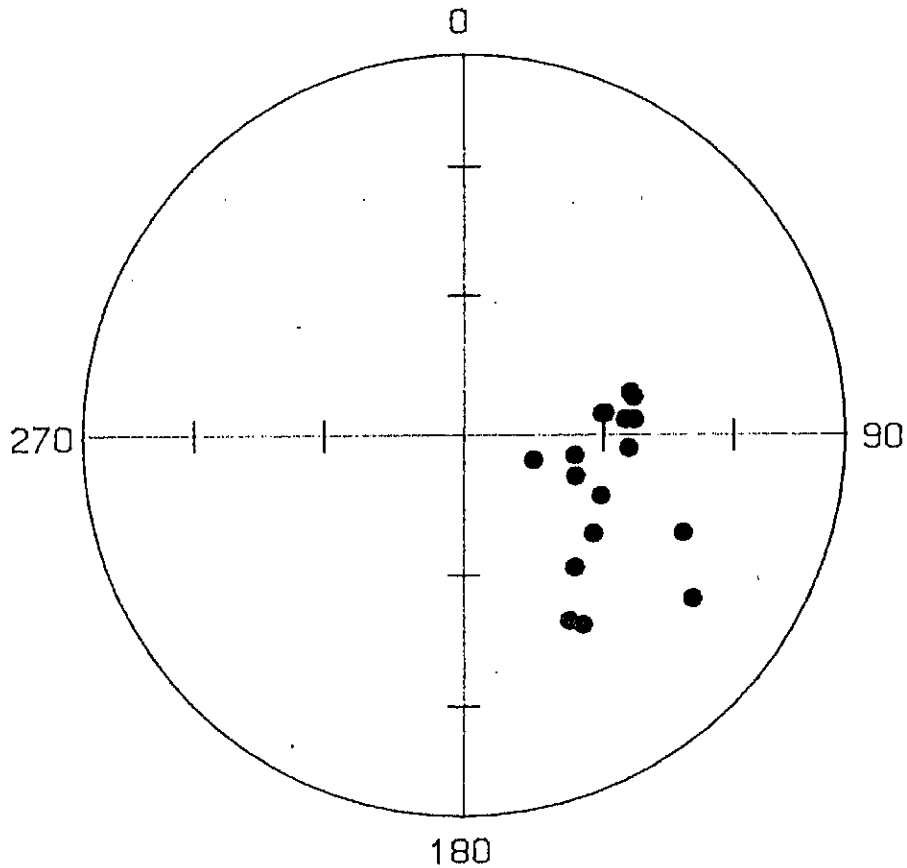

Fig.18. Low and high temperature remanence components from the Roamane hornblende diorite.

Hb diorite
Low temp

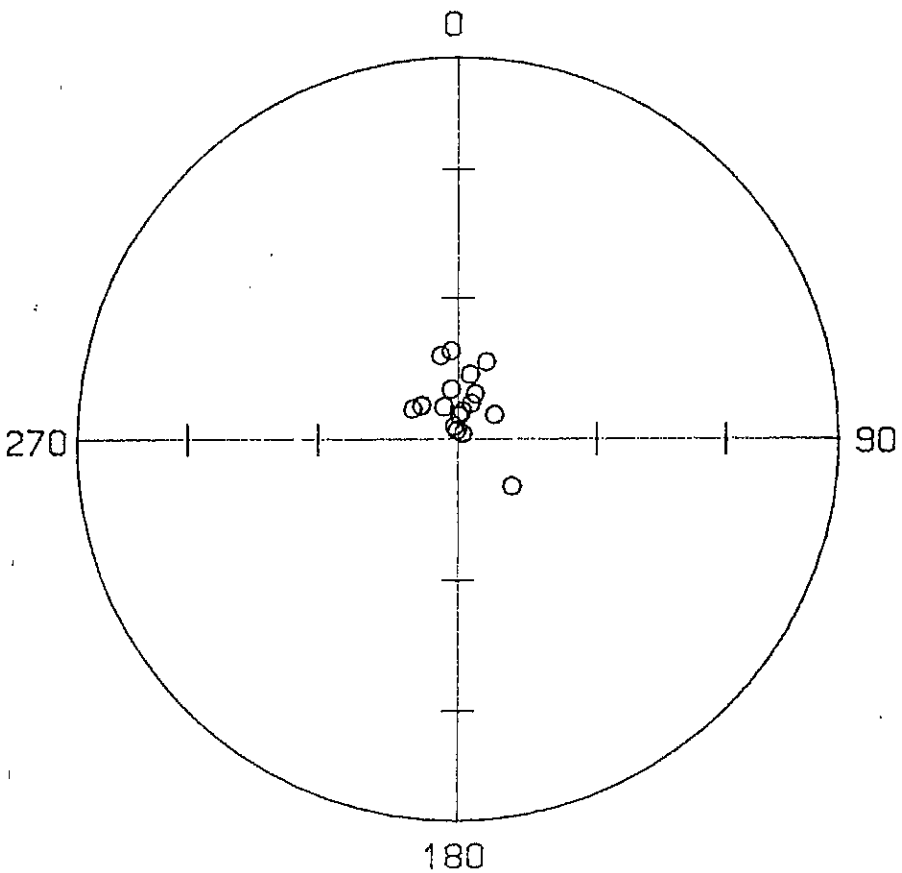

High temp

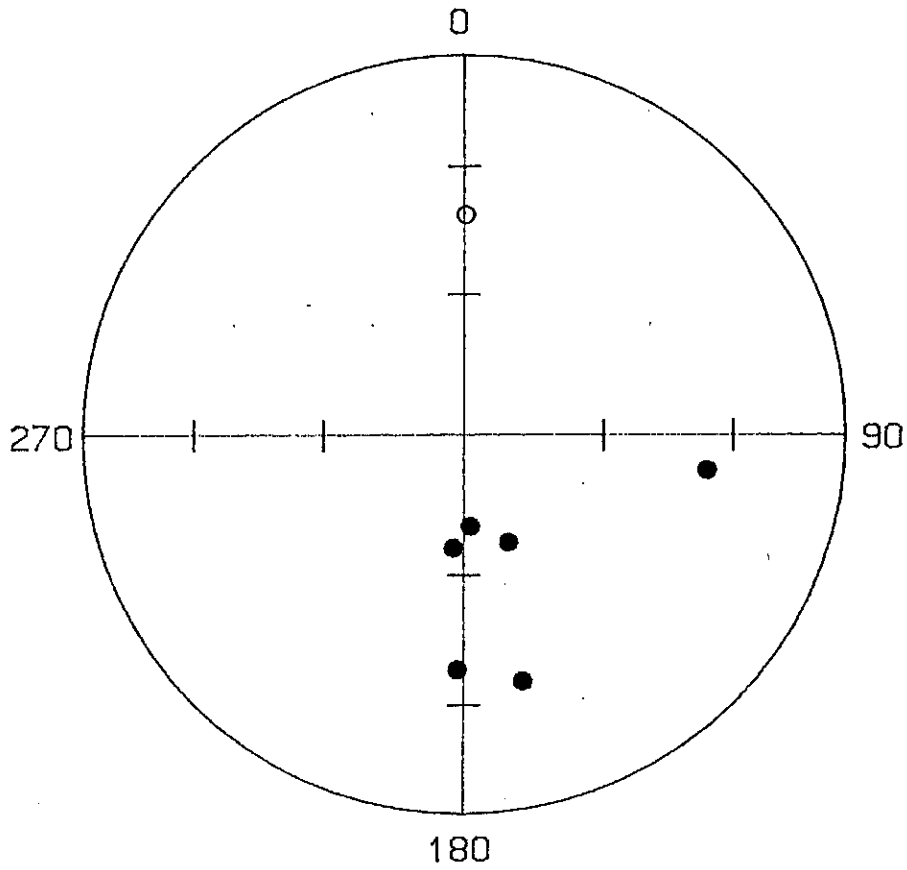

Fig.19. Low and high temperature remanence components from the Rambari/Roamane augite hornblende diorite.

Aug Hb diorite
Low temp

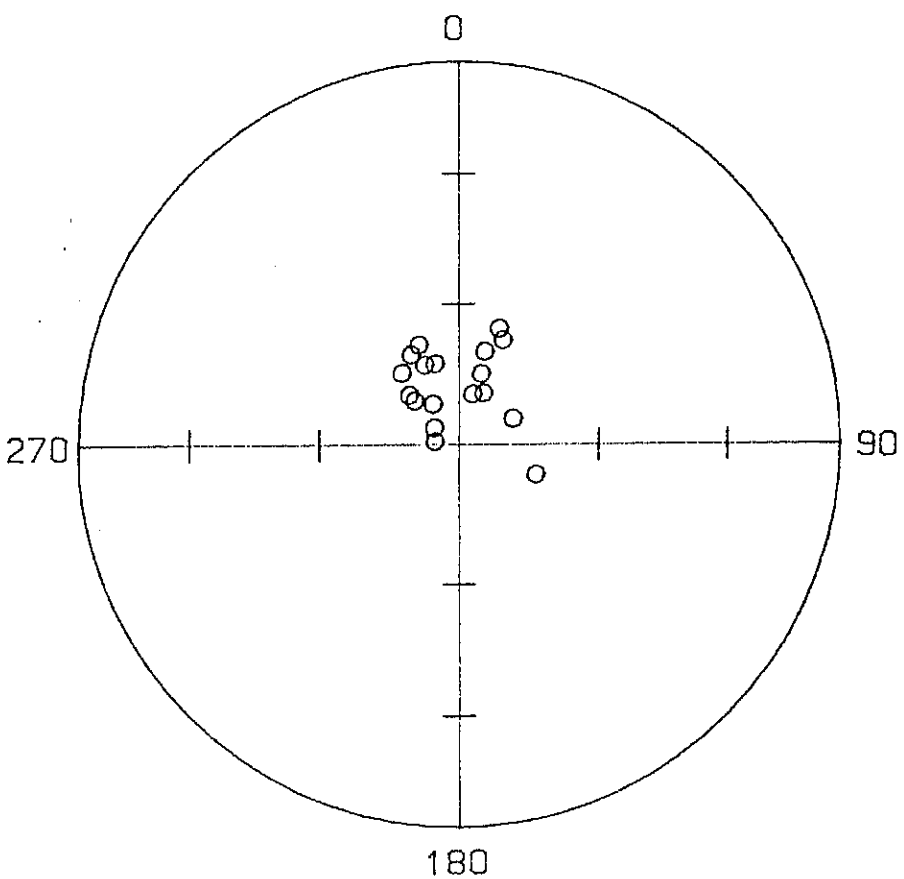

High temp

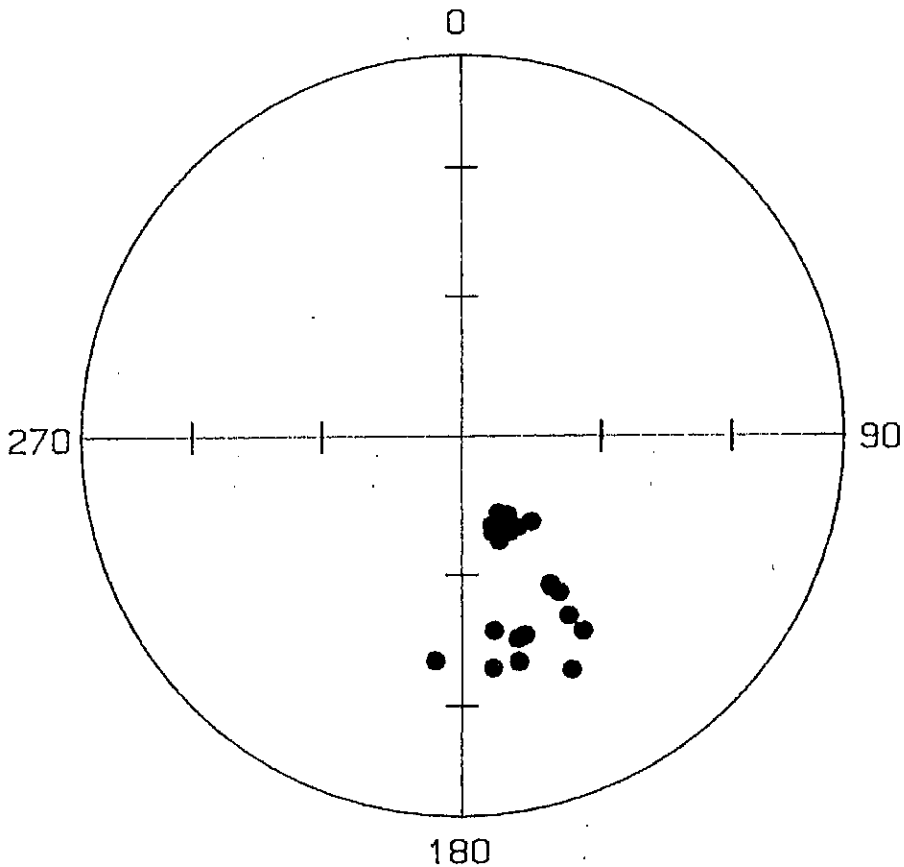

Fig.20. Principal susceptibility axes of specimens from sites 01-11. Major axes define magnetic lineations, magnetic foliation planes contain major and intermediate susceptibility axes, and minor axes represent poles (normals) to magnetic foliations.

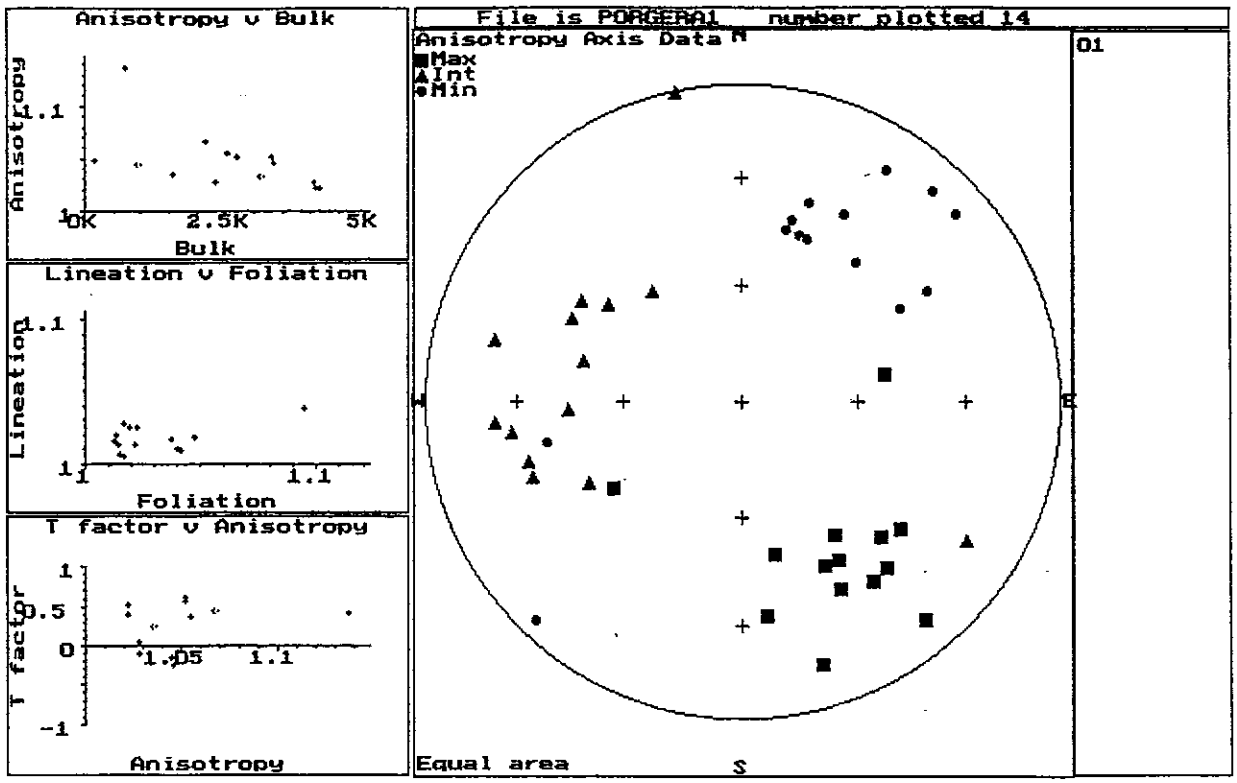
Anisotropy v Bulk
Anisotropy
1.1
1
0K
2.5K
5K
Bulk
Lineation v Foliation
Lineation
1.1
1
1
1.1
Foliation
T factor v Anisotropy
T factor
1
0.5
0
-1
1.05
1.1
Anisotropy
File is PORGERA1 number plotted 14
Anisotropy Axis Data N
Max
Int
Min
W
E
S
Equal area
01

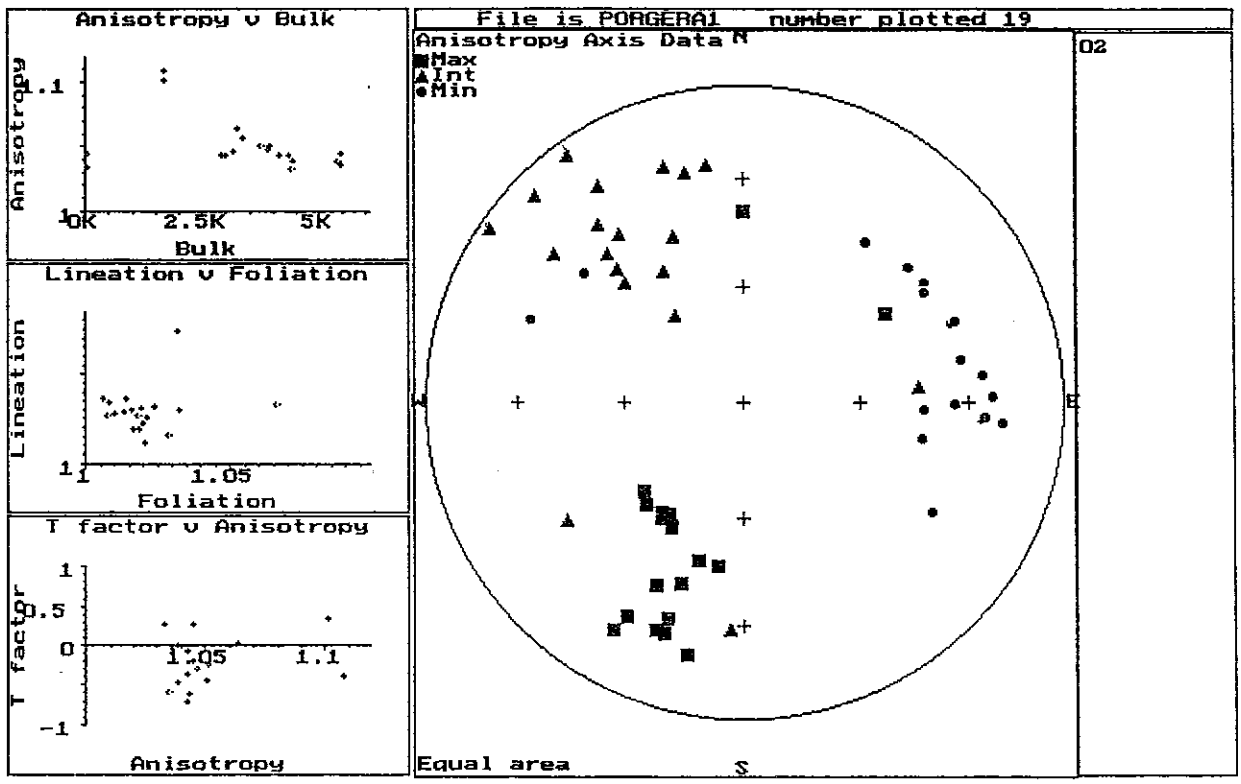
Anisotropy v Bulk
Anisotropy
1.1
1
0K
2.5K
5K
Bulk
Lineation v Foliation
Lineation
1
1
1.05
Foliation
T factor v Anisotropy
T factor
1
0.5
0
-1
1.05
1.1
Anisotropy
File is PORGERA1 number plotted 19
Anisotropy Axis Data N
Max
Int
Min
W
E
S
Equal area
02

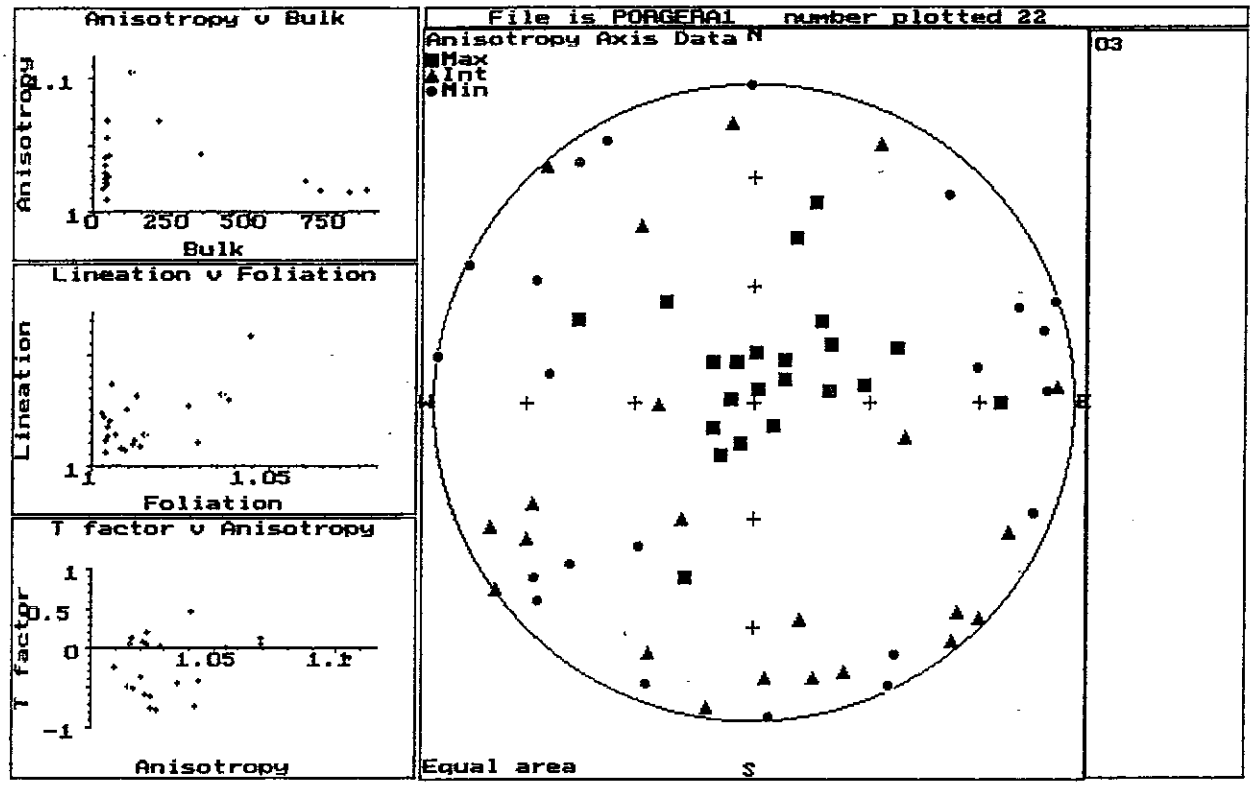
Anisotropy v Bulk
Anisotropy
1.1
1
0
250
500
750
Bulk
Lineation v Foliation
Lineation
1
1
1.05
Foliation
T factor v Anisotropy
T factor
1
0.5
0
-1
1.05
1.1
Anisotropy
File is PORGERA1 number plotted 22
Anisotropy Axis Data
Max
Int
Min
N
E
S
Equal area
03

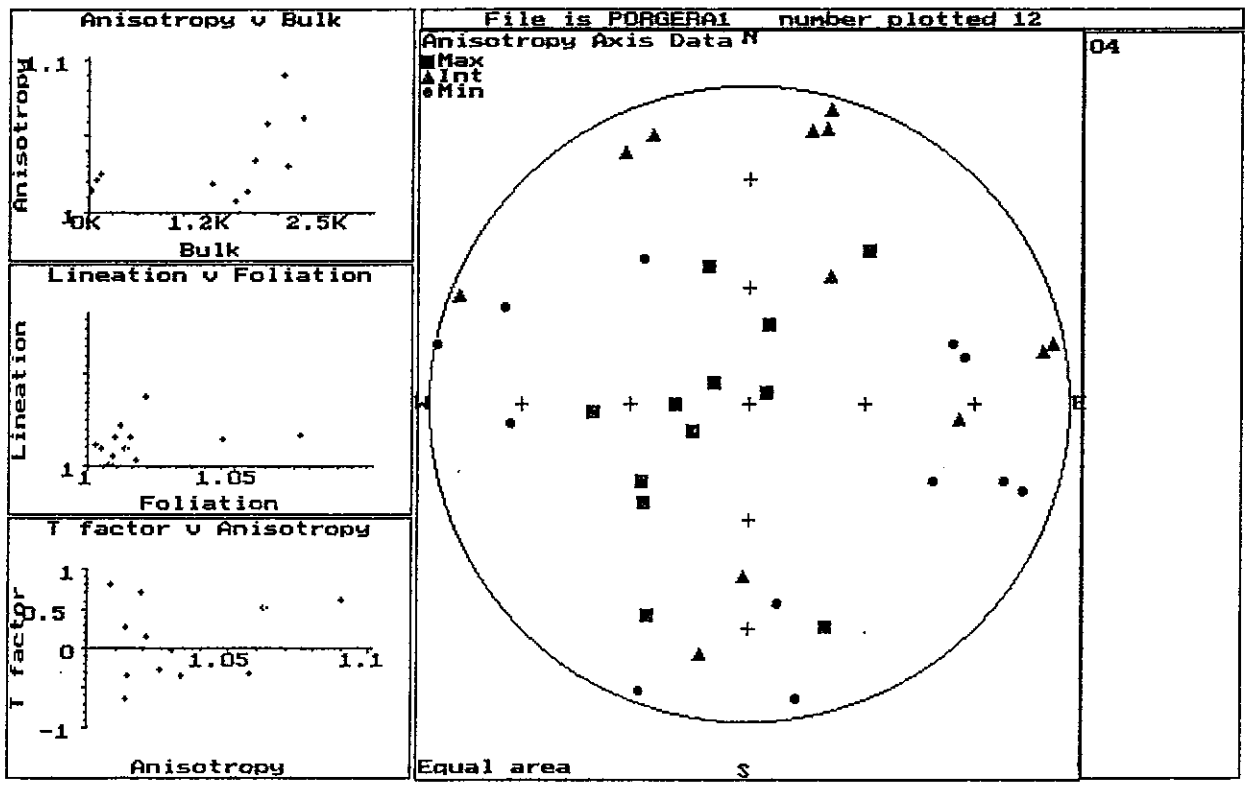
Anisotropy v Bulk
Anisotropy
1.1
1
0K
1.2K
2.5K
Bulk
Lineation v Foliation
Lineation
1
1
1.05
Foliation
T factor v Anisotropy
T factor
1
0.5
0
-1
1.05
1.1
Anisotropy
File is PORGERA1 number plotted 12
Anisotropy Axis Data
Max
Int
Min
N
E
S
Equal area
04

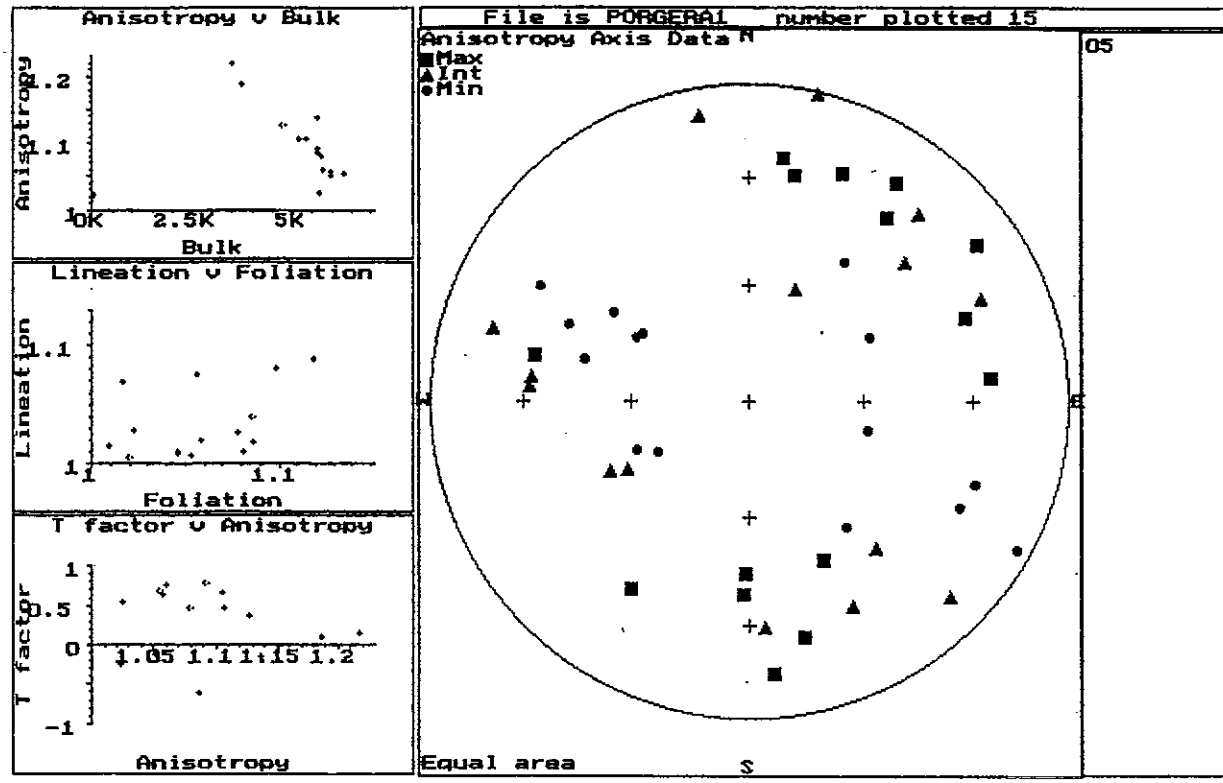
Anisotropy v Bulk
Anisotropy
1.2
1.1
1
0K
2.5K
5K
Bulk
Lineation v Foliation
Lineation
1.1
1
1
1.1
Foliation
T factor v Anisotropy
T factor
1
0.5
0
-1
1.05
1.1
1.15
1.2
Anisotropy
File is PORGERAI number plotted 15
Anisotropy Axis Data
Max
Int
Min
N
E
S
Equal area
05

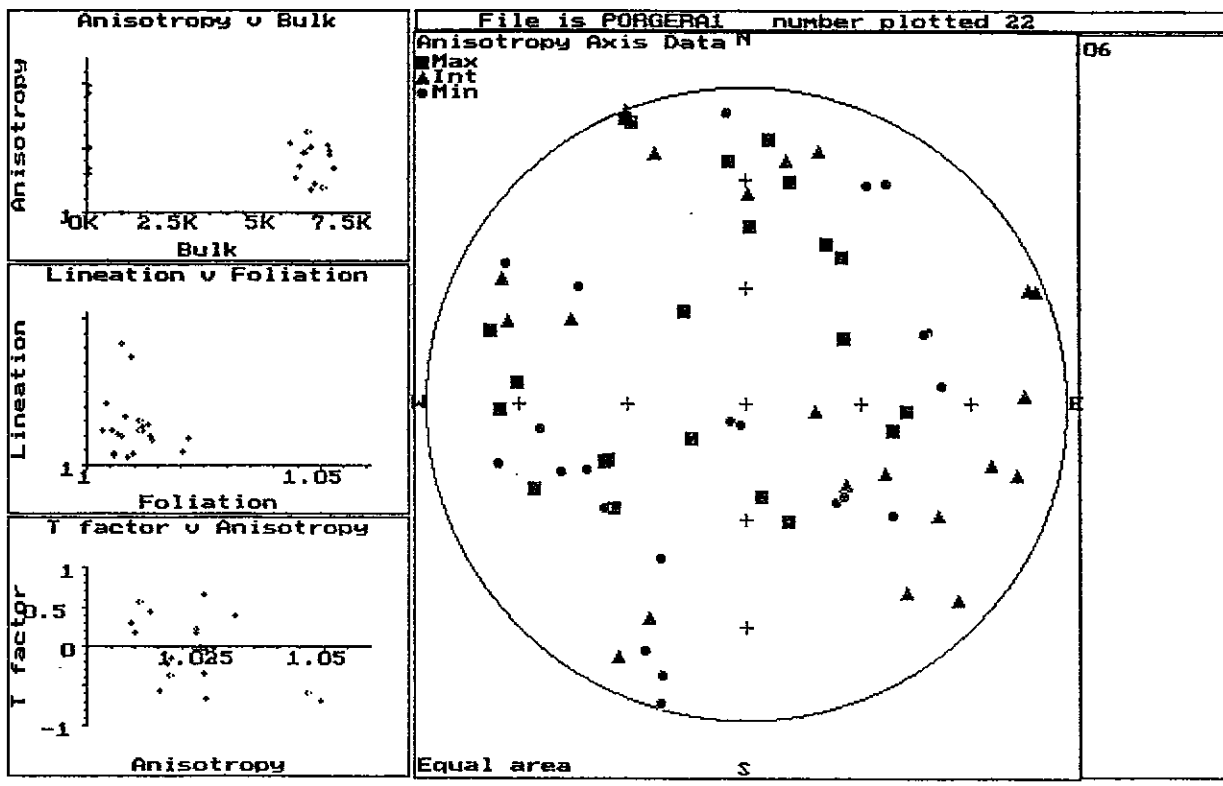
Anisotropy v Bulk
Anisotropy
1
0K
2.5K
5K
7.5K
Bulk
Lineation v Foliation
Lineation
1
1
1.05
Foliation
T factor v Anisotropy
T factor
1
0.5
0
-1
1.025
1.05
Anisotropy
File is PORGERAI number plotted 22
Anisotropy Axis Data
Max
Int
Min
N
E
S
Equal area
06

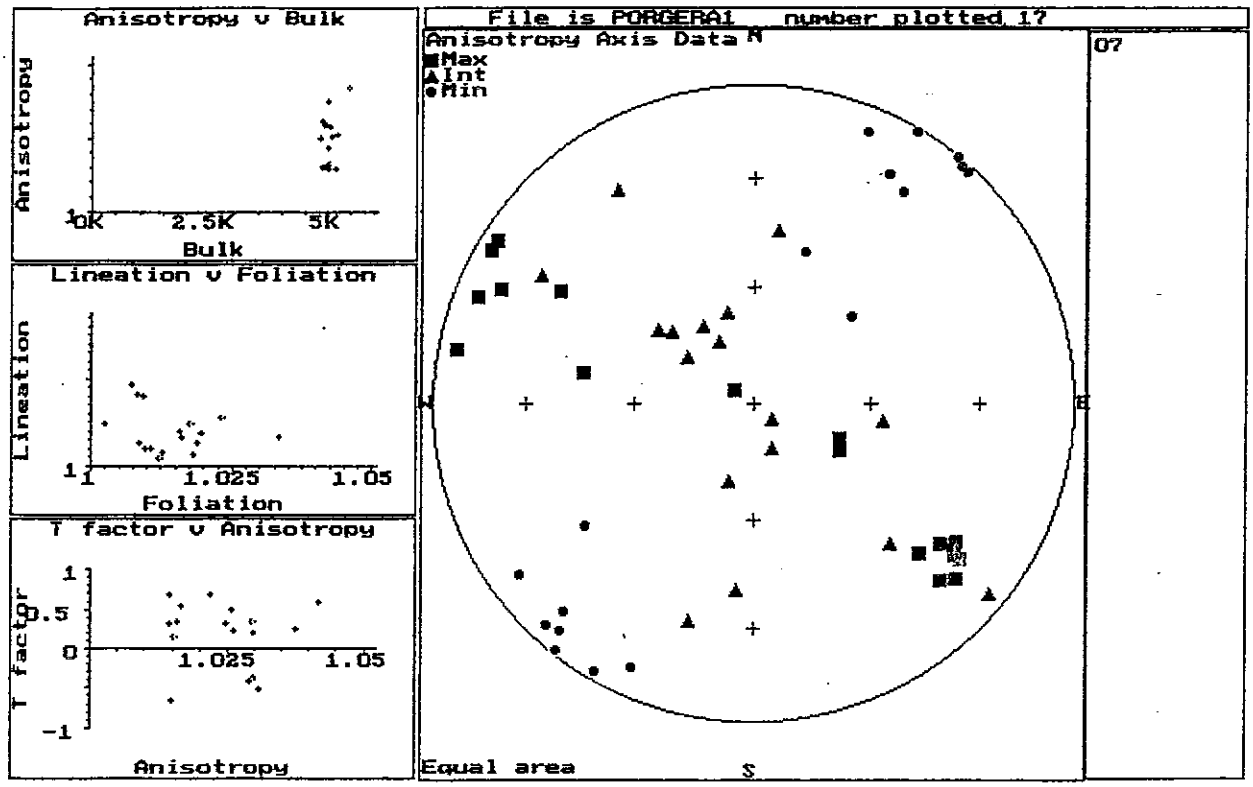
Anisotropy v Bulk
Anisotropy
1
0K
2.5K
5K
Bulk
Lineation v Foliation
Lineation
1
1
1.025
1.05
Foliation
T factor v Anisotropy
T factor
1
0.5
0
-1
1.025
1.05
Anisotropy
File is PORGERA1 number plotted 17
Anisotropy Axis Data
Max
Int
Min
N
W
E
S
Equal area
07

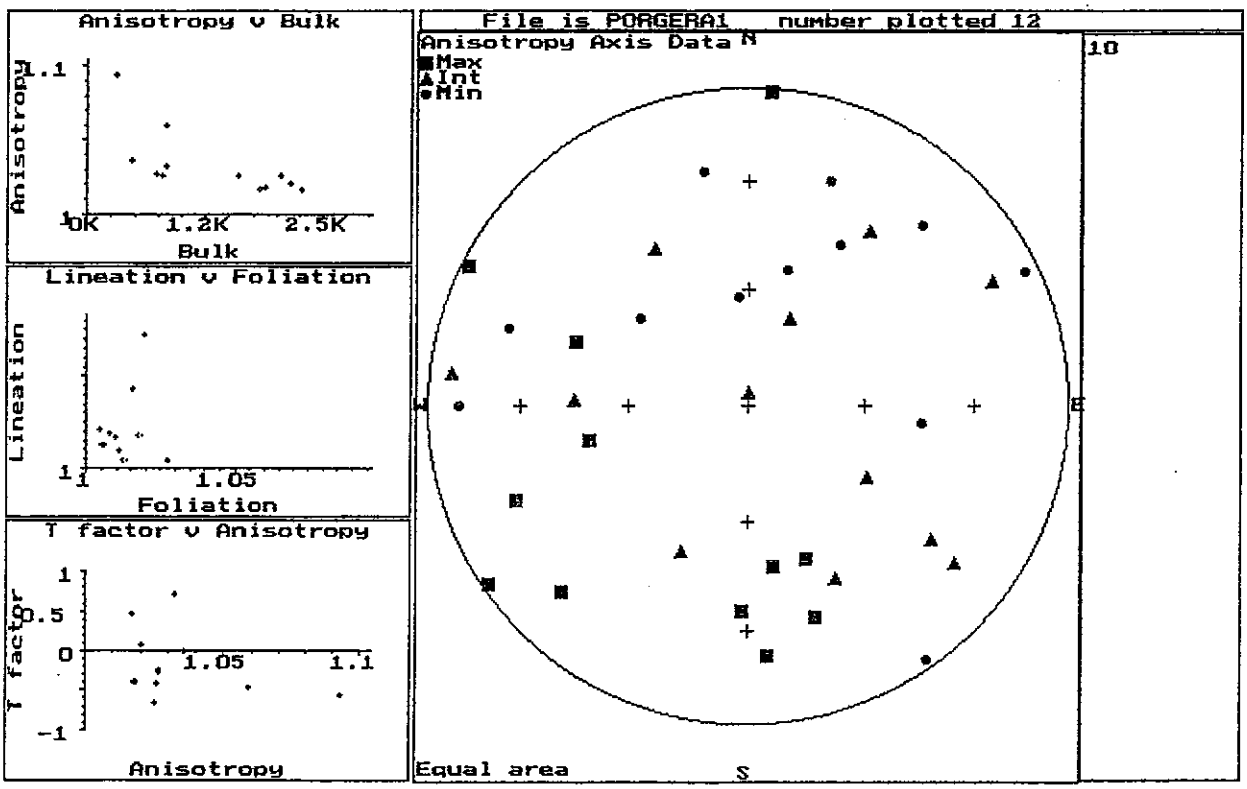
Anisotropy v Bulk
Anisotropy
1.1
1
0K
1.2K
2.5K
Bulk
Lineation v Foliation
Lineation
1
1
1.05
Foliation
T factor v Anisotropy
T factor
1
0.5
0
-1
1.05
1.1
Anisotropy
File is PORGERA1 number plotted 12
Anisotropy Axis Data
Max
Int
Min
N
W
E
S
Equal area
10

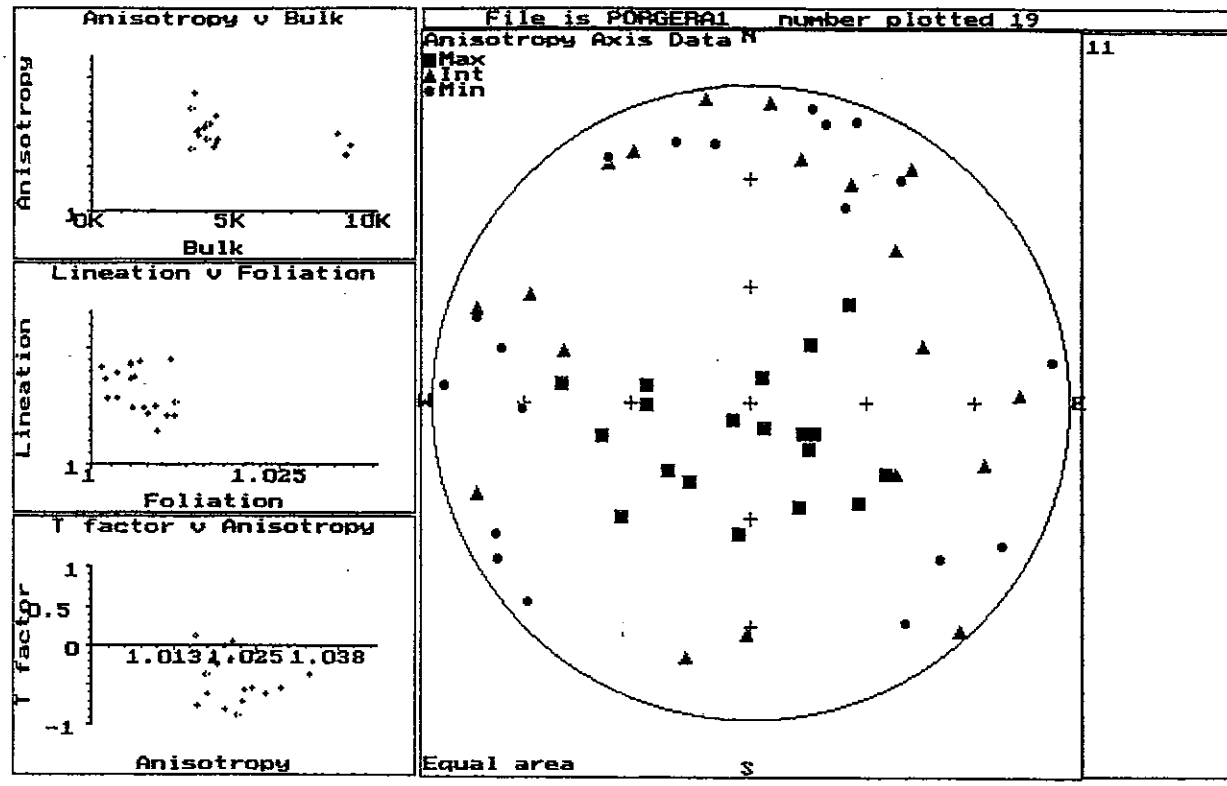
Anisotropy v Bulk
Anisotropy
0K
5K
10K
Bulk
Lineation v Foliation
Lineation
1
1
1.025
Foliation
T factor v Anisotropy
T factor
1
0.5
0
-1
1.013
1.025
1.038
Anisotropy
File is PORGERA1 number plotted 19
Anisotropy Axis Data
Max
Int
Min
N
W
E
S
Equal area
11

Fig.21. Principal susceptibility axes of specimens from Mt Kare.

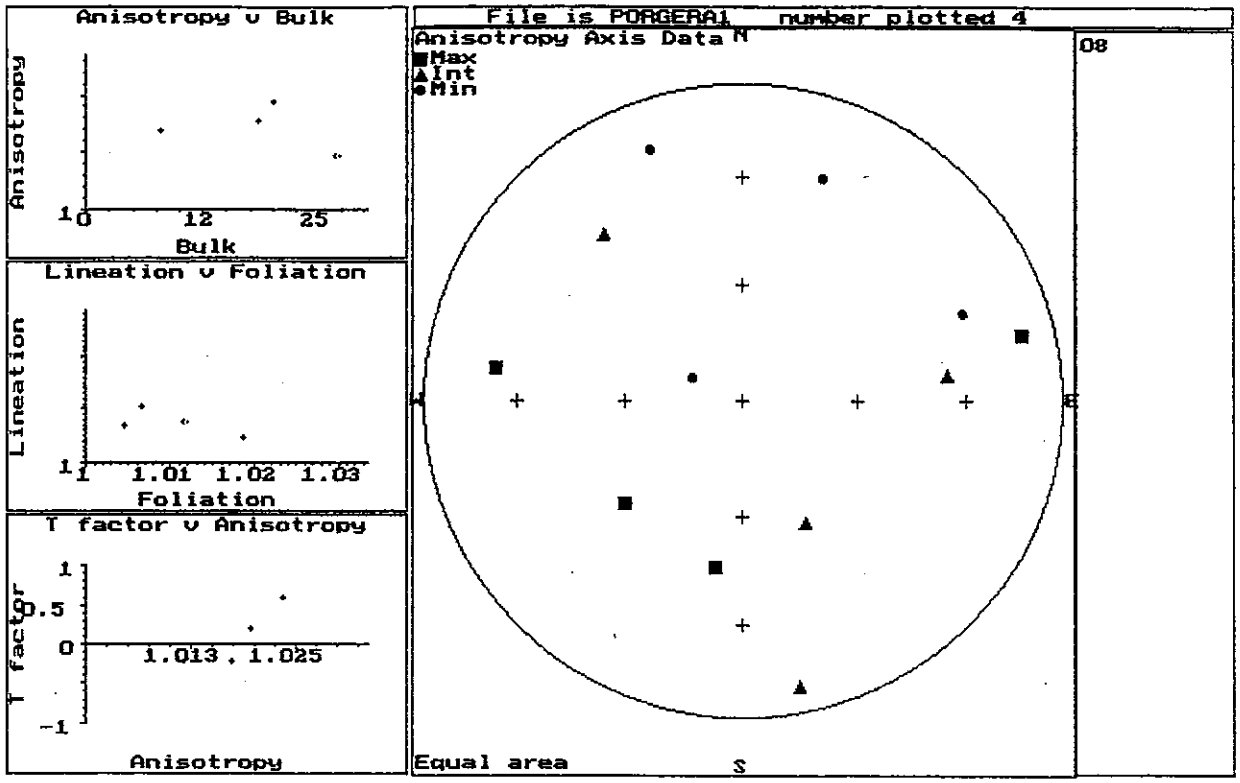
Anisotropy v Bulk
Anisotropy
1
0
12
25
Bulk
Lineation v Foliation
Lineation
1
1
1.01
1.02
1.03
Foliation
T factor v Anisotropy
T factor
1
0.5
0
-1
1.013 , 1.025
Anisotropy
File is PORGERA1 number plotted 4
Anisotropy Axis Data N
Max
Int
Min
08
E
Equal area
S

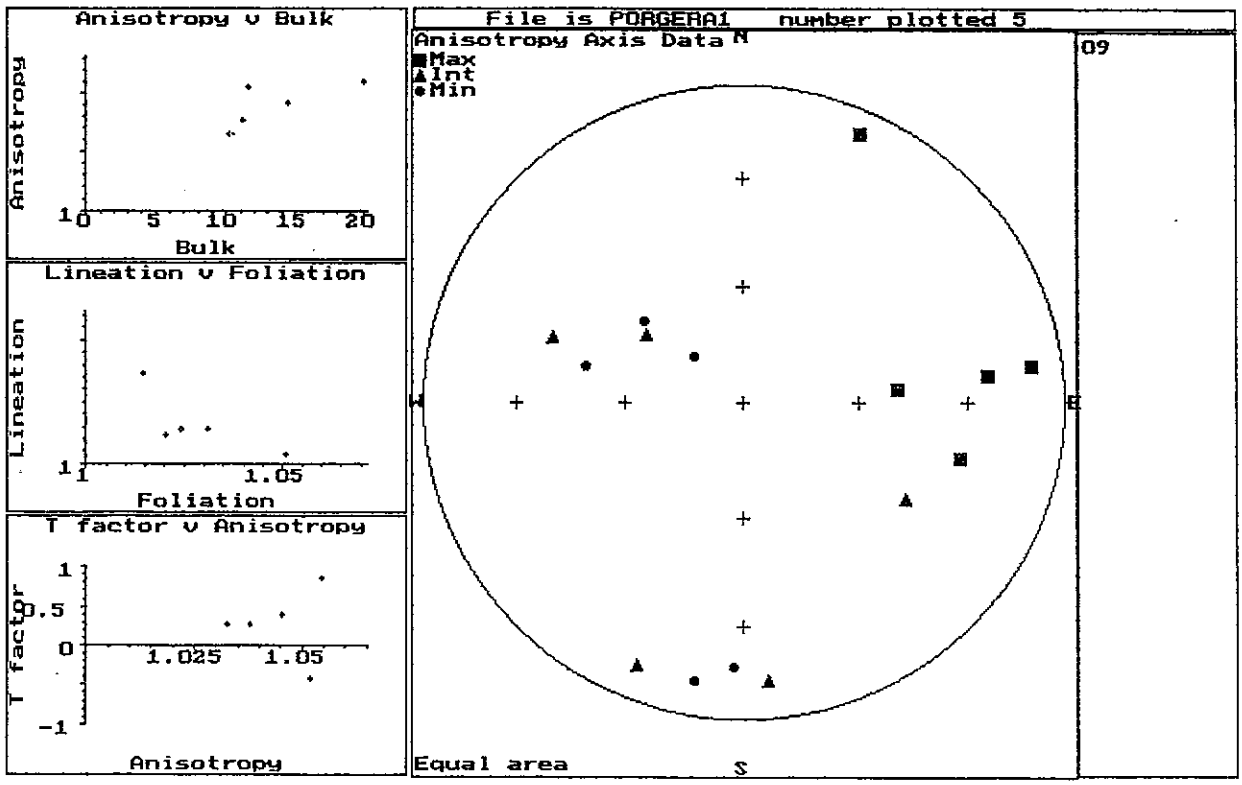
Anisotropy v Bulk
Anisotropy
1
0
5
10
15
20
Bulk
Lineation v Foliation
Lineation
1
1
1.05
Foliation
T factor v Anisotropy
T factor
1
0.5
0
-1
1.025
1.05
Anisotropy
File is PORGERA1 number plotted 5
Anisotropy Axis Data N
Max
Int
Min
09
E
Equal area
S

Fig.22. Principal susceptibility axes of hornblende diorite specimens from the underground mine.

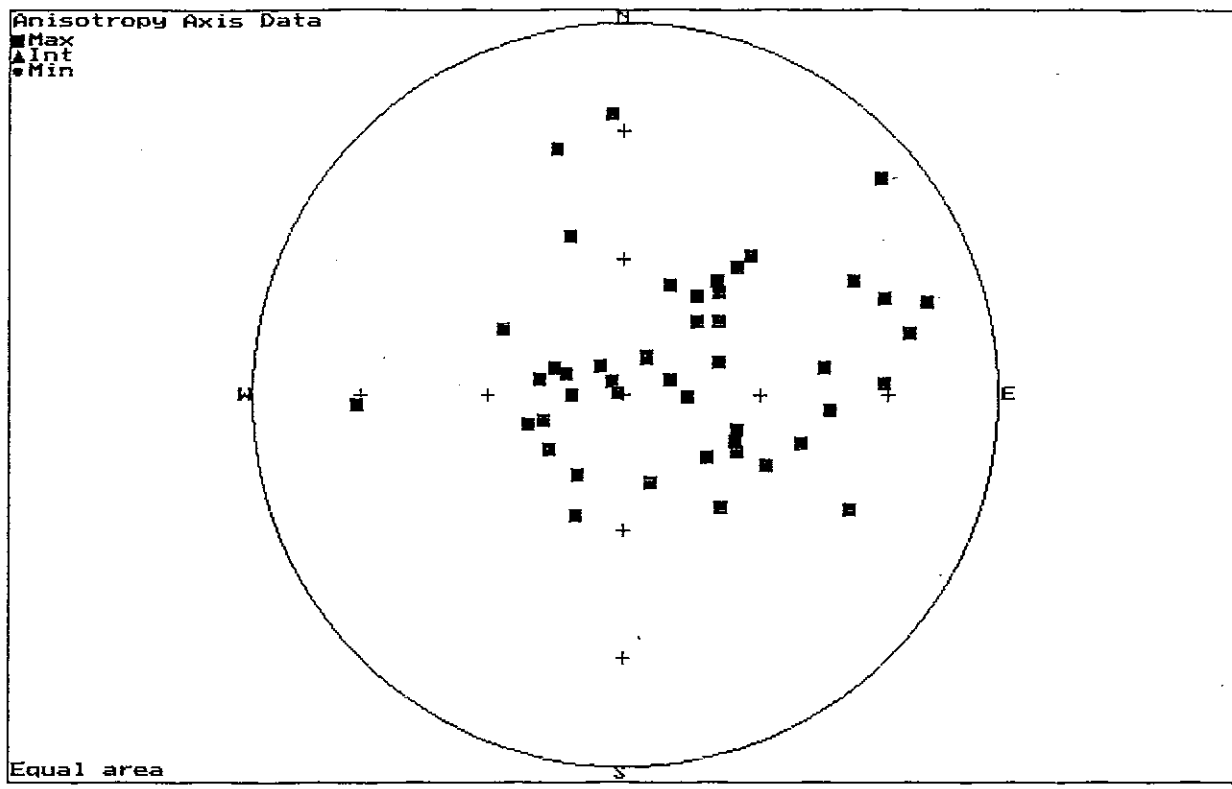
Anisotropy Axis Data
Max
Int
Min
N
W
E
S
Equal area

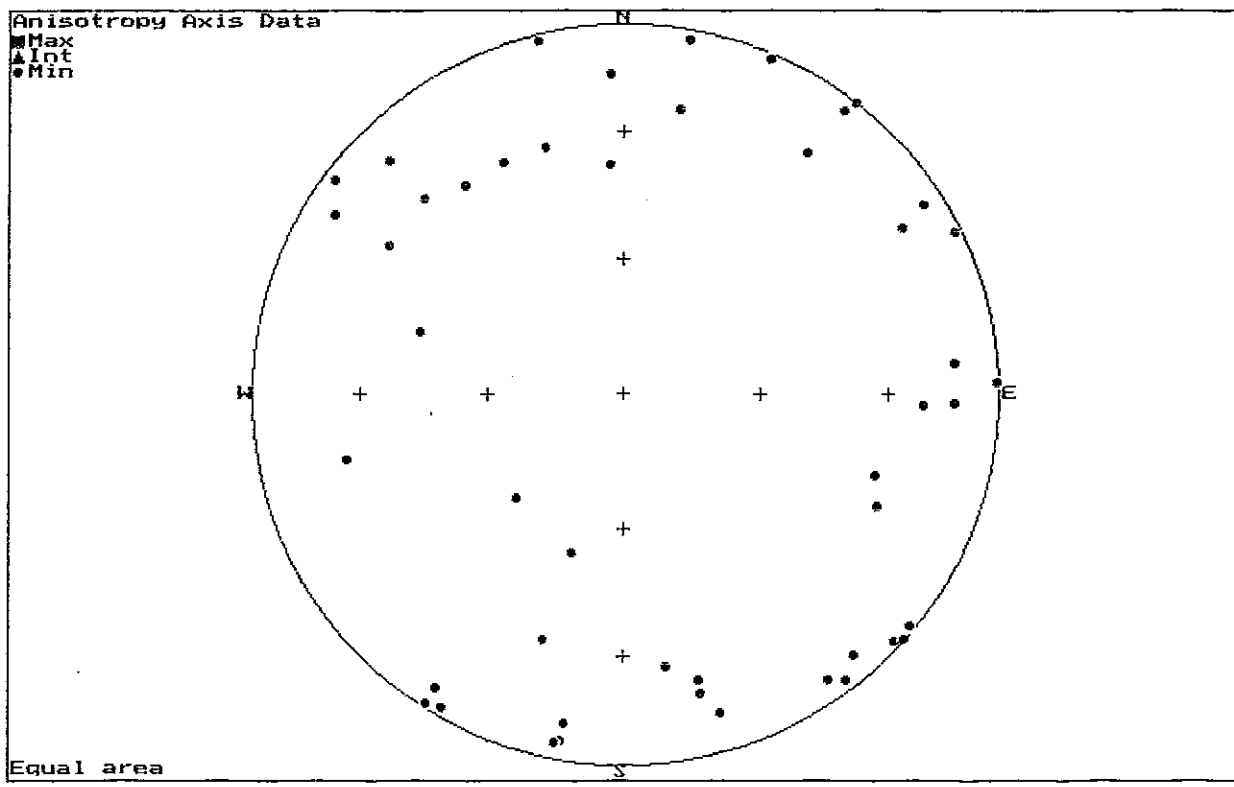
Anisotropy Axis Data
Max
Int
Min
N
W
E
S
Equal area

Fig.23. Principal susceptibility axes of augite hornblende diorite specimens from the undergound mine.

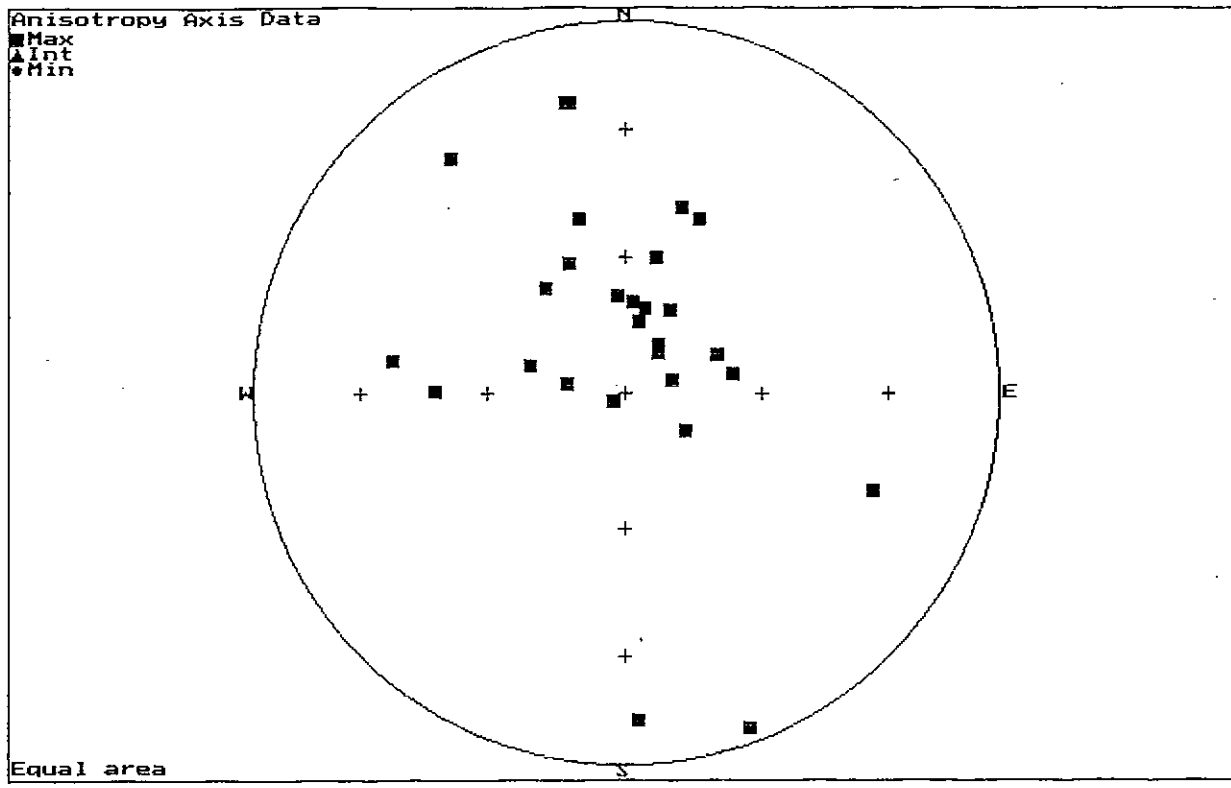
Anisotropy Axis Data
Max
Int
Min
N
W
E
S
Equal area

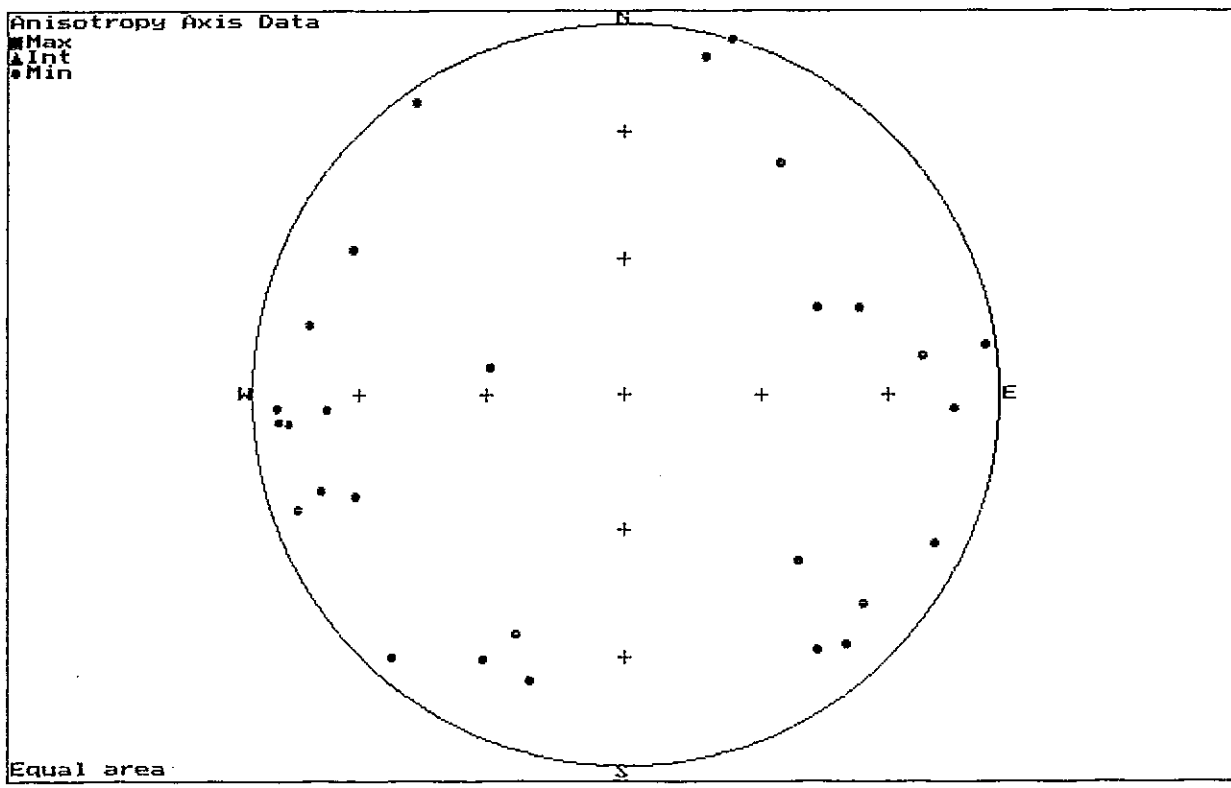
Anisotropy Axis Data
Max
Int
Min
N
W
E
S
Equal area